THE UNIVERSITY *of* EDINBURGH

Characterisation of the response of *Aedes* mosquito cells to Semliki Forest virus infection

Ricky Wai Chi Siu

Submitted for the degree of Doctor of Philosophy

July 2011

Table of contents

Declaration

I declare that all the work included in this thesis is my own except where otherwise stated. No part of this work has been, or will be submitted for any other degree or professional qualification.

Ricky Wai Chi Siu

2011

Centre for Infectious Diseases and The Roslin Institute

University of Edinburgh

Easter Bush

Edinburgh

EH25 9RG

Scotland, UK

Acknowledgements

I want to express my gratitude to the entire arbovirus team at University of Edinburgh. I consider it an honor and a privilege to work with such incredibly talented men and women. Without their support, hard work, passion and limitless dedications, this study would not exist.

In particular I would like to thank **John Fazakerley,** his patience, his support, and his forgiveness for me over the course of this PhD. John is a sophisticated supervisor with unlimited depth of knowledge coupled with fantastic logic and reasons, which is a perfect example for his fellow scientists. I would also like to thank my second supervisor **Alain Kohl** for his expertise, effort and support towards both my studies and publications.

Big Hugs for **Rennos Frakoudis, Gerald Barry, Julio Rodriguez-Andres, Ghassem Attarzadeh-Yazdi, Karen Sherwood, Mhairi Ferguson and Yi Chi**. They are wonderful colleagues who provided countless assistance and moral support and friends who shared both happiness and sadness in both work and personal life.

A special thanks to **Prof Peter Simmonds** for his knowledge and contribution in RNA secondary structure predictions. Another special thanks for **Prof David Taylor** for giving me this PhD opportunity.

Finally, to my parents, thank you for your support, understanding and love, thank you for your enormous effort to allow years and years of education. I wish I could have spent more time with you.

List of Figures

Chapter 1

Chapter 2

Chapter 3

Chapter 4

Chapter 5

Chapter 6

List of Tables

Chapter 1

Chapter 2

Chapter 5

Chapter 6

Abbreviations

Ae.aegypti	*Aedes aegypti*
Ae.albopictus	*Aedes albopictus*
AGO	Argonaute
An.gambiae	*Anopheles gambiae*
ANOVA	An analysis of variance
Apaf	Apoptotic protease activating factor
BHK-21	Baby hamster kidney
BSA	Bovine serum albumin
CARD	Caspase activation and recruitment domains
CDC	Centers for Diseases Control and Prevention
cDNA	complementary DNA
CHIKV	Chikungunya virus
CPE	Cytopathic effect
CpG	Cytosine-phosphate-guanine
CPV	Cytoplasmic vacuoles
DCV	Drosophila C virus
DCL	Dicer-like proteins
Dcr	Dicer
DD	Death domain
DENV	Dengue virus
DF	Dengue fever
DHF	Dengue hemorrhagic fever
DISC	Death-inducing signalling complex
DMSO	Dimethylsulfoxide
DNA	Deoxyribonucleic Acid
Dredd	Death-related ced-3/Nedd2-like protein
dNTP	Deoxy-nucleoside triphosphate
dsDNA	Double-stranded deoxyribonucleic acid
dsRBD	dsRNA binding domain
dsRNA	Double-stranded ribonucleic acid
DTT	Dithiothreitol

E. coli	*Escherichia coli*
EDTA	Ethylenediaminetetraacetic acid
EEE	Eastern equine encephalitis
EEEV	Eastern Equine Encephalitis Virus
eGFP	Enhanced green fluorescent protein
eIF2α	Eukaryotic transcription initiation factor 2α
ER	Endoplasmic reticulum
ERK	Extracellular signal-regulated protein kinases
FACS	Fluorescence-activated cell sorting
FADD	Fas-associated death domain protein
FCS	Foetal Calf Serum
FMDV	Foot-and-mouth disease virus
GMEM	Glasgow's minimal essential media
GTP	Guanosine triphosphate
H_2O	Water
HEPES	4-(2-hydroxyethyl)-1-piperazineethanesulfonic acid
ICAD	Inhibitor of caspase-activated deoxyribonuclease
IFN	Interferon
IFNAR	Interferon-alpha/beta receptor
IκB	Inhibitor of kappa B
IKK	Inhibitor of kappa B kinase
IMD	Immune deficiency
IRAK	Interleukin-receptor associated kinase
IRES	Internal ribosome entry site
IRF	IFN regulatory factor
ISGF	Interferon-stimulated gene factor
JAK	Janus family tyrosine kinase
JE	Japanese encephalitis
JEV	Japanese encephalitis virus
JNK	c-Jun N-terminal kinase
LAC	La Crosse
LAM	Lipoarabinomannan
LB	Luria-Bertani

LGP-2	Laboratory of genetics and physiology-2
LPS	Lipopolysaccharide
LRR	Leucine-rich repeat
LTA	Lipoteichoic acid
MAP	Mitogen-activated protein
MAPK	Mitogen-activated protein kinase
MAPKKK	Mitogen-activated protein kinase kinase kinase
MDA5	Melanoma differentiation-associated gene 5
MEFs	Mouse embryo fibroblasts
MKK	Mitogen-activated protein kinase kinase
MOI	Multiplicity of Infection
MHC	Major histocompatibility complex
MyD88	Myeloid differentiation-88
NBCS	Newborn calf serum
NFκB	Nuclear factor kappa-light-chain-enhancer of activated B cells
nsP	Non-structural protein
ONNV	O'nyong-nyong virus
ORF	Open reading frame
PAMP	Pathogen associated molecular pattern
PBS	Phosphate buffered saline
PBSA	Phosphate buffered saline albumin
PFU	Plaque forming unit
PGN	Peptidoglycan
PGRP	Peptidoglycan recognition proteins
PIWI	P-element induced wimpy testis
PKR	Protein kinase R
PRR	Pathogen recognition receptor
PTGS	Post-transcriptional gene silencing
RHIM	RIP homotypic interaction motif
RIG-I	Retinoic acid-inducible gene-I
RIP	Receptor interacting protein
RISC	RNA-induced silencing complex
RLR	RIG-I like receptor

RNA	Ribonucleic acid
RRV	Ross river virus
RT	Room temperature
RT-PCR	Reverse-transcription polymerase chain reaction
RVF	Rift Valley fever
SARM	SAM and ARM-containing protein
SFV	Semliki Forest Virus
siRNA	Small interfering RNAs
SLE	St. Louis encephalitis
SPBS	Sterile phosphate buffered saline
ssRNA	Single-stranded ribonucleic acid
STAT	Signal transducers and activators of transduction
TAK	Transforming growth factor-β (TGF-β) activated kinase
TAB	TAK binding proteins
TBE	Tris borate EDTA
TGF	Transforming growth factor
TIR	Toll/IL-1R
TIRAP	TIR domain containing adaptor protein
TISC	Toll-induced signalling complex
TLR	Toll-Like Receptor
TNF	Tumour necrosis factor
TRAF	TNF receptor associated factor
TRAM	TRIF-related adaptor molecule
TRIF	TIR domain containing adaptor inducing IFN-β
TSWV	*Tomato spotted wilt virus*
UV	Ultra-Violet
VEE	Venezuelan Equine Encephalitis
VEEV	Venezuelan Equine Encephalitis Virus
VRP	Virus Replicon Particles
WAGO	Worm Argonaute
WEE	western equine encephalitis
WEEV	Western Equine Encephalitis Virus
WNV	West Nile virus

Abstract

Arboviruses are transmitted to vertebrates by arthropod vectors such as mosquitoes or ticks. The replication of Semliki Forest virus (SFV) (*Togaviridae; Alphavirus*) in vertebrate cells is well established and triggers cell death. SFV infection of *Aedes albopictus* mosquito cells was characterised. Virus growth curves were compared in three cell lines. Infection of U4.4 cells was persistent and did not affect growth of the culture. In contrast, infection of C6/36 and C7-10 cells resulted in a static culture with no cell division and no cell death. The response of U4.4 cells was characterised in greater detail using viruses containing fluorescent or luciferase markers within the replicase or structural open reading frame of the virus genome. Activation of the STAT/IMD pathway prior to SFV infection significantly reduced virus driven luciferase expression and virus production. Activation of the Toll pathway prior to SFV infection had no effect. However, activation of Toll in addition to STAT/IMD had a cumulative effect on luciferase expression and virus production. viRNAs were characterised by Illumina Solexa sequencing. Two percent of the small RNA species found in virus infected cells were derived from virus RNA. These were predominantly 21 nt long and mapped along the entire SFV genome and genome complementary RNAs. Generation of these viRNAs was not random. Some areas produced high frequencies and others no or very few; hot and cold spots respectively. There were no correlations between viRNA frequency and base pairing or secondary structures predictions. Cold spot-derived viRNAs were more effective than hot-spot viRNAs in inhibiting virus replication. Similar results were observed in *Aedes aegypti*-derived cells. Attempts were made to investigate the source of these viRNAs using a virus containing an IRES element which had been reported to prevent virus replication in insect cells but which did not efficiently do so in this study. A virus containing the RNAi inhibitor p19 was characterised and shown to increase virus production.

Techniques for infecting mosquitoes via a blood meal feed were established. No infection was observed with virus replicon particles carrying a fluorescent marker gene. Infection was established using virus containing p19

Table of contents

Chapter 1: Introduction

Arboviruses are some of the most common pathogens impacting on human and animal health worldwide. In many cases, virus transmission relies on successful replication and dissemination within susceptible vector tissues. Different mosquito species such as *Aedes albopictus*, *Aedes aegypti* and *Anopheles gambiae* are common vectors for different arboviruses. However, we are just beginning to understand how mosquito vectors respond to arbovirus infections. Although, there are mechanisms and pathways conserved between insects and mammals, insects lack the fundamental anti-viral systems of vertebrates. In vertebrates, the immune system can be divided into innate and adaptive immunity. Adaptive immunity relies on the production of specific antigen receptors and acquisition of memory. Prior to the development of specific responses, a rapid and non-specific system detects and determines the biological context of antigens. These tasks are achieved by the innate immune system. The innate immune system detects foreign antigens by a set of structurally and functionally diverse receptors (Choe et al., 2002; Kurt-Jones et al., 2000; Michel et al., 2001; Söderhäll & Cerenius, 1998; Wyers et al., 1995). These receptors trigger mechanisms such as phagocytosis, expression of pro-inflammatory genes and interferons in vertebrates (Klotman & Chang, 2006). However, there is no adaptive immune system in insects. Extensive studies in *Drosophila melanogaster* have shown only an innate immune system (Hoffmann, 2003). It is generally assumed that all insect species utilise a similar system. To date, the systems identified in *Drosophila*, the Toll and IMD pathways, defend against fungi and bacteria. The nature of innate defences against viruses remains less clear. As mosquitoes are vectors for transmitting many medically important virus diseases including: dengue fever (DF) and dengue hemorrhagic fever (DHF), yellow fever, Rift Valley fever (RVF), and West Nile fever (Black *et al.*, 2002), therefore understanding the interaction between insects and viruses is not only important fundamental biological knowledge but also has relevance to human and veterinary medicine.

Medical and veterinary importance of arboviruses

Arboviruses (arthropod-borne viruses) are viruses that are maintained in nature through transmission between vertebrate hosts by blood feeding arthropods. The commonly known blood feeding arthropod vectors include mosquitoes, psychodids (moth and sand flies), ceratopogonids (midges), and ticks. Transmission occurs when the infected arthropod takes a blood meal from a susceptible vertebrate host. There are over five hundred different arboviruses registered in the international catalogue of arboviruses at the division of vector-borne infectious diseases (DVBID) under the Centers for Diseases Control and Prevention (CDC). The members of three families: the *Togaviridae* (genus *Alphavirus*), *Flaviviridae* and *Bunyaviridae* pose important human health problems worldwide (Table 1.1). These viruses are maintained in non-human vertebrates (birds and rodents and sometimes horses) and transmitted by mosquitoes and mosquitoes or ticks. In many cases, transmission to humans occurs when the virus escapes the natural cycle often through a secondary vector to a secondary host (dead end host) (Figure 1.1). Infected humans occasionally develop clinical illnesses such as mild febrile illness, arthralgia and encephalitis. More severe cases include neurological damage, the development of hemorrhagic fever and death.

Arthopod vector	Virus family	Human diseases
Mosquito	*Bunyaviridae*	La Crosse encephalitis, Rift Valley fever
	Flaviviridae	Japanese encephalitis, St Louis encephalitis, West Nile fever, Dengue fever, Yellow fever
	Togaviridae	Eastern equine encephalitis, Western equine encephalitis, Venezuelan equine encephalitis, Chikungunya, O'nyong-nyong fever, Ross River fever
Tick	*Bunyaviridae*	Crimean-Congo haemorrhagic fever
	Flaviviridae	Tick-borne encephalitis, Powassan encephalitis, Omsk haemorrhagic fever
	Reoviridae	Colorado tick fever

Table 1.1 Arboviruses of medical importance in different families.

Most arboviruses are RNA viruses of the families Bunyaviridae, Togaviridae and Flaviviridae with exceptions such as CTF of the double stranded RNA virus family *Reoviridae*.

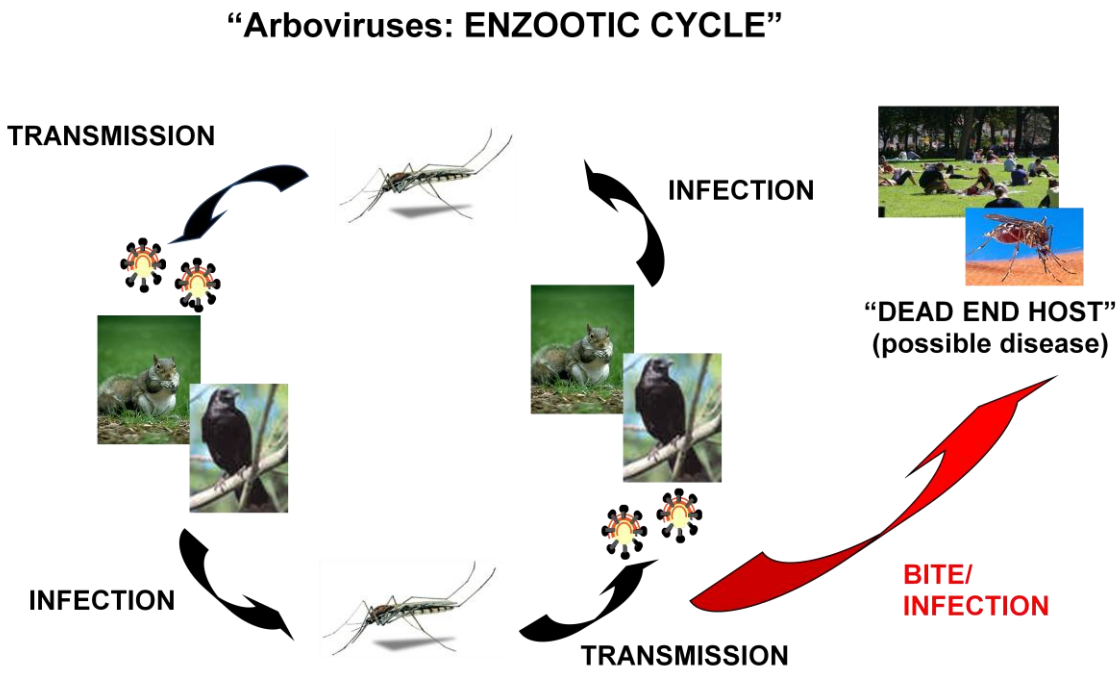

Figure 1.1: Enzootic cycle of arboviruses.

Arboviruses are maintained in complex life cycles involving a nonhuman vertebrate host and arthropod vector(s). These cycles remain intact until the virus escapes via a secondary vector or vertebrate host as the result of some ecologic change. Infected humans and domestic animals can develop mild febrile illness and occasionally viral encephalitis. Infection in humans usually leads to a dead end for the virus because "dead end hosts" do not usually contribute to the transmission cycle.

Arboviruses have been recognised as the leading cause of encephalitis worldwide since 1985 (Ho & Hirsch, 1985) . The outburst of arboviral infections often occurs during warmer seasons when it is most favourable for mosquitoes to breed. This reflects the importance of transmitting vectors for transmission. For example, incidence of yellow fever is often high during the rainy season in both South America and Africa. This reflects the importance of understanding the vector as one of the major keys to control the transmission cycles of all mosquito-borne diseases. Infections are mostly asymptomatic, a minority of patients develop mild febrile illness or viral meningitis (Tsai, 1991). Although only a minority develop encephalitis with arbovirus infection, the fatality rate in this group can be up to 70%.

Alphavirus

The genus Alphavirus contains approximately 30 members, which were estimated to have diverged a few thousand years ago (Powers *et al.*, 2001). Not all alphaviruses are pathogenic to humans, only some are highly infectious and cause clinical diseaseswhich ranges from mild to severe. Alphaviruses can be divided into New World and Old World viruses characterised by their distinctive ways of interacting with their respective hosts and differences in their pathogenicity, tissue and cellular tropism, cytotoxicity and interaction with the cell. The New World virus infections are predominantly associated with encephalitis, whereas the Old World virus infections are associated with polyarthritis and rash (Powers *et al.*, 2001; Weaver & Reisen, 2010).

Sindbis virus (SINV) is one of the most studied alphaviruses. It is named after the northern Egyptian district where the virus was first isolated from a mosquito in 1952 (Taylor *et al.*, 1955). The virus is present in Europe, Africa, Asia and Australia and transmitted between birds by *Culex* species mosquitoes (Jupp *et al.*, 1986; Tesh, 1982). SINV has been isolated from blood of migratory birds, but it does not cause mortality or sickness in them. The virus is naturally transmitted to humans by mosquitoes of the genera *Culex* and *Culiseta*, in laboratory studies it can also be transmitted by *Aedes* species (Taylor *et al.*, 1955). In Europe, outbreaks have been recorded since the early 1980s in Sweden, Finland, and the adjacent Karelia area of Russia. Clinical disease caused by SINV is called Ockelbo disease in Sweden, Pogosta disease in Finland, and Karelian fever in Russian Karelia. The most recent outbreak occurred in Finland in 2002 (Kurkela *et al.*, 2005). Pogosta disease was first recognised in Finland in 1974, and since then epidemics have taken place every 7 years. Nucleotide sequencing of the viruses isolated from these locations indicated that these viruses are geographically distinct genotypes (Norder *et al.*, 1996). During the acute phase of infection in humans, symptoms consist of fever, headache, fatigue, followed by progressive musculoskeletal pain, swollen joints, arthritis, inflamed tendons and rash. The joint symptoms can be incapacitating in the acute phase of the disease. Recovery usually takes a period of weeks, and joint pains may persist for

several years in one-third of the patients (Niklasson *et al.*, 1988). No vaccines against SINV and SINV-related viruses are presently available.

Eastern equine encephalitis (EEE) is caused by the alphavirus EEEV, transmitted to humans and equines by the bite of an infected mosquito. It was first isolated in 1933 after an equine epizootic in New Jersey and Virginia (TenBroeck & Merrill, 1933). EEEV occurs along the eastern seaboard of the United States and has a wide range of avian and mammalian hosts including turkeys, emus, whooping cranes, partridges, pheasants, horses and humans. Infection is more dangerous to horses but mostly asymptomatic for humans. However, in some cases, infected humans can develop sudden onset of fever, general muscle pains, and a headache of increasing severity. These individuals often progress to more severe symptoms such as seizures and coma. One in three who develop clinical encephalitis will die from the disease and those who recover often suffer permanent brain damage. Infection is often lethal for pheasants and horses whilst rapidly fatal for whooping cranes, turkeys and emus. Outbreaks of EEE were observed from May 2008 to August 2009 in Brazil. The disease occurred in 93 farms affecting 229 equids with a case fatality rate of 72.92% (Silva *et al.*, 2011). EEEV is maintained between birds and the mosquito *Culiseta melanura* (Armstrong & Andreadis, 2010). The virus is thought to escape its natural cycle through other mosquito vectors *Coquilletidia perturbans* and *Aedes sollicitans* which feed on birds and mammals.

Western equine encephalitis virus (WEEV) is an alphavirus that causes western equine encephalitis in horses and humans in western parts of the USA and Canada. It was first isolated in 1930 from a horse with encephalitis. Like other viral encephalitis, most WEEV infections in humans are asymptomatic or present as mild, nonspecific illness. Patients with clinically apparent illness usually have a sudden onset with fever, headache, nausea, vomiting, anorexia and malaise, followed by altered mental state, weakness and signs of meningeal irritation. Infants under 1 year old are affected more severely than adults and may be left with permanent sequelae (5 - 30% of young patients). The case mortality rate is about 3%. The enzootic cycle of WEEV is maintained between passerine birds and culicine mosquitoes, in particular *Culex tarsalis* (Kenney et al., 2010).

Venezuelan equine encephalitis (VEE) caused by VEEV, an alphavirus like EEEV and WEEV viruses, is a disease ranging from mild febrile illness to encephalitis or death in horses and humans. It is an important veterinary and public health problem in Central and South America because it is one of the most pathogenic members of the genus. This virus is a complex of antigenically related but epidemiologically and ecologically distinct viruses. Epizootic viruses emerge at unpredictable intervals of time; infect a large number of mosquito species, producing extensive outbreaks in equines and humans. It was estimated that 200,000 human cases and more than 100,000 equine deaths in the outbreak in 1969 in centra Colombia (Weaver *et al.*, 2004). In 1995, 90,000 humans were estimated to have been infected by a VEE epidemic in Venezuela and Colombia. A recent outbreak of VEE in 2004 caused at least one fatal case in Panama (Quiroz *et al.*, 2009). On the other hand, sylvatic VEEV subtypes are transmitted continuously in forest and swamps, causing sporadic human infections (Oberste *et al.*, 1998) . VEEV infection in humans is less severe than EEEV and WEEV, but has a 20-40% case fatality rate in horses and high mortality in experimentally infected dogs, rodents and coyotes. These viruses are maintained in cycles involving forest dwelling rodents and the mosquito *Culex melanoconion* (Anishchenko *et al.*, 2006).

Chikungunya is a disease caused by CHIKV, a member of the *Alphavirus* genus. It was first identified in Newala province (Tanzania) in 1953 (Robinson, 1955). The disease is transmitted by the vector mosquito *Ae. albopictus* (Vazeille *et al.*, 2007). Between the 1960s and the 1980s, the virus was isolated from numerous countries in Central, Southern and West Africa as well as many areas of Asia (Powers *et al*, 2000). The outbreak which took place in Madras had 400,000 estimated cases in 1964, and there were 40,000 to 70,000 paediatric cases in the Bangkok outbreak in 1962 (Halstead *et al.*, 1969). In 2005 and 2006, a Chikungunya outbreak occurred on the French island of Reunion in the Indian Ocean. During this outbreak, there were 244,000 cases and 237 deaths were reported (Bonn, 2006; Renault *et al.*, 2007). Madagascar, Mauritius and the Seychelles were also affected. An outbreak occurred in the following year in India, in which more than 1.25 million suspected cases were reported (GAR, WHO). In 2007, Chikungunya was transmitted locally in a small outbreak in Italy; about 200 cases were reported from two small towns in Ravenna

province (Vazeille *et al*., 2008). The spread of CHIKV into Europe is thought to have resulted from importation by infected travellers returning from areas with high incidence rates. Infection with CHIKV is not usually fatal but can cause fever, headache, fatigue, nausea, vomiting, muscle pain, rash, and joint pain. Acute Chikungunya fever typically lasts a few days to a few weeks. More importantly, after recovery from acute infection some patients suffer from incapacitating joint pain, or arthritis which may last for weeks or months (Yazdani & Kaushik, 2007). Epidemics have been reported in East and South Africa since 1952 with 50% polyarthritis in reported cases. Recurrent joint pain can last for years in 30-40% of those infected and this is thought to be the result of immune mediated swelling of joints similar to the pain caused by the related alphavirus Ross River virus (RRV) (Morrison *et al.*, 2006). The case fatality rate has been estimated to be 1 in 1,000, with most deaths occurring in neonates, immunocompromised adults and the elderly (Gérardin *et al.*, 2008). Although CHIKV is a member of the Old World viruses, it causes meningoencephalitis in neonates and haemorrhagic diseases. However, unlike other encephalogenic alphaviruses, which infect neurons, CHIKV infects the stromal cells of the central nervous system (CNS) (Schwartz & Albert, 2010). The virus is maintained naturally between monkeys or baboons and the mosquito *Ae. aegypti*. Transmission of CHIKV to humans usually occurs through the bite of infected *Ae. aegypti*, however, *Ae. albopictus* has been associated with all the recent outbreaks. An analysis of CHIKV genetic sequences was carried out and revealed independent mutation events in the CHIKV genome which provided selective advantage for transmission by *Ae. albopictus* mosquitoes (de Lamballerie *et al.*, 2008; Tsetsarkin *et al.*, 2007). *Ae. albopictus* has been shown to acquire blood exclusively from human hosts, this suggested the amplification and transmission were enhanced by this mosquito species (Muñnoz *et al.*, 2011). CHIKV initially replicates in the skin following transmission and then disseminates to the liver and joints through the bloodstream (Robin *et al.*, 2010). In tissue culture experiments, the virus replicates in various human cell lines and causes wide spread apoptotic cell death in epithelial cells, endothelial cells, fibroblasts, monocyte-derived macrophages and Hep-2 hepatic cells (Sourisseau *et al.*, 2007). CHIKV has also been shown to infect a broad range of non-human cell lines including Vero cells, chick embryo cells, BHK21 and

L929 fibroblast-like cells (Glasgow, 1966; Hahon & Zimmerman, 1970; Rinaldo Jr *et al.*, 1975; Simizu *et al.*, 1984).

O'nyong-nyong virus (ONNV), which causes O'nyong-nyong fever is closely related to CHIKV and serologically classified in the Semliki Forest virus complex (see below). The symptoms of infection resemble Chikungunya fever: joint pains, rash and lymphadenitis. Clinical symptoms appear in 40% of patients. The virus circulates locally in East Africa at a low level and transmission is maintained by local malaria vectors *Anopheles funestus* and *Anopheles gambiae* (Bessaud *et al.*, 2006). The first outbreak was recorded in 1959 in Uganda.. This spread rapidly in East Africa, south to Mozambique, and Malawi, and west to Senegal (Williams *et al.*, 1965). The outbreak lasted for three years and was estimated to have caused two million cases. The epidemic re-emerged again in 1996-1997 in southern Uganda (Kiwanuka *et al.*, 1999).

Ross River fever is a disease endemic to Australia, Papua New Guinea, and the South Pacific caused by Ross River virus (RRV). Infections in humans often lead to 20-60% of the patients developing fever, and 83-98% develop polyarthralgia. Joint pain may persist for several months. The joint pain is caused by immune-mediated swelling of joints (Morrison *et al.*, 2006). In RRV-infected mice, inflammatory macrophages infiltrate muscles and joints, and treatment of mice with macrophage-toxic agents (silica) prior to RRV infection completely abrogated disease symptoms (Lidbury *et al.*, 2000). The virus was first described in outbreaks during 1928 and 1956 and subsequently isolated from *Aedes vigilax* in 1963. A large epidemic outbreak occurred in 1979 and 1980 involving Fiji, New Caledonia, Samoa, and the Cook Islands. In Australia between 1991 and 2000, there were 4,745 reported cases each year on average (Harley *et al.*, 2001).

Flaviviruses

West Nile fever is caused by West Nile virus (WNV), a member of the *Flaviviridae*. Infection can cause encephalitis in both humans and horses. The virus is naturally maintained between birds and mosquitoes and was first isolated from a patient in Uganda in 1937 (Smithburn *et al.*, 1940). It can be found in Europe, Africa, the

Middle East, Asia, Australia and more recently in the US (Hayes, 2001). WNV can infect cells from humans, primates, swine, ticks and mosquitoes. Intracerebal injection of WNV to mice, hamsters, rhesus monkeys and bonnet macaques leads to fatal encephalitis. Encephalitis caused by WNV is unusual, as only 1% of infections are associated with clinical disease including encephalitis. Encephalitis can be fatal in both children and adults. Many small outbreaks have occurred in Israel, India, France, Egypt, Russia, Belarus, Ukraine, Romania, the Czech Republic, and the United States. Since 1996 a large outbreak affected Bucharest and surrounding areas of southern Romania; 800 clinical cases were recorded with a case fatality rate of 1.8% for patients with meningitis and 15% for encephalitis. Between 1998 and 2000, infection of horses occurred in Italy, southern France and New York (Trock *et al.*, 2000), and there were outbreaks of human disease in the Democratic Republic of Congo and Russia (Lvov *et al.*, 2000). The disease was identified for the first time in the US in 1999 where it caused 62 clinical cases and seven deaths in Queens, New York, and surrounding areas (Lanciotti, 1999), and another 18 cases with two deaths in the following year. Since then the virus had spread to all states of US except Hawaii, Alaska and Oregon. Subsequent outbreaks took place every year from 2002 to 2008 with an average of 4,115 cases and 159 deaths per year reported by the CDC. At least 30% of those cases were considered severe involving meningitis or encephalitis.

Yellow fever is a mosquito-borne disease caused by yellow fever virus, a prototype virus of the *Flaviviridae* family first isolated in 1927 (Stokes *et al.*, 1928). There are five distinct strains, three in Africa and two in South America. The virus is maintained between non-human primates and tree hole mosquitoes (*Haemagogus spp.* in the Americas and *Aedes africanus* in Africa) in the jungles of South Central America and Africa. Humans can acquire yellow fever from jungle mosquitoes and transmit it to other humans through urban adapted mosquitoes *Aedes aeypti*. Yellow fever caused major historically documented epidemics from the 17th to 19th centuries (Patterson, 1992). Since 1905, yellow fever has only been recorded to occur in tropical South America and sub-Saharan Africa. From 1987 to 1991, there were 18,735 reported cases and 4,522 deaths worldwide (Nasidi *et al.*, 1989; Robertson *et al.*, 1996). Between 1990 and 1999, there were 11,297 cases worldwide (83% in

Africa) and 2,648 deaths were officially recorded by the World Health Organization (WHO). Incidence of yellow fever is often high during the rainy season in both South America and Africa. The virus is maintained over the dry season by vertical transmission in mosquitoes (Aitken *et al.*, 1979). According to WHO, there are an estimated 200,000 cases of yellow fever, causing 30,000 deaths, worldwide each year. In America, *Ae. aegypti* has adapted to become an urban inhabitant and it is a concern that yellow fever could erupt in explosive outbreaks. Fortunately, *Ae. aegypti* has low vector competence for yellow fever virus. Patients infected with yellow fever virus suffer from headache, backache, muscle ache, haemorrhagic fever and hepatic, renal and myocardial failures (Monath, 2001). Like other arboviral diseases, infection is usually asymptomatic with a low chance of developing severe disease, but the case fatality rate of diseased patients ranges from 15% to over 50% .

Dengue fever (DF), one of the most important tropical diseases, is caused by four distinct but closely related dengue virus (DENV) serotypes and occurs in tropical and sub-tropical regions. The virus is transmitted by *Aedes* mosquitoes, mainly *Ae. aegypti*. On average, 5-10% of *Ae. aegypti* found within a household are infected with dengue virus and 10-20 females maybe found per room and each female has the propensity to probe several persons before completing a blood meal. *Ae. albopictus* only plays a secondary role in interhuman transmission of dengue. There are 2.5 billion people at risk of infection, and according to CDC there are as many as 100 million people infected every year including 100-200 travellers from the United States, Europe and Australia. Human infection with dengue virus can result in severe flu-like illness, and sometimes a potentially lethal complication called dengue haemorrhagic fever (DHF). DHF is a leading cause of serious illness and death among children in some Asian countries. Based on findings of serological surveys, there is a high risk of developing DHF when subsequent infection happens with a serotype different from the previous infection. For example, DENV-1 was introduced to Cuba in 1977 and 44% of the population was infected. Only mild disease was reported. Then DENV-2 was brought into Cuba four years later leading to an estimated 10,000 incidences of DHF (Guzmán et al., 1990; Kouri et al., 1989). In many areas of the world, two or more serotypes co-circulate. Dengue infections are mostly prevalent in Southeast Asia, where all four serotypes are continuously in

circulation. The transmission of DENV has been recorded all over the tropical regions of the world including: sub-continental India, southern China, Taiwan, the Oceanic islands, Queensland in Australia, the Seychelle Islands, coastal Kenya, Somalia, Sudan, Saudi Arabia, Yemen, Central America, the Caribbean region, and South America. It is believed that pre-existing heterotypic, non-neutralising antibody that binds with DENV would facilitate the entry of the virus into cells of the monocytic line which leads to positive feedback in production of cytokines and chemical mediators, resulting in vascular permeability (Gubler, 1998). The symptoms of DHF included rapid onset of capillary leakage accompanied by thrombocytopenia, altered haemostasis and damage to the liver. There are not yet any vaccines developed to prevent infection with DENV.

St. Louis encephalitis caused by St. Louis encephalitis (SLE) virus, *Flaviviridae*, is the leading cause of epidemic flaviviral encephalitis and the most common mosquito-transmitted human pathogen in the United States (Tsai, 1991). SLE virus is maintained between birds and *Culex* mosquitoes and distributed throughout the Southern US. In average, there have been 193 cases reported per year since 1964. However, less than 1% of infections show clinical symptoms and the majority of infections remain undiagnosed. Patients can develop a symptoms ranging from a simple febrile headache to meningoencephalitis, with an overall case-fatality ratio of 5-15 %. The disease is generally milder in children than in adults, but in those children who do have disease, there is a high rate of encephalitis. The elderly are at highest risk for severe disease and death.

Japanese encephalitis (JE) caused by Japanese encephalitis virus (JEV), *Flaviviridae*, is one of the most important endemic encephalitides; it occurs mostly in Asia (50,000 patients annually). JE is also asymptomatic in most people; however symptomatic individuals have a high fatality rate (15,000 deaths annually) and half of the survivors have neurological sequelae (Misra & Kalita, 2010). The virus is maintained between waterbirds and *culicine* mosquitoes and transmitted to man by *Culex* mosquitoes, primarily *Cx. tritaeniorhynchus*.

Bunyaviruses

La Crosse (LAC) encephalitis is caused by La Crosse virus, *Bunyaviridae*. The virus was first isolated from the brain of a child who died of encephalitis in La Crosse County, USA (Thompson *et al.,* 1965). LAC virus is naturally cycled between the mosquito, *Aedes triseriatus*, and vertebrate hosts (commonly chipmunks and tree squirrels). The virus is maintained over the dry season by vertical transmission in mosquitoes (Watts *et al.*, 1975). There are about 75 cases reported in the United States per year on average since 1963. Most infections occur in children under 16 years of age. LAC encephalitis initially displays nonspecific symptoms such as fever, headache, nausea, vomiting and lethargy. Severe disease occurs most commonly in children under the age of 16 and is characterized by seizures, coma, paralysis, and a variety of neurological sequelae after recovery. Death from LAC encephalitis occurs in less than 1% of clinical cases.

Rift Valley fever (RVF) is an endemic disease in Eastern and Sub-Saharan Africa affecting domestic animals (sheep, buffalo, cattle, goats and camels) and humans. The disease is caused by RVF virus, a member of the genus *Phlebovirus* in the family *Bunyaviridae.* The virus is maintained in a natural cycle between livestock and insect vectors (*Aedes* mosquitoes and sandflies). The disease was first reported in 1900. Major outbreaks occurred in Kenya in 1950 (resulting in the death of 100,000 sheep), Egypt in 1977 and 1993 (both animals and humans) and Saudi Arabia and subsequently Yemen in 2000 (Abu-Elyazeed *et al.*, 1996; Ahmad, 2000; Davies, 1975; Meegan, 1979). The infection has a mortality rate of 10 - 30% in sheep, cattle and goats and is associated with abortion and almost 100% mortality in pregnant animals (Madani *et al.*, 2003). Infection in humans can occur through insect vectors or direct contact with infected animals. Infection in humans is usually asymptomatic but occasionally causes a mild febrile illness. However, a small number of patients (1%) develop fatal haemorrhagic fever, shock, encephalitis, liver necrosis and ocular complications. Approximately 1-10% of affected patients may suffer vision loss (Al-Hazmi *et al.*, 2003).

The mosquito *Aedes albopictus*: classification, geographical distribution life cycle and disease association

Classification and geographical distribution

Mosquitoes make up the family *Culicidae* in the order *Diptera*. At present, there are about 3,523 species of *Culicidae* classified in two subfamilies and 113 genera. The two subfamilies are *Anophelinae* and *Culicinae*. *Anophelinae* contains three genera and *Culicinae* contains 110 genera and two groups of *incertae sedis* (of uncertain taxonomic position, broader relationships are unknown or undefined). *Aedes* mosquitoes are one of the *incertae sedis* groups under subfamily *Culicinae* (Harbach, 2011; Reinert et al., 2005).

There are 12 species within the genus *Aedes. Ae. aegypti and Ae. albopictus* are well known for their adaptability, aggressiveness, blood feeding requirement and viral disease associations. *Ae. albopictus* is also known as the Asian tiger mosquito because of its origin and its black and white stripes (Figure 1.2). It is geographically distributed in warm and humid parts of the world and areas that have been urbanised including: China, Japan, Vietnam, Singapore, Indonesia, Indian Ocean Islands, the islands of La Réunion and Mauritius, Madagascar, south-eastern Brazil, Florida, and Puerto Rico. (Bagny *et al*., 2009; Braks *et al*., 2003; Chan *et al*, 1971; Cox *et al*, 2007; Delatte *et al*., 2008; Higa *et al*., 2010; Ishak *et al*., 1997). *Ae. albopictus* has also become established in European countries such as: France, Spain (2004), Italy (1990), Greece, Belgium, Montenegro, Albania, Bosnia and Herzegovina, Croatia, Israel, Montenegro, Serbia, Slovenia, Switzerland, The Netherlands and Germany (Delaunay *et al*., 2009; Eritja *et al*., 2005; Pluskota *et al*., 2008; Roiz *et al*., 2008; Romi, 2001; Samanidou-Voyadjoglou *et al*., 2005). In the United States, the species was first discovered in Florida in 1986 and it has rapidly become the most common mosquito throughout the US. *Ae. albopictus* is often introduced to European countries by the importation of used tyres which retain water during transportation. *Ae. Albopictus* is a competent vector for numerous arboviruses, and its geographical distribution has continuously expanded and even replacing *Ae. aegypti* in some parts of the world (Gould & Higgs, 2009; de Lamballerie *et al.*, 2008).

A

B

Figure 1.2: *Ae. albopictus*

A) An unfed female *Ae. albopictus*. B) A freshly fed *Ae. albopictus*. These pictures were taken by James Gathany, and are available at Centers for Disease Control and Prevention's Public Health Image Library (PHIL).

Mosquito life cycle

There are four stages to the mosquito life cycle: egg, larva, pupa and adult (Figure 1.3). In *Ae. aegypti* the key biological process to initiate egg production, vitellogenesis (synthesis of yolk protein precursors), is in an arrested state before a female mosquito takes a blood meal. The repression on yolk protein precursor genes (*YPPs*) is lifted once blood feeding has taken place (Attardo *et al*., 2003) . Male mosquitoes only feed on plant nectar, not requiring a blood meal. A female mosquito can lay several hundred fertilised eggs on the surface of water in treeholes, or other water-holding containers. Eggs can be clustered or dispersed depending on the species of the mosquito. Mosquito larvae hatch from the eggs within 24 hours. The larvae feed on algae, bacteria, and other micro-organisms. Domesticated larvae kept in an insectary can be fed on commercial chicken liver powder. The larvae take 7-14

days before moulting into pupae. Mosquito pupae spend 1-4 days transforming into adult mosquitoes (metamorphosis) and then leave the pupal case.

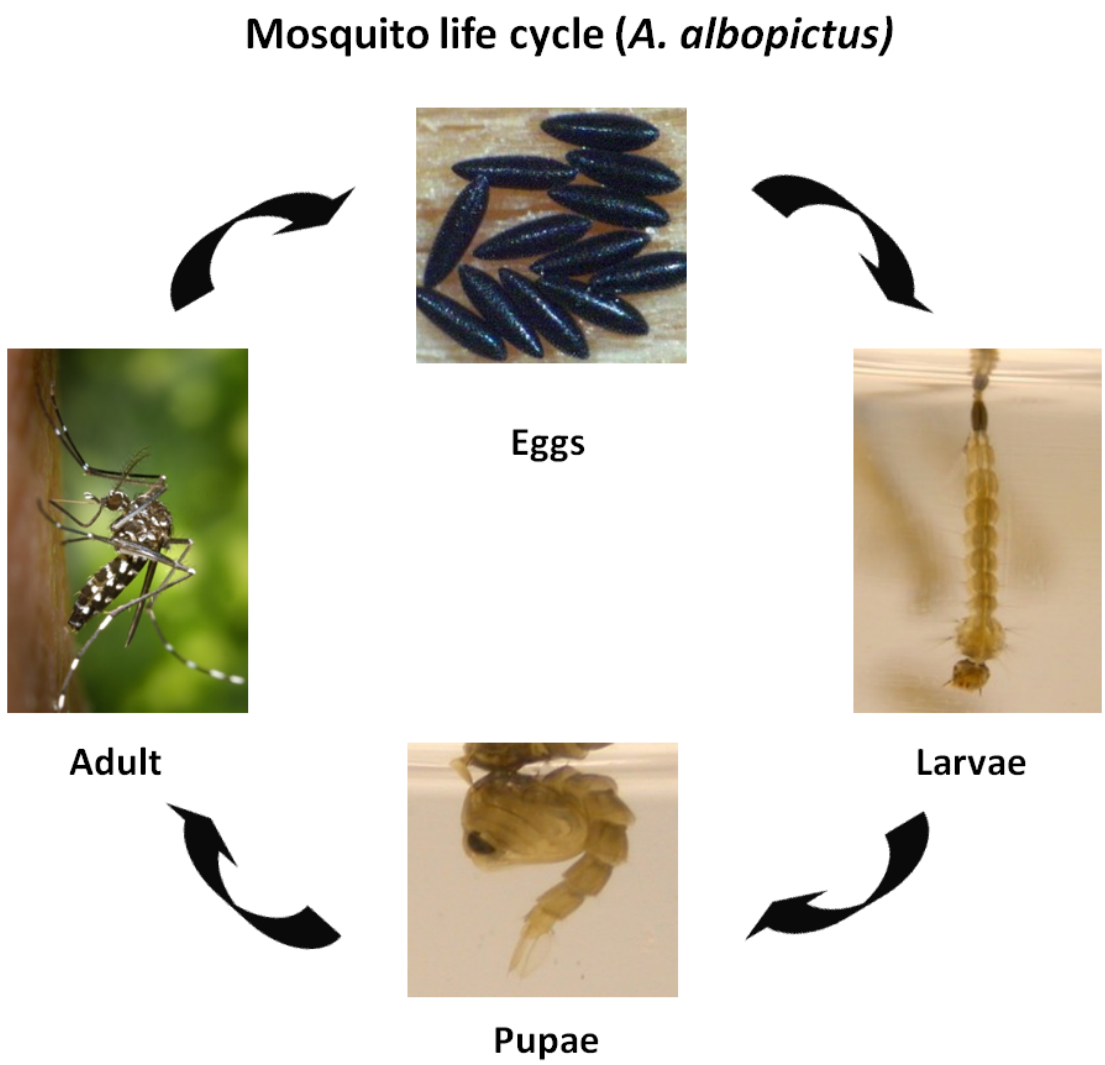

Figure 1.3: ***Ae. albopictus life cycle***

A female mosquito produces eggs after a blood meal has been taken (left). Several hundred eggs are laid on the surface of water in water-holding containers. *Ae. albopictus* eggs are black and dispersed (top), distinct from eggs of *Culex spp*. which form an egg raft. Larvae of mosquitoes (right) live in water and have four developmental stages, 1st, 2nd, 3rd and 4th instars. During this stage they actively feed and grow larger. It takes up to a week for the larvae to be fully developed and moult into the pupal stage (bottom). Feeding does not take place during the pupal stage. The pupa remains in the water for no more than a few days until the adult emerges from the pupal case on the surface of the water.

Disease associations

The disease association and the vector competence of a mosquito are often established by the following observations. i) isolation of infectious virus from wild-caught mosquito samples, ii) infection of the mosquito by feeding on a viraemic host, iii) virus transmission by subsequent bites, iv) association of infected mosquito with confirmed cases in an epidemic region.

Ae. albopictus is a vector of dengue viruses in Asia. In the United States, at least six arboviruses including WNV, EEEV, Keystone virus, Tensaw virus, Cache Valley virus, and Potosi virus have been isolated from this species. Of these six viruses, West Nile virus, Eastern equine encephalitis virus and Cache Valley viruses are known to cause disease in humans. As mentioned above, *Ae. albopictus* was responsible for the outbreak of Chikungunya in the French Indian Ocean islands in 2005 (Schaffner, 2000) and in Italy in 2007 (Romi *et al*., 1999). The feeding patterns of *Ae. albopictus* (acquire blood exclusively from human hosts) makes this species of major importance in the amplification and transmission of infectious viruses to humans.

Alphaviruses: classification, geographical distribution, morphology and replication cycle

Classification and geographical distribution

Alphaviruses belong to the *Togaviridae* family. Viruses in the *Togaviridae* family are enveloped positive-strand RNA viruses. In Latin, toga means cloak, indicating that viruses in this family are enveloped. *Alphavirus* and *Rubivirus* are the two genera in the *Togaviridae* family. This family was originally much larger and included flaviviruses, pestiviruses and some other viruses that had not been well characterised. They were originally grouped together by their size, the characteristics of their genome (single stranded non-segmented RNA), the ability of their RNA to be infectious and their transmission strategy via mosquito vectors. With the advance

in knowledge of virus genome structure and replication strategies, the *Flaviviridae* family was established apart from the *Togaviridae* family. The *Alphavirus* genus consists of 28 different members. Rubella virus is the only member of the genus *Rubivirus* (Strauss & Strauss, 1994). Alphaviruses are classified into seven distinct antigenic complexes based on the sequences of their E1 envelope glycoproteins. The complexes are VEE complex, WEE complex, Semliki Forest complex, Sindbis-like virus complex (SIN), Middelburg complex (MID), Barmah Forest complex (BF), and Ndumu complex (NDU) (Powers *et al*., 2001) . Members of the *Alphavirus* genus are globally distributed. Viruses from the VEE and EEE groups are found in America, Brazil and Peru. Sindbis virus and its group members are distributed in Africa, Asia, Europe, Australia, Brazil and the USSR. The SFV group viruses are distributed mainly in Africa and Australia.

Morphology

Alphaviruses contain a single positive strand of RNA which contains two open reading frames (ORFs) encoding nine functional proteins. The viral genome, 11-13 kb, is surrounded by an icosahedral capsid (T=4 symmetry) composed of 240 copies of a single capsid protein. The capsid is then enveloped in a lipid membrane derived from the infected host cell. Alphaviruses have two or three glycoproteins E1, E2 and E3 (species dependent) that associate to form a single spike, each virion contains 80 spikes. The C-terminus of the glycoprotein E2 is attached to the capsid and its membrane spanning domain anchors on the envelope membrane forcing the envelope to surround tightly and take on the shape of the capsid. The E1 protein is essential for membrane fusion between the viral envelope and the target membrane (Knipe, 1996).

Replication cycle of alphaviruses

Alphaviruses infect host cells via receptor-mediated endocytosis. Virus particles attach to the host cell surface receptor through the receptor-binding domain of the E2 glycoprotein (Strauss & Strauss, 1994). The host receptor involved in viral attachment remains unclear. One study reports that SFV has affinity for major histocompatibility antigen of humans (HLA-A and –B) and mice (H2-K and D)

(Helenius *et al.*, 1980, 1978), though this has never been confirmed. Sindbis virus attaches to cells via laminin and heparin sulphate receptors (Klimstra *et al*., 1998; Wang *et al*., 1992).

Following endocytosis, the endocytosed vesicle fuses with an endosome and then a lysosome. The acidic environment of the lysosome induces a low-pH-dependent conformational change in the glycoprotein spike complex which facilitates membrane fusion between the virus envelope and the lysosome membrane to allow the release of the nucleocapsid into the cytoplasm (Kielian, 1995). It has been proposed that passing through the acidic endosome destabilises the nucleocapsid, and reveals ribosomal binding sites on the capsid (Singh & Helenius, 1992). Ribosomes bind to the capsid resulting in release of viral RNA into the cytoplasm (Wengler, 1984, 1987).

The naked alphavirus genome is a single positive-strand of RNA with two ORFs (11.7 kb for SINV and 11.5kb for SFV). The viral genome has the features of a mature messenger RNA found in eukaryotes, containing a 5' terminal cap and a 3' terminal poly-A tail, and it encodes nine functional proteins. The 5' two thirds of the genome encodes four non-structural proteins (nsP 1, 2, 3 and 4). The four nsPs are translated as one or two large polyproteins (some viruses have an opal termination codon after nsP3 which can be read through). The nsPs are the components for viral replication. The 3' one-third of the genome encodes for the viral structural proteins, capsid, p62(E3+E2), 6K and E1, under the control of a subgenomic 26S promoter. These polyproteins are essential to make new virus particles and they are co- or post-translationally processed into individual proteins (Strauss & Strauss, 1994).

After the viral RNA genome has been released into the cytosol, it serves directly as mRNA resulting in the synthesis of a polyprotein containing nsP1 to nsP3 or nsP1 to nsP4 known as P123 or P1234 respectively. The polyprotein is processed into individual mature proteins by the catalytic activity of the C-terminal domain of nsP2, which is a papain-like protease domain (Vasiljeva *et al*., 2001). The processing of the non-structural polyprotein is highly regulated to promote different stages of the viral replication process. In SFV, the first cleavage takes place between nsP3 and nsP4 *in trans*, resulting in the release of nsP4 and formation of the early replication

complex (nsP123 and nsP4). This early replication complex is essential for synthesising the negative-strand RNA from the positive viral genome (Vasiljeva *et al*., 2003). There is a lag period following each cleavage event and the next cleavage is between nsP1 and nsP2 *in cis*, then between nsP2 and nsP3 *in trans* (Figure 1.4A). Once nsP1 is processed from the polyprotein or nsP2 is separated from nsP3, the early replication complex loses its ability for making negative strand.

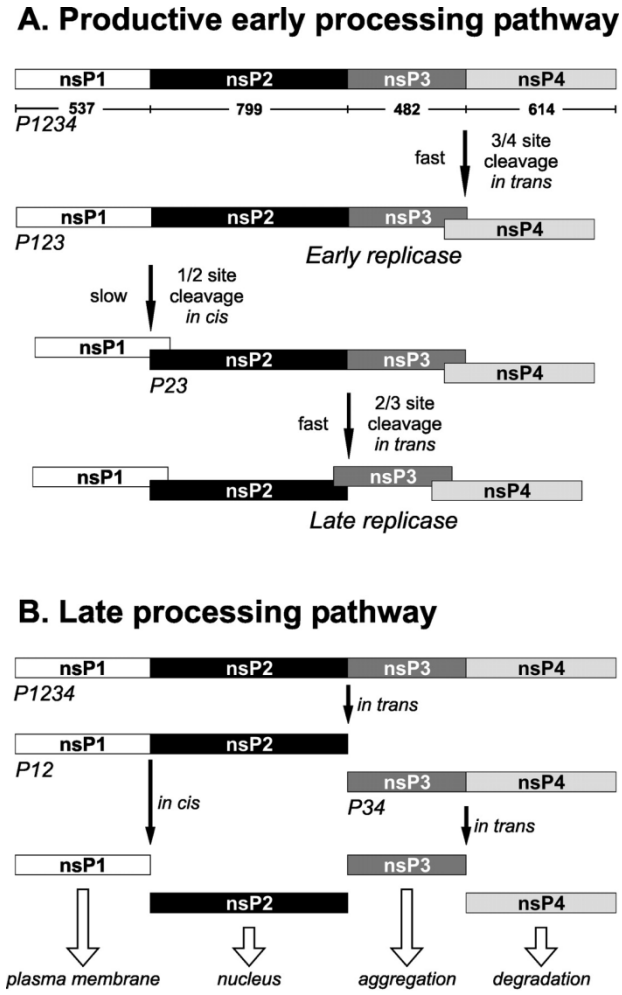

Figure 1.4: Early and late processing pathways of SFV P1234. (A) processing pathway during early infection produces a functional replication complex. This is essential for the production of the genome complimentary RNA. (B) processing pathway during late infection which inhibits the formation of new replication complexes and synthesis of minus-strand. RNA Figure adapted from Vasiljeva *et al*, 2003 with permission.

The four processed nsPs form the mature replication complex which synthesises full-length 42S genome (positive strand RNA) and 26S sub-genomic RNAs. The transcription of positive strand RNA can either start at the 3' end so that the complete strand is transcribed or it can start at a subgenomic promoter located at the 3' of the structural protein genes. The mature replication complexes are anchored to membranous structures of endosomal and lysosomal origin known as cytoplasmic vacuoles (CPVs). On the external surface of CPVs are numerous invaginations called

spherules. The synthesis of viral RNA takes place in these spherules. At a late stage of infection, due to abundant processed nsPs in the cytosol, newly produced non-structural polyproteins (nsP1-4) are being cleaved *in trans* between nsP2 and nsP3. This inhibits the formation of early replication complexes (nsP1-3+4) and the synthesis of negative-strand RNA (Figure 1.4B).

Translation of the sub genomic RNA leads to the production of the structural polyprotein NH_2-capsid-p62(E3+E2)-6K-E1-COOH. The capsid protein has autoprotease activity and it cleaves itself from the polyprotein. The remaining polyprotein is then translocated to the endoplasmic reticulum (ER) by a signal sequence located on the p62 protein. Another signal sequence on the 6K protein leads to the translocation of E1 to the ER lumen. p62 and E1 are transmembrane proteins which are released from the polyprotein by signal peptidase and transported from the ER through the Golgi apparatus to the cell surface. During the transportation through the secretory pathway, p62, E3 and E2 are cleaved and modified (Melancon & Garoff, 1987). These processed glycoproteins are then anchored into the cell membrane while the viral genome is being packaged by capsid proteins.

Virus particle assembly starts from the encapsidation of the genomic RNA. The capsid protein binds and encapsulates the genomic RNA from a packaging sequence in nsP2 for SFV and nsP1 for SINV (Frolova *et al*., 1997). Then the nucleocapsid interacts with the cytoplasmic tail of transmembrane E2 spike proteins. New virus particles are released via budding mediated by structural protein 6K (Loewy *et al*., 1995). The exact mechanism remains unclear, but 6K-deficient SFV does not form new virus particles.

Dissemination of alphaviruses in mosquitoes

To begin the alphavirus life cycle in a mosquito, a haematophagous mosquito has to ingest viraemic blood from a vertebrate host. Once the viraemic blood has reached the mosquito midgut, the virus must establish a productive infection in midgut epithelial cells by overcoming the midgut infection barrier (Bosio *et al.*, 2000). Following the replication in midgut epithelium, the virus progeny exits the infected

cell either by budding or through apoptotic cell death. The virus must pass through a midgut escape barrier before it infects secondary tissue such as muscle surrounding the alimentary tract, the fat body, haemocytes, nerve tissue, and finally the salivary glands (Myles *et al*., 2004). The virus is then shed into the ducts of the salivary gland. Once the virus enters the saliva, the virus has completed its extrinsic incubation and the mosquito can transmit the virus to a new host through a subsequent bite. The molecular and cellular biology of alphavirus replication in mosquito cells have not been studied in detail but are generally presumed to be similar to the well-described process in mammals.

Pathogenesis of Semliki Forest virus (SFV)

SFV is an alphavirus naturally found in sub-Saharan Africa and it was first isolated in Uganda in 1942 from the mosquito *Aedes abnormalis* (Smithburn & Haddow, 1944). However, it is spread predominately by *Aedes africanus* and *Ae. aegypti* mosquitoes. SFV infections have been repoted in horses, monkeys and human (Mathiot *et al.*, 1990; Robin *et al.*, 1974). There is only one reported case of human death from infection with SFV; a scientist who was working with the Osterrieth strain of SFV (Willems *et al.*, 1979). An outbreak of SFV was reported in Central African Republic in 1987, with 22 isolations of SFV made from serum samples collected from 22 paitients presenting with fever, severe persistent headache, myalgia (muscle pain), and arthralgia (Mathiot *et al.*, 1990).

There are various strains of SFV including the strain L10, V13, Osterrieth, A8, A7, A7(74), SFV4 (molecular clone of prototype), and MRS MP 192/7. Four of these strains, L10, prototype, A7 and A7(74) have been studied most extensively. The strains L10 and prototype are virulent in adult mice and A7 and A7(74) are avirulent in adult mice. Whether they are virulent or avirulent, all strains of SFV are neuroinvasive and virulent in neonatal mice (Bradish *et al.*, 1971; Fazakerley *et al.*, 2002; Glasgow *et al.*, 1991; Smithburn & Haddow, 1944). The strains that have been cloned and sequenced are prototype, SFV4, L10, and Viet Nam strains (Garoff *et al.*, 1980; Glasgow *et al.*, 1994; Santagati *et al.*, 1995, 1998; Takkinen, 1986; Tan *et al.*, 2008; Tarbatt *et al.*, 1997).

The cell lines which are commonly used to study SFV infection are Chicken embryo fibroblasts (CEF) and baby hamster kidney (BHK) cells. SFV also infects experimental animals including mice, rats, rabbits and guinea pigs (Bradish *et al.*, 1971). Following intraperitoneal (IP) inoculation into adult mice, SFV replicates in the muscles, including skeletal, smooth, and cardiac muscle (Amor *et al.*, 1996; Fazakerley, 2002). A high titre transient plasma viraemia is produced within 24 hours. In neonatal mice, the A7(74) and L10 strains of SFV are virulent. However, in 3- to 4- week-old mice only L10 strain is virulent. The distribution of viral RNA in the brain shows the virus first apparent as small foci of infected cells around cerebral capillaries (Fazakerley *et al.*, 1993). Once in the CNS, the SFV infects neurons and oligodendrocytes but not astrocytes. In both neonatal and 3- to 4- week-old mice infected with L10 or neonatal mice infected with A7(74), the infection spreads rapidly from the original foci to infect large areas throughout the brain resulting in pycnosis and death (Oliver & Fazakerley, 1998). In contrast, 3- to 4- week-old mice infected with A7(74) virus showed little spread in the brain from the original perivascular foci. The same pattern of A7(74) infection is observed in 3- to 4- week-old *nu/nu* mice (mice that make immunoglobulin (Ig) M antibodies but cannot class-switch to produce IgG antibodies and have no T cells) and mice with severe immunodeficiency, indicating that failure to spread is an age-related virulence characteristic of the avirulent SFV strains (Fazakerley *et al.*, 1993). This age related virulence of avirulent SFV strains is related to the maturation of the CNS. Upon completion of the CNS maturation, there is a decrease in susceptibility to virus infections. The decrease in susceptibility may be linked to shutdown of metabolic processes required by the virus, e.g. production and transport of smooth membrane vesicles (Oliver *et al.*, 1997) or to up-regulation of inhibitory processes, e.g. anti-apoptotic genes (Scallan *et al.*, 1997). It is believed that virulent strains induce death because of their ability to replicate productively and destroy a large number of mature neurons before intervention of immune responses.

Apart from causing CNS disease, another interesting property of some SFV strains, e.g. A7, is their ability to cross the mouse placenta which can either lead to abortions or have a teratogenetic effect in developing foetuses (skeletal, skin, and neural tube defects)(Atkins *et al.*, 1982).

Alphavirus reverse genetics

Alphaviruses are positive strand RNA viruses and the genomic RNA can directly be translated to produce the proteins required for its own replication and to produce new virus particles, the genomic RNA is therefore considered to be infectious. This RNA can be generated by capped *in vitro* transcription from a cDNA plasmid. If this plasmid contains the full length virus genome, it is generally refereed to as an infectious cDNA (icDNA). The virus genome can be reverse engineered by changing the sequence of the icDNA plasmid by standard molecular biology techniques. This can include deletions, insertions and point mutations. In addition, there are replicon systems available which are cDNA plasmids containing the sequence for the virus non-structural genes, or replicase; capped in vitro transcription of this gives rise to an RNA which within cells produces the virus non-structural proteins and replicates this RNA. This RNA can be packaged into virus replicon particles (VRP) by virus structural proteins encoded *in trans* on a separate RNA species. The icDNA clones of several alphaviruses, including SFV, SINV, VEEV and CHIKV have been developed (Caley *et al.*, 1999; Davis *et al.*, 1989; Hahn *et al.*, 1992; Liljeström & Garoff, 1991; Rice *et al.*, 1987; Vanlandingham, Dana L Tsetsarkin *et al.*, 2005; Vähä-Koskela *et al.*, 2003)

Alphavirus systems have been used by many laboratories to express foreign proteins. One strategy to construct a replication-competent alphavirus vector is to insert the foreign gene of interest under the control of a duplicated subgenomic promoter. this results in high levels of transcripts for the foreign gene. The duplicated subgenomic promoter and foreign gene can be inserted either into the short non-translated region between the replicase and the structural ORF, or into the 3’ non-translated region of the genome. Figure 1.5 shows examples of the possible ways to insert a second subgenomic promoter and a foreign gene.

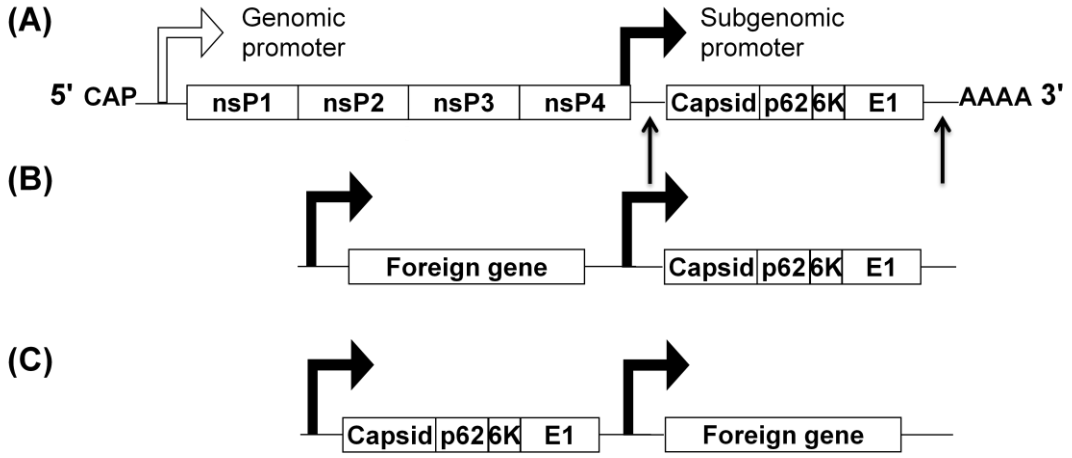

Figure 1.5: Schematic representation of alphavirus replication-competent vectors

(A) Schematic representation of the alphaviral genome. **(B)** Insertion of a second 26S promoter and a foreign gene of interest at the 5' end of the structural polyprotein. **(C)** Insertion of a second 26S promoter and a foreign gene of interest at the 3' end of the structural polyprotein

Most studies suggested that expression is stronger if the foreign gene is inserted with the subgenomic promoter at the 3'of the structural ORF. Examples of stronger expression through insertion at the 3' end of the structural ORF include expression of immunogenic proteins of Japanese encephalitis virus (JEV) under duplicated subgenomic vectors in SINV, expression of MA/CA domain of HIV gag protein in a VEEV vector, and expression of eGFP in CHIKV vectors (Caley *et al.*, 1999; Pierro *et al.*, 2003; Pugachev *et al.*, 1995; Vanlandingham *et al.*, 2005). These authors have also shown that the strategy of inserting the second subgenomic promoter and the foreign gene at the 5' of the structural ORF remains useful because it provides greater genetic stability compared to vectors carrying an insert at the 3' of the subgenomic ORF.

Recombination between the duplicated subgenomic promoter sequences is thought to be the main mechanism that causes genetic instability in these vector constructs. The main factors that influence the genetic instability are the length and the nature of the transgene. For example, vector viruses expressing a 3-4 kb long foreign sequence are less stable than constructs carrying a 1-2 kb shorter sequence, and natural selection favours the virus that eliminates the inserted sequence and is capable of replicating faster (Caley *et al.*, 1999; Chen *et al.*, 1995). Constructs with a duplicated subgenomic promoter are often used to express foreign marker genes that do not

provide any selective advantage to the virus; examples include influenza haemagglutinin, bcl-2, eGFP, luciferase, and antisense RNAs (Fragkoudis *et al.*, 2008, 2009; Hahn *et al.*, 1992; Johnson *et al.*, 1999; Levine, 1996). These vector viruses exhibit high levels of genetic instability because inserted sequences are incorporated as separate transcription units which can be eliminated easily to gain advantage in replication (Thomas *et al.*, 2003; Vähä-Koskela *et al.*, 2003).

As an alternative to duplicating the subgenomic promoter for transgene expression in alphavirus vectors, the gene of interest can be fused with one of the viral replicase sequences (Figure 1.6A). By fusing the transgene with the replicase gene, recombinant SINV and SFV expressing eGFP or luciferase in fusion with nsP2 or nsP3 have been produced (Atasheva *et al.*, 2007; Fragkoudis *et al.*, 2008; Frolova *et al.*, 2006; Tamberg *et al.*, 2007). However, in this approach, the transgene expression is driven by the genomic promoter. This limits the expression of the transgene to early infection. Another alternative is to insert the gene of interest followed by the 2A sequence from foot-and-month disease virus (FMDV) into the structural ORF as a cleavable component (Figure 1.6B). This utilises the autocatalytic activity of the capsid protein at the 5' end of the foreign protein and the autoprotease activity of the 2A peptide to release the transgene (Donnelly *et al.*, 2001; Fragkoudis *et al.*, 2008; Thomas *et al.*, 2003). Both of these approaches improve genetic stability when compared to duplicated subgenomic constructs.

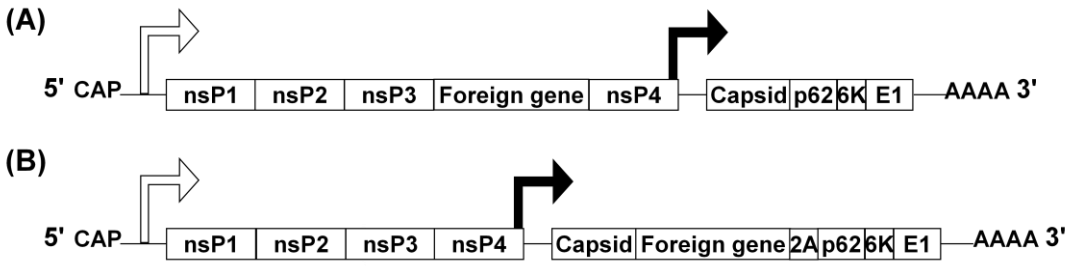

Figure 1.6: Schematic representation of "fusion" alphavirus replication-competent vectors

(A) Insertion of a foreign gene fused at the 3'-end of the nsP3 protein **(B)** Insertion of a foreign gene followed by a 2A sequence between the capsid and the p62 sequence.

All of the above icDNA constructs share a common problem when amplified in *Escherichia coli* cells. It appears that *E. coli* cells transformed with the SFV icDNA

constructs grow poorly. It is believed that in the nsP2 sequence of SFV, there are cryptic promoters active in *E. coli* cells. These promoters drive the expression of viral structural proteins and these are toxic for the bacterial cells (Prof. Andres Mertis, personal communication). This problem is reduced by using low-copy number plasmids for icDNA constructs to limit the toxicity in *E.coli* cells (Petrakova *et al.*, 2005)

Propagation-deficient vectors provide a high level of biosafety and are preferred for clinical use (i.e. vaccination and gene therapy) and experiments that require a non-propagating virus particle for a single round of infection. This is achieved by removing the subgenomic sequences to generate a replicon RNA. If required, a foreign gene of interest placed under the control of the subgenomic promoter can be inserted. Figure 1.7 shows examples of the propagative-deficient alphavirus vector system

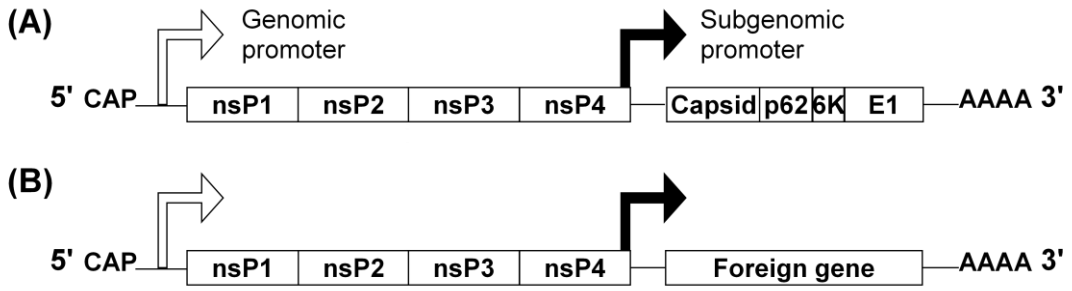

Figure 1.7: Schematic representation of alphavirus propagative-deficient vector

(A) Schematic representation of the alphaviral genome. **(B)** In the propagative-deficient alphavirus vector the subgenomic sequence is replaced by a foreign gene and placed under the control of a subgenomic promoter.

There are three different strategies to insert the propagative-deficient vector to the inside of a cell. The first strategy is to synthesise suicidal viral particles known as virus replicon particles (VRPs). VRPs are capable of only one round of replication. To synthesise VRPs, the structural genes are provided *in trans* either as separate RNA messages (helper) or in packaging cell lines (Karlsson & Liljeström, 2003; Polo *et al.*, 1999). In the early studies, the structural genes were provided as a single helper RNA transcript. This allowed recombination between the replicon and the

helper RNA to take place easily and led to the production of infectious virus (Berglund *et al.*, 1993). Therefore, to overcome this problem a split-helper system was developed where structural genes were provided as two separate RNA transcripts and a mutation was introduced in the structural genes. In the split-helper system, the capsid and glycoproteins are separated into two different RNA transcripts and are expressed separately (Fayzulin *et al.*, 2005; Smerdou & Liljeström, 1999). The production of VRPs by the split-helper system is shown in Figure 1.8.

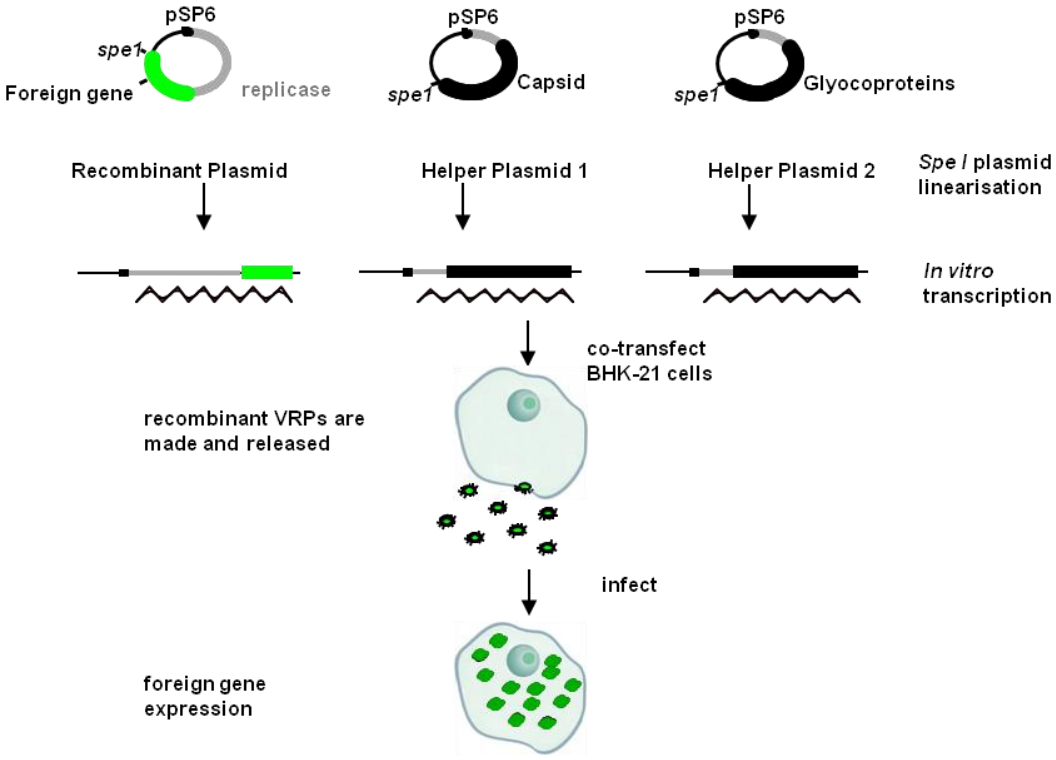

Figure 1.8: Schematic representation of production of VRPs by split-helper system.

The recombinant plasmid is coding for the replicase genes with the foreign gene of interest under the control of a subgenomic promoter. The two helper plasmids are coding for the capsid and glycoprotein genes. The three plasmids are linearised using *Spe I* followed by *in vitro* transcription. Three RNA transcripts are used to co-transfect BHK-21 cells. Recombinant VRPs are made and released. The released VRPs can be puriflied and used to infect cells to produce transient expression of foreign gene (see also Material and Methods).

The second approach involves converting the replicase genes followed by a foreign gene (placed under the control of subgenomic promoter) into DNA and cloning them into a DNA plasmid placed under the control of a eukaryotic promoter derived from the CMV – IE (cytomegalovirus immediate-early) promoter. This DNA plasmid is

then directly transfected or electroporated into cells and this system is known as a layered DNA/RNA vector. This method is less time-consuming and more cost-effective because *in vitro* transcription is not required (Berglund *et al.*, 1998; Dubensky Jr *et al.*, 1996). The third approach involves transfection or electroporation of *in vitro* transcribed RNA encoding the replicase followed by the gene of interest (Karlsson & Liljeström, 2003). The disadvantage of the second and third approaches is that it is often difficult to achieve high transfection efficiency and electroporation is often damaging to cells. Nevertheless, all the approaches have been proven to be efficient to express transgenes up to 5 kb at high levels for up to seven days (Morris-Downes *et al.*, 2001).

Innate immunity in mammals

Toll-Like Receptors (TLR)

Toll-like receptors (TLRs) are a family of type I transmembrane receptor proteins responsible for the detection of infections. These receptors are characterised by an extracellular leucine-rich repeat (LRR) domain and an intracellular Toll/IL-1R (TIR) domain. The first member of this family, Toll, was first identified in *Drosophila* in 1988 during a screening of genes responsible for embryonic polarity (Hashimoto *et al*., 1988). Five human Tolls were then discovered by Rock and co-workers and termed "Toll-like receptors" (TLR) (Rock *et al*., 1998). TLRs recognise different types of conserved pathogen associated molecular patterns (PAMPs). Activation of TLRs through the detection of specific PAMPs leads to activation of NFκB and phosphorylation of interferon regulatory factor (IRF) -3 and -7 (Fitzgerald *et al.*, 2003). Characterised PAMPs include bacterial cell wall components such as lipopolysaccharide (LPS), peptidoglycan (PGN), lipoteichoic acid (LTA), and lipoarabinomannan (LAM). Viral-related PAMPs recognised by TLRs include: cytosine-phosphate-guanine (CpG) motifs on pathogen DNA by TLR 9, single-stranded RNA (ssRNA) rich in guanine and uridine by TLRs 7 and 8 and double-stranded RNA (dsRNA) by TLR 3 (Alexopoulou, 2001; Bauer *et al*., 2001; Diebold *et al*., 2004; Lund *et al*., 2004). To date at least 11 TLRs have been identified in

humans and 13 in mice. The localisation of TLR is dependent on both the type of TLRs and the cell type. For example, TLR3 localises to the cell surface in human lung fibroblast cells and to intracellular vesicles such as phagosomes and endosomes in human monocyte-derived dentritic cells (Johnsen *et al*., 2006; Matsumoto *et al*., 2002); TLR 7 and 9 localise to endosomes (Nishiya *et al*., 2005).

Toll immune pathways

In mammals, TLR signalling involves the binding of the receptor to a selection of downstream adaptor proteins. These adaptor proteins include myeloid differentiation-88 (MyD88), TIR domain containing adaptor protein (TIRAP), Toll/IL-1R domain containing adaptor inducing IFN-β (TRIF), TRIF-related adaptor molecule (TRAM) and sterile α motif (SAM) and Armadillo repeat motif (ARM)-containing protein (SARM). Upon binding of ligand to the TLR, MyD88 mediates the association of a serine/threonine kinase called interleukin-receptor associated kinase-4 (IRAK-4) to the receptor complex. IRAK-4 recruits and phosphorylates IRAK-1 and IRAK-2. TNF receptor associated factor-6 (TRAF6) is then activated by IRAK-1, allowing translocation and interaction with membrane-bound TGF-β activated kinase (TAK1) and TAK-1 binding proteins (TAB) complex. TRAF6 and TAK-1 undergo polyubiquitination and TAK1 and TAB-2 undergo phosphorylation allowing the complex to translocate from membrane to cytosol, and the degradation of IRAK-1. Activated TAK-1 phosphorylates downstream targets such as IκB kinases (IKKs). The activated IKK complex phosphorylates and induces degradation of IκB which leads to activation of nuclear factor-κB (NF-κB). Activated NF-κB can freely translocate to the nucleus and promotes transcription of proinflammatory cytokines, such as TNFα, IL-1, and IL-2. The MyD88 pathway is utilised by TLR 7, 8 and 9 (Takeuchi & Akira, 2007). However, TLR 3 associated with the endosomes utilises a MyD88-independent pathway with different adaptor proteins, TRIF and TRAM. Through interaction with TRIF and TRAM, IKKs, IKKε and TANK-binding kinase-1 (TBK1) mediate activation of IRF3 to induce IFNβ promoter (Doyle *et al*., 2002; Kawai *et al*., 2001). Alternatively, TRIF can directly recruit and activate TRAF6, this

leads to the formation of the TAK1-TAB2 complex which activates the IKK complex which then activates NF-κB.

The c-Jun N-terminal kinases (JNKs) signal transduction pathways

The JNKs are an evolutionarily conserved sub-group of mitogen-activated protein (MAP) kinases (MAPK). Other sub-groups of MAPKs include extracellular signal-regulated protein kinases (ERK) and the p38 MAP kinases. In mammals, JNK is activated in response to inflammatory cytokines (e.g. interleukin-1, lymphotoxin-β, tumor necrosis factor, and transforming growth factor-β), activation of TLRs (TLR-3, TLR-4 and TLR-9) or exposure to environmental stress. JNKs are phosphorylated/activated by upstream MAPK kinases (MKKs), MKK4 and MKK7. MKKs are in turn phosphorylated/activated by upstream MAP kinase kinase kinases (MAPKKK). MAPKKKs respond to diverse stimuli, examples include: Ras or Rho family GTPase, ubiquitination by IL-1 receptor signalling complex for TAK1, phosphorylation by PAK, GCK and HPK. It is well-established that JNK is related to apoptotic cell death. It appears to promote ubiquitination of the caspase-8 inhibitor cFLIP. JNK also phosphorylates H2AX, a DNA damage repairing protein which may be responsible for DNA fragmentation. The use of JNK knock-out primary fibroblast cells shows that JNKs are responsible for the downstream release of pro-apoptotic protein from mitochodria in stress-induced apoptosis. Another important role of MAPKs is regulation of T cell development, activation and differentiation. However, the contribution of the JNK signalling pathway to these processes has not been resolved (Rincón et al., 2001).

Retinoic acid-inducible gene-I and melanoma differentiation-associated gene 5

Retinoic acid-inducible gene-I (RIG-I), melanoma differentiation-associated gene 5 (MDA5) and laboratory of genetics and physiology-2 (LGP-2) are protein receptors within the RIG-I like receptors (RLRs) family. These proteins are present in the cytoplasm and characterised by containing a DExD/H-box RNA helicase domain. In addition to the DExD/H-box RNA helicase domain, RIG-I and MDA5 have two N-

terminal caspase activation and recruitment domains (CARDs). A CARD domain is also present on the mitochondrial adaptor protein MAVS, also known as Cardif, IPS-1 or VISA. In the present of viral RNA ligand, RIG-I interacts with MAVS through CARD-CARD interaction. MAVS then activates downstream signalling leading to the activation of transcription factors such as IRF-3, IRF-7 and NF-κB (Yoneyama & Fujita, 2009). Therefore, RIG-I and MDA5 are key mediators of antiviral immunity responsible for detection of infection by RNA viruses and induction of interferons. The natural RIG-I ligands include: virus genome containing 5'-PPP groups (Figure 1.9), such as genomes from flu and rabies viruses (Hornung *et al.*, 2006; Pichlmair *et al.*, 2006; Plumet *et al.*, 2007); non-genomic viral transcripts or replication intermediates and RNA derived from host cells that is cleaved by RNase L (Malathi *et al*., 2007; Samanta *et al*., 2006). On the other hand, the natural MDA5 ligands are less well defined. MDA5 recognises polyinosine-polycytidylic acid (poly(I:C)) and high levels of dsRNA during viral infection but also mixed structures of single and double stranded RNA (Kato *et al.*, 2006; Pichlmair *et al.*, 2009). Nevertheless, RIG-I and MDA5 have different roles in the recognition of RNA viruses (Kato *et al.*, 2006).

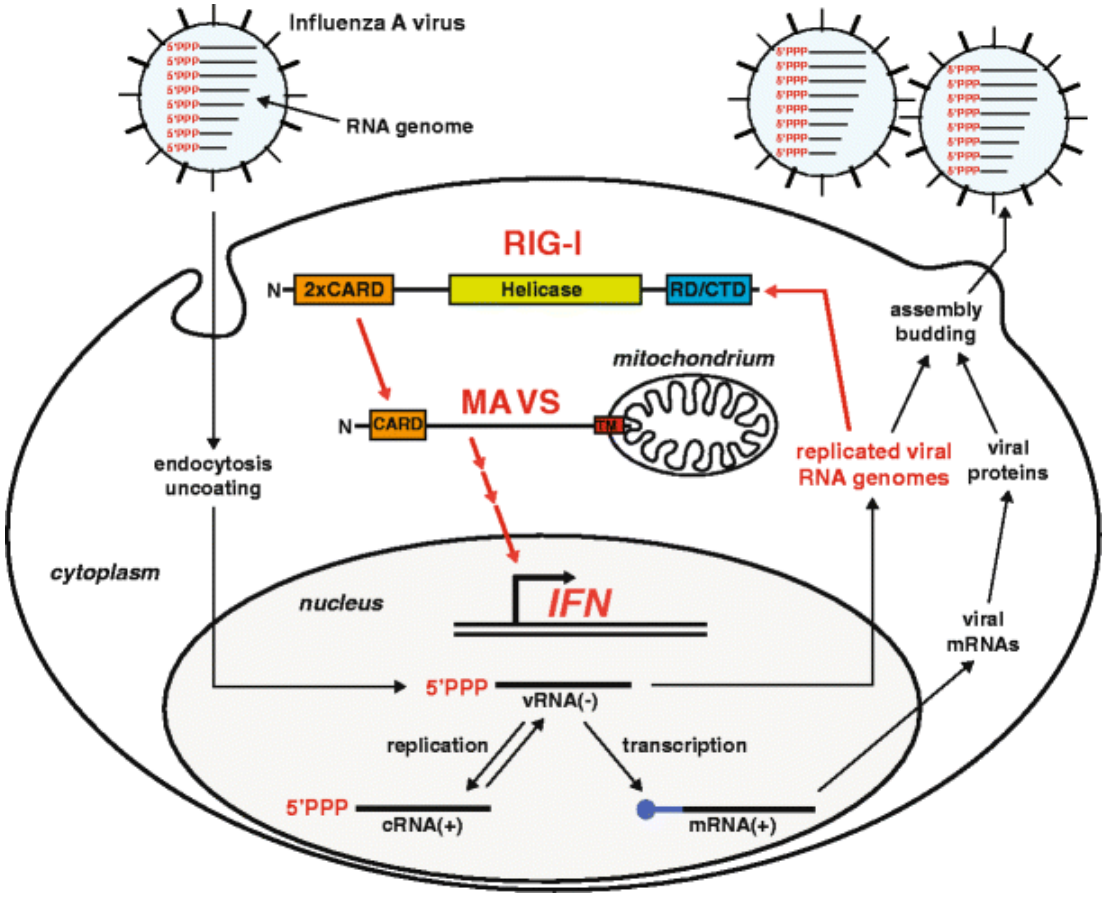

Figure 1.9: Illustration of dsRNA detection by RIG-I and the downstream signalling pathway.

This is a diagram of the flu virus life cycle and the detection of viral RNA molecules carrying 5'-PPP groups by a cell. Viral RNA molecules containing 5'-PPP groups are detected by RIG-I. Activated RIG-I signals MAVS via the CARD domain. NF-κB and IRF-3 are activated in turn and induce transcription of antiviral genes. RD/CTD (repressive domain/C-terminal domain); TM (transmembrane domain). Figure adapted from Rehwinkel, 2010 with permission.

Protein Kinase R

Protein kinase R (PKR) is an interferon induced enzyme which is activated by double-stranded RNA or PKR-activating protein (PACT). PKR is a 65-KDa protein first discovered in mouse L cells by treatment of sepharose bound Poly (I:C). The protein was isolated by chromatography on columns of Poly I:C-Sepharose (HOVANESSIAN & KERR, 1979). PKR consists of a dsRNA binding domain located at the N-terminal and a kinase domain and PACT binding motif at the C-

terminal. The protein is constitutively expressed at a low level in cells and expression is enhanced when the cell is exposed to IFN-α/β or virus infection. PKR remains inactive until it binds with specific activators such as dsRNA, e.g. dsRNA from viral replication intermediates. Activated PKR becomes auto-phosphorylated and in turn phosphorylates the eukaryotic transcription initiation factor 2α (eIF2α) which modulates translation in cells (Li *et al*., 2006). Phosphorylation of eIF2 impedes recycling of eIF2 to its active guanosine triphosphate (GTP) bound form, which leads to a global reduction in the levels of eIF2-GTP-transfer (t)RNA^{Met}. eIF2-GTP-transfer (t)RNA^{Met} is required for loading the initiator methionine onto the 48S preinitiation complex to begin translation (Wek *et al*., 2006).

In mammals SFV infection highly activates PKR, leading to almost complete phosphorylation of eIF2α and subsequent translational shut down (Barry *et al.*, 2009; Ventoso *et al.*, 2006). This shut-off affects host protein synthesis and the production of viral non-structural proteins but not structural protein (McInerney *et al*., 2005). Structural protein escapes translational shut-down and is translated efficiently in the presence of eIF2α phosphorylation due to a hairpin loop structure located downstream of the AUG initiator codon at the 5' end of the subgenomic RNA. This loop structure stalls the ribosomes on the correct site to initiate translation on subgenomic mRNA (26s), bypassing the requirement for eIF2α (Ventoso *et al.*, 2006). PKR also activates the transcription factor NF-κB by phosphorylation of its inhibitor, IκB, for targeted polyubiquitination and subsequent degradation by proteosomes (Kumar *et al*., 1994). This allows NF-κB to bind on promoters of pro-inflammatory genes such as IFN and promote transcription. In some viral infections, PKR has been shown to be an essential defence mechanism. For instance, mice lacking PKR are predisposed to lethal intranasal infection by the usually innocuous vesicular stomatitis virus, and also display increased susceptibility to influenza virus infection (Balachandran *et al.*, 2000). Also, in Herpes simplex virus 1-infected cells, NF-κB is activated in wild-type murine embryonic fibroblast cells (MEFs) but not in PKR-null cells which strongly supports the idea that PKR plays an important role in the innate immune response (Taddeo *et al*., 2003). In MEFs, PKR delayed virus protein synthesis, production of infectious virus and caspase-3-activated cell death and reduced the yield of infectious virus by 90%. Furthermore, PKR contributes to a

large proportion of the IFN-β response, the levels of IFN-*β* transcripts in $PKR^{-/-}$ MEFs at 8 h were 80% lower than those in wt MEFs and levels of functional IFN at 24 h were 95% lower (Barry *et al.*, 2009).

Endoribonuclease (RNase L)

RNase L is an effector enzyme in the 2-5A enzymatic pathway, and the pathway is under interferon regulation. It is constitutively expressed in most mammalian cell types and it remains inactive under normal circumstances. The pathway is activated by IFN, inducing transcription of several 2-5A synthetase genes. These synthetase proteins will be activated when they bind with dsRNAs. Activated 2-5A synthetase converts ATP into 5'-triphosphorylated oligoadenylates; these contain 2'-5' phosphodiester bonds, unlike 3'-5' linkages in RNA and DNA. 2-5A acts as a specific activator of RNase L. Upon binding, RNase L is activated to cleave single-stranded RNAs at UpN (mainly UpU and UpA) sequences in single stranded regions of RNA (both cellular and virus). The role played by RNase L in IFN-induced antiviral activity has been demonstrated by i) transfection of 2-5A or stabilised 2-5A analogues to cells to inhibit the pathway (Watling *et al*., 1985) which restores encephalomyocarditis virus (EMCV) RNA synthesis and virus yield, ii) constitutive expression of 2-5A synthetase and RNase L, which confers resistance to picornavirus infection (Chebath *et al*., 1987; Ghosh *et al*., 2000) , iii) *in vitro* study in mice which shows RNase L is activated in WNV infected cells and responsible for antiviral response to flaviviruses (Scherbik *et al*., 2006) iv) *in vivo* studies on *RNASEL*$^{-/-}$ mice which show increase in susceptibility to infection with EMCV, Coxsackievirus B4, WNV and Herpes simplex virus 1 (Samuel *et al*., 2006; Zheng *et al*., 2001; Zhou *et al*., 1997).

RNA interference (RNAi)

To date there is no evidence of that RNAi function as an antiviral defence in mammals. There is no evidence that long double stranded RNA are being processed into 21–23 nt in human cells. However, introduction of small interfering RNA (siRNA) can trigger RNAi in human Hela cells (Hall & Alexander, 2003).

Apoptosis

Apoptosis is a vital process in development, in the regulation of cell numbers in the mature organism and in the elimination of damaged cells. It also functions as an early defence against virus infection at least in mammals and possibly also in invertebrates. The term apoptosis was used to describe a dying cell displaying unique morphology including cell shrinkage, nuclear condensation and cytoplasmic blebbing. In mammals, apoptosis can be triggered by at least two different paths, the intrinsic and extrinsic pathways. The intrinsic pathway involves permeabilisation of the mitochondrial outer membrane and subsequent release of mitochondrial contents (such as: cytochrome c, complex of apoptotic protease activating factor (Apaf) -1 molecules, pro-caspase-9 and ATP). Upon the release of mitochondrial contents, the apoptosome forms and caspase-9 is activated. Caspase-9 cleaves and activates the effector caspases-3 and -7. The extrinsic pathway is cell surface receptor-mediated. The receptors involved in initiating this pathway are predominantly from the tumour necrosis factor (TNF) receptor family. Receptors of this family have an intracellular death domain (DD). Ligands induce oligomerisation of the receptors and conformational change which allows the binding and activation of the adaptor protein Fas-associated DD protein (FADD). The receptors and FADD proteins form a death-inducing signalling complex (DISC). Multiple caspase-8 molecules can bind to a DISC complex allowing the proteolytic activation of neighbouring caspase-8. Activated caspase-8 can directly activate caspase-3. Notably, both intrinsic and extrinsic pathways lead to the activation of caspase-3 and -7. Upon activation, caspase-3 cleaves a variety of downstream proteins, including inhibitor of caspase-activated deoxyribonuclease (ICAD), which leads to degradation of chromosomal DNA, a DNA repairing protein Poly (ADP-ribose) polymerase and cytoskeleton proteins.

For some viruses apoptosis may aid propagation, but in most virus infections, apoptosis is a cellular altruistic response which terminates the infected cell prematurely to prevent the virus from replicating and being released to infect surrounding cells. Numerous viruses have evolved pro- and anti-apoptotic genes to mediate their propagation and replication. There are multiple interactions between

viruses and host cells which lead to the apoptotic response of the host cell. For example, attachment and entry can trigger caspase-8 via the Fas signalling pathway (Liu & Zhang, 2007). Presence of dsRNA in the cytoplasm also triggers an apoptotic response. During replication, RNA viruses produce dsRNA replication intermediates. These are detected by mechanisms including TLR, PKR, RIG-I and MDA5. On the translational level, viral protein synthesis at the endoplasmic reticulum (ER) can also trigger an apoptotic response by activation of the unfolded protein stress response. This attempts to restore balance by increasing protein folding capacity and inhibiting translation but if this fails it induces cell death (Barry *et al.*, 2010).

Interferon (IFN) system

Interferon was first discovered during an experiment in which a transferable anti-viral state was produced by fluid from a chick chorio-allantoic membrane infected with heat-inactivated influenza virus (Isaacs & Lindenmann, 1957) . IFNs are a multi-gene family of inducible protein cytokines. Their best characterised role is the ability to inhibit replication of viruses through induction of an antiviral state. The IFN proteins consist of two families, the type I viral induced IFN family including IFN-α and IFN-β and the type II immune induced family (induced by mitogenic or antigenic stimuli of leukocytes) IFN-γ. Most virus-infected mammalian cell types are capable of producing IFN-α/β. In contrast, IFN-γ is only produced by cells of the immune system including natural killer (NK) cells, CD4 Th1 cells, and CD8 cytotoxic suppressor cells (Samuel, 2001) .

In human there are 13 IFN-α genes, 1 IFN-β gene, and 1 IFN-γ gene. IFN-α genes can be divided into two groups: an immediate-early response gene (IFN-α4) which is induced rapidly and without the need for ongoing protein synthesis; and a set of IFN-α genes consisting of IFN-α2, IFN-α5, IFN-α6, and IFN-α8, that display delayed induction and are induced more slowly and require cellular protein synthesis (Marié et al., 1998) . The alpha4 and beta IFNs initially stimulate the JAK-STAT pathway through a common cell surface receptor consisting of two interferon-alpha/beta receptor (IFNAR) subunits, IFNAR-1 and IFNAR-2. This results in activation of transcription factor interferon-stimulated gene factor 3 (ISGF3). IFN-stimulated

genes are induced by ISGF3 and activated IFN regulatory factor 7 (IRF7) is produced. IRF7 is activated (phosphorylated) in response to detection of virus and in turn induces the delayed IFNα gene set. IFNs are essential to protect against many viruses. IFN-$\beta^{-/-}$ mice and $IFNAR^{-/-}$ mice are highly susceptible to many viruses (Deonarain *et al.*, 2000).

Janus kinases (JAK) & signal transducers and activators of transcription (STAT)

The Janus kinases (JAK) and signal transducers and activators of transcription (STAT) are key components of the JAK/STAT signalling pathway. The pathway begins with activation of the IFN receptor by IFN-mediated heterodimerisation of the cell surface receptor subunits, IFNAR-1 and IFNAR-2 with IFN-α/β and IFNGR-1 and IFNGR-2 with IFN-γ. The intracellular domains of the IFN receptor subunits are already in association with JAK. There are four members of the JAK family, Jak-1, Jak-2, Jak-3 and Tyk-2. Activation of the interferon receptor (heterodimerisation) brings two JAK tyrosine kinases enzymes together, allowing transphosphorylation of tyrosine residues in juxtaposition. Transphosphorylation of JAKs allows cytosolic STAT protein to dock onto the receptor complex via their SH domain. The STAT family of proteins are latent cytoplasmic transcription factors that become tyrosine phosphorylated by the JAK kinase after recruitment. There are seven known members of the STAT protein family, Stat-1, Stat-2, Stat-3, Stat-4, Stat-5a, Stat-5b, and Stat-6. Activated STATs form either heter- or homo-dimers prior to nuclear translocation (Figure 1.10). Different members of the JAK and STAT families have different functions in cytokine signalling. The Jak-1, Jak-2 and Tyk-2 kinases and the Stat-1 and Stat-2 transcription factors are the main players in IFN-dependent signalling for induction of anti-viral responses. In mammals, there are four JAK and seven STAT genes which are activated in different combinations by more than 30 cytokines and growth factors (Darnell Jr., 1997).

Once localised in the nucleus, STATs bind to specific DNA sequences (TTCNNNGAA) and induce transcription of specific genes (Agaisse & Perrimon, 2004). Activation of STAT proteins can lead to macrophage activation, increase in expression of MHC proteins, cytokine and interferon synthesis, and stimulation of the production of granulocytes and macrophages.

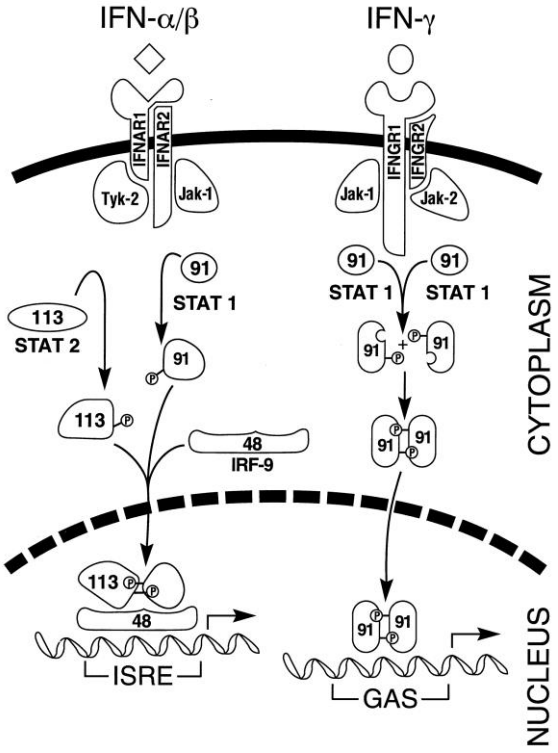

Figure 1.10: A schematic representation of IFN signaling by the JAK-STAT pathway.

The signalling cascade begins with binding of the IFN-α/β or IFN-γ to their respective receptor subunits. IFN binding leads to receptor dimerisation and transphosphorylation of pairs of Jak. Stat are in turn phosphorylated. IFN-α/β activated pathway leads to the phosphorylation and dimerisation of the Stat-1 (p91) and Stat-2 (p113) proteins and subsequent translocation, along with IRF-9 (p48), to the nucleus. This protein complex is known as IFN-stimulated gene factor 3 (ISGF-3), which activates the transcription of IFN-α/β inducible genes through the ISRE. IFN-γ activates and dimerises 2 Stat-1 proteins through Jak-1 and Jak-2 kinases. The Stat-1 dimer complex, known as GAF for gamma activation factor, activates the transcription of IFN-γ inducible genes through the GAS enhancer element. Figure adapted from Samuel, 2001 with permission.

Innate immunity in insects

Like mammals, insects are also vulnerable to invading pathogens but unlike mammals they do not have an IFN system or any adaptive immunity. However, arboviral infection of arthropod cell cultures often leads to a non-lethal persistent infection. The ability to efficiently control arboviral infection is solely achieved by the innate immune system. Upon detection of Gram-positive bacterial or fungal

infection, the proteolytic signal cascade pathway Toll is activated whilst the detection of Gram-negative bacterial infection activates the immunodeficiency (IMD) pathway. Although, these two pathways are homologues of the nuclear factor-κB (NF-κB) signalling pathways in mammals, they do not appear to share any intermediate components and they mediate differential expression of antimicrobial peptide (AMP) -encoding genes via distinct NF-κB-like transcription factors. Activation of these defence pathways leads to transcriptional induction of AMPs including attacin, ceropin, defensin, diptericin, drosocin, drosomycin, and metchnikowin. These are made in the fat body, a functional equivalent of mammalian liver, and secreted in the haemolymph to control and eliminate invading pathogens (Hoffmann *et al*.., 2002). Other evolutionary conserved signalling pathways include Janus kinase (JAK)/signal transducer and activator of transcription (STAT), c-Jun N-terminal kinase (JNK) and RNAi pathways.

Toll pathway

In *Drosophila* there are three NF-κB homologues, Doral, Dif and Relish. Toll does not act as a pathogen recognition receptor (PRR). Upon Gram positive bacterial or fungal infection, the toll pathway is triggered by PAMPs such as peptidoglycan binding with peptidoglycan recognition proteins (PGRPs) leading to an uncharacterised serine protease cascade and the processing of Spätzle. Cleaved Spätzle becomes a dimeric cytokine that binds to extracytoplasmic regions of Toll and cross links two Toll ectodomains. Activated dimeric Toll recruits adaptor proteins dMyD88 (myeloid differentiation primary-response gene 88), a functional homologue of mammalian MyD88, Tube and Pelle via its intracytoplasmic TIR domain. MyD88 recruits and activates Tube and in turn, Tube recruits and activates protein kinase Pelle, a homologue of mammalian serine/threonine kinase a homologue of IL-1R-associated kinase (IRAK-1). All three adaptor proteins contain death domain (DD). Pelle phosphorylates the I-κB like protein Cactus for degradation, possibly through polyubiquitylation, allowing nuclear translocation of the NF-κB like transcription factors DIF (dorsal-related immune factor) and Dorsal

to promote transcription of antimicrobial peptide genes (Rämet et al., 2002; Weber et al., 2003). Figure 1.11 shows the Toll pathway and its components schematically.

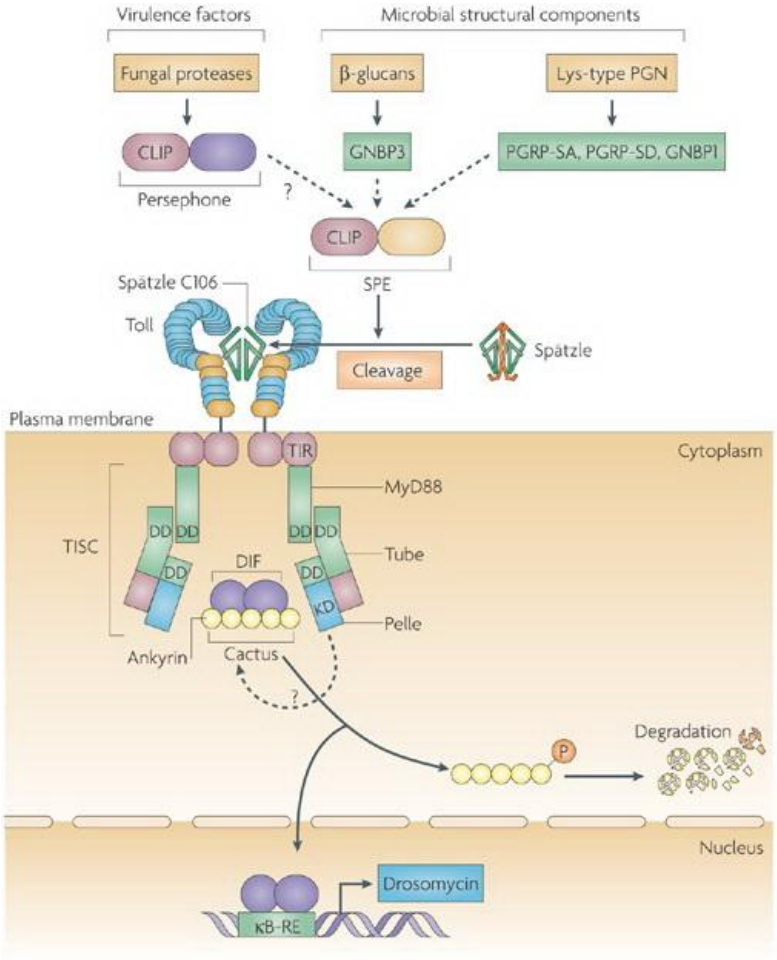

Figure 1.11: A schematic representation of Toll pathway in Drosophila.

The antifungal and anti-Gram positive bacteria Toll pathway. Toll pathway is initiated when the Spatzle protein binds to its ligand. Cleaved Spatzle binds and activates Toll receptor, lead to the formation of Toll-induced signalling complex (TISC) consisting of dMyD88, Pelle, Tube, and possibly dTRAF2. Pelle phosphorylates Cactus, an IκB homologue, for degradation. This allows DIF and Dorsal (NF-κB homologues in flies) in the cytoplasm to translocate into the nucleus and induce transcription of antifungal factors such as Drosomycin. Figure adapted from Ferrandon *et al.*, 2007 with permission.

Immune deficiency (IMD)/ JUN N-terminal kinases (JNKs) signal transduction pathways

In *Drosophila*, the IMD pathway responds to interaction of peptidoglycans in Gram-negative bacteria with peptidoglycan recognition proteins (PGRP), PGRP-LC and PGRP-LE (Choe et al., 2002; Ferrandon et al., 2007; Gottar et al., 2002; Kaneko et al., 2006; Rämet et al., 2002). PGRP-LC is a transmembrane receptor of the IMD pathway, whereas PGRP-LE is a secreted receptor in the haemolymph. Both PGRPs contain a receptor interacting protein (RIP) and a homotypic interaction motif (RHIM) and are presumed to be responsible for initiating signal transduction cascade of the IMD pathway. However, it is unclear whether there are unidentified adaptors that mediate the interaction between PGRP and IMD (Kaneko *et al.*, 2006). IMD is a death domain protein which is homologous to the mammalian receptor interacting protein 1 (RIP1) from the tumour necrosis factor (TNF) pathway which is essential for NF-κB and mitogen activated protein kinase (MAPK) activation (Georgel *et al*., 2001). Activation of IMD also ultimately targets the NF-κB-like transcription factor Relish for activation (Hedengren *et al.*, 1999). Unlike other NFκB-like transcription factors, Relish is bipartite, consisting of an N-terminal Rel/NF-KappaB homology domain and a C-terminal IκB -like domain with Ankyrin repeats. Upon bacterial infection, IMD initiates two different processes signalling the endoproteolytic cleavage of Relish.

The first process is to phosphorylate Relish. IMD activates the downstream MAPKKK, transforming growth factor-β (TGFβ)-activated kinase 1 (TAK1). TAK1 then forms a complex with regulatory subunit TAK-binding protein 2 (TAB2). TAK1 complex (TAK1/TAB2), also known as *Drosophila* TAK1 (dTAK1), mediates the activation of the IKK signalling complex formed by the catalytic subunit IRD5 (immune-response deficient 5; the fly homologue of mammalian IKKβ) and a regulatory subunit Kenny (the fly homologue of mammalian IKKγ). This phosphorylation process is thought to target Relish for subsequent cleavage but direct evidence of this process is still lacking. This process shares striking similarities with mammalian activation of TAK1 and IKK, as they both require K63-

linked polyubiquitin conjugation (Chen, 2005; Hasdemir *et al*., 2009; Zhou *et al*., 2005).

The second process is the cleavage of Relish. This involves 3 genes: *imd*, *Fadd* (FAS-associated death domain), and *Dredd* (death-related ced-3/Nedd2-like protein). IMD recruits the DD-containing adaptor FADD which interacts with the caspase-8 homologue DREDD. This process is absolutely required for DREDD to interact with Relish to direct endoproteolytic cleavage (Leulier *et al*., 2000; Leulier *et al*., 2002; Naitza *et al*., 2002). Endoproteolytic cleavage separates N and C terminal domains. C-terminal Ankyrin domain remains in the cytoplasm and N-terminal Rel-homology domains translocate to the nucleus to promote transcription of antimicrobial peptide genes include Cecropin, Diptericin, Attacin, Defensin and Metchnikowin (Stöven et al., 2000). The FADD-DREDD complex is also required upstream of the dTAK1 complex in the first process to activate the IKK complex (Figure 1.12).

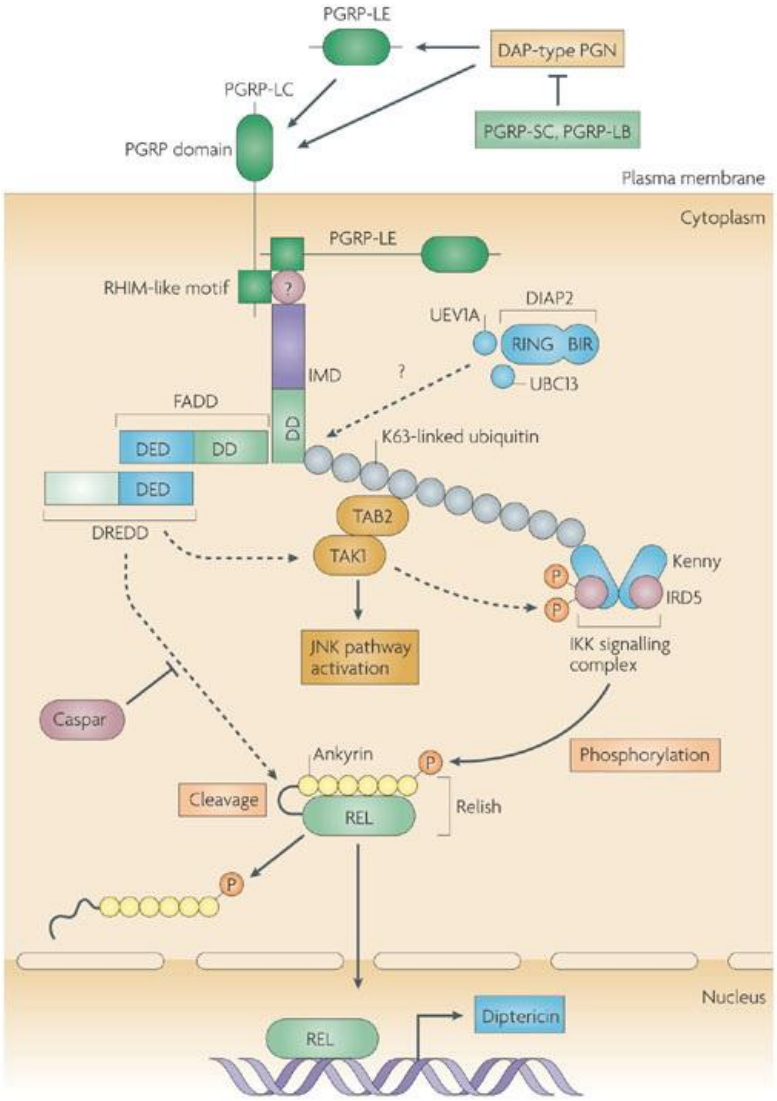

Figure 1.12: A schematic representation of the IMD pathway in Drosophila.

The anti-Gram negative bacteria IMD pathway. This cascade signals through the receptor PGRP. Relish is activated by endoproteolytic cleavage in response to bacterial infection, leading to the production of N-terminal Rel-homology domains that translocate to the nucleus. Figure adapted from Ferrandon *et al*., 2007 with permission.

Besides Relish activation, the IMD pathway splits into a second branch which also activates the JUN N-terminal kinase (JNK) pathway. The branch point begins downstream from the TAK1/TAB2 complex, which may signal a TNF-like signalling cascade controlled by Eiger and Wengen (Geuking *et al*., 2005). Genome-wide expression profiling has revealed that JNK and JAK/STAT pathways contribute to

the temporal expression of microbial challenge-induced genes (Boutros *et al*., 2002). Medeiros and co-workers showed that the JNK pathway was triggered in *Frankliniella occidentalis* by infection with *Tomato spotted wilt virus* (TSWV). A 4 fold increase in transcriptional level of JNK cascade receptor signalling protein was observed (Medeiros *et al*., 2004).

Janus kinases (JAK) & signal transducers and activators of transcription (STAT)

In insects, no interferon or interferon homologue has been identified. However, STAT exists in insects and it is activated in response to bacterial infection in the mosquito *Anopheles gambiae* (Barillas-Mury *et al*., 1999). Activation of the *Drosophila* JAK-STAT pathway is initiated by binding of ligand Upd to a homodimer subunit of the transmembrane cell surface receptor Domeless (Dome), a homologue of the vertebrate type I cytokine receptors (Brown *et al*., 2001). Upd is a protein encoded by *unpaired* (*upd*) to regulate cell proliferation in *Drosophila* growth and development (Arbouzova & Zeidler, 2006). The intracellular domains of the Dome receptor subunits are already in association with the homologue of JAK tyrosine kinase, Hop. Activation of Dome receptor (homodimerisation) brings two Hop together, allowing transphosphorylation. The activated Hop will in turn phosphorylate Dome resulting in the formation of docking sites for cytoplasmic STATs. This activated Dome/Hop complex recruits and mediates dimerisation/activation of STATs. Activated STAT dimers translocate into the nucleus and induce transcription of target genes. Infection of *Drosophila* with *Drosophila* C virus (DCV) did not trigger the induction of antimicrobial peptides but triggered transcription of a set of genes which contain consensus binding sites for the transcription factor STAT (Dostert *et al.*, 2005). In another study, Souza-Neto and co-workers have shown that the JAK-STAT pathway in *Ae. aegypti* is responsible for controlling dengue virus infection. RNAi-mediated silencing of Hop and Dome increased the mosquito's susceptibility to dengue virus infection, whereas silencing of protein inhibitor of the activated STAT (PIAS), the negative regulator of the JAK-STAT pathway, increased the resistance to virus infection. This suggested the JAK-

STAT pathway is part of *Ae. aegypti*'s antiviral defence independent from other pathways (Souza-Neto *et al*., 2009).

Apoptosis

Apoptosis also takes place in insect cells. An example of apoptosis in insect cells as a response to infection is observed in baculovirus infection of *Spodoptera frugiperda* cells (SF-21) (Prikhod'ko & Miller, 1996). Baculoviruses have evolved mechanisms to regulate apoptosis during infection by expressing proteins that inhibit caspase activation, for example, caspase inhibitor p35 and the inhibitor of apoptosis (IAP) proteins. Infection of SF-21 cells with a mutant strain of *Autographica californica* multicapsid nucleopolyhedrovirus (AcMNPV) containing mutations in the p35 gene triggers early apoptosis and results in 100-fold decrease in virus production and the loss of occluded virus. Infectivity is reduced compared to wild type virus when p35-mutant viruses infect *S. frugiperda* larvae. Apoptosis has been observed in the mosquito midgut epithelia after WNV infection (Vaidyanathan & Scott, 2006).

RNA interference (RNAi) in insects

RNAi is an evolutionarily conserved cellular process which was first discovered in plants and termed co-suppression (Napoli *et al*., 1990) and is also known as post-transcriptional gene silencing (PTGS). This discovery was first made when an antisense chalcone synthase gene was introduced into transgenic plants resulting in suppression of both introduced gene and the homologous endogenous gene of flower pigmentation (van der Krol *et al.*, 1988). Since then, the phenomenon has been observed in other plant species and in fungi (*Neurospora crassa).* The gene responsible for post-transcriptional transgene-induced gene silencing was identified and silencing was termed as quelling in fungi (Cogoni & Macino, 1997). PTGS can be triggered by introduction of transgenes or plant virus, and the silencing effect is transmitted from cell to cell, and spreads throughout the entire plant. Fire and co-workers decided to utilise and investigate a technique called antisense inhibition in *Caenorhabditis elegans*, this later became known as RNAi. Antisense inhibition was first manipulated by by reinserting a clone of the thymidine kinase (TK) gene in

reverse orientation and expressing it in mouse L cells resulting in transient reduction of the TK gene (Izant & Weintraub, 1984). Fire and co-workers discovered that production of antisense RNA through a DNA vector disrupts target gene expression (Fire *et al*., 1991). This group later observed that injection of double stranded RNA molecules into a cell produced a target gene silencing effect far more potent than injecting sense or antisense RNA alone. This suggested a catalytic or amplification component in the interfering process (Fire *et al*., 1998). Then Hamilton and Baulcombe made the important discovery of 25nt RNA species in plants undergoing co-suppression. These small RNAs were complementary to both the sense and antisense strands of the gene being silenced (Hamilton & Baulcombe, 1999). Then Zamore and co-workers demonstrated that dsRNAs are processed to RNA segments of 21-23 nucleotides in *Drosophila* embryo lysates (Zamore *et al*., 2000).

RNAi is triggered by the presence of (exogenous or endogenous) long double-stranded RNA (dsRNA) in the cell. Long dsRNA is processed by the enzyme Dicer, into 21 to 26-nt siRNAs with 2-nucleotide overhangs at the 3'-ends. These siRNAs are then assembled into a RNA-induced silencing complex (RISC). During assembly, one strand (passage strand) of the siRNA duplex is removed and the other (guiding strand) is assembled into the RISC to direct target degradation. This results in the degradation of any RNA with sequence homology to the siRNA (Bernstein *et al*, 2001).

Dicer

Dicer is an enzyme of the RNase III endonuclease family. There are 3 classes of proteins within this family but all contain one or two RNase III domains in tandem, and are conserved in bacteria, bacteriophages, and fungi. Class 1 RNase III enzymes were discovered in bacteria. They consist of a single N-terminal RNase III domain and a single C-terminal dsRNA binding domain (dsRBD). Class 2 RNase III enzymes consist of two RNase III domains and one dsRBD at the C-terminal with an uncharacterised structural motif at the N-terminal. An example of a class 2 enzyme is the human Drosha protein responsible for processing pri-miRNA into pri-miRNA hairpin. Class 3 enzymes have multiple domains including two ribonuclease domains, one or two dsRBD at the C-terminus, an N-terminal DExD/H-box helicase

domain, a small domain with unknown function (DUF283), and a PAZ domain. An example of class 3 RNAse III endonuclease is the *Giardia intestinalis* Dicer (Gi-Dicer). X-ray crystallography shows the protein contains two endonucleases, PAZ, and platform domains (Macrae *et al*., 2006). A single RNase III domain has seven α-helices and dimerisation of two RNase III domains provides a valley-shaped dsRNA-binding surface which is the active site for cleavage. In additional, a divalent metal ion Mg^{2+} is required for the catalytic cleavage reaction (Nowotny & Yang, 2009). The hallmark of RNase III cleavage is a product with a 5'-phosphate and a 2nt 3'-OH overhang. Both Drosha and Dicer can process imperfectly base paired dsRNA, furthermore Dicer is reported to cleave substrates with bulges or bubbles 6-10 bps away from the endonuclease active site (MacRae *et al*., 2007).

Plant and insect genomes encode multiple Dicers or Dicer-like proteins. Different Dicer-like proteins function either independently or redundantly within the RNA silencing pathway. In Drosophila, miRNA are generated by Dicer-1 (Dcr-1), whereas siRNAs and viRNAs are generated by Dicer-2 (Dcr-2). In *Arabidopsis thaliana*, there are four Dicer-like proteins (DCL), DCL1-4. Each has a different role. DCL1 is responsible for miRNA processing, whereas DCL2, DCL3 and DCL4 process long dsRNA into 22, 24 and 21 base pair products, respectively. However, the situation is different in helminths and vertebrates, in which there is only one Dicer encoded in the genome.

RNA-induced silencing complex (RISC)

Once dsRNA is processed, siRNA is transferred into the RISC complex. In *Drosophila*, Dcr dimerises with R2D2 to present siRNA into AGO2-RISC. The RISC complex is the effector of silencing in the RNAi pathway. The exact molecular composition of the RISC is not well defined due to its wide range of binding partners. However, at the core of the RISC complex is a member of the Argonaute protein family. The eukaryotic Argonaute family is classified into three major phylogenetic classes based on amino acid sequence homology. The three classes include Argonaute (Ago), Drosophila protein P-element induced wimpy testis (PIWI) and nematode-specific worm Argonaute (WAGOs). Protein structural analysis carried out mostly on prokaryotic Argonautes has revealed a bilobed structure, with

each lobe responsible for binding opposite ends of the guiding strand. The N-terminal contains a PAZ domain, which binds to the 3' end of the guiding strand. The C-terminal contains a middle domain which binds to the 5'-phosphate of the guiding strand and a RNase H-like PIWI domain which hydrolyses target RNA. Upon transfer of siRNA into RISC, the 5'-phosphate and the first base are held in a pocket between the middle and PIWI domains. Therefore the first base of the guiding strand does not contribute to target recognition. The rest of the guiding strand stays in contact with the Argonaute protein with its phosphodiester backbone. The 3' two nucleotides are clamped into a hydrophobic cleft in the PAZ domain. Bases 2-6 of the guiding strand, named the "seed region", are fully exposed and face out from Argonaute and act as an initial probe for RNA targets. Once the guiding strand is in place, Argonaute engages target RNA for degradation (Kim, 2008; Mi *et al*., 2008; Nowotny & Yang, 2009).

It is now understood that RNAi is an evolutionarily conserved mechanism that provides a sequence-specific immunity against viruses in plants and insects (Baulcombe, 2004; Lecellier & Voinnet, 2004), regulates expression of cellular genes by sequence-specific degradation of RNA transcripts and maintains the genome by suppressing mobilisation of transposable elements (Ketting *et al*., 1999). The primary function of RNAi is to destroy viral RNA transcripts in a sequence-specific manner (Jorgensen *et al*., 1998). As a defence mechanism, RNAi is especially effective against virus present in a cell as dsRNA because RNA can form double stranded structures throughout the course of viral replication.

In insects, RNAi is capable of post-transcriptional gene silencing, destroying foreign dsRNA and mounting a sequence specific antiviral response. In *Drosophila melanogaster*, Dicer is responsible for cleaving dsRNA into 21-23 bp siRNA (Zamore *et al*., 2000) and RNAi is an essential part of the antiviral response against Drosophila X Virus (DXV) infection. RNAi pathway mutants were found to be highly susceptible to DXV infection (Zambon *et al*., 2006). The RNAi pathway was shown to exist in *Ae. albopictus* C6/36 cells by using dsRNA to silence transgene expression from plasmids, SFV replicons and DENV replication. (Adelman *et al*., 2002; Caplen *et al*., 2002). RNAi was shown to interfere with DENV-2 replication in

C6/36 cells previously infected with genetically modified SINV that contained a 290 base region of DENV-2 prM in either sense or antisense orientation (Sanchez-vargas *et al*., 2004). In *Anopheles gambiae*, virus spread was significantly inhibited when ONNV was coinjected with dsRNA of ONNV nsP3 sequence (Keene *et al*., 2004). These authors demonstrated that the silencing *An.gambiae Arganaute2* (*AgAgo2*) made mosquitoes more permissive to virus infection. Since then attempts have been made to produce transgenic mosquitoes expressing dsRNA in midgut or salivary gland tissues to block DENV infection in the mosquito vector (Travanty *et al*., 2004).

Effect of alphaviruses on the innate immune response

The interaction between replicating virus and host innate immune response is a critical factor in viral pathogenesis. Alphaviruses do not encode any protein that functions solely as an inhibitor of the innate immune response. However, replication of alphaviruses strongly down-regulates transcription and translation of cellular mRNAs which in turn affects activation of viral stress-inducible genes and suppresses the development of an antiviral state. Sarver & Strollar have demonstrated that host RNA synthesis is inhibited 1.5 to 1.7 fold in SINV infected *Ae. albopictus* cells by measuring ^{3}H-uridine incorporation into cellular RNA (Sarver & Stollar, 1977). This host gene expression reduction was also observed in SFV infected *Ae. albopictus* cells and mouse NIH 3T3 cells (Fragkoudis *et al.*, 2008). The expression of EEEV and VEEV capsid protein inhibits general cellular gene expression (Aguilar *et al.*, 2007; Garmashova *et al.*, 2007). As mentioned above, SFV infection highly activates PKR, leading to almost complete phosphorylation of eIF2α and subsequent translational shut down (Barry *et al.*, 2009; Ventoso *et al.*, 2006). This global shut-off effect affects host protein synthesis and is likely to play a part in dampening the activation of viral stress-inducible genes (McInerney *et al*., 2005).

In contrast to non-specific suppression, the multi-functional nsP2 plays a role in suppression of the type I interferon response (Breakwell *et al.*, 2007). The effect of nsP2 on interferon production is demonstrated by infection with SINV with a mutation in the nsP2, which induces significantly higher levels of IFN-α/β secretion

both *in vivo* and *in vitro* (Frolova *et al.*, 2002). In addition, SINV has also been shown to inhibit cellular transcription (Gorchakov & Frolova, 2005). The higher level of IFN-α/β could be due to the inability of this mutated virus to inhibit host gene expression, leading to activation of viral stress-inducible genes, which may be involved in development of an antiviral state. The same phenomenon has also been observed in cells infected with SFV (Gerald Barry, personal communication). Recently, the nsP2 of CHIKV has been shown to inhibit type I/II interferon-stimulated JAK-STAT signalling by blocking STAT1 phosphorylation and nuclear translocation in mammalian cells (Fros *et al.*, 2010). Individual expression of CHIKV nsPs showed that nsP2 is a powerful inhibitor of IFN-induced JAK-STAT signalling.

In *Ae. albopictus* mosquito cells, SINV infection resulted in an increase in translocation of Relish into the nucleus. This strongly implies that SINV activates Relish-mediated transcription (Avadhanula *et al.*, 2009). In *Ae. aegypti* mosquitoes, SINV infection leads to changes in the transcription levels of 135 genes. Sanders and co-workers have shown that during early infection (PID 1) there was an almost 2-fold increase in transcription level of Dorsal-related immunity factor (Dif). This suggests that the Toll innate immunity pathway responds to alphavirus infection. However, this transcript returned to the background level by (PID 4). At the same time (PID 4), transcription of three ubiquitin-ligase pathway components was down-regulated. This ubiguitin-ligase pathway is a known regulator of NF-κB-like proteins. The Toll pathway requires ubiquitin ligase-mediated degradation of Cactus to activate Dif. Therefore, decrease in ubiquitin ligase levels may inhibit activation of the Toll pathway. This suggests that alphavirus infection can lead to modulation of NF-κB mediated innate immune pathways, whether this modulation is a direct effect of interaction between viral proteins and innate immune components has not yet been proven. On PID 8, there was a 4-fold increase in transcriptional level of a JNK cascade receptorsignalling protein, suggesting induction of the JNK cascade in response to SINV infection. More importantly, this study also showed that the transcription levels of a large number of genes with unidentified function changed upon SINV infection (Sanders *et al.*, 2005). These unidentified genes may represent unidentified innate immune pathways in insects that are responsible for controlling

alpha virus infection. Sanders and co-workers have provided evidence that indicates that SINV may respond to innate immune defences by inhibiting Toll pathway activation In *Drosophila* S2 cells, SINV infection leads to up-regulation of 210 genes and down-regulation of 68 genes at PID 5. These genes encode for cytoskeletal and membrane trafficking components, immune-related components, transcription factors, cell cycle and cell division factors. Four of the immune-related genes are, again, involved in ubiquitination. The transcription level of Relish was also increased 1.5-2 folds (Mudiganti *et al.*, 2010). Avadhanula and co-workers have shown that Relish has a role in controlling SINV in *Drosophila*, as a *relish*$^{-/-}$ mutant showed higher viral load and enhanced replication compared with the wild type (Avadhanula *et al.*, 2009). Mudiganti and co-workers also showed that Thiol-ester containing protein II (TEP II) was up-regulated in S2 cells at PID5. TEP II is a member of the TEP family which plays an important role in immune responses as a component of the complement system in vertebrates, and is induced upon bacterial challenge in *Drosophila* (Meister & Lagueux, 2003). It has been suggested that expression of TEPs is under the direct regulation of the JAK-STAT pathway (Mathey-Prevot & Perrimon, 1998). In *An. gambiae* mosquitoes, Sim and co-workers have shown that ONNV infection leads to changes in the level of transcription of 18 genes on PID14. Seven of these genes have been proven to be infection-induced and are involved in modulation of translation/replication factors and intracellular transport pathways. However, none of these seven genes are related to the innate immune signalling pathways. These genes included: EF-1α which is involved in host translational elongation and has been shown to bind with the positive strand of RNA viruses (BLACKWELL & BRINTON, 1997; Joshi *et al.*, 1986); RpL35 encoding for ribosomal protein which may interact with the capsid protein of SFV (Ranki & Ulmanen, 1979); HSP70 encoding for heat shock molecular chaperone which may be involved in ONNV entry and protecting the vector vells from ONNV-induced molecular damage; DAN4 and agglutinin encoding for host membrane proteins .

The findings of these authors have shown that different member of the alphavirus family can induce change in levels of gene transcription in *Ae. aegypti* and *An. gambiae* mosquitoes, and induce innate immune pathways such as Toll, JAK-STAT and IMD. However, viruses within the same family do not induce changes in level of

transcription of the same set of infection-inducible genes. To date, there is no evidence that alphaviruses suppress immune signalling in mosquitoes. However, mosquito immune signalling is prone to interference by other viruses such as Japanese Encephalitis Virus (JEV). The NS5 protein of JEV has been shown to prevent STAT1 and TYK-2 phosphorylation in vertebrates and has been implicated in blocking phosphorylation of STAT in *Ae. albopictus* C6/36 cells (Lin *et al.*, 2004, 2006).

Hypothesis

Infection of mosquito cells with SFV activates anti-viral defences which reduce virus replication to levels below that required to trigger cell death resulting in a persistent infection.

Aims and objectives

AIM

To characterise mosquito cell defence mechanisms against SFV infection.

OBJECTIVES

- Determine whether SFV infection of mosquito cell lines can be established.
- Characterise SFV infection of mosquito cell lines.
- Determine whether SFV triggers anti-viral defence mechanisms in mosquito cells.
- Determine whether defence mechanisms include signalling from infected to uninfected cells.
- Determine whether activation of known defence systems triggered by bacteria affects SFV infection.
- Determine whether STAT gene expression affects virus replication.
- Characterise viRNA biogenesis from SFV genome in mosquito cells.
- Determine the efficiency of RNAi silencing in SFV infected mosquito cells. .

Table of contents

Chapter 2: Materials and Methods

Bacterial protocols

Bacterial culture

Escherichia coli (*E. coli)* strains were grown in Luria-Bertani (LB) medium or on LB plates with 1.5% agar. (Please see Appendix 1 for composition of LB.) Media and agar were sterilised and melted during autoclaving. For selection purposes, appropriate antibiotics were added to the medium prior to use; 100μg/ml ampicillin or 50μg/ml kanamycin (depending on strength of antibiotic resistance conferred by plasmids). To prepare agar plates, LB agar was poured into Petri dishes (10 cm). A suspension of bacteria was spread out on the surface of the agar with a glass spreader. Plates were inverted and incubated at 37^{o}C overnight (16 hr). Single colonies retrieved from agar plates were picked to inoculate liquid medium. Liquid cultures were incubated overnight (16 hr) at 37^{o}C with constant shaking (225 rpm). All procedures were carried out under aseptic conditions.

Transformation of XL 10-Gold® Ultracompetent cells

The infectious SFV cDNA plasmid clone is a relatively large plasmid construct. The transformation of this large construct in regular competent cells i.e. DH5α cells does not often produce viable bacterial colonies. Therefore XL 10-Gold ultracompetent cells were used for efficient transformation of large DNA constructs (Please see Appendix 1 for source of competent cells). A vial of ultracompetent cells was thawed on ice and 100 μl were aliquotted into 1.5 ml sterile pre-chilled eppendorf tubes. One μl of β-mercaptoethanol was added to the cells and incubated for 10 minutes on ice, and gently mixed every 2 minutes for the duration. Approximately 200ng of plasmid was added to the cells and the mixture was incubated on ice for 30 minutes. Cells were then heat-shocked at 42 ^{o}C for approximately 30 sec followed by 2 minutes of incubation on ice. The time of heat shock is crucial as it affects the uptake of DNA. Nine hundred μl of pre-warmed SOC medium (Sigma-Aldrich) was added and the mixture was incubated at 37^{o}C in an orbital shaker (225 rpm) for 1 hour.

During incubation, LB agar plates supplemented with corresponding antibiotics, 50 to 100 μg/ml of ampicillin or kanamycin were placed in an incubator at 37 ^{o}C with the lid slightly tilted to warm and air dry the surface of the agar. Ten, 50 or 100 μl of transformed cells were pipetted on agar plates and evenly distributed across the surface with a sterile glass spreader beside a Bunsen burner. Transformation of pUC 19 plasmid was carried out as a positive control. The agar plates were then inverted and incubated overnight (16 hr) at 37^{o}C. The plates were examined for colony growth.

Only uptake of plasmid would confer antibiotic resistance and allow formation of colonies. A single colony was used to prepare a small bacterial amplification (up to 10 ml) as later described in "miniprep", or to create a large plasmid stock as later described in "maxiprep".

Preparation of frozen stocks of transformed bacteria

A single colony was isolated from an LB agar plate and used to inoculate 5ml of LB medium containing appropriate antibiotic. The culture was grown overnight (16 hr) in an orbital shaker (225rpm) at 37^{o}C. The cultured bacteria were pelleted by centrifugation (6 minutes at 1500 x g) and the pellet was resuspended in 1 ml of sterile 50% glycerol in H_2O. The sample was transferred to a sterile eppendorf tube and snap frozen using dry ice. The tube was stored at -80^{o}C.

Eukaryotic tissue culture

Baby hamster kidney (BHK-21) cells

BHK-21 cells were used to produce and titrate viruses. BHK-21 cells were cultured in T175 flasks (Nuclon, UK) with Glasgow's minimum essential medium (GMEM) (Gibco, UK) until a confluent monolayer was formed. The medium contains an energy source (D-glucose), amino acids, inorganic salts and all vitamins required for cell growth. Additionally, the medium was supplemented with 10% (volume/volume (v/v)) new born calf serum (NBCS) (Invitrogen), 10%

(v/v) tryptose phosphate broth (TPB), and L-glutamine (2 mM) (10% GMEM+). As required, antibiotics were added to the medium (penicillin/streptomycin – 100 units/ml and 100 μg/ml, respectively) to protect cells from contamination by Gram positive and Gram negative bacteria. BHK-21 cells grow at optimum pH of 7.2 to 7.4, therefore the pH indicator phenol red is incorporated into the medium to monitor pH during cell growth. The medium turns yellow when the pH is acidic and pink when it is basic.

Harvesting, counting and passaging BHK-21 cells

Adherent cells were passaged to new flasks when 80-90% confluence was reached. To passage the cells, old medium was removed from the flask and the cell monolayer was rinsed with 5 ml of 0.02% versene (EDTA) to chelate any Ca^{2+} ions. After the versene was removed, 5 ml of Trypsin-ethylene diamine tetraacetic acid (EDTA) (0.05% Trypsin, 0.53 mM EDTA, Invitrogen) was added to the cell monolayer and incubated at 37^{o}C until the cells had detached. The trypsin-cell mixture was diluted in twice the volume of complete medium (10% GMEM+) to inactivate the trypsin. The cells were then pelleted at the bottom of a universal tube by centrifugation (378 x g) for 5 minutes. The pellet was resuspended in 10 ml of medium, 10 μl of this was diluted with 90 μl of trypan blue (1 in 10) and a haemocytometer was used to count the cells. To prepare the next passage of cells, fresh T175 flasks were then seeded with $5x10^6$ cells in 30 ml of medium (10% GMEM+) and incubated at 37^{o}C in an atmosphere of 5% CO_2 in air. Cells were used between passages 4 and 40 at which point their growth became obviously slowed. All tissue culture procedures were carried out in a class II microbiological safety cabinet under aseptic conditions.

Culture of mosquito cell lines

The *Aedes albopictus*-derived cell lines C6/36, C7.10 and U4.4 (Condreay & Brown, 1986) and *Aedes aegypti*-derived cell line Aag2 (Peleg, 1968) were grown in L-15 (Leibovitz) Medium (Sigma-Aldrich) with 10% v/v foetal calf serum (FCS), 10% v/v TPB, and 2mM L-glutamine (Merck) (10% L-15) in T175 flasks (Nunclon, UK) at 28^{o}C (without addition of extra CO_2).

Harvesting, counting and passaging mosquito cells

Cells were passaged when 80-90% confluence was reached. To passage the cells, old medium was removed from the flask and 5 ml of fresh incomplete medium (L-15) was added to gently wash the cell monolayer. The medium was then removed, 10 ml of fresh complete medium (10% L-15) was then added and the cells were gently dislodged with a cell scraper (Falcon). The suspension was then transferred into a universal tube. Ten µl of the resuspended solution was taken and diluted into 90 µl of trypan blue, then 10 µl of this was diluted with 90 µl of trypan blue (final dilution 1 in 100) and a haemocytometer was used to count the cells. To prepare the next passage of cells, fresh T175 flasks were then seeded with $5x10^6$ cells in 30 ml of medium (10% L-15) and incubated at 28^oC without addition of extra CO_2. All tissue culture procedures were carried out in a class II microbiological safety cabinet under sterile conditions.

Freezing and thawing cells

Cells were prepared for cryogenic storage when they were healthy, in the middle of a growth phase and below 80% confluency. To prepare cells for freezing, cells were trypsinised or mechanically agitated, pelleted and resuspended in 10 ml of complete media and then counted using a haemocytometer. Once cells were counted, the cell suspension was pelleted by centrifugation (500 x g) for 5 minutes and then resuspended in freezing medium (10% dimethyl sulfoxide (DMSO) and 90% FCS) to the optimal freezing concentration of $5x10^6$ cells per ml. One ml aliquots of this suspension were then put into 1.5 ml cryovials (Nunc), the tubes were placed in a freezing container (Mr. Frosty, Sigma) filled with 200 ml of isopropanol. The container was transferred to -80^oC and stored overnight. The isopropanol insulation allows the cells to cool at approximately 1^oC per minute which permits water to escape from cells to avoid freezing damage (avoid formation of ice crystals which fragments and damages cells). Frozen cells were transferred to a liquid nitrogen storage container at -130^oC.

To thaw cells, the cryovial was transferred from liquid nitrogen to dry ice. The frozen cells were then rapidly thawed by placing the cryovial in a 37^{o}C water bath. Once defrosted the freezing medium containing the cells was transferred into a universal tube with 10 ml of pre-warmed complete growth medium. The cell suspension was centrifuged at 478 x g for 5 minutes, the supernatant was removed and the cell pellet was resuspended in 1 ml of growth medium and the whole suspension was transferred into a 25 cm^2 flask with 10 ml of pre-warmed medium. For BHK-21 cells, the flask was then placed in the incubator at 37^{o}C in an atmosphere of 5% CO_2 in air. For insect cells, the flask was then placed in the incubator at 28^{o}C without addition of CO_2. The cells were allowed to grow normally. A high level of cell death is expected from the freeze/defrosting process, and a 25 cm^2 flask is appropriate for keeping the surviving cells in close enough contact for proliferation. The procedures described were carried out in a class II microbiological safety cabinet under aseptic conditions.

Mosquito rearing and feeding

Rearing of mosquitoes

Adult *Ae. aegypti* mosquitoes were kindly provided by Professor Rick Maizels, Institute for Infection and Immunity, School of Biological Sciences, University of Edinburgh. Live mosquitoes were kept in a stockinette sleeve openable cage (mesh panels on all sides) and reared at 28^{o}C, 70% relative humidity, with a 10 hours light 14 hours dark photoperiod (Figure 2.1). To maintain the mosquitoes, a sugar meal was given to the mosquitoes by placing cotton wool soaked with 10% fructose sugar solution on the top of the mosquito cage.

Figure 2.1: Mosquito cage

Live mosquitoes were reared in stockinette sleeve openable cage with mesh panels on all sides.

Mosquito feeding container

The mosquitoes were caged in waxed paper cartons (ice-cream carton) during feeding. The feeding cartons were modified to allow a one way entry point and a semi-accessible area for feeding. The entry point was created by cutting a small square hole (approx. 2 cm) in the side of the carton which was taped over with two layers of elastic latex (cut from latex gloves). A small hole was cut on each of the latex layers (approx. 2 mm). The lid of the carton was replaced with nylon mesh and sealed with multiple elastic bands. (Figure 2.2)

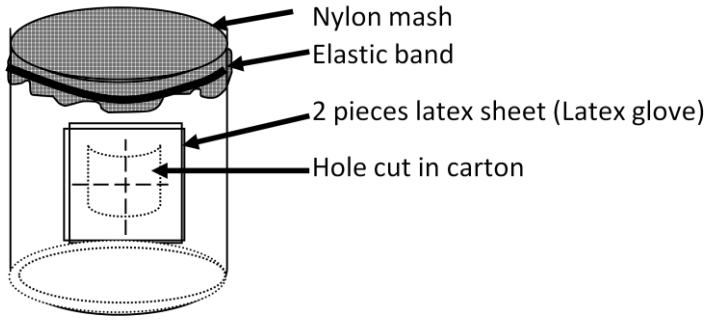

Figure 2.2: Mosquito feeding container.

Oral infection

To infect mosquitoes, defibrinated blood was mixed with virus or virus like particles and 10 µl droplets of this infectious mixture were placed on top of the nylon mesh. During feeding, the feeding containers were kept in a 28^{o}C incubator. This method had been used by Cirimotich and co-worker (Cirimotich *et al.*, 2009). Approximately one hour was allowed for feeding to take place and fed mosquitoes were selected to keep alive for further experimention. To select fed mosquitoes, the feeding container was wrapped in a plastic bag and placed on ice in the middle of a large ice bucket for 10 minutes. Following that, the mosquitoes were checked to confirm that they were anaesthetized and unfed mosquitoes were taken out and submerged in ethanol. Once selection was completed, the feeding container was sealed again and kept in a 28^{o}C incubator.

Nucleic acid techniques

Plasmid DNA extraction

Miniprep

DNA plasmids were purified on a small scale using a Qiagen Miniprep kit. The procedure was carried out according to the manufacturer's instructions. In brief, a small plasmid amplification in up to 10 ml of LB media was prepared in a universal container. To harvest the bacteria, the bacteria were pelleted and resuspended in 250 µl of buffer P1 and transferred into a 1.5 ml eppendorf tube. The cells were then lysed by addition of 250 µl of lysis buffer P2. This alkaline lysis buffer solubilises the bacterial membrane and denatures the DNA and protein. The mixture was gently mixed by inverting the tube 4 - 6 times. To neutralise the reaction and precipitate all protein and lipid, 350 µl of buffer N3 was added to the lysate and mixed by inverting 4 - 6 times and then centrifuged at approximately 17,900 x g for 10 minutes. After centrifugation, a white pellet at the bottom was observed, and DNA was left in the supernatant. The supernatant was then transferred into a Qiaprep mini column and centrifuged at 17,900 x g for 1 minute. The flow-through was discarded and the filter

was washed with 750 µl of PE buffer and centrifuged at 17,900 x g for 1 minute. The flow-through was again discarded and the filter was centrifuged dry at 17,900 x g for further 2 minutes. The plasmid DNA was then eluted by adding 30 µl of RNase and DNase free water directly onto the centre of the filter and allowing to sit for 1 minute. The DNA plasmids were collected by placing filter column in an eppendorf and centrifuged at 17,900 x g for 1 minute. The DNA was stored at -20^{o}C.

Maxiprep

To generate large amounts of plasmid DNA, a Qiagen EndoFree Plasmid Maxi Kit was used. To prepare large amount of plasmids, a single *E. coli* colony (containing the plasmid of interest) was picked from an LB agar plate and inoculated into 2 ml LB medium starter culture containing an appropriate antibiotic e.g. 50 µg/ml ampicillin. The starter culture was incubated on an orbital shaker (225 rpm) at 37^{o}C for 6 to 8 hours. Then 500 µl of the starter culture was transferred to 250 ml of LB medium containing the appropriate antibiotic and again incubated overnight (16 hr) at 37^{o}C in an orbital shaker (225 rpm). To harvest the bacteria, the bacteria were pelleted by centrifugation (6000 x g) at 4^{o}C for 15 minutes. The bacterial pellet was resuspended in 10 ml of buffer P1 and transferred into a 50 ml sterile centrifuge tube (Falcon), followed by addition of 10 ml of lysis buffer P2. The mixture was gently mixed by inverting the capped tube 4 to 6 times and allowed to sit at room temperature for 5 minutes to break down cell walls and release the DNA. To neutralise the reaction, 10 ml of pre-chilled buffer P3 was added to the lysate and mixed. The lysate was then poured into the barrel of the QIAfilter Cartridge and pushed through the filter into a new 50 ml centriguge tube. Following that, 2.5 ml of Buffer ER was then added to the filtered lysate, mixed by gently inverting the tube 10 times and incubated on ice for 30 minutes. Meanwhile, a QIAGEN-tip 500 was equilibrated by allowing 10 ml of Buffer QBT to flow through it. After 30 minutes, the filtered lysate was passed through the equilibrated QIAGEN-tip. Supernatant (flow-through) was discarded and the QIAGEN-tip was washed twice by passing through 30 ml of Buffer QC. Plasmid DNA was eluted from the filter with 15 ml of Buffer QN. To precipitate the DNA, 10.5 ml of isopropanol at room temperature was

added to the eluted DNA and the mixture was then centrifuged at 15,000 x g at 4°C for 30 minutes. The supernatant was discarded and the DNA pellet was washed with 5 ml of 70% ethanol and further centrifuged at 15,000 x g for 10 minutes to remove all traces of isopropanol. The supernatant was removed carefully by inverting the tube, and the remaining ethanol was allowed to evaporate at room temperature for no more than 5 minutes. The pellet was redissolved in 300 µl of endotoxin-free buffer TE. Samples were stored in 1.5 ml eppendorf tubes at -80°C.

Restriction enzyme digestion

To perform a restriction digestion, up to 1 µg of plasmid DNA was digested with 1 unit (U) of restriction endonuclease. The enzyme unit (U) is a unit for the amount of a particular enzyme that catalyses the cleavage of 1 µg of DNA at the appropriate temperature per hour. The restriction digestion reaction had a final volume of 20 µl, and contained 2 µl of 10X restriction enzyme buffer, 2 µl of 10X acetylated bovine serum albumin (BSA), 1 µl of enzyme (1 unit/µl), plasmid DNA, and DNase-free H_2O made up to a final volume of 20 µl. The reactions were incubated at the enzyme's optimum temperature for 2 to 4 hours. The restriction product(s) was analysed using agarose gel electrophoresis or purified for further manipulation.

The products of a plasmid DNA restriction digestion could result in multiple bands on an agarose gel if the DNA plasmid was not completely digested by the enzyme. The three resulting products are uncut supercoiled plasmid (migrates furthest), linearised plasmid, and nicked plasmid (migrates slowly).

Purification of restriction digestion products

After restriction digestion, DNA fragments were purified. Jetquick (Genomed), a DNA purification kit, was used. The volume of digestion product was brought up to 100 µl with DNase-free H_2O. Then 400 µl of H1 solution was added. The mixture was transferred into the binding column and centrifuged for 1 minute at 12,000 g. The flow-through was discarded, and the column was washed twice with 500 µl of H2 solution each time. To elute the DNA fragments, 30 µl of DNase-free H_2O pre-

heated to 65-70^{o}C was added directly onto the binding matrix. The column was held for 1 minute before it was centrifuged for 1 minute in a sterile eppendorf tube. The eluted DNA was stored at -20^{o}C.

In vitro transcription of capped infectious complementary DNA(icDNA)

Approximately 1.66 μg of *Spe I* linearised icDNA was used in the transcription reaction. The RNA was synthesised at 37^{o}C for 1 hour, using the cap analogue m^{7}G(5')ppp(5')G to produce capped transcripts. The composition of the reaction is listed in following table. The further details of each reagent are tabulated in Appendix 1.

Reagents	Volume
Spe I cut plasmid (1.66μg)	xx.x μl
10x SP6 buffer (GE Healthcare)	5.0 μl
10 mM m^{7}G(5')ppp(5')G (cap) (GE Healthcare)	5.0 μl
50 mM DL Dithiothreitol (Sigma)	5.0 μl
rNTP mix (10 mM ATP, CTP, UTP, 5 mM GTP) (Promega)	5.0 μl
Recombinant RNasin Ribonuclease Inhibitor (60 U/1.5 ul) (Promega)	1.5 μl
SP6 RNA polymerase (50 U/μl) (GE Healthcare)	1.5 μl
Nuclease-free H_2O to Total volume	50.0 μl

Table 2.1 Reagents and quantity for *in-vitro* transcription.

Synthesised RNA was verified by using agarose gel electrophoresis. *In vitro* transcripts were generally used immediately, but were sometimes stored at -80^{o}C.

Agarose gel electrophoresis

DNA and RNA were separated on gels containing 1% or 1.25% agarose in TBE buffer (fragment size dependent). To prepare a 1% agarose gel, 1 g of electrophoresis grade agarose powder was added to 100 ml of tris-borate (TBE) buffer in a conical flask and boiled in a microwave for 1 minute at full power to dissolve the agarose.

The gel mix was allowed to cool down before adding ethidium bromide (0.5 μg/ml). Once mixed, the gel was transferred into a plastic frame and a comb was placed into the gel to produce wells. Bubbles on the gel were removed with pipette tips and the gel was allowed to set (15-30 minutes). Once set, the comb was removed and DNA samples mixed with 6x loading buffer were loaded into the wells of the gel and run at 100 V for 45 to 60 minutes. The nucleic acid bands were visualised under a UV transilluminator. Molecular weight markers i.e. 100 bp and 1 kb DNA ladder (Promega) were loaded alongside the samples.

Nucleic acid quantification

All nucleic acid samples were quantified using a NanoDrop ND-1000 spectrophotometer. One μl of nucleic acid sample was placed on the lens of the NanoDrop ND-1000 spectrophotometer and the quantity was measured.

Polymerase chain reaction

PCR was used to amplify a specific region of DNA between 2 primers for diagnostic purposes. For different samples, different primers and reaction cycles were used as listed below. The PCR reaction mix had a final volume of 20 μl, and contained 2 μl of 10X PCR buffer (15mM $MgCl_2$ included), 0.4 μl dNTPs (10 mM) (Promega), 0.5 μl of each primer, forward and reverse (50 pM) (Invitrogen), 0.3 μl of *Taq* polymerase (Promega), DNA sample and DNase/RNase-free water to a final volume of 20 μl. The reactions were incubated in a thermal cycler (Veriti®, Applied Biosystems) using the following settings: an initial denaturation stage of 5 minutes at 95^{o}C followed by an amplification stage which consisted of 27 cycles of three steps; denaturation at 94^{o}C for 30 seconds, annealing at 55^{o}C for 30 seconds and extension at 72^{o}C (duration depends on length of application region); then a final extension stage at 72^{o}C for 15 minutes. A negative (no template) and a positive (β-actin) control were used as control to test for possible contamination and to confirm that the reaction itself was functional. The PCR products were examined by agarose gel electrophoresis and stored at -20^{o}C.

Negative control β-actin primers

Forward (Start 225 nt): 5'- CGTTGACATCCGTAAAGACC -3'

Reverse (End 465 nt): 5'- CTGGAAGGTGGACAGTGAG -3'

Annealing temperature: 60 ^{o}C. Product size: 241.

SFV nsP3, C-terminal region primers

Forward (Start 4974 nt): 5'- ATACCATGTAGATGGGGTGCAGAAGGT -3'

Reverse (End 5523 nt): 5'- TGCGGTCCAGGAGGAGAAAATGTACC -3'

Annealing temperature: 62 ^{o}C. Product size: 589 nt

SFV capsid primers

Forward (Start 7855 nt): 5'- ACGTGAAAGGAGTCATCGAC -3'

Reverse (End 8682 nt): 5'- GGTGGCTACCTTCAAAGATG -3'

Annealing temperature: 62 ^{o}C. Product size: 827 nt

Reverse transcription PCR

Reverse transcription RCR (RT-PCR) was used to create cDNA copies of an RNA template using an oligo dT primer. For each reaction, 1 µl of deoxyribonucleotide triphosphate solution (dNTPs, 10 mM) (Promega), 1 µl oligo dT (500 µg/ml) (Promega), dH_2O and 5 µg RNA made up to a total volume of 10.5 µl were mixed and placed at 65^{o}C for 5 minutes and followed by 5 minutes on ice. Meanwhile, 4 µl of 5x first strand buffer, 2 µl dithiothreitol (DTT, 0.1 M) (Sigma) and 0.5 µl RNasin (Promega) were mixed together and kept on ice. The two mixtures were combined and incubated at 42^{o}C for 2 minutes, followed by addition of 1 µl of Superscript II (Invitrogen). The reaction mix was incubated at 42^{o}C for 1 hour. The reaction outcomes were examined by agarose gel electrophoresis.

Total RNA extraction

Total RNA was isolated from U4.4 or Aag2 cells by using Trizol (Invitrogen), a phenol-based reagent. Approximately 5x10^{5} U4.4 or Aag2 cells were grown in 6-

well plates overnight (16 hr) at 28 ^{o}C. The cells were then infected with SFV (MOI=10). Total RNA was extracted at 24 h postinfection (p.i.). To extract total RNA, medium was removed from the well, and 1 ml of Trizol was added into each well (1 ml per 10 cm^2) followed by passing the cell lysate several times through a pipette. The lysate was transferred to a 1.5 ml RNase free tube and incubated at room temperature for 5 minutes to allow complete dissociation of nucleoprotein complexes. Then 200 µl of chloroform was added to the lysate (0.2 ml chloroform per 1 ml of Trizol used) and shaken vigorously for 15 seconds followed by incubation at room temperature for 2 to 3 minutes. To remove extracellular membranes, polysaccharides, fat, and high molecular weight DNA, the cell lysate was centrifuged at approximately 12,000 x g for 15 minutes at 2-8^{o}C. To precipitate RNA, the top aqueous phase (containing RNA) was transferred to a sterile 1.5 ml RNase free tube by a pipette followed by the addition of 500 µl of molecular grade isopropyl alcohol (Invitrogen) (0.5 ml isopropyl alcohol per 1 ml of initial Trizol used). The mixture was incubated at room temperature for 10 minutes and centrifuged at approximately 12,000 x g for 10 minutes at 2-8 ^{o}C. The supernatant was removed and the RNA pellet was left untouched at the bottom of the tube. The RNA pellet was then washed by addition of 1 ml of 75% molecular grade ethanol (7.5ml ethanol (Invitrogen) and 2.5 ml RNase-free water (Invitrogen)) and mixed by gentle vortexing, followed by 5 minutes of centrifugation at approximately 7,500 x g at 2-8 ^{o}C. The supernatant was then discarded and the pellet was air dried for 5-10 minutes. The pellet was dissolved in 50 µl of RNase-free water and stored at -80^{o}C.

Virus and Virus Replicon Particles (VRPs)

The viruses used for experiments in this study are detailed in Table 2.2.

Virus	Backbone	Description
SFV4	n/a	Virus derived from the molecular clone of the prototype strain of SFV. (GenBank accession number X04129) corrected by the recent resequencing of SFV4 (GenBank accession number AJ251359)
A7(74)	n/a	Naturally occurring strain of SFV without modification.
SFV-steGFP	SFV4	Maker gene *eGFP* inserted in the structural ORF between the capsid and p62(E2/E3) coding region.
SFV4-st*Rluc*	SFV4	Marker gene *Renilla* luciferase inserted in the structural ORF between the capsid and p62(E2/E3) coding region.
SFV4(3H)-*Rluc*	SFV4	Marker gene *Renilla* luciferase inserted between nsP3 and nsP4. Designed for early expression from non-structural polyprotein.

Table 2.2 List of viruses used in the project.

All the recombinant viruses were made from plasmids kindly provided by Prof Andres Merits, University of Tartu, Estonia. Viruses were transported to Edinburgh in the form of infectious plasmid cDNA (icDNA). These cDNA plasmids, capable of giving rise to complete infectious virus, are designated icDNA plasmids. These plasmids were amplified by transforming chemically competent *E. coli*, growing up the *E. coli* cultures and harvesting the plasmids. To produce virus, the icDNA plasmids were linearised using Spe I and used as templates for *in vitro* transcription to produce capped viral RNA. Viral RNAs were then electroporated into baby hamster kidney (BHK-21) cells. Virus was harvested in the supernatant at 24 and 48 hours after electroporation. All viruses were stored at -80^{o}C.

The VRPs used for experiments in this study are detailed in Table 2.3.

Virus Strain	System	Modification
SFV1-d1eGFP	Split-helper system	Structural genes replaced with marker gene eGFP.
SFV1(3F)-IRES-ZsGreen	Split-helper system	An IRES element was inserted at 5' end of nsp1 coding region. Subgenomic region was deleted. Marker gene zsGreen was fused at the end of nsp3.
SFV1(3F)-ZsGreen	Split-helper system	Subgenomic region was deleted. Marker gene zsGreen was fused at the end of nsp3.

Table 2.3 List of VRPs used in this project.

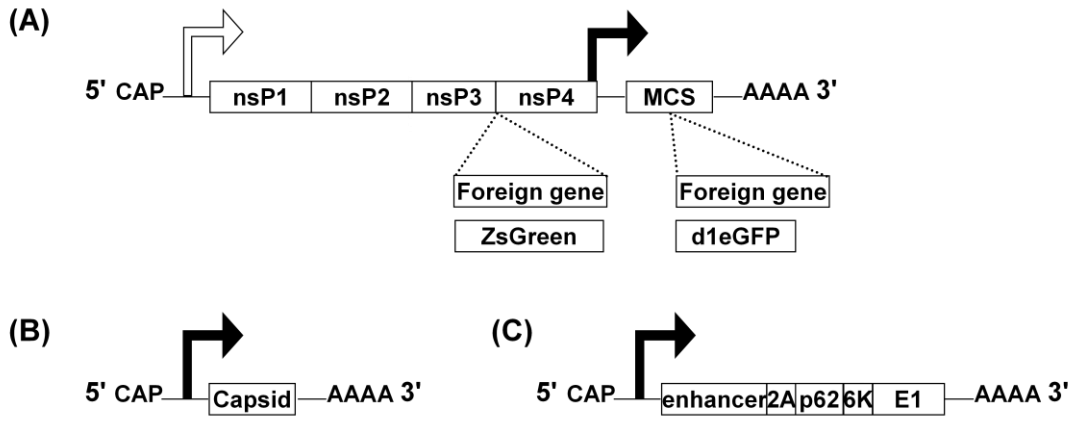

Figure 2.3: A Schematic representation of the SFV1 VRP and split-helper system

(A) SFV1 VRP is based on SFV4 construct with viral subgenomic region replaced with a multiple cloning site (MCS). SFV1 VRP is unable to produce any viral strauctral proteins. Foreign gene can be inserted at locations indicated. E.g. ZsGreen sequence can be inserted between nsP3 and nsP4, producing SFV1(3F)-ZsGreen; d1eGFP can be inserted at the MSC to produce SFV1-d1eGFP **(B)** The helper 1 construct consists of a 5' cap, subgenomic promoter, capsid and a 3' poly A tail. **(C)** The helper 2 construct consists of a 5' cap, subgenomic promoter, enhancer sequence from the capsid protein, 2A sequence, p62(E3+E2), 6K and E1 and a poly A tail.

The "split-helper system" was used to produce non-propagating marker gene carrying VRPs (Smerdou & Liljeström, 1999). The cDNA plasmids for making

VRPs have viral structural genes removed, and are thus only capable of giving rise to the 5' 2/3 of the viral RNA transcripts (Figure 2.3 A), they are designated pSFV1 plasmids. The helper plasmids, one encoding the viral capsid and the other encoding the viral envelope genes, were constructed to viral transcripts to produce structural proteins *in trans* for virus packaging (Figure 2.3 B & C). DNA plasmids were kindly provided by Prof Andres Merits, University of Tartu, Estonia. To make VRPs, pSFV1 plasmids and pSFV-helper plasmids were amplified by transformation and growth in chemically competent *E. coli* cultures. The plasmids were then harvested by plasmid extraction (see Transformation and Maxiprep, page 49 and 56). The plasmids were then linearised (1.66 µg of each plasmid) using Spe I and *in vitro* transcribed (see *in vitro* transcription, page 58) to produce RNA. The three RNA transcripts were co-transfected into BHK-21 cells by electroporation. The split helper system provides the viral structural proteins in trans for the packaging of SFV1 RNA to form infectious particules. The viral structural genes were splitted into two part helpers to reduce the chance of recombination which produces propagating virus. of Transfected cells were incubated for 48 hours and VRPs were harvested in the supernatant.

Virus or VRP purification

Forty-eight hours after viral RNA(s) was electroporated into BHK cells, the supernatant containing virus or VRPs was collected and clarified three times to remove cell debris by centrifugation (27,000 x g) at 4^{o}C for 30 minutes, using a JA 20 rotor in a J2-21 centrifuge (Beckman Instruments). To pellet the virus or VRPs, the clarified supernatant was ultracentrifuged through a 20% sucrose cushion. Aliquots of 17.5 ml of virus or VRP supernatant were added to four Beckman SW28 ultracentrifuge tubes followed by addition of 20% (w/v) sucrose (Sigma) in TNE buffer pH 7.4 (50 mM Tris HCl pH 7.4, 100 mM NaCl and 0.1 mM EDTA pH 8.0, filter-sterilised) underneath the supernatant using a pipette until the tube was filled. Virus particles were sedimented through the sucrose cushion at 84,600 x g for 90 minutes at 4^{o}C. Following that, supernatants were decanted from the ultra-centrifuge tube. Virus or VRP pellets were re-suspended by adding 100 µl of TNE buffer to the

pellet and the tube was left vertically on ice on a rocker for 2 hours. All re-suspended virus or VRP was transferred to a sterile eppendorf tube. The centrifuge tube was rinsed with 50 µl of TNE buffer to collect any remaining virus/VRP which was transferred to the eppendorf tube. The pooled purified virus or VRP was aliquoted into eppendorf tubes, 50 µl per tube, snap frozen on dry ice and stored at -80^{o}C.

Titration of virus: Plaque assays

Virus titres were measured by plaque assay. Six-well plates (Nuclon, UK) were seeded with 2 ml of 10% GMEM+ containing 3.5x10^{5} BHK-21 cells per well. Plates were left at room temperature (RT) to settle before incubating in 5% CO_2 in air at 37^{o}C overnight. Meanwhile, GMEM with 2% NBCS, 0.75% bovine serum albumin (BSA) in phosphate buffered saline (PBS) (PBSA) and 4% agarose in PBS (Difco, UK) were prepared and sterilised. In the following day, the BHK-21 cell monolayers in the six-well plates were confirmed to have reached 80% before serial dilution of virus sample was carried out. PBSA was used to make serial dilutions of virus samples from 10^{-1} to 10^{-10}. Plates were labelled with date and sample number. The medium was removed from each well and 400 µl of each virus dilution were added to duplicate wells (in the order of highest to lowest dilution). The plates were incubated for an hour at RT inside a humid box to avoid dehydration of the monolayer and shaken gently every 5 minutes to ensure equal coverage of the monolayer. The 4% agarose was melted in a boiling water bath and then allowed to cool to 57^{o}C in a separate water bath. The agarose was mixed with 2% GMEM+ pre-warmed to 37^{o}C (38 ml of medium to 12 ml of agarose to cover 4 plates). 2 ml of the agarose/medium mixture was added to each well to cover the monolayer completely. Once the agar was set, the plates were incubated for 48 hours (depending on the virus strain) at 37^{o}C in 5% CO_2 in air. After this incubation, the monolayers were fixed by adding 3 ml of 4% neutral buffered formaldehyde to each well for at least an hour (in a fume cupboard). The fixative was then removed and 0.1% toluidine blue was added to each well to stain the monolayer for at least 30 minutes. Finally, the plates were washed with water and after the plates were dried the numbers of plaques were counted.

Plaque Forming Unit and Limit of Detection

The plaque forming units (pfu) per ml was calculated with the following formula:

$$\frac{\text{Average number of plaques x dilution factor}}{\text{Amount (ml) of inoculum per well}}$$

The "limit of detection" of each assay is the threshold below which the assay is not able to detect infectious virus. The limit of detection was determined using the formula above and assuming the lowest dilution used in each assay caused the formation of one plaque. For example, if a plaque assay was carried out with sample dilutions of 10^{-4}, 10^{-5} and 10^{-6}, and 0.4 ml of each dilution was used to infect monolayers of cells in 6 wells plates, 1 plaque observed at 10^{-4} dilution would give a titre of $2.5x10^4$ PFU/ml. The logarithm of that value is 4.4, meaning that the limit of detection of that particular assay was 4.4 Log_{10}; virus below $2.5x10^4$ PFU/ml will not be detected by this assay. Normally, plaque assays are performed with the lowest dilution at -1. Therefore the limit of detection is $10^{1.4}$ PFU/ml.

Microscopic examination of cell cultures

The confluence or cytopathic effect of cell cultures were checked under a Nikon inverted microscope. To check for the presence of eGFP fluorescence a Nikon inverted microscope fitted with UV light (with excitation filter 485 and emission filter 530) was used.

Titration of VRPs

BHK-21 cells were prepared as a suspension of single cells as described above. Six well plates were seeded by placing 22x22 mm cover slips (Chance Propper) into each well and then 2 ml of cell suspension, $4x10^5$ cells per well. The following day, medium was removed followed by one wash with sterile PBS (SPBS). Two wells of the plate served as negative controls to which 450 μl of 10% GMEM+ was added. The material to be titrated was diluted from 10^{-1} to 10^{-6}. 400 μl of each dilution were added to duplicate wells (in the rder of highest to lowest dilution). The cells were

then left on a shaker for 1 hour for the VRPs to attach. Two ml of 10% GMEM+ was then added to cover each well, and the plate was incubated overnight at 37^{o}C in 5% CO_2 in air. The next day, the medium was removed from each well and cells were fixed for 20 minutes with 2 ml of 4% paraformaldehyde (Sigma) per well. Fixed cells were then washed with SPBS. For eGFP VRPs, cover slips were carefully removed with forceps and mounted onto pre-cleaned microscope slides (Surgipath) with fluorescent mounting medium containing DAPI (Vector). For other VRPs cover slips were immuno-stained with antibody to nsp3 before being mounted on a glass slide. Details of immuno-chemistry are described in the histology section.

The slides were examined with a standard Zeiss Axioskop2 microscope equipped with filters suitable for visualisation of eGFP (green), Alexa Fluor 594 (red) and DAPI (UV). An infectious unit (IU) titration was carried out by counting 15 random fields using the X40 objective lens.

Formula for calculating VRP titre (IU/ml):

$$\frac{\text{Mean cell count (from 15 random locations) x (constant = 4365.3) x dilution factor}}{\text{Volume (ml)of VRPs added}}$$

This constant = total area of a well in a 6 well plate (1133.54 mm^2) divided by the area viewed through the 40X lens the microscope (0.25967 mm^2)

Electroporation: delivery of RNA transcripts into BHK-21 cells

One T175 flask containing confluent BHK-21 cells was trypsinised and the cells were counted. The cell suspension was spun at 378 x g for 5 minutes at room temperature. The cell pellet was resuspended in SPBS to give a density of 5x10^6 cells per 400 μl. Then 800 μl of cells were placed in a sterile eppendorf tube and 50 μl of RNA transcript was added. 450 μl of this mixture was then placed in the cuvette of an electroporator (Gene Pulser X cell^{TM} Electroporation System, Bio-Rad Laboratories Inc). The pre-set protocol for the BHK-21 cell line was used, 140 volt per square wave pulse with a pulse length of 25 ms. Electroporated cells were then placed into a T175 flask containing 25 ml of 10% GMEM+ medium (pre-warmed to 37 ^{o}C) which was then incubated at 37^{o}C in 5% CO_2 in air. A total of 1x10^7 cells

were electroporated. Electroporation was carried out in a class II microbiological safety cabinet under aseptic conditions.

Nucleic acid transfection using liposomes (Lipofectamine 2000)

To prepare mosquitoe cells for transfection, 24-well plates were seeded with $1x10^5$ cells in 500 µl of medium per well. Plates were incubated at 28°C overnight (16 hr). To transfect DNA plasmids or RNA preparations or small RNAs to a well of cells, the nucleic acid preparation (amount depends on required final concentration) was diluted in 50 ul of Opti-MEM® medium (Invitrogen) and mixed gently in a polystyrene tube. Following that, 1 µl Lipofectamine 2000™ (Invitrogen) was diluted in 50 µl of Opti-MEM® medium in a separate polystyrene tube. The two different mixtures were incubated at room temperature for 5 minutes and then mixed together. The mixture was mixed gently and further incubated for 20 minutes at room temperature. Meanwhile, the medium in the wells of the 24-well plate was replaced with 400 µl of antibiotic-free medium. 100 µl of the Lipofectamine nucleic acid mixture was added to each well. The plate was then incubated at 28°C for 5 hours before the supernatant mixture was removed and replaced with new 10% L15 medium.

One-step growth curve

A one-step growth curve of a virus assays the accumulation of virus in the supernatant over time when virtually all the cells in the population are infected. Six well plates were seeded with BHK-21 cells, as described in the plaque assay section and incubated overnight at 37°C in 5% CO_2 in air. Medium in each well was removed and monolayers were washed with SPBS. Virus was diluted in 0.75% PBSA to provide an MOI of 10 in 400 µl. Virus/PBSA was added on to the monolayers and infection was allowed to take place. The plates were incubated for 1 hour at RT inside a humid box to prevent dehydration of the monolayer and shaken gently every 5 minutes to ensure equal coverage of the monolayer. After 1 hour, each well was washed 3 times with SPBS to remove any unbound virus followed by addition of 2 ml pre-warmed 10% GMEM+. This point was taken as time-point zero. Aliquots of

100 µl of supernatant were collected every 2 hours and replaced with the same amount of fresh medium for the following 12 hours. Samples were kept in eppendorf tubes at -80^{o}C. All samples were titrated by plaque assay.

Histology

Immunostaining

Immunochemistry was used to visualise viral protein to define viral infection in a cell. To stain cell cultures on a glass slide, cells were fixed with 10% neutral buffered formaldehyde for 45 minutes. The glass slide was then washed in PBS 3 times for 5 minutes each. To increase cell membrane permeability prior to staining, the glass slide was covered in 0.3% Triton-X100 for 20 minutes at room temperature. Following membrane permeabilisation, the slide was inserted into a staining rack and washed in PBS 3 times for 5 minutes each. The slide was then treated with CAS block (Invitrogen) for 30 minutes at room temperature inside a humid chamber. The blocking solution was then replaced with primary antibody diluted with CAS block solution (Zymed) (Table 2.4). The primary antibody was incubated on the slide for 2 hours before the slide was washed 3 times in PBS for 15 minutes each. Then a secondary biotinylated antibody (diluted in CAS block, Table 2.4) was added onto the slide, followed by 1 hour of incubation before the slide was washed with PBS 3 times for 15 minutes each. Streptavidin-conjugated Alexa Fluor 594 (excitation 590 and emission 617 nm) was diluted 1:1400 in H_2O and added onto the slide which was incubated for 45 minutes at RT. The slide was then washed in PBS twice (10 minutes each) before being mounted with fluorescence mounting medium under a coverslip sealed with nail varnish. The completed slide was kept at 4^{o}C, out of sunlight.

Name	Type	Host	Isotype	Optimum Dilution	Source
α-nsP3	Primary	Rabbit	Polyclonal	1:800	Tero Ahola
Biotinylated α – Rabbit IgG	Secondary	Goat	IgG	1:500	Vector Labs
SA-Alexa Fluor 594	Tertiary	-	-	1:1400	Invitrogen

Table 2.4 List of antibodies used in this project.

To check for the presence of eGFP fluorescence or fluorophore emission, a Nikon inverted microscope fitted with UV light (with excitation filter 485 and emission filter 530) was used.

Video microscopy

For live cell imaging of mosquito cells, 5 x 10^5 mosquito cells were seeded in a T20 flask and incubated overnight at 28 ^oC. All internal surfaces were rinsed with medium before filming started to prevent condensation forming inside the top surface of the flask during the course of filming. The flask was then placed under a Zeiss Axiovert microscope and the microscope was programmed to take 1 frame every 3 minutes under visible and UV light. The temperature of the room was maintained at 28 ^oC throughout the course of filming.

WST-1 Assay

Cell viability and proliferation rate were measured by WST-1 assays. 96-well plates (Nuclon, UK) were seeded with 100 μl of 10% L-15 medium containing 5x10^3 cells per well. Following that, the plates were incubated at 28^oC overnight. The plates were labelled with date and sample number. The medium was removed from each well and 30 μl of virus in PBSA was added to give the required MOI. The plates were incubated for an hour at room temperature inside a humid box to avoid dehydration of the monolayer and were shaken gently every 5 minutes to ensure equal coverage of the monolayer. The inoculum was then replaced by fresh 10% L-

15 medium. The 96-well plate was returned to incubation at 28°C. At the required time post-infection, 10 µl of the cell proliferation assay reagent WST-1 (Roche) was added to each well and the plate was incubated at 28°C for 1 hour. The plate was then scanned at 420-480 nm in a microtiter plate reader.

Dual luciferase assays

The dual luciferase assay is a method of quantifying the level of gene expression through the measurement of luminescence produced by the reaction between the luminescent substrate and the expressed reporter gene product, firefly and *Renilla* luciferase. To measure luciferase expression, the dual luciferase reporter assay system, Dual-Glo Luciferase Assay System (Promega) was used. In brief, cells were grown in a 6-well plate and infected with viruses that express *Renilla* luciferase or transfected with plasmids that express *Renilla* luciferase. To release the luciferase from the cells, medium was removed 24 hours post-infection and 200 µl of passive lysis buffer (1 in 5 dilution) was added directly to the monolayer of cells. For experiments carried out in 24-well plates, 50 µl of passive lysis buffer was used per well. The plates were then incubated at room temperature in a sealed humid box on a shaker for 15 minutes for the cells to lyse. To quantify the amount of luciferase being expressed by the cells in each well, 1 µl of the lysate was used for luminescence measurements with a Turner Designs model TD-20/20 luminometer. The following steps were used for luminescence measurements: One µl of the lysate was mixed with 70 µl of the firefly luciferase assay reagent II (LARII). The luminescence emitted from the mixture was then measured in the luminometer with a 10-s equilibration time and a 10-s integration time. After quantifying the firefly luminescence, the reaction was quenched, and the *Renilla* luciferase reaction was initiated by addition of 70 µl of Stop & Glo® reagent. The reaction mixture was quantified once again with 10-s equilibration time, and a 10-s integration time. All reagents were prepared as described by the manufacturer. The data are represented as individual activities of each luciferase and the ratio of firefly to *Renilla* luciferase activity (*Fluc/Rluc*).

Illumina Solexa sequencing

All of the total RNA samples were subsequently processed at GenePool, University of Edinburgh (http://genepool.bio.ed.ac.uk/). Small RNAs below 44 nt were purified from a 15% TBE-Urea polyacrylamide gel, and RNA adapters (see below) were ligated to the 5' and 3' of the small RNAs. These small RNAs which were flanked by adapter sequences were then converted to complementary DNA (cDNA) by reverse transcription with a reverse transcription primer (see below). These small cDNA sequences containing the adaptor sequences were then used as templates for PCR using primer 1(see below) to synthesise double-stranded DNA containing an additional 23 nt attachment sequence which allows all the PCR products to attach on to the inside surface of the flow cell channels. The DNA sequences attached on the inside of the flow cell were then bridge amplified into DNA clusters. The flow cell was then loaded into the sequencer for automated cycles of extension with the sequencing primer (see below) and imaging. Each extension cycle incorporated a single fluorescent nucleotide followed by high resolution imaging of the entire flow cell. These images contained the physical location of all the clusters and the fluorescent emission identified which of the four bases was incorporated at that position. A detailed schematic representation of the sequencing process is available at
http://www.illumina.com/documents/products/techspotlights/techspotlight_sequencing.pdf

To identify SFV-derived viRNAs, small RNA sequences were compared to the SFV4 reference genome sequence (GenBank accession number X04129) corrected by the recent resequencing of SFV4 (GenBank accession number AJ251359) (compiled by Prof A. Merits, personal communication) using SOAP software (with the help of Gene- Pool bioinformatics support) (Li, et al., 2008).

RNA adapters and PCR Primers

The RNA adaptors attached on the 5’ and 3’ of small RNA oligonucleotide samples were:

5' RNA Adapter:

5' GUUCAGAGUUCUACAGUCCGACGAUC

3' RNA Adapter:

5' P-UCGUAUGCCGUCUUCUGCUUGUidT

The small RNA oligonucleotide samples flanked by adaptor sequences were reverse transcribed to cDNA with a reverse transcription primer:

Reverse transcription primer:

5' CAAGCAGAAGACGGCATACGA

The small cDNA were amplified by PCR with PCR primers 1 and 2. PCR primer 1 contains an additional 23 nt attachment sequence which is added to all the PCR products and allows them to attach on to the inside surface of the flow cell channels.

PCR Primer 1 (with attachment sequence):

5' AATGATACGGCGACCACCGACAGGTTCAGAGTTCTACAGTCCGA

PCR Primer 2:

5' CAAGCAGAAGACGGCATACGA

Sequencing Primer:

5' CGACAGGTTCAGAGTTCTACAGTCCGACGATC

Fluorescence-activated cell sorting (FACS)

Cell sorting was kindly carried out by Shonna Johnston at Optical Imaging Services in the Centre for Inflammation Research, University of Edinburgh.

RNA secondary structure prediction

The existence and position of RNA secondary structures in SFV genomic RNA were predicted by thermodynamic folding energy calculations that used comparative sequence data from the available SFV complete genome sequences (SFV4 as described above and GenBank accession numbers EU350586, DQ189086, and Z48163). This analysis was performed using the programme UNAFold (Zuker, 2000). For calculations of folding energies, sequences in the SFV alignment were split into sets of 150 base fragments incrementing by 1 base across the genome. Folding energies were compared with those of 50 copies of each fragment whose sequence order was scrambled using the algorithm NDR, which preserves dinucleotide frequencies of the native sequence automated using the programme Folding Energy Scan as implemented in the Simmonic2005 v1.8 package (Davis et al, 2008). The minimum free energies (MFEs) of each native sequence fragment were compared with the mean MFE of the NDR-scrambled controls to produce an MFE difference (MFED) as previously described (Simmonds et al., 2004). MFED values for each fragment were averaged across the four available SFV complete genome sequences. The prediction of specific structures using the available comparative sequence data for SFV was done by using the programme StructureDist in the Simmonics package. This programme compares minimum energy structures from sequence data sets and computes phylogenetically conserved pairings and secondary structures. The results were expressed in the form of pairing frequencies, which were calculated from the proportion of pairwise comparisons of connect files for each sequence with the same pairing predictions, as previously described (Simmonds *et al.*, 2004).

.

Table of contents

Chapter 3: Infection of mosquito cells with SFV

Introduction

The ability of alphaviruses to infect cells of the mosquito *Aedes albopictus* has previously been studied in three cell lines, C6/36, C7-10, and U4.4 which were derived from neonate larva *Ae. albopictus* (Singh, 1967). The cell line C6/36 is one of twenty clones isolated from cultured *Ae. albopictus* cells, a characteristic of this clone is the ability to produce high virus yield up to 7 days after dengue and Chikungunya virus infections. Sub-clone 36, one of the 43 sub-clones of C6, shows mild to extensive cytopathic effect (CPE) several days post-infection with SINV (Igarashi, 1978). C7-10 cells are also a sub-cloned population derived from Singh's cells which display CPE upon alphavirus virus infection (Sarver & Stollar, 1977).

In this study, there are a number of experiments designed to determine the innate immune responses against SFV infection in mosquito cultures. However, all three cell lines behave uniquely upon virus infection; some are resistant to infection and some are susceptible to infection and display CPE. This project will explore different aspects of the mosquito immune system response to alphaviruses using SFV as a model virus. The first experiments, described in this chapter were carried out to characterise SFV infection in each of the cell lines to determine the ideal cell line for subsequent studies.

Replication of SFV in *Aedes albopictus* cells

To determine whether SFV would infect and replicate in U4.4, C7-10 and C6/36 mosquito cell lines, these cell lines were infected individually with a genetically modified marker virus, SFV4-steGFP, a SFV strain with an enhanced green fluorescence protein gene inserted in the structural region of the genome followed by a foot-and-mouth disease virus (FMDV) 2A sequence to allow for automatic release of eGFP protein (Figure 3.1). This virus construct was used for 3 reasons. The experiment was designed to determine infection at 12 and 24 hours, therefore a virus construct with marker gene expressed in late infection (after 4-6 hours) under the

control subgenomic promoter is suitable for this experiment. Secondly, the eGFP gene is expressed at a high level under the control of a subgenomic promoter at late infection which helps visualisation. Finally, eGFP is self-released as explained in chapter 1 which makes this construct ideal for visualisation of infected cell because eGFP is not specificically localisised in any part of the infected cell.

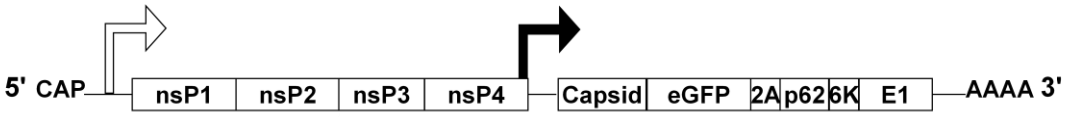

Figure 3.1: A Schematic representation of the SFV4-steGFP.

SFV4-steGFP is based on SFV4 construct with enhanced fluorescence protein gene inserted between Capsid and p62 proteins, flanked by three N-terminal amino acids (SAP) of p62 protein at the N-terminus and a 2A peptide sequence from FMDV at the C-terminus.

U4.4, C7-10 and C6/36 cells were seeded in 6 well plates with a cover slip placed at the bottom of each well. The plates were incubated overnight at 28^{o}C before infection with SFV-steGFP (MOI=10). Cells were fixed with neutral buffered formaldehyde at 12 and 24 hours post-infection and examined under a microscope with UV light. All 3 cell types expressed eGFP 12 hours post-infection. A photomicrograph was taken at 24 hours post-infection of U4.4, C7-10 and C6/36 cells and immunostaining using antibodies against nsp3 was carried out on infected C7-10 and C6-36 cells (Figure 3.2). The nsP3 staining is in red.

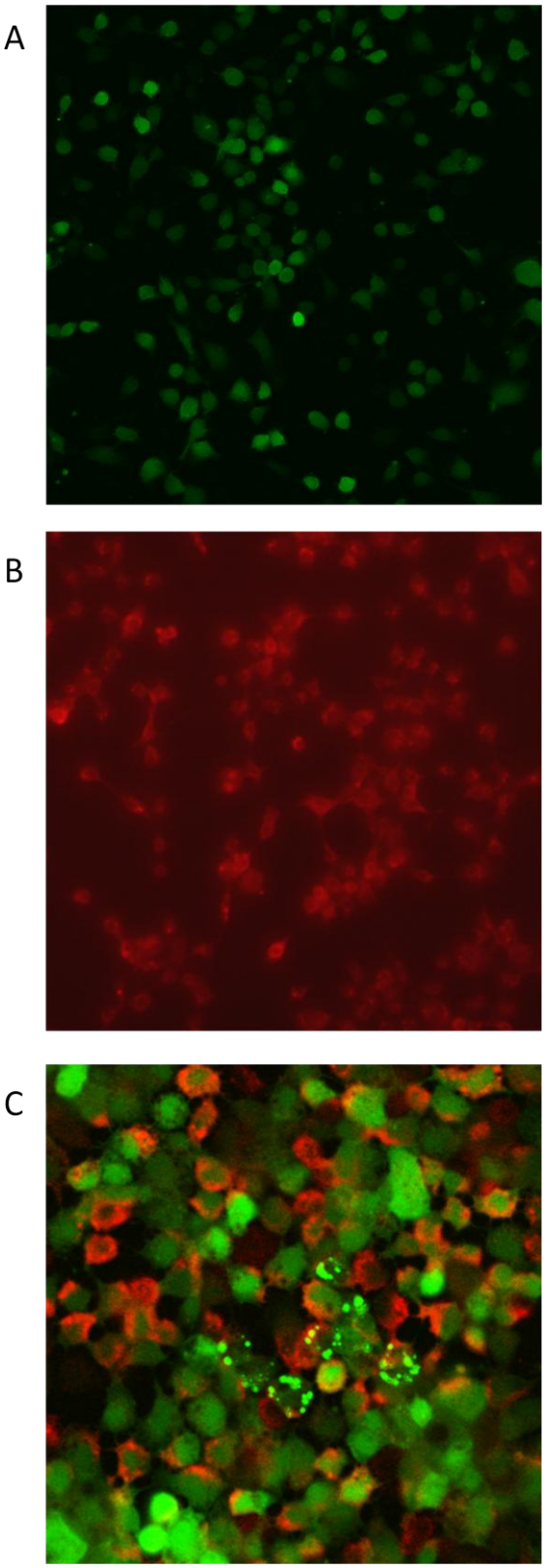

Figure 3.2: Infection of *Aedes albopictus*-derived (A) U4.4 (B) C7-10 and (C) C6/36 cells with SFV4-steGFP (MOI=10).

Photomicrograph taken using confocal microscope: (A) U4.4 cells showing the expression of eGFP at 20x magnification; (B) C7-10 cells immune-fluorescence stained against nsp3 of SFV at 20x magnification; (C) C6/36 cells showing the expression of eGFP and positive immunostaining

During the course of infection, each cell line exhibited different distinctive characteristics in cell numbers and morphology. Therefore, SFV4 infection was characterised in each cell line by determining virus growth in the first 12 hours post-infection. Cells were seeded in a 6-well plate and infected with SFV4 (MOI=10) in triplicate. 100 µl of supernatant were collected and replaced with the same amount of fresh medium every 2 hours for 12 hours. Samples were stored at -80^{o}C and titrated by plaque assay (Figure 3.3).

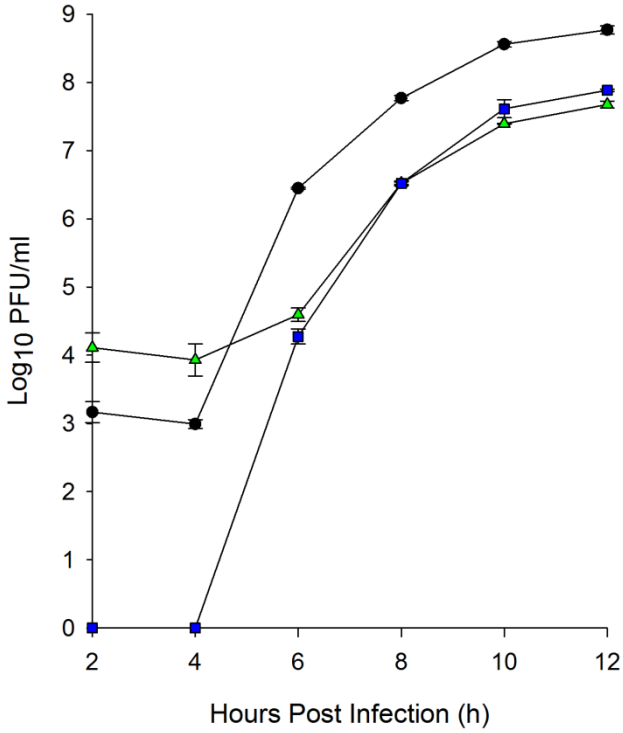

Figure 3.3: One step growth curves of SFV4 in different mosquito cell lines.

SFV4 growth kinetics in U4.4 (▲), C7-10 (■) and C6/36 (●) cells. Each point is the mean of triplicate samples. The error bars indicate the standard error of the mean.

The growth curves show that SFV4 replicates efficiently in all three mosquito cell lines and shows a typical virus growth pattern going from stationary to exponential and then to a plateau phase. As shown by the results, virus growth went through an exponential phase from 4-8 hours and started to reach a plateau from 8-12 hours. C6/36 cells produced virus most rapidly out of the 3 lines, reaching almost 1 log higher titre at 12 hours in comparison to the others. Due to the observation of change in cell number and morphology, more experiments were designed and carried out in an attempt to characterise the viability of cells during the course of infection.

The viability of infected mosquito cells

To determine whether infected cells remained viable, WST-1 cell viability assays were carried out. This assay system uses tetrazolium as a substrate for succinate-tetrazolium reductase, an enzyme of the mitochondrial respiratory chain. The enzyme is only active in viable cells and cleaves the tetrazolium to a soluble formazan dye which can be measured at 420-480 nm. The absorbance value is interpreted as the metabolic activity of the culture and an indicator of cell viability. Replicate cell cultures were set up in 96-well plates, each well was seeded with 5,000 cells. Cells were infected at MOI of 10 with SFV4 for one hour. At each time point, a set of triplicate wells were measured and discarded. Uninfected controls were included and measured at the same time points.

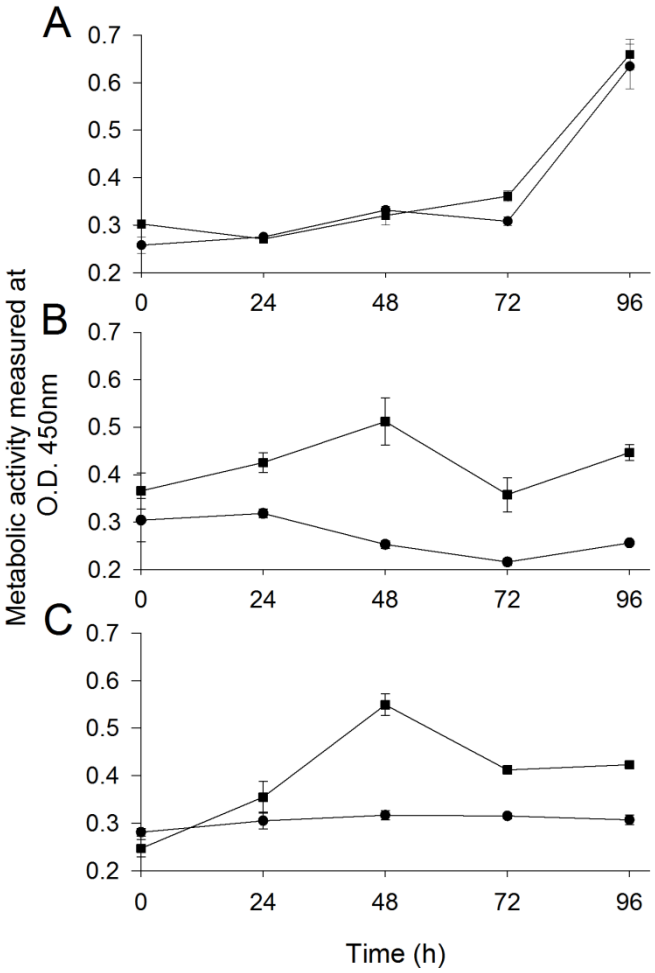

Figure 3.4: Comparison of the metabolic activity of infected (MOI=10) and uninfected U4.4, C7-10 and C6/37 cells.

(A) U4.4 cells. **(B)** C7-10 cells. **(C)** C6/36 cells. The O.D. at 450 nm gives a measure of the metabolic activity of the culture. Each time point is the mean of triplicate samples. The error bars indicate the standard error of the mean. ■ and ● indicate the uninfected and infected cultures respectively.

In U4.4 cells, the metabolic activity of the uninfected cultures increased over the 96 hours of the study. There did not appear to be any overgrowth of the culture due to the slow-growing nature of this cell type. The metabolic activity of the infected cultures was not affected; it remained very similar to the uninfected cultures, as shown in figure 3.4.

In C7-10 and C6/36 cells, the metabolic activity of the uninfected cultures reached a maximum at 48 h, decreased from 48 to 72 h and thereafter remained stable from 72

to 96 h. The decrease after 48 h was probably due to the accumulation of cells over time, contact inhibition and exhaustion of nutrients leading to decreased cell metabolism or possible cell death. The metabolic activity of infected cells remained constant throughout the 96 h studied indicating that the culture was viable for up to 96 h after infection. WST-1 only measures metabolic activity which is a product of several parameters including the number of cells, the cell proliferation rate and the cell death rate. The WST value did not change over time in the infected culture. That could indicate (i) all cells were static neither proliferating nor dying or (ii) that cells were dying and proliferating at the same rate with the metabolic activity of individual cells being unaffected by infection.

The cellular growth of infected mosquito cells

To directly determine the numbers of C6/36, C7-10 and U4.4 cells in infected and mock-infected cultures, a cell counting experiment was set up. Replicate cultures were set up in 24-well plates infected at 10 MOI with SFV4 or mock-infected. Cells were scraped off the plate and diluted with trypan blue at 0, 24, 48, 72 and 96 h post-infection for counting.

For all 3 cell types, the number of cells in the mock-infected cultures increased steadily over time (Figure 3.5). Infection had no effect on the number of U4.4 cells, the number continued to increase slowly as for the mock-infected cells. In contrast, the number of cells in infected C6/36 and C7-10 cultures did not change with time. Again as with the WST-1 data, these data do not distinguish between the possibility for the C6/36 and C7-10 infected cultures that, (i) the culture was static with no cell division and no cell death or (ii) cells in the culture were proliferating and dying at the same rate. However, the cell counts and the WST-1 data are in agreement that SFV4 has no effect on the growth of U4.4 cultures but strongly affects C6/36 and C7-10 cultures.

Trypan blue was used to dilute cells for counting to aid better visualisation of live cells as dead cells stain blue due to trypan blue uptake. The cell diluent in the U4.4 cell suspension was observed to be clear and blue, whilst noticeable amounts of very small cellular debris were observed in the cell diluent from C6-36 and C7-10. This

would be consistent with the hypothesis that cells in these cultures were proliferating and dying at similar rates.

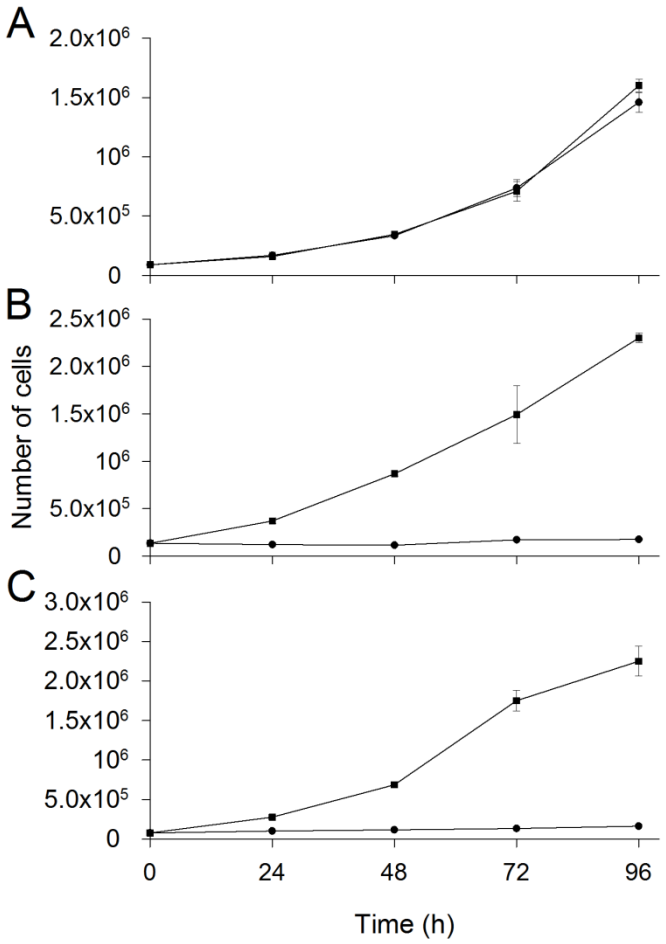

Figure 3.5: Cell growth after SFV4 infection (MOI=10) as measured by cell count.

(A) U4.4 cells. **(B)** C7-10 cells. **(C)** C6/36 cells. The cell count shows the number of cells present in the culture. Each point is the mean of triplicate samples. The error bars indicate the standard error of the mean. ■ and ● indicate the uninfected and infected cultures respectively.

There is an apparent difference in the cellular growth pattern between U4.4 , C6/36 and C7-10 infected cells. However, the virus growth curves are fairly similar from cell type to cell type (Figure 3.3).

The amount of virus being produced in mosquito U4.4 cell line from acute to persistent phase of infection.

Given the cell viability data it can least be concluded that unlike mammalian cells, mosquito U4.4 cells do not undergo apoptosis after SFV4 infection. The next study was designed to determine the amount of virus being produced by U4.4 cells during acute and persistent phases of infection and also to monitor the time of transition between phases. Cultures of $5x10^5$ U4.4 cells were infected synchronously with SFV4 (MOI=10). Aliquots of 100 µl supernatant were collected at 12, 24, 48, 72, 96 and 120 h post-infection. The remaining supernatant in the cells was completely replaced with fresh medium each time after an aliquot of supernatant was collected. Supernatant samples were kept in eppendorf tubes at -80^{o}C. All samples were titrated by plaque assay. As shown in Fig 3.6, high levels of virus production were observed from 0 to 24 hours post-infection. Thereafter, virus production dropped to low levels as the culture entered the persistent phase of infection.

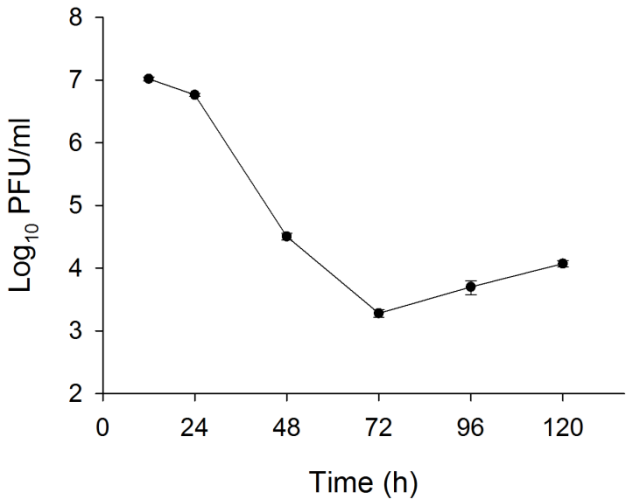

Figure 3.6: SFV4 production between each time interval up to 120 hours post-infection.

U4.4 cells were infected synchronously with SFV at MOI of 10. Supernatant was collected for titration at 12, 24, 48, 72, 96 and 120 h post-infection. The error bars indicate the standard error of the mean.

Video microscopy (See attached CD)

In the previous cell counting experiment, infected C6/36 and C7/10 had shown no increase in number of cells over 120 hours post-infection. Therefore, video microscopy was used to determine if these cultures maintained cell numbers by growing and undergoing apoptosis at the same rate or by cells becoming static post-infection. Video microscopy was also carried out on VRP infected U4.4 and C6/36 cells to observe viral marker gene expression from the acute phase to the persistent phase of infection in the absence of new virion production and new infection. A T25 flask was seeded with $5x10^5$ mosquito cells and incubated overnight at 28 ^oC. Cells were then infected with SFV1(3F)-ZsGreen at MOI=1. SFV1(3F)-ZsGreen is a propagating-deficient replicon with the ZsGreen fluorescent protein gene inserted at and fused with the C-terminus of nsP3. This suicidal replicon particle was used to infect cells at low MOI to show that a small amount of infected cells (with no second round of infection) were sufficient to cause arrest in number of cells in C6/36 culture. Secondly, ZsGreen fusion protein was used in attempt to produce greater emission signal for videomicroscopy, however, due to the nature of this construct, ZsGreen signal will be localised at the nucleus. The flask was then placed under the microscope for 16 hours of filming. All internal surfaces of the flask were rinsed with medium before filming started to avoid condensation forming on the inside of the top surface of the flask during the course of filming. The microscope was programmed to take one frame every three minutes under visible and UV light. An attempt to film one frame per minute resulted in total cell death due to over-exposure to UV light. A compact disk containing the video clips of video microscopy on U4.4 and C6/36 cell lines, infected and uninfected, is included at the back of the thesis. The videos are each 1 min 4 sec in length, 5 frames per sec, 320 frames in total.

The U4.4 cell cultures were heterogeneous and contained more than one cell type (this cell line was derived from whole mosquito larva.). In figure 3.7 U4.4(A), 4 frames of the uninfected U4.4 culture at 0 hour, 5 hours 15 min, 10 hours 45 min, and 16 hours of video time are shown. This video was filmed under 20 times magnification. As observed in the video of the non-infected culture, there were a variety of cells with different morphologies. Most of the observed cells were

rounded, and relatively stationary. However, approximately a quarter of the cells were highly motile and capable of travelling in and out of the microscopic field of observation. The morphologies of these motile cells resembled macrophages, and these cells could be haemocytes. These motile cells engaged with one cell and then actively travelled to another and appeared to engulf very small cell debris. The number of cells in the microscopic field increased from 40 to 53 over the period of observation thought this is not a good indication of the actual growth rate of the culture as different area of the flask had different numbers of settled cells. For the SFV infected cultures, videos were started at 6 hours post-infection. Therefore, video time label 0 hour is 6 hours post-infection. In SFV1(3F)-ZsGreen infected U4.4 cultures (figure 3.7 U4.4(B)), infected cultures appeared to behave like uninfected cultures, cell migration and cell division were observed. A video under UV light of the infected culture was taken and infected cells appeared green (figure 3.7 U4.4(C)). This showed that the viral marker gene from the structural region of the virus genome is expressed from 6 hours post-infection and the reporter eGFP remained visible throughout the entire course of filming. No second round of infection was observed.

The uninfected C6/36 cultures also appeared to contain more than one cell type. The first type of cells was rounded and was the predominant type of cell in the culture making up 90% of the population. These cells were rounded and appeared to be slightly smaller than U4.4 cells. None of the cells were capable of travelling a great distance (figure 3.7C6/36(A)). In infected C6/36 cultures, all cells appear to become static at video clip time 10 sec, which was 2 hours 30 after filming started and post-infection time 8 hours 30 minutes. No cell division and no cell death were observed throughout this static phase (figure 3.7C6/36(B)). Figure 3.7C6/36(C) shows the infected culture under UV light. This showed that infected C6/36 cells are going into static phase when infected, ruled out the possibility of cells dying and growing at the same rate.

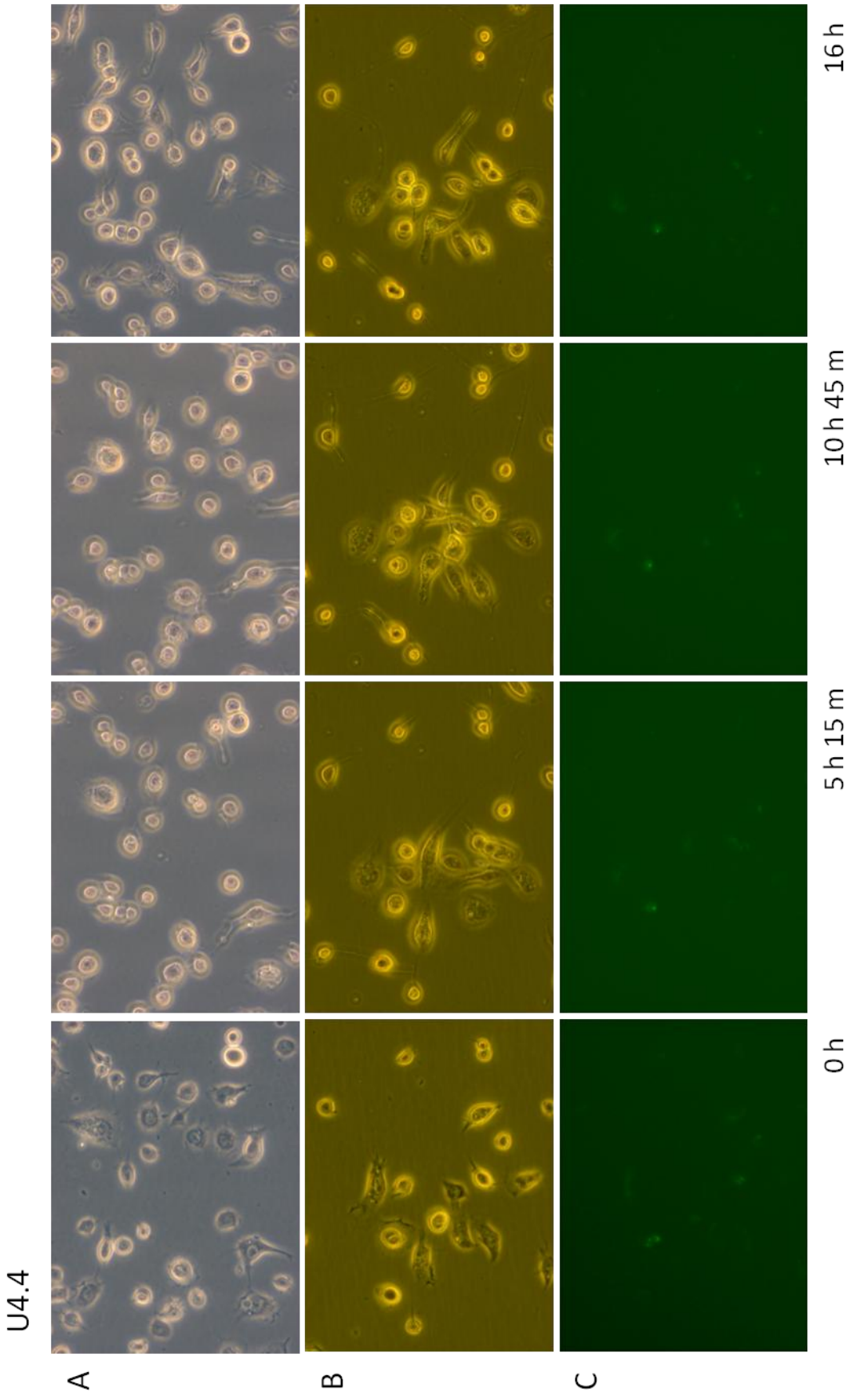
U4.4
A
B
C
0 h
5 h 15 m
10 h 45 m
16 h

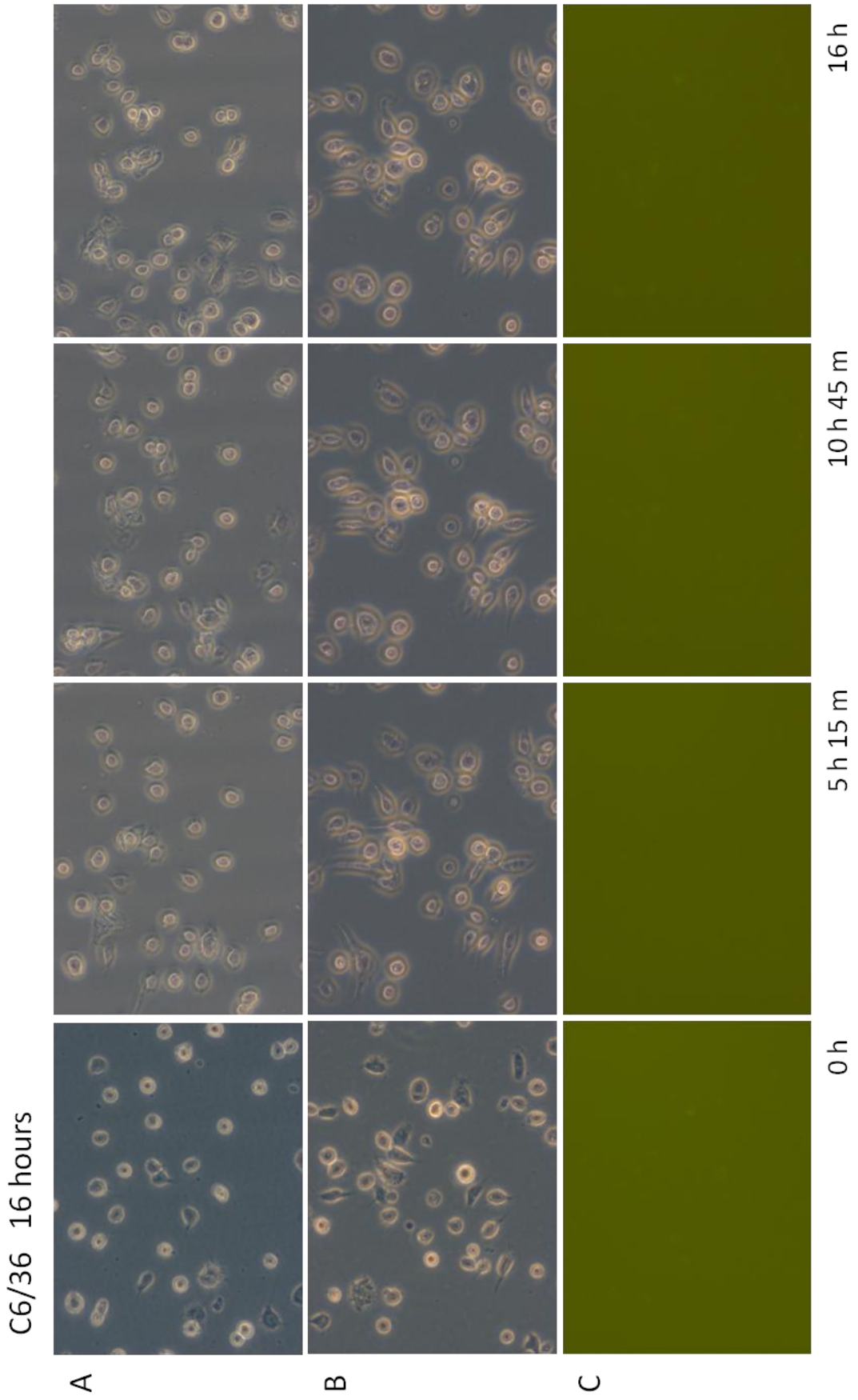
C6/36 16 hours
0 h
5 h 15 m
10 h 45 m
16 h
A
B
C

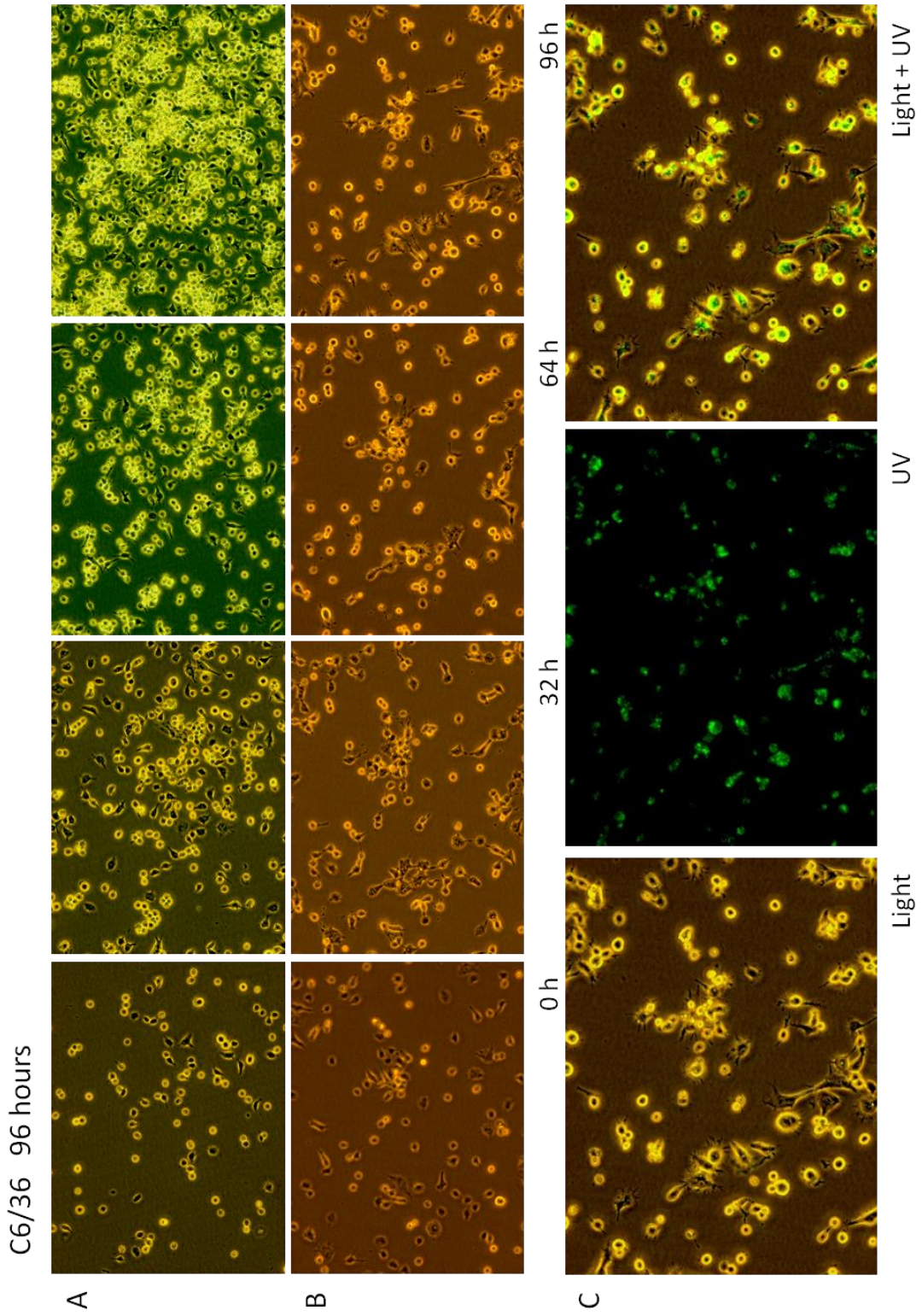

Figure 3.7: Video microscopy of SFV1(3F)-ZsGreen infected U4.4 and C6/36 cells.

U4.4 cells (page 87) and C6/36 cells (page 88) were infected with SFV1(3F)-ZsGreen, and light and UV video microscopy was performed as described in Chapter 2. Four subsequent frames are

displayed separately. (A) Top row, uninfected cells. (B) Middle row, infected cells. (C) Bottom row, infected cells under UV light. The total number of frames is 320, recorded during 16 hours, 20x magnification. Additional panel (page 89) shows C6/36 cells infected with SFV1(3F)-ZsGreen at 10 MOI, video microscopy was carried out under visible light. Four subsequent frames are displayed separately. (A) Top row, uninfected cells. (B) Middle row, infected cells. The total number of frames is 1920, recorded during 96 hours, 20x magnification. (C) Bottom row, photomicrographs of infected C6/36 cells taken at 96 hours post-infection (same culture as middle row). This showed C6/36 were infected with SFV1(3F)-zsGreen.

Summary of Findings

Infection of mosquito cells with SFV

- Infection of U4.4, C6/36 and C7-10 cells with SFV was established. Infection of U4.4 and C6/36 cells with SFV4-steGFP resulted in expression of eGFP. Immunostaining of SFV4-steGFP infected C7-10 cells using antibodies against nsp3 showed these cells were infected.
- The growth of SFV4 in the first 12 hours post-infection was characterised in all three mosquito cell lines. Growth was exponential from 4 to 8 hours post-infection. C6/36 cells produced virus most rapidly and reached almost 1 log higher titre at 12 hours in comparison to U4.4 or C7-10 cells.
- Infected U4.4 cells showed no change in the growth of the culture. In contrast, C6/36 and C7-10 infected cultures showed no growth.
- SFV production in U4.4 cells showed virus was being produced most rapidly during the acute phase of infection. The amount of virus being produced declined after 24 hours. Low level virus production was maintained from 72 hours onwards.

Video microscopy

- U4.4 cell cultures were heterogeneous and contained more than one cell type. Most of the cells were rounded, and relatively stationary. However, approximately a quarter of the cells were highly motile. These motile cells engaged with other cells in the culture and appeared to engulf cell debris.

SFV1(3F)-zsGreen VRP infected U4.4 cultures appeared to behave like uninfected cultures. Only a single round of infection was observed. A video of one of these cultures showed expression of the marker gene for 16 hours.

- C6/36 cultures were also heterogeneous. Cells were rounded and appeared to be slightly smaller than U4.4 cells. None of the cells were extensively motile. As shown in a video, infected C6/36 cultures became static. No cell division and no cell death were observed throughout this static phase.
- Video microscopy confirmed that infected C6/36 cells became static after infection. No cell division and no cell death resulted in maintenance of the cell number at the same level after infection.

Discussion

In this series of initial experiments, infection with SFV was established in three *Ae. albopictus* cell lines. U4.4, C7-10 and C6/36 cells were infected with SFV4-steGFP. The expression of virus promoter driven eGFP marker gene was observed 24 hours post-infection in U4.4 and C6/36 (Figure 3.2A & 3.2C). Immunostaining of SFV4-steGFP infected C7-10 and C6/36 cells using antibodies against SFV nsP3 showed these cells were infected and contained nsP3 in the cytoplasm (Figure 3.2B & 3.2C). Figure 3.2C showed eGFP signal overlapping with signal from immunostaining of nsP3 in C6/36 cells. In this figure, some cells contained eGFP signal only, some cells only contained red signal (staining for nsP3) and a few showed both signals. This indicated that infection at 10 MOI did not infect all the C6/36 cells in the culture simultaneously because different stages of the virus life cycle were observed. The green cells are cells which were initially infected by the virus and are at a late stage of viral replication. At the late stage of infection, nsP3 is not being made and only viral genes driven by the non-structural promoter are being expressed. The red cells represent cells which were not initially infected but were subsequently infected by virus released from initially infected cells. Therefore, the red cells are at an early stage of infection, and only non-structural genes are being transcribed and translated. The cells showing both red and green are going through the transition from early to

late stage of infection where nsPs are not yet fully degraded and structural genes are being transcribed and translated.

The growth of SFV4 in each of the mosquito cell lines was characterised by 12-hour one step growth curves which showed that all three cell lines are capable of supporting the growth of virus from stationary through exponential to plateau phase. The exponential growth phase took place from 4 to 8 hours and started to reach plateau from 8 hours post-infection. Cell line C6/36 produced the highest yield of SFV4 in comparison to U4.4 and C7-10 which is in agreement with previous observations that C6/36 produces highest virus yield amongst other clones and viruses tested (Igarashi, 1978). In C7-10 cells, the virus titres at 2 and 4 hours post infection were below the limit of detection. These time points are inconclusive and time constraints did not allow me to repeat it to resolve this matter. However, based on the later time points I would expect the virus to follow a very similar pattern to the U4.4 cells.

Although all three of the mosquito cell lines support virus infection and have been shown to maintain infection in low titre through passages, their morphological and growth responses are different during the course of infection. Only U4.4 cells displayed no change in the growth of the culture after SFV infection, whereas the growth of C6/36 and C7-10 cells appeared to be adversely affected. Therefore, WST-1 assay and cell counting was carried out. In the U4.4 cells the uninfected and infected cultures had similar metabolic activity and numbers of cells over 96 hours. At 72 hours post-infection the metabolic activity of both infected and uninfected cells did not double from 48 hours post-infection (Figure 3.4A) and generate a smooth curve as observed in the results in cellular growth of infected mosquito cells (Figure 3.5A). This could be due to the number of cells seeded in that column of the 96-well plate (the column used for the 72 hour assay) being slightly lower than other columns because cells in suspension precipitate over the course of manual pipetting. Nevertheless, figure 3.4A shows that the metabolic activity of infected and uninfected U4.4 cells closely resembled each other. The C6/36 and C7-10 cells showed no increase in metabolic activity or cell number in infected cultures 96 hours post-infection. However, these results did not determine whether infected C6/36 and

C7-10 become (i) static with no cell division and no cell death or (ii) were proliferating and dying at the same rate. It was later revealed by video microscopy that these cells remained static with no cell division and no cell death caused by SFV1(3F)-zsGreen infection of C6/36 culture. The use of suicidal SFV1 particles to infect cells at low MOI also showed perhaps an extracellular signal was produced from the few infected C6/36 cells to the rest of the uninfected C6/36 in the culture. This signal is perhaps also contributed in the anitiviral activity reported by Riedel and Brown in 1978. In fact, a pilot experiment was carried out and showed a putative signal factor was produced which influenced growth and affected subsequent infection by transferring supernatant from SFV1 infected C6.36 cells (MOI=1) to uninfected C6/36 culture (results not shown). The results were not further pursued because it is beyond the scope of interest and the involvement of extracellular signalling, low molecular weight fractionation require different equipments and skill set from this laboratory. Video microscopy also showed that U4.4 cells were heterogeneous and contained cells resembling macrophages. These motile cells were capable of travelling great distance and engulfing cell debris.

In conclusion, U4.4 cells displayed a number of characteristics ideal for experiments to investigate virus replication. The growth rate of U4.4 cells is much slower than C7-10 and C6/36 cells. This allows experiment to be performed at a higher cell density without the complication of over-growth and contact inhibition. The growth of U4.4 cultures was not affected by infection with SFV, and they showed the acute phase of virus production from 12 to 24 hours and transition to low virus production during the persistent phase of infection (Figure 3.8, below). This pattern of infection was similar to the earlier experiments of Davey & Dalgarno (Davey & Dalgarno, 1974). These properties of U4.4 cells were also in agreement with infection of U4.4 cells with Sindbis virus (Mudiganti *et al*., 2006). This means during the course of infection, cell metabolism was not under stress whilst the ability to control SFV infection was maintained.

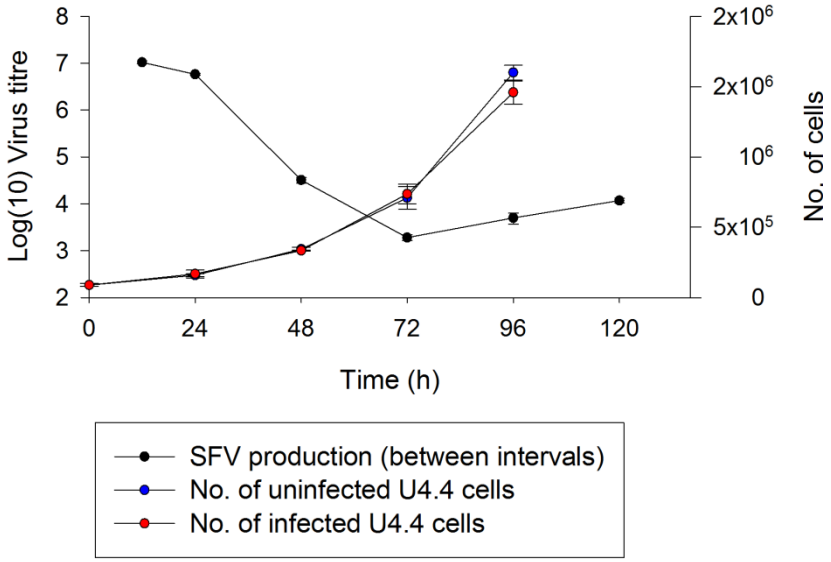

Figure 3.8: SFV4 production in U4.4 cells and characteristics of U4.4 cells infected with SFV4.

U4.4 cells were infected synchronously with SFV at MOI of 10. Supernatants were collected for titration at 12, 24, 48, 72, 96 and 120 h post-infection. Virus titre ● is represented in Log_{10}(PFU) ● indicated on the left Y-axis. Infected and uninfected U4.4 cell numbers were counted up to 96 hours, represented in number of cells on the right Y-axis. Each point is the mean of triplicate samples. The error bars indicate the standard error of the mean.

Table of contents

Chapter 4: Investigation of the effect of mosquito innate immune pathways on virus replication

Introduction

Viruses and other intracellular pathogens have to overcome cellular host defences to replicate efficiently. In vertebrates, detection of viral molecular patterns, for example dsRNA, is an important trigger of antiviral defences.

Insects have a potent innate immune response that effectively protects them against fungi and bacteria (Silverman & Maniatis, 2001). For example, *Drosophila* produces seven types of antimicrobial peptides (AMPs) in response to fungal or bacterial infection (Hoffmann & Reichhart, 2002). Insect innate immune defences have been studied mostly in *D. melanogaster*; in which fungi and Gram-positive bacteria activate the Toll pathway (Ferrandon *et al*., 2004). The activation of Toll pathway leads to the production of AMPs such as Drosomycin and Metchnikowin in *Drosophila*. Mutant flies fail to produce these two AMPs are susceptible to infections with the filamentous fungus *Aspergillus fumigates* (Lemaitre *et al.*, 1996). Gram-negative bacteria activate the IMD pathway (Royet, 2004) and JNK pathway (Silverman & Maniatis, 2001). The activation of IMD pathway induces the production of AMPs such as attacin, cecropin, defensin, diptericin, and drosocin. *Drosophila* failed in producing these AMP genes due to a recessive mutation in the IMD pathway has been shown to be more susceptible to Gram-negative bacteria (Lemaitre *et al.*, 1995). In *Anopheles* mosquitoes, dsRNA RNAi-mediated knockdown of defensin has been shown to be essential for defense against Gram-positive bacteria (Blandin *et al.*, 2002). Defensin is important as innate antiviral immunity in mammals, which can block viral infection by directly interacting with the viral envelopes or through interaction with the host cell (Chang *et al.*, 2005; Daher *et al.*, 1986; Wang *et al.*, 2004).

These fundamental immune signalling pathways and the RNAi response (Sanchez-vargas *et al*., 2004; Zdobnov *et al*., 2002) are conserved in *Aedes* and *Anopheles* mosquitoes. However, little is known about how these pathways respond to virus

infections. Arboviruses establish persistent infections in insect cells, as opposed to causing cell death in vertebrate cells. This suggests that the insect's ability to control of viral infections lies within the functions of innate immune defences.

Although the IMD and Toll pathways are activated upon bacterial and fungal stimulation, activation of these pathways ultimately activates the transcription factors Relish and Dif, the homologue of NF-κB. Therefore, activation of these innate immune pathways may induce transcription of genes that share the same promoter element which is involved in the defence against virus infection. In *Drosophila*, the STAT and IMD pathways are involved in responses to drosophila C and *Drosophila* X viruses (Dostert *et al.*, 2005; Zambon *et al.*, 2005). The Toll pathway has been shown to be involved in the control of Dengue virus infection in Aag2 cells, with up-regulation of two Tolls, MyD88, and Rel1. Furthermore, a comparison between the transcriptomes of DENV-infected Aag2 cells and Toll pathway-activated Aag2 cells (RNAi-mediated silencing of Cactus) revealed a great percentage of overlap genes that changed in expression level (Sim & Dimopoulos, 2010). DNA micro-array analysis of the gene expression by midgut cells of *Ae. aegypti* infected with Sindbis virus showed that genes involved in Toll and IMD were up-regulated early in infection, whereas JNK and RNAi (dicer-2) genes were down-regulated in the midgut of infected mosquitoes (Sanders *et al.*, 2005). The JAK-STAT pathway is activated in *Ae. Aegypti* mosquitoes infected with DENV and the mosquito's susceptibility to DENV infection increases when JAK-STAT pathway is suppressed through RNAi depletion of its receptor Dome and the Janus kinase Hop. Furthermore, mosquitoes become more resistance to DENV infection when JAK-STAT is up-regulated prior to infection (Souza-Neto *et al.*, 2009).

The interplay between mosquito cell signalling pathways and alphaviruses is not understood. The principle aim of this series of experiments was to determine whether activation of STAT/IMD or Toll pathways had any anti-viral effect on SFV replication (represented by viral gene expression). The STAT/IMD or Toll pathways were activated in U4.4 cells prior to infection and viral gene expression was determined by the level of viral reporter gene expression. Two reporter viruses SFV4(3H)-*RLuc* or SFV4-st*RLuc* were used to determine the effect of these

pathways on the early and late stage of virus replication. The expression of *Renilla* luciferase is driven by the viral non-structural promoter of SFV4(3H)-*RLuc* and the structural promoter of SFV4-st*RLuc*. The effect of these pathways on early or late virus replication can be interpreted as the changes of *Renilla* luciferase expression by these reporter viruses.

Characterisation of SFV4(3H)-*RLuc* and SFV4-st*RLuc* marker viruses in U4.4 mosquito cells

New reporter viruses with a *Renilla* luciferase (*RLuc*) gene inserted into either the non-structural or the structural ORF were available for this study (Figure 4.1). These viruses were constructed by Prof. Andres Merits but had not previously been characterised. To examine the replication ability of these viruses, one-step growth curves were determined.

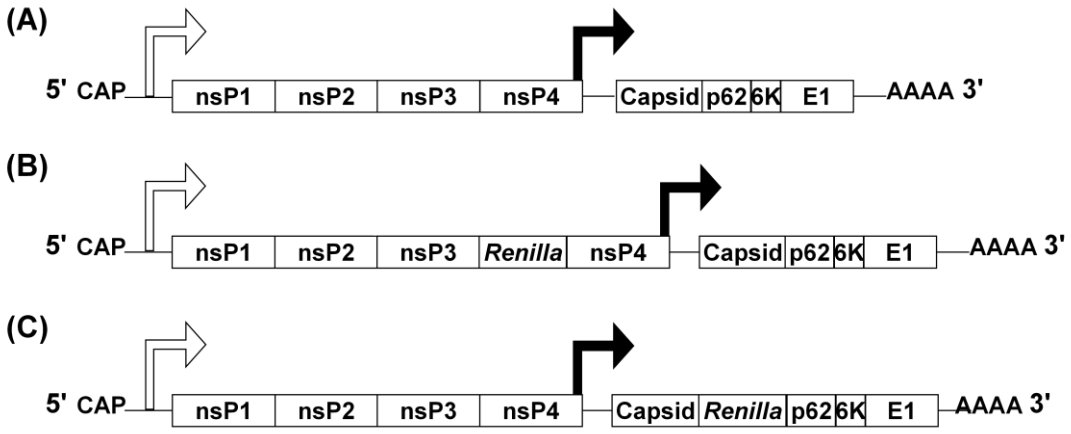

Figure 4.1: A Schematic representation of SFV4, and *RLuc* expressing SFV4 constructs.

(A) SFV4. **(B)** SFV4(3H)-*RLuc*. This is an SFV4 construct with the *RLuc* gene inserted between nsP3 and nsP4. *RLuc* is translated as part of the non-structural polyprotein. The native nsP2 protease recognition site (C-terminus of nsP3) and its duplicate (fused at the C-terminus of *RLuc*) gives rise to mature *RLuc* through expression of non-structural genes. **(C)** SFV4-st*RLuc*. This is an SFV4 construct with the *RLuc* gene inserted between the capsid and p62 genes. *RLuc* is flanked by three N-terminal amino acids (SAP) of the p62 protein at the N-terminus and a 2A peptide sequence from FMDV at the C-terminus translated as part of the structural polyprotein.

One step growth curve analysis was carried out to characterise SFV4(3H)-*RLuc* and SFV4-st*RLuc* along with the control SFV4 in U4.4 mosquito cells (Figure 4.2). All three growth curves started with the stationary phase, then went into exponential phase at 6 hours post-infection. At early time points (2 and 4 hours post-infection), SFV4(3H)-*RLuc* had higher average titres than SFV4. However, the error bars on those two time points were large and overlapped the average titre of SFV4. This indicates that determination of the replication kinetics of SFV4(3H)-*RLuc* was

inconclusive. Based on the titres of SFV4 and SFV4(3H)-*RLuc* at 2 and 4 hours post-infection, the steep descrease of SFV4-st*RLuc* titre at 2 and 4 hours post-infection is unlikely to be the natural replication pattern. I would expect the virus titre of SFV4-st*RLuc* to follow a similar pattern to SFV4 at those time points. However, time constraints did not allow me to repeat the experiment to resolve this matter. All three viruses reached maximum titre at 12 hours post-infection. At 10 hours post-infection, the virus tires of both recombinant viruses, SFV4(3H)-*RLuc* and SFV4-st*RLuc*, were significantly lower than the SFV4 titre (P = 0.0001 and 0.0003 respectively, by statistical comparison with a nonparametric unpaired t test). The titres of SFV4(3H)-*RLuc* and SFV4-st*RLuc* were also significantly lower than SFV4 at 12 hours post-infection (P = 0.0028 and 0.0038 respectively, by statistical comparison with a nonparametric unpaired t test). The lower titre of the recombinant marker viruses suggested that insertion of the marker gene had compromised the replication of the virus.

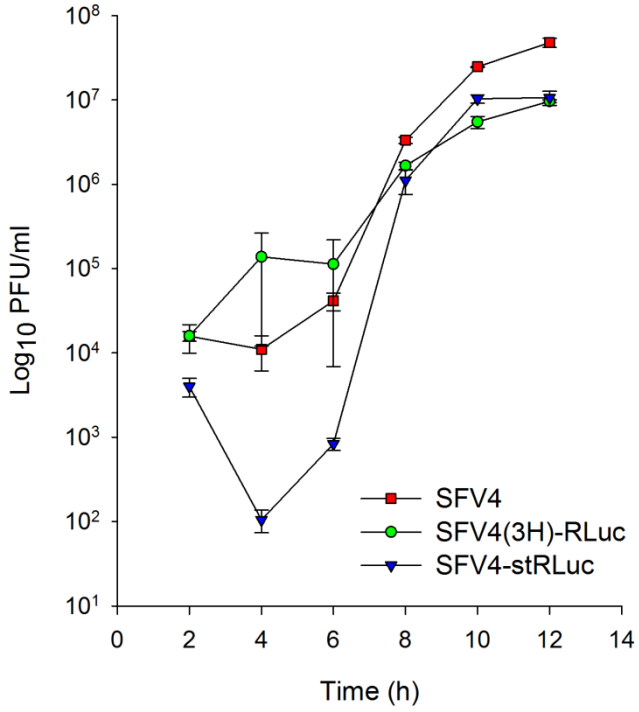

Figure 4.2: Growth curves of SFV4, SFV4(3H)-*RLuc* and SFV4-st*Rluc* in U4.4 cells up to 12 hours post-infection (MOI=10).

Virus titres were determined every two hours by plaque assay. Each point is the mean of triplicate samples. The error bars indicate the standard error of the mean.

Activation of STAT/IMD pathways in U4.4 cells

To activate STAT/IMD pathways in U4.4 cells, U4.4 cultures were incubated with heat killed bacteria for one hour. The control experiment to determine the activation of STAT/IMD pathways was carried out by Rennos Fragkoudis and Yi Chi (Fragkoudis *et al.*, 2008). The Firefly luciferase expression plasmids p6x2DRAF-Luc or pJL169 (containing respective promoters for STAT or IMD inducible signalling pathways) were transfected prior to stimulation with heat-killed bacteria. The activation of STAT and IMD pathways were detected as Firefly luciferase expression after heat-killed bacterial stimulation.

Effect of activation of STAT/IMD pathways on SFV gene expression in U4.4 cells

To activate the STAT/IMD pathways, triplicate cultures were set up in 6-well plates with 5 x 10^6 U4.4 cells in each well. *E. coli* JM109 was grown overnight, harvested and resuspended in 500 µl of SPBS. The bacterial suspension was killed by heating to 98^{o}C for 5 minutes. Five µl of heat killed bacteria was added to each well of U4.4 cells to stimulate their STAT/IMD pathways. An hour later, stimulated cells were infected (MOI=1) with SFV4(3H)-*RLuc* or SFV4-st*RLuc*. A mock-infection was included as a negative control. A separate control experiment carried out by Yi Chi, another student in the laboratory, showed that SFV infection of U4.4 mosquito cells does not activate the STAT or IMD signalling pathways (Data not shown) (Fragkoudis *et al.*, 2008).

The ideal time to measure viral marker gene expression had to be determined. Therefore, to determine the ideal time post-infection to observe the effect of STAT/IMD activation on viruses, experiments were set up and cells were lysed at 1, 2, 3, 4, 5, 6 and 12 hours post-infection and viral marker gene expression was determined by luciferase assay (Figure 4.3). The experiment was carried out in triplicate. The luciferase expression for both SFV4-st*RLuc* and SFV4(3H)-*RLuc* was reduced by 40% when the cells had been previously simulated with heat-killed bacteria at all the tested time points. At 12 hours post infection, the luciferase

activities for SFV4(3H)-*RLuc* infected U4.4 cells and U4.4 cells stimulated with heat-killed bacteria were $4x10^4$ and $2.3x10^4$ respectively; for SFV4-st*RLuc* infected U4.4 cells and U4.4 cells stimulated with heat-killed bacteria were $9.5x10^5$ and $5.2x10^5$ respectively. In both control and heat-killed bacteria stimulated U4.4 cells, SFV4-st*RLuc* had 23-fold more luciferase activity than SFV4(3H)-*RLuc*. This is because by 12 hours post-infection the virus replication entered the late phase in which mature replication complexes focus on the production of positive strand and 26S sub-genomic RNA. The large quantity of 26S sub-genomic RNA was being translated into structural proteins (including the marker gene). In contrast at 6 hours post-infection, the luciferase activities measured from SFV4-st*RLuc* were only 3.6- and 2.2-fold more than SFV4(3H)-*RLuc* infected control and heat-killed bacteria-stimulated cells respectively. This indicated that, at 6 hours post-infection, virus replication had just made the transition to produce positive-strand and 26S sub-genomic RNA. This suggested that 12 hours post-infection is a more suitable time to measure the fully-expressed structural and non-structural marker genes.

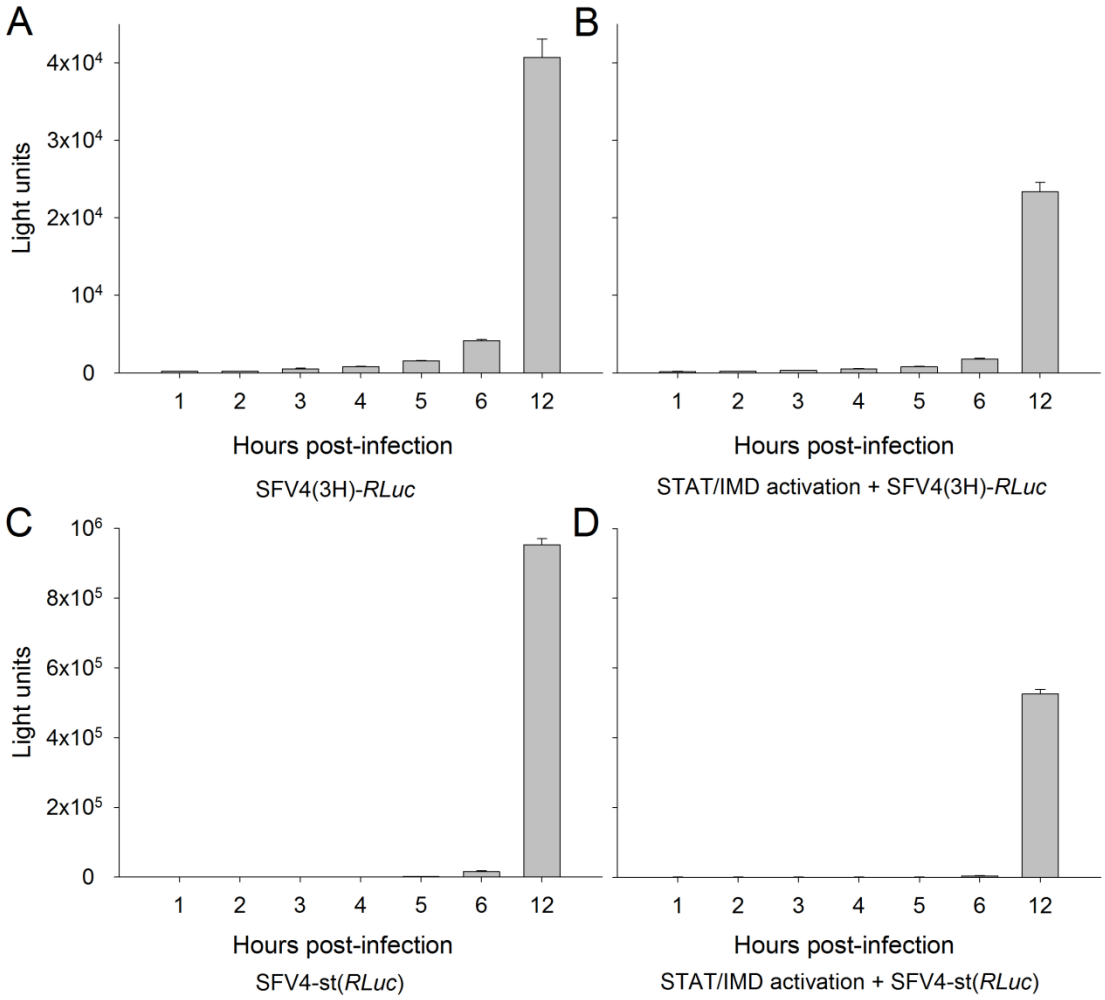

Figure 4.3: Effect of activation of STAT/IMD pathway on virus driven *RLuc* expression, measured between 1 and 12 hpi; U4.4 cells infected at MOI=1 with SFV4(3H)-*RLuc* and SFV4-st*RLuc*.

(A) A control experiment for SFV4(3H)-*RLuc*, showing luciferase expression at 1, 2, 3, 4, 5, 6 and 12 hours post-infection without prior activation of STAT/IMD. **(B)** Luciferase expression at indicated hours post-infection. STAT/IMD pathways were activated by heat killed bacteria prior to SFV4(3H)-*RLuc* infection. **(C)** A control experiment for SFV4-st*RLuc*, showing *RLuc* expression at indicated hours post-infection without prior activation of STAT/IMD. **(D)** Luciferase expression at indicated hours post-infection. STAT/IMD pathways were activated by heat killed bacteria prior to SFV4-st*RLuc* infection. Each bar is the mean of triplicate samples. *RLuc* expression measured in activity by luminometer. The error bars indicate the standard error of the mean.

To determine the ideal MOI for infection and the effect of STAT/IMD activation on SFV4(3H)-*RLuc* and SFV4-st*RLuc*, three independent experiments were carried out with infection at MOI of 0.1, 1 and 10. SFV4 infection was carried out a as control. Cultures were lysed 12 hours post-infection and viral marker gene expression was determined by luciferase assay (Figure 4.4).

At MOI=0.1, the mean luciferase expression of SFV-st*RLuc* in control U4.4 cell cultures was 1.4 x 10^4 light units (Figure 4.4A bar 3). In heat-killed *E. coli* stimulated cultures, mean expression was 6.6x10^3 light units (Figure 4.4A bar 4). For SFV4(3H)-*RLuc*, mean luciferase expression in the control experiment was 1.4x10^4 light units (Figure 4.4A bar 5), and 8.6x10^3 light units (Figure 4.4A bar 6) in stimulated cultures. At this MOI, luciferase expression controlled by the structural gene promoter was reduced by 54% and by 41% for the non-structural gene promoter after activation of STAT/IMD pathways. At MOI=1, a 44% reduction was observed in SFV4-st*RLuc* expression from 9.5x10^5 to 5.2x10^5 light units (Figure 4.4B bars 3&4) and also a 44% reduction observed in SFV4(3H)-*RLuc* from 4x10^4 to 2.3x10^4 light units (Figure 4.4B bars 5&6). At MOI=10, a 48% reduction was observed in SFV-st*RLuc* expression from 1.3x10^6 to 6.8x10^5 light units (Figure 4.4C bars 3&4) and a slight gain of 1.5% in SFV4(3H)-*RLuc* (Figure 4.4C bars 5&6).

At MOI of 0.1 and 1, the luciferase activity expressed by both SFV-st*RLuc* and SFV4(3H)-*RLuc* infected cells was reduced by a similar percentage after stimulation with heat-killed bacteria. However, the luciferase expression from cells infected with SFV-st*RLuc* at MOI=0.1 was low (e.g. mean expression from stimulated cells was 6.6 x 10^3 light units) which makes measurement more prone to errors. In contrast, at MOI=1 luciferase expression was much higher and produced less error within replicate experiments. At MOI=10, the luciferase expression from SFV4(3H)-*RLuc* was not reduced in cells stimulated by heat-killed bacteria. This indicates that, at a higher multiplicity of infection, early virus replication could overcome the pre-activated STAT/IMD pathways. It is interesting that although early replication had apparently overcome the pre-activated STAT/IMD pathways, the late replication stage remained suppressed as indicated by the reduction in luciferase expressed from SFV-st*RLuc*. In conclusion, infection at MOI=1 produced accurate results and

showed that the effect of activated STAT/IMD pathways can interfere with early and late SFV replication in U4.4 cells. This MOI was therefore used in subsequent experiments.

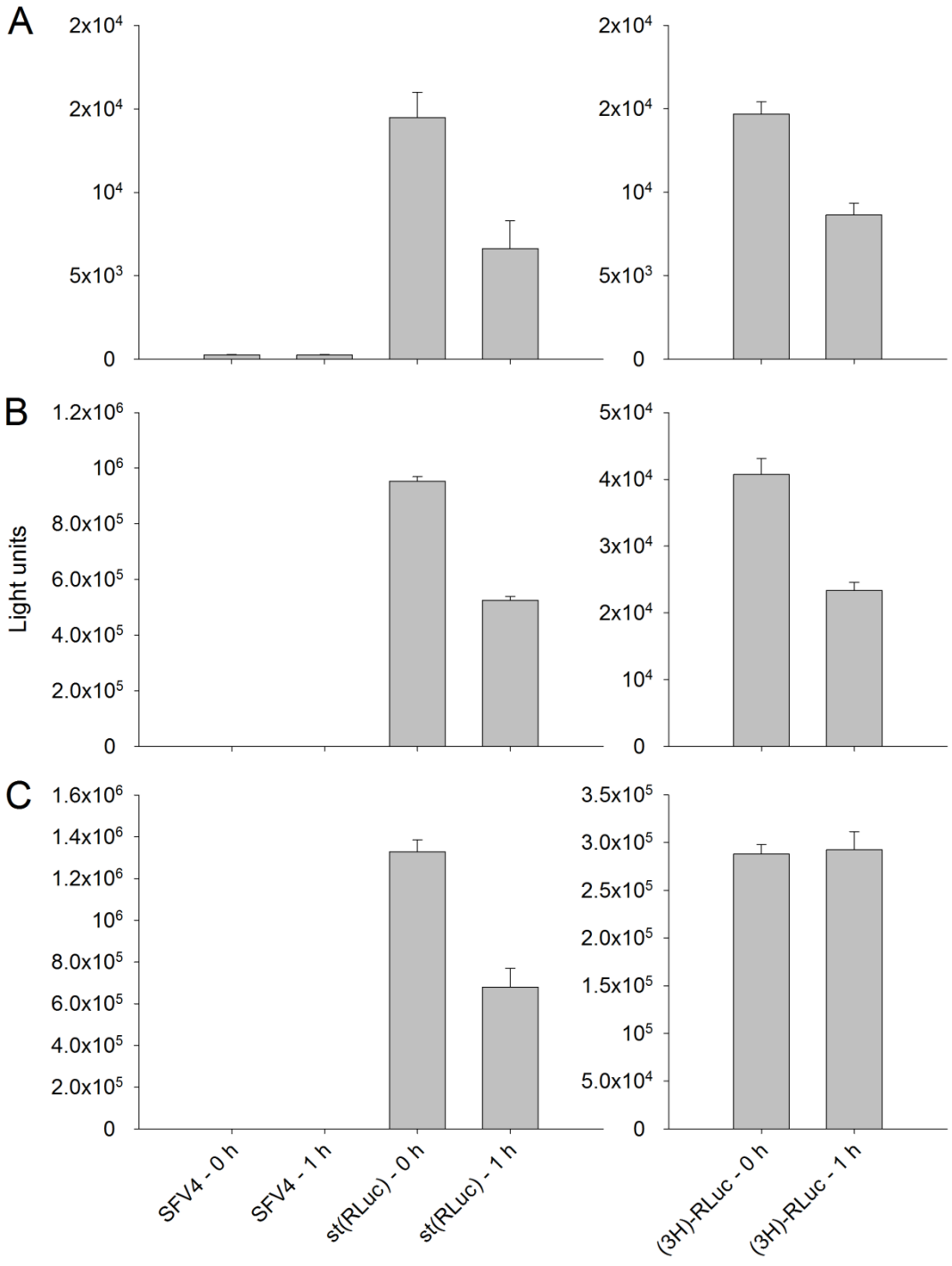

Figure 4.4: The effect of activated STAT/IMD pathway at different multiplicity of infection.

RLuc expression measured in light units from U4.4 cells at 12 hours post-infection at **(A)** MOI=0.1, **(B)** MOI=1, and **(C)** MOI=10 with SFV4, SFV4-st*RLuc* and SFV4(3H)-*RLuc*. 0 h and 1 h indicates the amount of time the cell cultures had been stimulated with *E. coli*. *RLuc* production measured as activity by luminometer. Each bar is the mean of triplicate samples. The error bars indicate the standard error of the mean.

Effect of activation of STAT/IMD pathways on SFV replication in U4.4 cells

To determine the effect of STAT/IMD activation on SFV replication, STAT/IMD pathways were activated in cultures prior to infection and progeny virus titrated. Triplicate cultures were set up in 6-well plates with $5x10^6$ U4.4 cells in each well. STAT/IMD pathways were activated on the next day with heated-killed *E. coli* prior to SFV4 infection. STAT/IMD pathways were activated by 5 µl of heat-killed bacteria per well of U4.4 cells for 1 hour prior to SFV4 infection (MOI=1). Control wells received SPBS alone followed by infection. The supernatants were collected 12 and 24 hours after infection. All samples were titrated by plaque assay. An unpaired non-parametric t test indicated the virus titres between non-activated and activated (STAT/IMD) cultures at 12 hours post-infection were not significantly different, P = 0.3571. However, the titres were significantly lowered by 60% at 24 hours, P = 0.0336 (Figure 4.5).

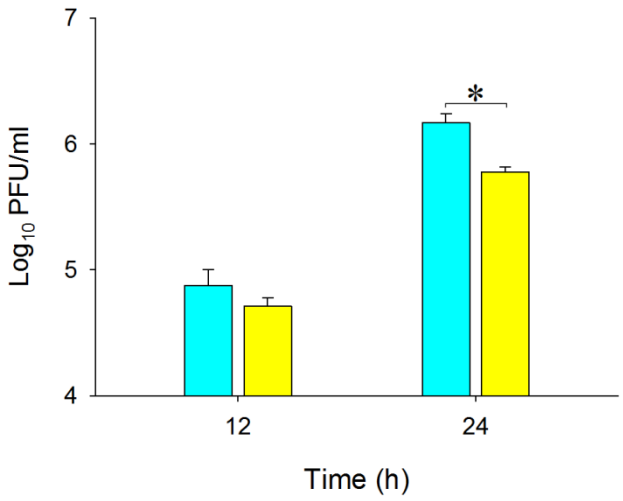

Figure 4.5: The effect of activation of the STAT/IMD pathway on SFV4 replication in U4.4 cultures.

The amount of virus produced in U4.4 cells was measured at 12 and 24 hours post-infection (MOI=1) by plaque assay. The blue bars are control cultures in which STAT/IMD were not activated. The yellow bars represent STAT/IMD activated cultures. Each bar is the mean of triplicate samples. The error bars indicate the standard error of the mean. * $p<0.05$ by (unpaired nonparametric t tests)

Activation of Toll pathway in U4.4 cells

To activate the Toll pathway in U4.4 cells, plasmid pJL195 (a construct based on the insect competent plasmid pIB-V5/His into which a mutated toll receptor gene sequence was inserted) was transfected into mosquito cells. This mutated toll receptor (Toll Δ LRR) is constitutively active, recruits and phosphorylates downstream signalling molecules (Tauszig *et al*, 2000). The control experiment to determine the activation of Toll pathway was carried out by Rennos Fragkoudis and Yi Chi (Fragkoudis *et al.*, 2008). The Firefly luciferase expression plasmid pJM648 (containing Toll responsive promoter for STAT or IMD inducible signalling pathways) were co-transfected with pJL195. Activation of the Toll pathway was detected as Firefly luciferase expression.

Effect of activation of Toll pathway on SFV gene expression in U4.4 cells

To determine whether activation of the Toll pathway has any effect on SFV replication, the Toll pathway was activated in U4.4 cells prior to infection and virus replication was determined by the level of marker gene expression. Twelve hours after the pJL195 plasmid was transfected, cells were infected with SFV4(3H)-*RLuc* or SFV-st*RLuc* at MOI=1. A control experiment was carried out with cells transfected with an empty plasmid, pIB-V5/His, followed by infection with SFV4(3H)-*RLuc* or SFV4-st*RLuc* at MOI=1. Cells were lysed at 12 h post-infection and viral marker gene expression was determined by luciferase assay.

Luciferase expression of SFV4-st*RLuc* and SFV4(3H)-*RLuc* in Toll-activated cultures was similar to the expression in the controls. These results showed that production of luciferase within infected cells was not affected by activation of the Toll pathway. An unpaired non-parametric test indicated that expression levels in non-activated and activated Toll cultures for SFV4-st*RLuc* and SFV4(3H)-*RLuc* were not significantly different; $P = 0.7194$ and 0.1399 respectively. Therefore, activation of the Toll pathway does not affect production of proteins encoded by either the structural or non-structural ORF of the viral genome.

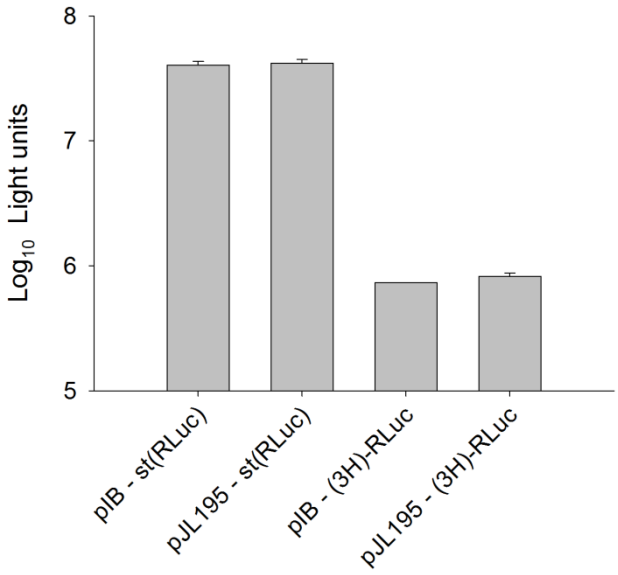

Figure 4.6: The effect of activation of the Toll pathway on virus-driven *RLuc* expression in U4.4 cells infected with SFV4-st*RLuc* and SFV4(3H)-*RLuc* (MOI=1) at 12 hours post-infection.

Y-axis legends: pIB – st(*RLuc*) = control non-activated culture which received a blank pIB-V5/His plasmid, followed by infection with SFV4-st*RLuc*; pJL195 – st(*RLuc*) = activated culture in which Toll pathways in the cell culture were activated by transfection of plasmid pJL195, followed by infection with SFV4-st*RLuc*; pIB – (3H)-*RLuc* = control non-activated culture which received a blank pIB-V5/His plasmid, followed by infection with SFV4(3H)-*RLuc*; pJL195 – (3H)-*RLuc* = activated culture in which Toll pathways in the cell culture were activated by transfection of plasmid pJL195, followed by infection with SFV4(3H)-*RLuc*. Each bar is the mean of triplicate samples. The error bars indicate the standard error of the mean.

Effect of activation of Toll pathway on SFV replication in U4.4 cells

To determine the effect of activated Toll pathway on SFV titres, triplicate cultures were set up in 6-well plates with $5x10^6$ U4.4 cells in each well. The toll pathway was activated by transfection of plasmid pJL195. The plates were then incubated for 12 hours before infection with SFV4 (MOI=1). As controls, cultures were transfected with an empty plasmid, pIB, prior to SFV4 infection (MOI=1). The supernatants from transfected and control cultures were collected 12 and 24 hours post-infection. The supernatants were titrated by plaque assay. The resulting titres indicated little or no difference between Toll activated and non-activated cultures at 12 and 24 hours post-infection. An unpaired non-parametric t test indicated that the virus titres in

non-activated and Toll-activated cultures at 12 hours and 24 hours post-infection were not significantly different; P = 0.4738 and 0.5455, respectively (Figure 4.7).

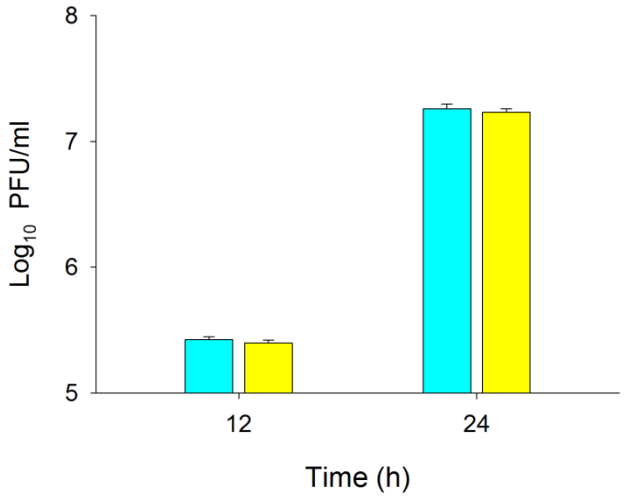

Figure 4.7: The effect of activated Toll pathway on SFV4 titres in U4.4 cultures.

The amount of virus produced in U4.4 cells was measured 12 and 24 hours post-infection (MOI=1) as plaque forming units by plaque assay. The blue bars are control cultures in which Toll was not activated. The yellow bars represent Toll activated cultures. Each bar is the mean of triplicate samples. The error bars indicate the standard error of the mean.

Effect of activation of STAT/IMD and Toll pathways on SFV gene expression in U4.4 cells

To determine if STAT/IMD and Toll together have a combined effect on SFV viral gene expression, both pathways were activated in cultures prior to infection. Triplicate cultures were set up in 6 well plates with 5 x 10^6 U4.4 cells in each well. Cells were transfected with pJL195 or pIB-V5/His as control. Plates were then incubated for 12 hours prior to addition of 5 µl of heat-killed bacteria followed by one hour of incubation. Cultures were then infected at MOI=1 with SFV4(3H)-*RLuc* or SFV4-st*RLuc*. Cells were lysed at 12 hours and viral marker gene expression was determined by luciferase assay. An unpaired non-parametric t test indicated that, for SFV4-st*RLuc*, expression levels in STAT/IMD/Toll activated cultures were significantly increased by 28.9% (P = 0.0300) than in STAT/IMD only activated cultures, whereas for SFV4(3H)-*RLuc* , they were significantly reduced by 20% (P = 0.0021) (Figure 4.8).

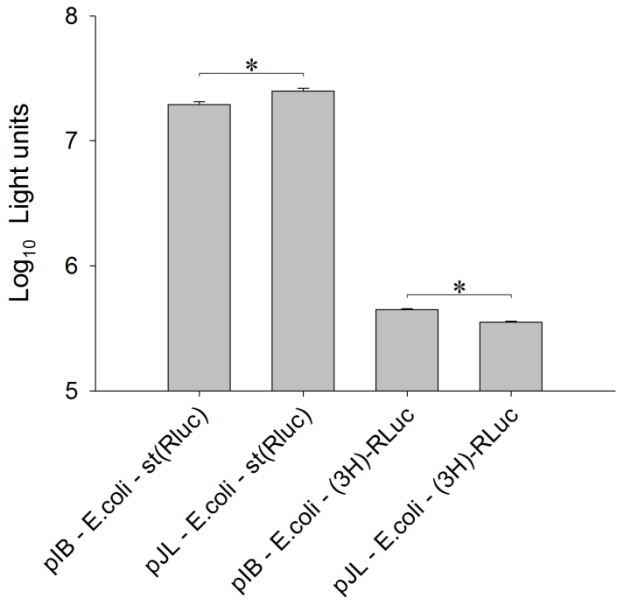

Figure 4.8: Effect of Toll and STAT/IMD activation on SFV replication measured in luciferase light units.

U4.4 cultures transfected with pIB-V5/His (STAT/IMD activation) or pJL195 (STAT/IMD/Toll activation) and treated with heat-killed *E. coli* prior to SFV infection. *RLuc* was measured in U4.4 cells 12 h after infection (MOI=1) with SFV4-st*RLuc* or SFV4(3H)-*RLuc*. Each bar is the mean of triplicate samples. The error bars indicate the standard error of the mean. * $p<0.05$ (unpaired nonparametric t tests)

Effect of activation of STAT/IMD and Toll pathways on SFV replication in U4.4 cells

To determine if STAT/IMD and Toll together have a combined effect on SFV titres, both pathways were activated in cultures prior to infection. Triplicate cultures of U4.4 cells were set up in 6-well plates (5×10^6 in each well). The following day, the Toll pathway was activated by transfection with plasmid pJL195. Plates were incubated for 12 h followed by addition of 5 µl heat killed *E. coli* followed by one hour incubation to activate STAT/IMD pathways. Pathway activated cultures, and control cultures in which Toll alone was activated, were then infected with SFV4 (MOI=1). The supernatants from test and control cells were collected 12 and 24 h after infection to determine virus tire. An unpaired non-parametric t test indicated that the virus titres in STAT/IMD only and STAT/IMD/Toll activated cultures at 12

hours post-infection were not significantly different (P = 0.0975). However, at 24 hours virus titres were significantly reduced by 60% in the supernatants from the STAT/IMD/Toll-activated cultures (P = 0.0083) (Figure 4.9).

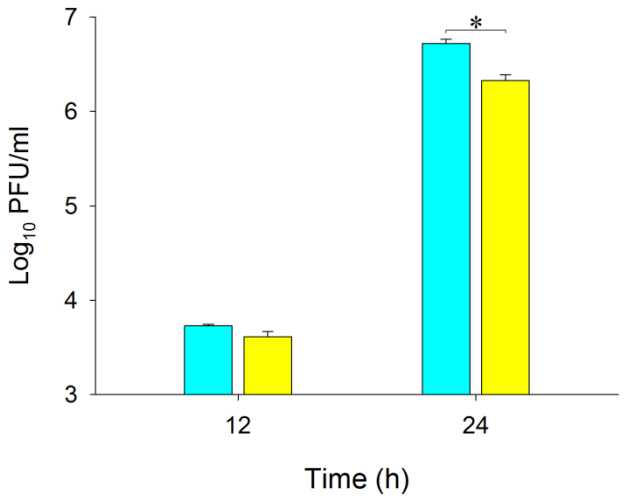

Figure 4.9: The effect of Toll and STAT/IMD pathways on SFV4 replication in U4.4 culture.

The amount of virus produced in U4.4 cells was measured 12 and 24 hours post-infection (MOI=1) as plaque forming units by plaque assay. The blue bars stand for control cultures in Toll alone was activated. The yellow bars represent STAT/IMD and Toll activated cultures. Each bar is the mean of triplicate samples. The error bars indicate the standard error of the mean. * $p<0.05$ (unpaired nonparametric t tests)

Summary of Findings

- SFV4(3H)-*RLuc* and SFV4-st*RLuc* replicated in U4.4 cells with growth kinetics similar to SFV4. Both recombinant viruses had a slightly lower maximum virus titre which indicated marker gene insertion slightly attenuated virus replication.
- Activation of the STAT/IMD pathway prior to infection reduced virus-driven luciferase expression by 40% between 1 and 12 hours post-infection in both SFV4(3H)-*RLuc* and SFV4-st*RLuc* infected cultures.
- Activation of the STAT/IMD pathway prior to SFV4-st*RLuc* or SFV4(3H)-*RLuc* infection reduced subsequent luciferase expression at low MOI levels

(0.1 or 1). However, at high MOI, non-structrual protein expression overcame the pre-activated STAT/IMD pathways (no luciferase reduction) but structural protein expression remained suppressed.

- Activation of the STAT/IMD pathway prior to SFV4 infection reduced virus production.
- Activation of the Toll pathway prior to SFV4-st*RLuc* or SFV4(3H)-*RLuc* infection had no effect on virus-driven luciferase expression.
- Activation of the Toll pathway prior to SFV4 infection had no effect on virus production.
- Activation of the STAT/IMD and Toll pathways prior to SFV4-st*RLuc* infection showed no further reduction of luciferase expression than activation of STAT/IMD alone. However, luciferase expression from SFV4(3H)-*RLuc* infected culture was further reduced when both STAT/IMD and Toll were activated.
- Activation of STAT/IMD and Toll pathways prior to SFV4 infection reduced virus production more than activation of STAT/IMD alone.

Discussion

In insects, STAT/IMD and Toll have been studied predominately in the context of bacterial and fungal infections and have been shown to activate a number of anti-bacterial and anti-fungal systems including anti-bacterial and anti-fungal peptides. However, there is a growing amount of evidence that these pathways are responding to virus infection. The data presented in this chapter have shown that activation of these pathways prior to virus infection can affect subsequent virus replication.

The effects on SFV infection of immune responses initiated by activation of IMD/STAT or Toll, or both pathways, were determined using SFV4 and its recombinant viruses SFV4(3H)-*RLuc* and SFV4-st*RLuc*. One step growth curves showed that SFV4(3H)-*RLuc* and SFV4-st*RLuc* replicate in U4.4 cells with growth kinetics similar to SFV4 with a slightly lower maximum virus titre at 12 hours post-infection. These viruses allowed quantitative assessment of early and late virus gene expression, as well as virus production and spread in mosquito cells (Flynt *et al*,

2009; Keene *et al*., 2004). The effects of immune signalling involving IMD and STAT on SFV gene expression are shown in figure 4.4B. Activation of host defences with heat-killed bacteria prior to SFV infection reduced virus-driven gene expression from both the genomic and the sub-genomic promoters by around 40%. This reduction in luciferase expression was not caused by a reduced number of infected cells resulting from heat-killed bacterial stimulation. Immunostaining of stimulated and control (PBS) cultures was carried out by Dr Rennos Fragkoudis. His results demonstrated that the percentage of virus-infected cells in both the bacterial-treated and PBS control cells were identical indicating that prior stimulation with bacteria did not affect the number of cells infected. As for virus production, the virus titre was reduced by 30% at 12 hours and 60% at 24 hours post-infection (Figure 4.5). These results suggest that the IMD/STAT pathways in mosquito cells have a role in controlling SFV replication. This concurs with other findings involving the control of virus replication in other insect systems. For example, in *Drosophila*, mutations in components of the IMD pathway including relish, resulted in a higher viral load and enhanced replication of SINV compared to wild type (Avadhanula *et al.*, 2009). For the STAT pathway, Dostert and co-workers showed that the JAK kinase Hopscotch was involved in the control of the DCV viral load in infected *Drosophila* and was required for the induction of some virus-regulated genes (Dostert *et al.*, 2005). Souza-Neto and co-workers have shown that depletion of Dome and Hop in the JAK-STAT pathway leads to increase in the susceptibility of *Ae. aegypti* mosquitoes to DENV infection and suppression of the JAK-STAT negative regulator PIAS leads to increase in the resistance to DENV infection. These authors (Souza-Neto *et al*) had depleted PIAS which resulted in up-regulation of 63 genes and down-regulation of 66 genes. Of all the regulated genes, 14% of them were putative JAK-STAT-regulated genes based on sequence homology, changeds in the transcription level of 18 of these genes were induced by both PIAS depletion and DENV-2- infected mosquitoes. Amongst the induced genes, the putative JAK-STAT pathway-regulated DENV restriction factors DVRF1 and DVRF2 were identified as the effectors of JAK-STAT. These genes contain JAK-SAT binding sites and are regulated by JAK-STAT activation and DENV infection. Furthermore, RNAi-mediated depletion of these effectors resulted in a 2-fold increase of DENV-2 infection in midgut tissue.

Conversely, DENV infection induced DVRF1 and DVRF2 expression by 3-6 fold (Souza-Neto *et al.*, 2009). In contrast, the present study use of heat-killed bacteria activates the IMD/STAT pathways from the receptor level. This may result in activating numerous of gene sets or even specific effector genes non-specifically. The results of the present study provided evidence that immune response gene clusters or maybe even effector genes that act as SFV restrictor factors may exist in mosquito cells. Through the activation of the receptors of IMD/STAT pathways, the viral gene expression is suppressed. These results could be further investigated in the future by RNAi-mediated depletion of PIAS to determine if specific gene clusters under the control of the JAK-STAT pathway is responsible for the reduction of viral gene suppression.

The immune responses initiated by expression of constitutively active Toll receptor (Toll ΔLRR) for 24 h, followed by infection with *RLuc*-expressing SFV constructs had no effect on virus gene expression at 12 hours post-infection (Figure 4.6). Virus titres from Toll-activated and non-activated cultures did not show any significant difference (Figure 4.7). Interestingly, this result concurs with the findings of SINV infection in Drosophila *relish*$^{-/-}$ or *dif* $^{-/-}$ mutants. SINV viral RNA level was 9.3-fold higher in the *relish*$^{-/-}$ mutant compared to the wild type, whereas *dif* $^{-/-}$ mutant has the same viral RNA level compared with wild type (Avadhanula *et al.*, 2009). In contrast, the Toll pathway, but not the IMD pathway, plays a key role in the antiviral response against DXV infection in *Drosophila* immunity mutants (Zambon *et al*, 2006). The Toll pathway has also been shown to control DENV infection, loss of Toll pathway activation by silencing of the MyD88 factor prior to DENV infection leads to increase in the virus load (Xi *et al.*, 2008). Together, these results indicate that different innate immune pathways may have a differential role in controlling infection with viruses of different families. As the results presented here and by Avadhanula and co-workers indicate, alphavirus infection may be controlled by the IMD/STAT pathway, but not by the Toll pathway. However, Toll has antiviral effect on viruses of other families such as the Birnavirus DXV and Flavivirus DENV. As mentioned in Chapter 1, Sanders and co-workers showed that SINV infection induced transcription of Toll but not of the IMD pathway. However, it is not known whether Toll activation has an effect on SINV replication.

The effect of immune responses initiated by a combination of IMD/STAT and Toll reduced viral non-structural gene expression by 20% but increased structural gene expression by 30% when compared with the controls (Figure 4.8). The reason behind the increase in viral structural gene expression is unclear. The contradicting effects on the expression of subgenomic and genomic viral genes did not permit a conclusion of whether or not activation of both pathways has a greater effect on viral gene expression. SFV4 replication under the effect of both pathways was reduced significantly by 60% at 24 hours post-infection (Figure 4.8); this level of reduction is the same as observed in virus titre in IMD/STAT activated cultures (figure 4.5), indicating that activation of both pathways did not further reduce the virus titre. Interestingly, the DNA microarrays used to analyse gene expression changes in *Ae. aegypti* following infection by SINV showed that the activated Toll pathway was deactivated and followed by activation of the IMD pathway (Sanders *et al.*, 2005). Furthermore, during this transition from Toll to IMD activation, a set of ubiquitin-ligase genes were down-regulated. These ubiquitin-ligases may be responsible for Dif activation, and down-regulation of these genes may also be responsible for IMD pathway activation (Khush *et al.*, 2002; Spencer *et al.*, 1999). Therefore, it is possible that there is an antagonistic effect between these two pathways. This can be an interesting area for further investigation in the future.

To conclude, activation of STAT and IMD, but not Toll prior to SFV infection inhibited virus replication. The results suggested that STAT and/or IMD pathways may be important mediators of antiviral effects against SFV4 in mosquito cells, but at the same time other immune pathways which also respond to Gram-negative bacterial stimulation might also be involved. This is in contrast to other reports such as: i) screening of *Drosophila* immunity mutants found that the Toll pathway, but not the IMD pathway plays a key role in the antiviral response against DXV infection (Zambon *et al*, 2006); ii) loss of Toll pathway activation by silencing of the MyD88 factor prior to DENV infection leads to increase in the virus load (Xi *et al.*, 2008). The reason behind these contrasting observations is not clear, however these results are derived from three different virus systems. This alone may provide explanation. The antiviral ability of other immune pathways in mosquito cells remains to be determined in greater detail. Despite the evolutionary distance and molecular

difference between *Aedes* and *Drosophila* (Christophides *et al.*, 2002), their conserved immune responses and pathways enabled the use of pathogenic stimuli (*E. coli*) and an upstream mutated receptor (Toll Δ LRR) to study the effects of these pathways on SFV infection. The conservation of important physiological processes between related insect species is an advantage for insightful research on mosquitoes which are of particular medical and veterinary importance.

Table of contents

Chapter 5: The biogenesis of viRNA in mosquito U4.4 cells infected with Semliki Forest virus.

Introduction

In mosquitoes, the RNAi pathway has been shown to effectively modulate the replication of arboviruses. Virus dissemination and replication often become more rapid when RNAi is being suppressed, examples include: i) the silencing of *AgAgo2* expression in *A. gambiae* which results in wider spread and higher virus titres in ONNV infection (Keene *et al.*, 2004), ii) silencing of RNAi components in *Aedes aegypti* results in increases in SINV infection (Campbell *et al.*, 2008), iii) use of small RNAs sequestering B2 protein in SINV infection in *Ae. aegypti* mosquitoes results in increased infection, dissemination, virus titre and mortality (Cirimotich *et al.*, 2009; Myles *et al.*, 2008), iv) recombinant ONNV expressing an RNAi suppressor leads to higher motality in *Ae. aegypti* infection (Myles *et al*., 2008), v) silencing RNAi components in *Ae. aegypti* results in increased DENV2 replication (Sánchez-Vargas *et al.*, 2009) and vi) temporal impairment of RNAi in whole mosquitoes lead to increased infection and dissemination (Khoo *et al.*, 2010). That suppression of RNAi components often leads to increase in mortality rate in mosquitoes suggests RNAi may function as a mechanism to keep arbovirus replication below a harmful level. Therefore, RNAi is believed to have a major role in control of arbovirus replication, spread and transmission. Central to antiviral RNAi is the production of virus-derived small interfering RNAs (viRNAs) from viral dsRNA by the Dicer protein, and the formation of the RNA-induced silencing complex (RISC), followed by degradation of homologous viral RNA sequences (Kemp & Imler, 2009).

In *D. melanogaster* and *Ae. aegypti*, the RNAse III enzyme and DExD/H-box RNA helicase Dcr-2 initiate RNAi by cleavage of virus-derived long dsRNA into double-stranded viRNAs. There are a number of possible dsRNA substrates for this process. The formation of viral dsRNA could involve double-stranded regions in single viral genome or genome complementary RNA molecules, or two-molecule replication

intermediates (Lacomme, 2005; Myles *et al.*, 2010). There are also questions on whether all areas of the virus genome, subgenomic and genome complementary RNA generate viRNAs or only specific areas. Therefore an investigation was carried out to characterise SFV-4 derived viRNAs in *Ae. albopictus* cells for better understanding of viRNA biogenesis in mosquito cells

Characterisation of SFV4-derived viRNAs in *Aedes albopictus*-derived U4.4 cells

The biogenesis of viRNA was determined by Solexa Illumina deep sequencing of RNA extracted from SFV4 infected U4.4 cells. U4.4 cells were used for these studies as they have been shown to be RNAi competent (Brackney *et al*., 2010). $5x10^5$ cells per well were seeded in 6 well-plates and incubated overnight (16 hours). Three wells of U4.4 cultures were then infected simultaneously with SFV4 (MOI=10). Total RNA was extracted from the three infected cultures using Trizol (Invitrogen, Paisley, UK) 24 hours post-infection and pooled. The concentrations and purity of RNA samples were determined using a NanoDrop 1000 (Thermo Scientific). All subsequent RNA processing was performed at GenePool, University of Edinburgh (http://genepool.bio.ed.ac.uk/) as described in Chapter 2. In, brief, small RNAs below 44 nt were purified from a 15% TBE-Urea polyacrylamide gel, and RNA adapters were ligated to small RNAs before sequencing according to the manufacturer's instructions (Illumina Inc., USA). Small RNAs were then sequenced using an Illumina® Solexa Genome Analyzer. RNA of uninfected cells was sequenced as control. This approach has been previously shown to be a reliable way to analyse viRNA (Flynt *et al*., 2009; Szittya *et al*., 2010). To identify SFV4 derived siRNA, sequences were aligned and filtered according to the SFV4 reference genome/genome complementary sequence (Genbank accession number: NC_003215) using SOAP software (GenePool bioinformatics support) (Li *et al.*, 2008).

A total of 3.2×10^6 small RNA reads were generated. Small RNA reads which, i) aligned to the SFV4 sequence and, ii) were 20-26 nt in length were filtered out from the data. The sum of all 20-26 nt viRNA was 7.5×10^4. This represented 2.1% of all

small RNA reads. Of all the aligned SFV4-derived viRNAs, 21 nt long viRNAs were found to be the predominant species and accounted for 91.1% of 21-26 nt sequences. 60% of all the 21 nt viRNAs mapped to the genome and 40% to the complementary genome (Figure 5.1).

The first base of each 21 nt viRNA was mapped to its corresponding location on the SFV4 genome or genome complementary sequence. As shown in figure 5.2, 21 nt viRNAs were scattered over the entire SFV genome and genome complementary sequence in a non-random manner. Some areas generated high frequencies of viRNAs and others generated no (or only very few) viRNAs, these are referred to as hot spots and cold spots respectively. The biogenesis of viRNAs from genome and genome complementary RNA appeared to be asymmetric. SFV4-aligned viRNA sequences were analysed. There was no obvious skewing towards a particular base at the first position (28% A, 28% C, 12% G, 32% U). There was no bias in GC-content, and no obvious common sequence motifs. The sequencing results from uninfected control cells showed 131 reads aligned to the SFV genome and 76 reads to the genome complementary sequence. None of these sequences are above 4 reads and these matches can only be interpreted as background. A small number of viRNAs were also found in an uninfected control experiment from subsequent experiments.

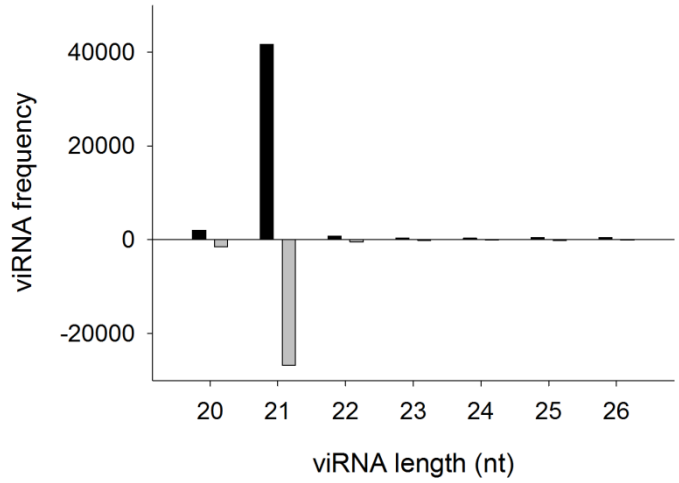

Figure 5.1: Size distribution of viRNAs (21-26 nt) from SFV-infected U4.4 cells at 24 hours post-infection.

Positive numbers on the Y axis indicate the frequency of viRNAs of various sizes mapping to the SFV genome; negative numbers on the Y axis indicate the frequency of viRNAs mapping to SFV complementary genome.

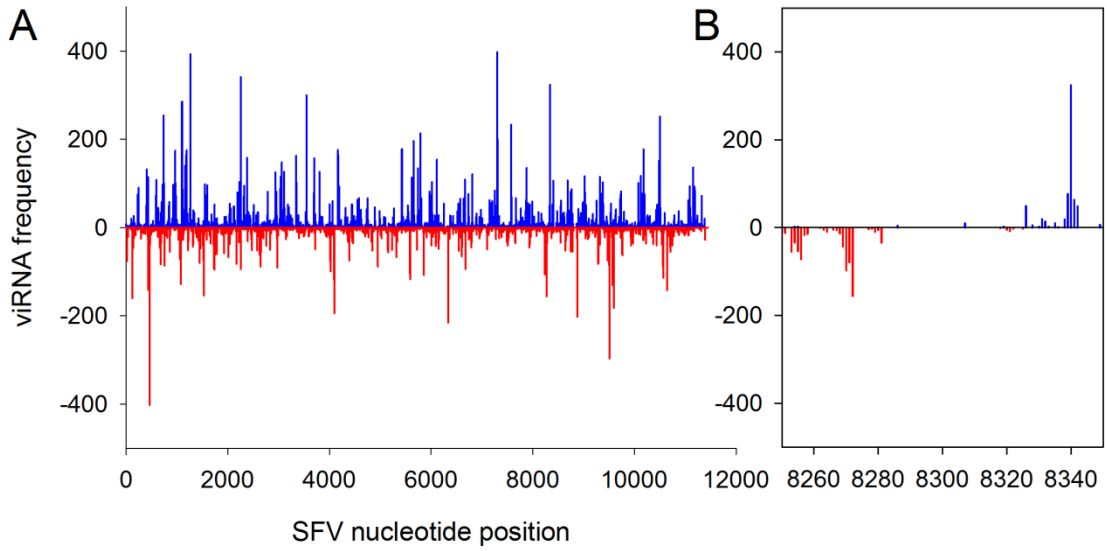

Figure 5.2: Frequency distribution of 21 nt viRNA-generating loci in SFV genome.

Total RNA was extracted from SFV4 infected U4.4 cultures 24 hours post-infection and small RNAs were sequenced and aligned to: SFV genome (5'-3'; viRNAs starting with 5' terminal nucleotide) or genome complementary sequence (3'-5'; viRNAs starting with 3' terminal nucleotide) starting at nucleotide 1 on the X axis. Numbers on the Y axis correspond to frequencies of viRNAs mapping to SFV genome (positive) or genome complementary sequence (negative). Blue peaks indicate loci of viRNAs mapping to SFV genome, red peaks indicate loci of viRNAs mapping to SFV antigenome. A representative section is magnified (panel B), to illustrate hot and cold spots visually.

The experiment was repeated to determine if the frequency pattern of viRNA biogenesis remained similar between studies. The repeat experiment showed a viRNA distribution patterns that resembled the initial pattern with little variation (Figure 5.3B). The major difference between repeat experiments was the depth of read frequency due to several upgrades and replacements of the sequencer (Illumina® Solexa Genome Analyzer) through the course of the project. Upgrades resulted in overall enrichment of read frequency as shown by the Y-axis values (Figure 5.3). Despite the depth of the frequency, the overall pattern in the two experiments was very similar, and there were many identical peaks sharing the same loci.

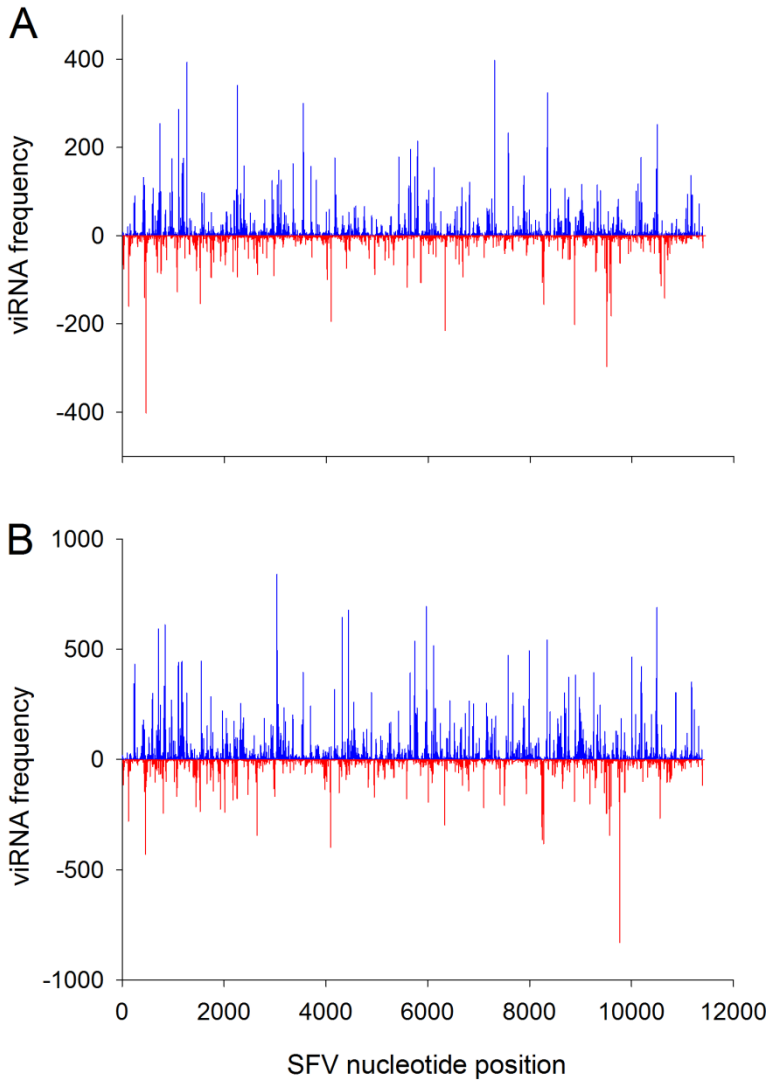

Figure 5.3: Frequency distribution of 21 nt viRNA-generating loci in the SFV genome in initial and repeat experiments.

A. Produced in late 2008 with maximum depth of 400 reads. **B.** Produced in early 2009 with maximum depth of 400 reads.

Characterisation of SFV-derived viRNAs in *Aedes aegypti*-derived Aag2 cells

Aag2 cells have previously been shown to be RNAi competent (Scott *et al.*, 2010) and can mount an RNAi response to Dengue virus (Sánchez-Vargas *et al.*, 2009). In addition, *Ae. aegypti* and *Ae. albopictus* share 80% sequence identity in Dicer 2, (J. Rodriguez and A. Kohl personal communication). To determine the influence of a different host species on viRNA biogenesis, Aag2 cells from embryonic tissues of *Ae. aegypti* (Peleg, 1968) were infected with SFV4. A culture of U4.4 cells was infected in parallel with the same stock of virus as control. 24 hours post-infection RNA extraction was performed. Aag2 and U4.4 viRNA sequences were determined synchronously in the same Illumina Solexa sequencing flow cell as described previously for U4.4 cells. This was carried out to eliminate any variability that might exist between flow cells. 97.6% of viRNAs were 21 nt in length, which was similar to U4.4 cells. 59.6% of all 21nt viRNA mapped to the SFV genome RNA and 40.4% mapped to the genome complementary RNA (Figure 5.4). Unfortunately, Gene Pool (sequencing service) had changed their isolation protocol for small RNA species and excluded 26 nt species (unknown to me). Therefore only 20-25 nt species are displayed in the size distribution. The viRNAs from Aag2 cells and U4.4 cells infected in parallel were mapped along the SFV4 genome and genome complementary sequence (Figure 5.5a and 5.5b respectively). The results once again emphasised the non random distribution of viRNA which generates hot and cold spot viRNA. The biogenesis of viRNAs from genome and genome complementary also appeared to be asymmetric in Aag2. viRNA sequence analysis showed no obvious skewing towards a particular base at the first position (28% A, 28% C, 22% G, 22% U). There was no bias in GC-content, and no obvious common sequence motifs (GenePool bioinformatics support).

However, the overall Aag2 viRNA frequency pattern differed from that of U4.4 cells. The Aag2 pattern had peaks solely focused on the structural region of the genome, whereas peaks were spread throughout the length of the whole genome in the U4.4 cells. This result suggested that different protein interaction partners or perhaps the slight change in the Dicer 2 sequence identity have an effect on viRNA generation.

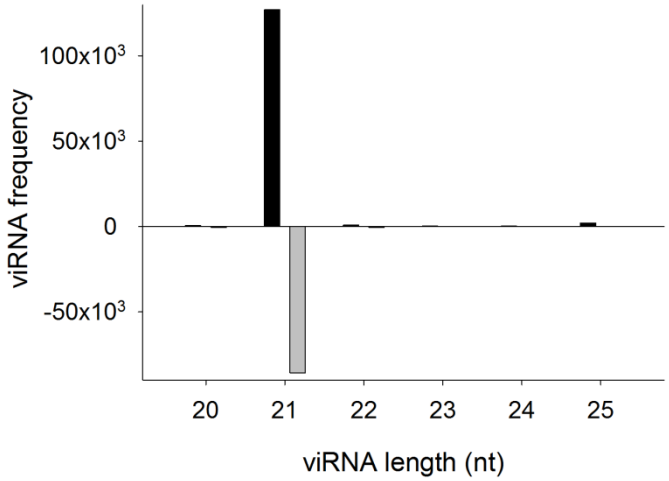

Figure 5.4: Size distribution of viRNAs in SFV-infected Aag2 cells at 24 h p.i.

Positive numbers on the Y axis indicate the frequency of viRNAs mapping to the SFV genome (black boxes); negative numbers on the Y axis indicate the frequency of viRNAs mapping to the SFV antigenome (grey boxes).

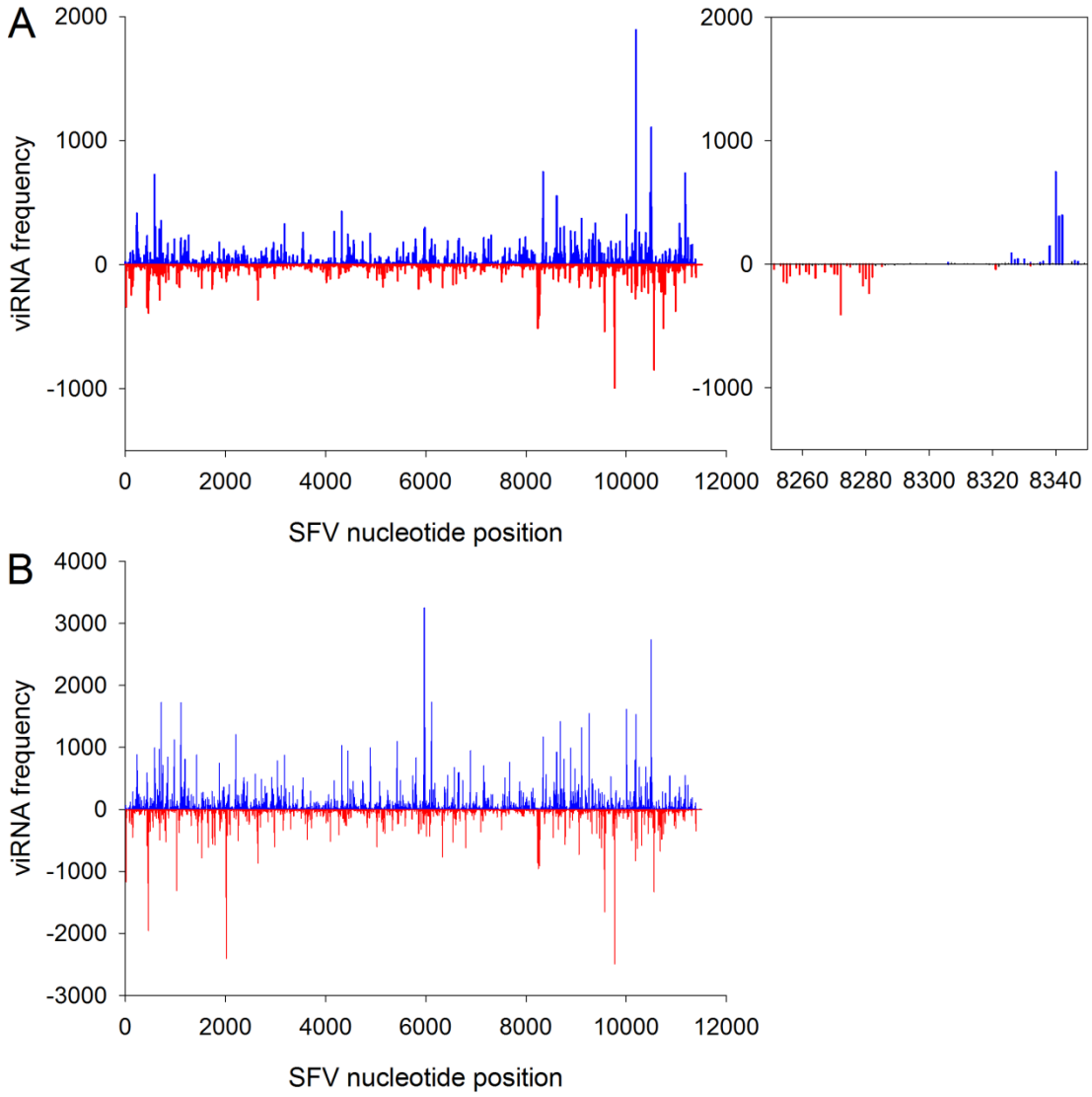

Figure 5.5: Frequency distribution of 21 nt viRNA-generating loci in SFV genome.

Total RNA was extracted from SFV4 infected (A) Aag2 and (B) U4.4 cultures 24 hours post-infection and small RNAs were sequenced and aligned to: SFV genome (5'-3'; viRNAs starting with 5' terminal nucleotide) or antigenome (3'-5'; viRNAs starting with 3' terminal nucleotide) starting at nucleotide 1 on the X axis. Numbers on the Y axis correspond to frequencies of viRNAs mapping to SFV genome (positive) or complementary genome (negative). Blue peaks indicate loci of viRNAs mapping to SFV genome, red peaks indicate loci of viRNAs mapping to SFV antigenome. A representative section is magnified (right panel), to highlight hot and cold spots in more detail.

The characterisation of viRNA origins in mosquito U4.4 cells.

RNAi occurs when dsRNA structures are recognised in the cytoplasm by Dicer. Dicer binds to dsRNA and cleaves it into siRNA duplexes. In virus infection, dsRNA can arise from at least three different sources i) double-stranded regions in the single viral genome, ii) in genome complementary RNA molecules, or iii) the replication intermediate duplex (Myles *et al*, 2010). To determine the origins of viRNAs generated by U4.4 cells, replication-deficient SFV genomes were introduced into the cytoplasm. This eliminated viRNAs generated from double-stranded replication intermediates; any viRNAs remaining would be generated from double-stranded structures on the introduced single stranded genomic RNA. To do this, a strategy is required to efficiently deliver a large amount of replication-deficient SFV genomic RNA into all the cells in U4.4 cell culture.

There are multiple strategies to produce replication-deficient SFV genomic RNA, including introduction of a point mutation or a stop codon in the virus replicase sequence or use uncapped SFV genomic transcripts. However, these methods require transfection in order to introduce the replication-deficient genomic RNA into cells. First of all, transfection is not an ideal method to introduce a large amount of RNA in every cell in the cell culture as transfection has a limited efficiency. Second of all, these methods rely on the limited amount of replication-deficient transcripts produced by *in vitro* transcription. To overcome these disadvantages, a SFV replicon SFV1(3F)-IRES-ZsGreen, with an IRES element at the 5' end of the genome was constructed by Prof. Andres Merits (Figure 5.6). The IRES of encephalomyocarditis virus (EMCV) was inserted between the duplicated nsP1 sequences. IRES element has been used by other to mediate cap-independent translation of alphavirus constructs in mammalian cells (Wiley *et al*., 2010), however, the IRES of EMCV has previously been shown to attenuate alphavirus replicon expression in insect cells (Finkelstein *et al*., 1999; Volkova *et al*., 2008; Woolaway *et al*., 2001). Furthermore, complete attenuation of SFV replication by EMCV IRES was observed in mosquito cells by Prof. Andres Mertis (Prof. Andres Mertis, personal communication). This construct allows a large amount of SFV genomic RNA to be produced in mammalian cells through virus replication (EMCV IRES permits translation in mammalian cells)

and these SFV genomic RNA can be packaged into VRPs when viral structural sequences are provided *in trans*. The purified VRPs can be used to infect U4.4 cells at high MOI as an efficient and effective way to deliver multiple copies of replication-deficient genome (EMCV IRES does not permit translation in mosquito cells) into all the cells in the culture.

SFV1(3F)-IRES-ZsGreen cDNA was created by inserting an IRES element at the 5' untranslated region under the duplicated N-terminus of nsP1 sequence and fusing a ZsGreen fluorescent protein sequence to the 3' end of nsp3. An SFV1(3F)-ZsGreen construct which does not contain IRES was used as a control. To deliver the largest possible amount of non-replicating SFV1 genome to cells in order to generate viRNAs for analysis, VRPs were generated and used to infect U4.4 cells at 100 IU (infectious units) per cell. The experiment was also attempted at 1000 IU but this proved lethal to the U4.4 culture.

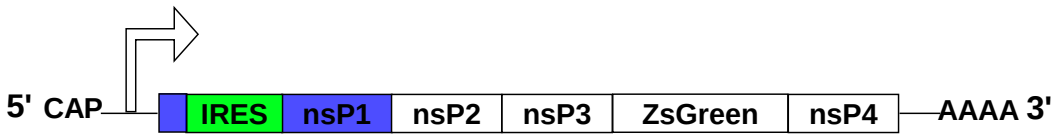

Figure 5.6: A Schematic representation of the SFV1(3F)-IRES-ZsGreen.

SFV1(3F)-IRES-ZsGreen is based on SFV1 construct with ZsGreen protein gene inserted and fused with the 3' end of the nsP3 sequence. The N-terminus of nsP1 was duplicated (highlighted in blue). IRES element was inserted between the duplicated region, at 276 – 853 nt (highlighted in green).

Unfortunately, 50% of the U4.4 culture infected with SFV1(3F)-IRES-ZsGreen appeared to be green indicating that replicon replication or at least translation of the input RNA had occurred. In the control experiment, all cells in the U4.4 culture infected with SFV1(3F)-ZsGreen expressed green fluorescence protein. This showed that the EMCV IRES does attenuate virus replication in insect cells as reported by others but that this is an incomplete block.

That all the cells in the control experiment were green indicted that at 100 IU all cells were infected. Therefore in the SFV1(3F)-IRES-ZsGreen infected culture, the non-

green 50% of the cells should contain copies of non-replicating genomes. To isolate the non-green cells, an infected culture was sorted by fluorescence-activated cell sorting (FACS). Total RNA of the non-green population of cells was extracted and sequenced. SFV1(3F)-IRES-ZsGreen and SFV1(3F)-ZsGreen sequences were used respectively as the reference sequence for SFV1(3F)-IRES-ZsGreen and SFV1(3F)-ZsGreen derived viRNAs (Figure 5.7A&B). The results showed that biogenesis of viRNAs from genome and genome complementary RNA of SFV1(3F)-IRES-ZsGreen was asymmetric with 69.7% of all the 21 nt viRNAs mapped to the genome and 30.3% to the complementary genome. SFV1(3F)-ZsGreen showed a very similar asymmetry, with 70.6% of all the 21 nt viRNAs mapped to the genome and 29.4% to the complementary genome.

In the SFV1(3F)-IRES-ZsGreen viRNA distribution map (Figure 5.7A), no viRNA appeared to align to region 250 to 990 nt. This region is where the IRES was inserted (Appendix II). The exact location of the IRES sequence is between 276 -853 nt. The Solexa sequencing data of SFV1(3F)-IRES-ZsGreen infected U4.4 cells over that region (including the 5' and 3' junctions), showed that there are four viRNA reads (one read for each of the four different locations) within the IRES region on the genomic sequence and no viRNA read matched to the IRES region from the genome complementary sequence (Table 5.1 & 5.2). The four individual sequences that aligned to the IRES region on the genomic sequences were below the control threshold of four reads, therefore they can only be considered as background.

The observation that no viRNAs were generated from the IRES region in the isolated non-green cells suggested that IRES was absent from the replicon. In addition, the absence of the IRES was unlikely to caused by deletion in the SFV1(3F)-IRES-ZsGreen sequence because no viRNA read was identified at the IRES-nsP1 junctions. The presence of zsGreen viRNA in the SFV1(3F)-IRES-ZsGreen infected U4.4 cells sequencing data suggested SFV1(3F)-IRES-ZsGreen VRP stock was contaminated by SFV1(3F)-ZsGreen VRPs. This contamination was likely to come from residual unmodified SFV1(3F)- ZsGreen during the insertion of the IRES.

To conclude, the results showed non-green SFV1(3F)-IRES-ZsGreen infected cells isolated by FACS did not contain any SFV1(3F)-IRES-ZsGreen derived viRNA.

This could mean that SFV1(3F)-IRES-ZsGreen is not a viable replicon and a low level of SFV1(3F)-ZsGreen replication was occurring in non-green cells.

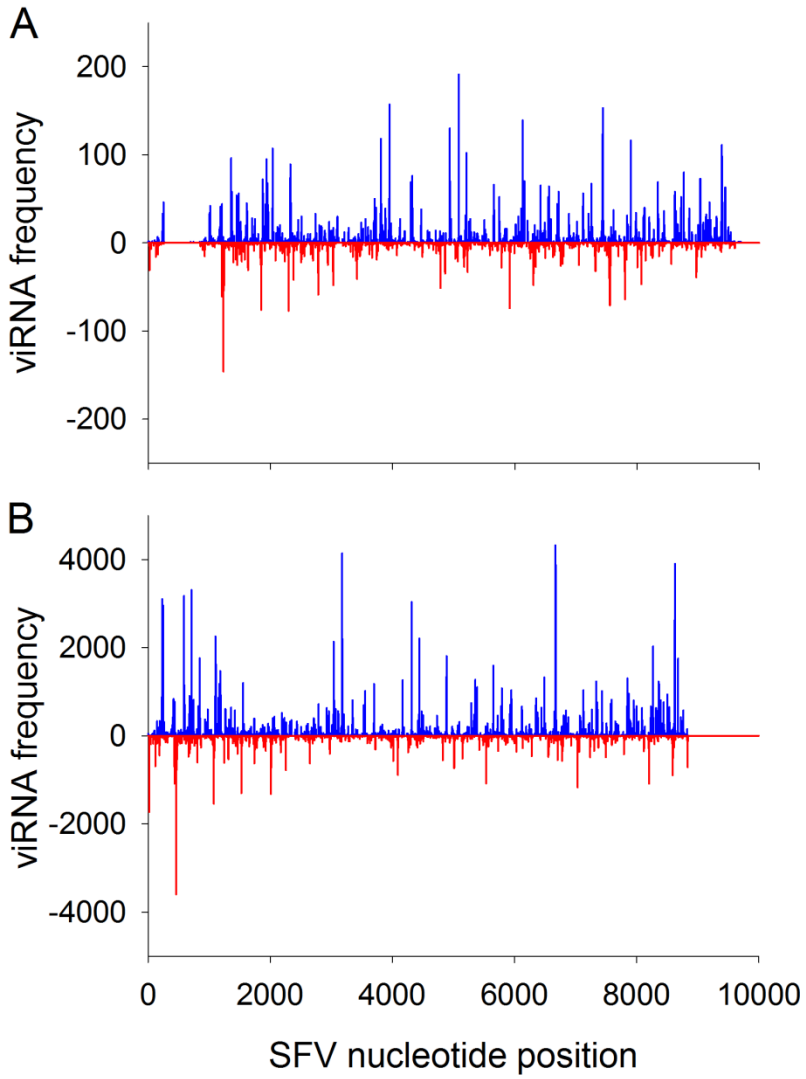

Figure 5.7: Characterisation of viRNAs in *Ae. albopictus*-derived U4.4 cells 24 hours after infection with SFV1(3F)-IRES-ZsGreen or SFV1(3F)- ZsGreen VRPs.

Frequency distribution of 21 nt viRNA-generating loci in the SFV VRP genome (5'-3'; viRNAs starting with 5' terminal nucleotide) or antigenome (3'-5'; viRNAs starting with 3' terminal nucleotide) starting at nucleotide 1 on the X axis. Numbers on the Y axis correspond to frequencies of viRNAs mapping to SFV genome (positive) or antigenome (negative). Blue peaks indicate loci of viRNAs mapping to SFV genome, red peaks indicate loci of viRNAs mapping to SFV antigenome. **(A)** viRNA profile of SFV1(3F)-IRES-ZsGreen. **(B)** viRNA profile of SFV1(3F)-ZsGreen.

First base location (nt)	Nucleotide sequence	Frequency
256	ACAAAGACACACTCATCTTGG	1
258	AAAGACACACTCATCTTGGAT	1
610	ATTCAACAAGGGGCTGAAGGA	1
691	TTCAACAAGGGGCTGAAGGAT	1
738	ATCTGATCTGGGGCCTCGGTG	1
839	AAACACGATGATAATATGGCC	1
864	AAGTGCATGTTGATATTGAGG	1
869	CATGTTGATATTGAGGCTGA	2

Table 5.1: Solexa sequencing data of viRNAs aligned to positive strand of SFV1(3F)-IRES-ZsGreen from 255 - 868 nt.

This segment of data shows the solexa sequencing data from the 5' to the 3' junction of the IRES insert. The IRES insert is located at 276 – 853 nt. There are 4 individual reads scattered at 4 different location within this region and no viRNA were located overlapping the insertion junction.

First base location (nt)	Nucleotide sequence	Frequency
225	CTGGCTACCAAATTGATCGAG	1
254	TGACAAAGACACACTCATCTT	1
854	ATGGCCGCCAAAGTGCATGTT	4
867	TGCATGTTGATATTGAGGCT	1

Table 5.2: Solexa sequencing data of viRNAs aligned to the complementary sequence of SFV1(3F)-IRES-ZsGreen from 255 - 868 nt.

This segment of data shows the solexa sequencing data from the 5' to the 3' junction of the IRES insert. The IRES insert is located at 276 – 853 nt. No viRNA was sequenced and aligned to the IRES region.

Characterisation of viRNA biogenesis in mosquito U4.4 cells - structural analysis of SFV genomic RNA and role of RNA structures in viRNA generation by Minimal Folding Energy (MFE)

Central to biogenesis of viRNA is the source of virus-derived dsRNA. As mentioned previously, formation of viral dsRNA could involve double-stranded regions in single-stranded viral genome or antigenome RNA molecules, or two-molecule replication intermediates (Myles *et al*., 2010). One way to assess the likely origin of the viRNAs is to determine whether frequency of viRNA generation has any correlation to secondary structure of the RNA. The secondary structure of an RNA molecule should form according to the base sequence and given thermo-dynamics. In theory, two separate RNAs molecules should form the same secondary structure if given variables remain the same in two separate instances i.e. base sequence, thermo-dynamics of the environment and interacting partners. Therefore, an RNA molecule will fold up according to its' sequence and surrounding environment. Bioinformatics and advances in computing power have allowed secondary structure predictions on single molecules of RNA (Zuker & Stiegler, 1980).

One of the methods to predict RNA secondary structure is comparative sequence analysis. This method determines common Watson-Crick base-pairing between multiple homologue sequences. By comparing between homologue sequences, locations which tend to have specific pairings can be found. For example, a CG pair in one sequence is replaced by an AU pair in another, showing pairing takes place at that location. Comparative analysis is reasonably robust when there are enough homologous sequences available to make it statistically relevant. The robustness of this method is shown, in that over 97% of predicted base pairs in ribosomal RNA were proven by subsequent crystal structures. Another secondary structure prediction method involves calculation of free energy of base-pairing. This method predicts the most stable secondary structure of a given RNA sequence by using a mathematical algorithm (based on empirically determined stacking and destabilising energy values for the various base pairs that form simple stem loops) to find a conformation of minimum free energy (MFE). This method involves a dynamic

programming algorithm from applied mathematics and is widely used in RNA fold prediction programmes like MFOLD and RNAFold (Mathews *et al*, 1999; Zuker & Stiegler, 1980). However, the accuracy of RNA secondary structure prediction by free energy minimisation alone has several drawbacks because dynamic programming algorithms do not anticipate some strong sequence-dependent stability of motifs. Therefore, control sequences (e.g. the analysed sequence is SFV4 and its control would be genetic variants within the same genus) would be used to generate a mean scramble (MFE of sequence-order randomized controls) as a reference scale to predict genome-scale ordered RNA structure (GORS) (Simmonds *et al*., 2008; Simmonds *et al*, 2004).

RNA structure can also predicted by covariance analysis. For example, alignments of published virus genome sequences can be used to generate a consensus sequence. This consensus sequence will then be used to calculate the most energetically-favoured folding by MFOLD. Each sequence in the alignment would be scored for frequencies of substitutions that maintained or disrupted predicted base-pairing in the consensus predicted RNA structure. Sequence changes that maintained RNA structure would be divided into those that occurred at covariant sites (associated with paired changes in the base-paired nucleotide to maintain binding) and semi-covariant changes (where base-pairing was maintained without compensatory changes, corresponding to changes between G–C and G–U binding). For calculation of the null expectation (i.e. randomly occurring) frequencies of each type of sequence change, Perl scripts (Zuker, 2003) were used to generate all synonymous variants of the consensus sequence (or 10 000 unique sequences that were selected at random if the possible number of synonymous variants exceeded this number) that were maximally 10% divergent from the input sequence. By using the connect file as a framework, the number of base-paired (identical or covariant) or unpaired sites in the dataset, generated in silico, were determined (Tuplin *et al*, 2004). The prediction of specific structures using the available comparative sequence data was done by using the programme StructureDist v.1.3 in the Simmonics package (Simmonds *et al*., 2004). This programme compares minimum energy structures from sequence data sets and computes phylogenetically conserved pairings and secondary structures. The results were expressed in the form of pairing frequencies, which were calculated

from the proportion of pairwise comparisons of connect files for each sequence with the same pairing predictions.

An analysis of the SFV4 sequence for secondary structure has not been carried out previously, but alphavirus genomes have been reported to contain overall few areas of secondary structure (Davis *et al.*, 2008). The only known structured region in alphaviruses is in the 5' untranslated region of the genome, including Venezuelan equine encephalitis, Sindbis viruses and SFV (Jing-Hsiung *et al*., 1983; Kulasegaran-Shylini *et al*, 2009; Logue *et al*., 2008; Nickens & Hardy, 2008). Under the supervision of Prof. Peter Simmonds, the SFV4 genome (GenBank accession number AJ251359) was fully analysed and thermodynamic minimum free energy (MFE) was calculated at each nucleotide position using UNAFold. MFE values were calculated in frames of 150 nucleotides (75 nucleotides up and 74 downstream), and the frame incremented by 1 nucleotide across the complete SFV genome. The folding energies were then compared with 50 copies of fragments whose sequence order was scrambled using the algorithm NDR, which preserves dinucleotide frequencies of the native sequence automated using the programme Folding Energy Scan as implemented in the Simmonic2005 v1.8 package (Simmonds *et al*., 2008). The minimum free energies (MFEs) of each native sequence fragment were compared with the mean MFE of the NDR-scrambled controls to produce an MFE difference (MFED), which is the percentage difference between the MFE of the native sequence and the mean of a scrambled control of the same sequence, as in the formula below (Simmonds *et al.*, 2004). MFED values for each fragment were averaged across the 4 available SFV complete genome sequences (GenBank accession numbers EU350586, DQ189086, and Z48163).

$$\text{MFED (\%)} = [(\text{MFE}_{\text{native}}/\text{MFE}_{\text{scrambled}}) - 1] \times 100$$

The MFED value provides a scale to quantify sequence order-dependent RNA structure formation over the length of the genome. The MFED values for each position of the SFV4 genome were calculated and plotted in figure 5.8A. The red line represents mean values of five consecutive prediction fragments. The result showed MFED values close to zero along the entire SFV genome, which indicated an absence of structured RNA, with the exception of the 5' untranslated region. The

frequency pattern of 21-nt genome-derived viRNAs was aligned and compared with the pairing and MFED values (Figure 5.8A, red). Paired regions (high probability of pairing indicated by values close or equal to 1) in the SFV4 genome were predicted by using StructureDist (Figure 5.8A, green).

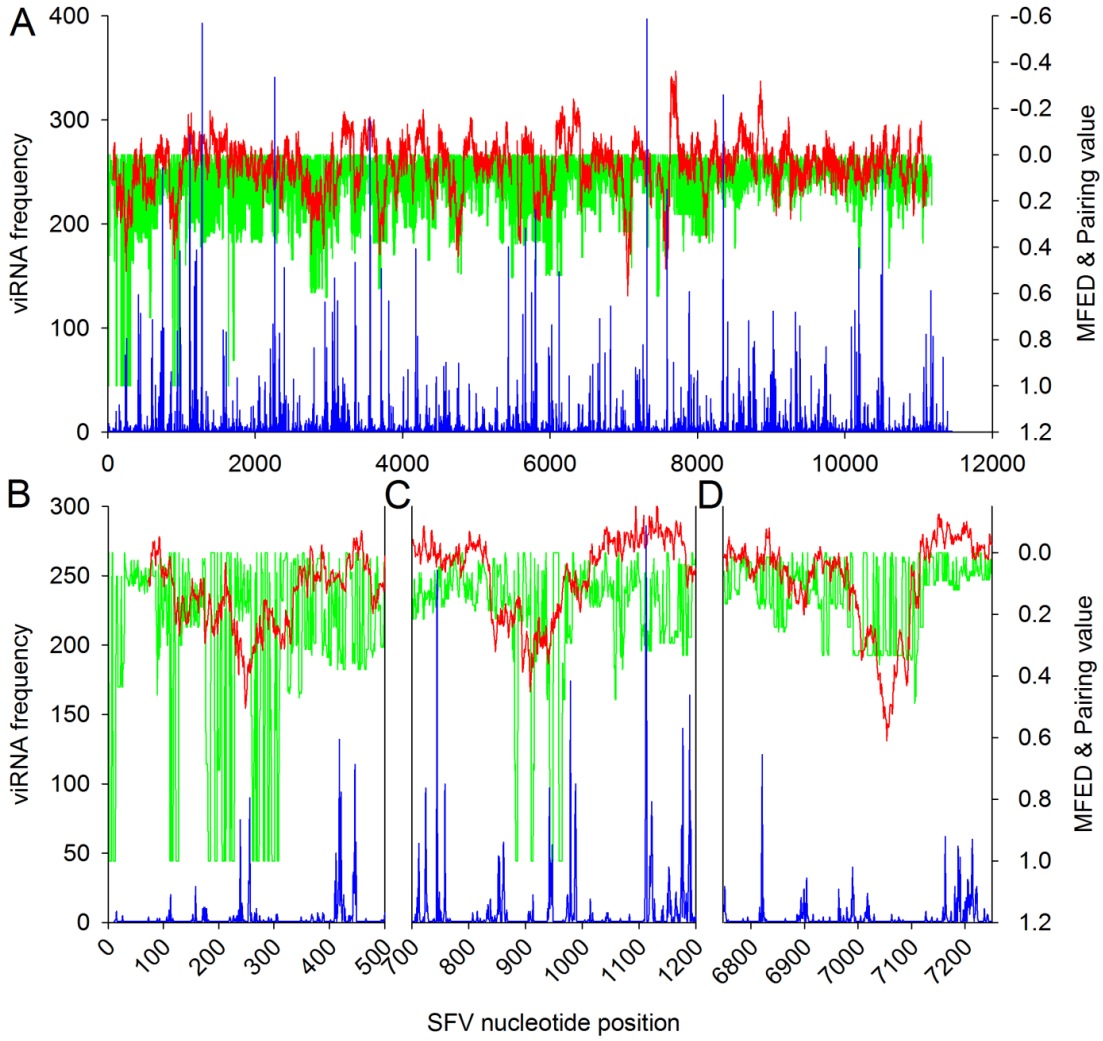

Figure 5.8: Prediction of RNA secondary structures (MFED) and pairing within the SFV genome, and correlation to 21 nt viRNA frequency in U4.4 cells.

Genomic viRNAs described in Fig. 3 were used for this analysis. (A) Distribution of MFED values (right Y axis; indicating probability of secondary structure) and pairing values (right Y axis, indicating probability of paired regions) along the SFV genome (X axis, starting at nucleotide 1) as red line and green shadow, respectively. High positive MFED values suggest areas with RNA secondary structures, respectively while values around 0 or negative do not. Pairing values close to, or equal to 1 suggest paired regions whereas low pairing values indicate absence of pairing. For clarity of the figure, ascending values on the right Y axis are indicated from top to bottom. viRNA frequencies on locations along the SFV genome (blue peaks) are indicated on the left Y axis. Bottom three panels **(B, C, D)** represent magnifications of selected regions from the top panel **(A)**. The diagram was generated using data produced by Prof. Peter Simmonds.

The alignment of MFED values to their nucleotide positions enabled categorisation of viRNA frequencies to compare mean MFED values between each category. viRNA frequencies were put into four ordered catagories according to the frequency of their appearence, 1, <10, 10 to 100, and >100. An analysis of variance (ANOVA) (Minitab, version 15) was carried out to determine any relationship between MFED values and viRNA frequency catagories. The results showed that there are no significant differences in MFED values across all designated levels of viRNAs ($F = 0.56$; $df = 3, 10{,}882$; $P = 0.643$). The relationship was also determined when viRNA frequency catagories were narrowed down into 7 ranges: 0, 1-10, 11-50, 51-100, 101-200, 201-300 and 301-400 (Figure 5.9). One way ANOVA was used to determine significant difference across all 7 groups and showed that the means are not significantly different from each other ($P = 0.6964$).

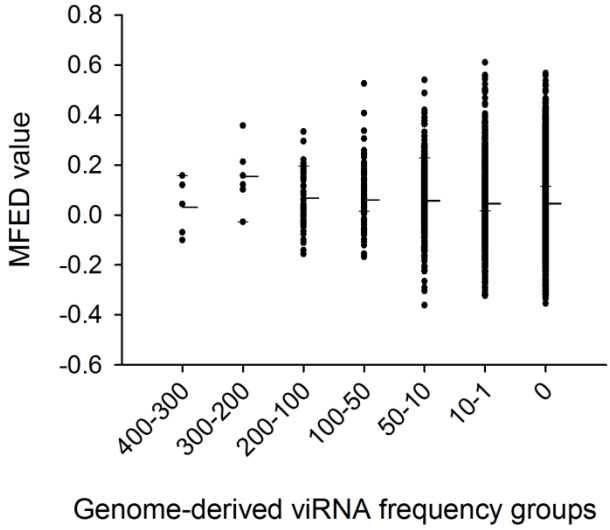

Figure 5.9: MFED prediction value distribution in different read frequency catagories.

A plot of ordered viRNA frequency groups against the MFED values of all of its group members. MFED value were assigned to each viRNAs by shifting 11 bases down to centre the MFED value prediction to the middle of each viRNAs. viRNAs were put into 7 ordered catagories according to the frequency of their appearence, 0, 1-10, 11-50, 51-100, 101-200, 201-300 and 301-400. MFED values (right Y axis) along different groups of viRNA frequency groups (X axis, starting with viRNAs having 301 to 400 reads). Number of members increase exponentially as X axis reduce to smaller read groups. The line in the middle of each group indicates the mean MFED value of each group.

Furthermore, the relationships between pairing values and viRNA frequency catagories (as described above) were analysed by using Fisher's exact tests (StatXact v8; Cytel Software Corp., Cambridge, MA). The pairing values were categorized above or below cutoff values of 0.4 or 0.6 in two separate tests. The results showed that there was no significant association between pairing values and levels of viRNAs ($P = 0.286$ for a cutoff of 0.4; $P = 0.1147$ for a cutoff of 0.6).

Althought the statistical analysis showed no correlation between predicted secondary structures and viRNA frequencies, there were however regions where predicted secondary structures in the genomic RNA were associated with interesting viRNA patterns. For example, the viRNA peaks at nucleotides 204 to 258 mapped on a trough of MFED value where secondary structure is likely to be present and also mapped between two pairing values close or equal to 1, suggesting presence of a stem-loop structure (Figure 5.8B). Unfortunately, there were also regions with consistant pairing and MFED predictions which did not associate with a viRNA peak and vice versa. For example, figure 5.8C showed a high viRNA frequency (1100-1140 nt) which did not coincide with high pairing or high MFED values; figure 5.8D showed a structured region predicted by both MFED and pairing values (7000-7100 nt) but this did not appear to produce any viRNAs. A long-distance pairing analysis of the genome identified 22 regions with complementary sequences which could allow folding back to form secondary structures. Analysis of the viRNA frequency at these 22 regions showed that these regions produced no viRNAs or only a low frequency of viRNAs.

Analysis of the ability of hot spot- and cold spot-derived viRNAs to inhibit SFV replication

The non-random generation of viRNAs along the SFV genome gave rise to hot- and cold-spots for viRNA generation. "Hot spots" refers to areas that gave rise to a high frequency of viRNA and "cold spots" refers to areas that produced few or no viRNA. It is unclear whether this non-randomised generation serve any purpose. To answer this question, the ability of hot spot- and cold spot-derived viRNAs to inhibit SFV replication was determined. To determine if hot spot- and cold spot-derived viRNAs

differ in their ability to inhibit SFV replication, 21 nt artificial siRNAs derived from hot (areas of high frequency) or cold (areas produced no viRNA) spots on the SFV4 genome were tested using SFV4 expressing an *RLuc* reporter gene, SFV4(3H)-*RLuc* (Figure 4.1B). As explained in chapter 4, *RLuc* activity provides a quantitative measure of early and late viral gene expression, SFV4 replication and virus production. Seven hot- and cold-spot siRNA mimics of viRNAs were selected from comparison of the U4.4 and Aag2 viRNA frequency maps (figure 5.2 and 5.5A). Selected sequences were complemented with their natural opposite stand, and designed to become duplexes with 3' 2nt overhang on both ends. These viRNA mimics were then ordered from Ambion with no chemical alterations for enhanced stability.

The viRNA mimics were introduced into RNAi competent U4.4 cells followed by SFV4 infection and measurement of luciferase activity. The viRNA mimics should function like natural viRNAs by mediating degradation of viral RNA and in turn reduce *RLuc* expression. Through degradation of viral genome, the *RLuc* expression is reduced. The efficiency of each viRNA mimic can be determined by the level of reduction in *RLuc* expression.

Location	Sequence	viRNA frequency (read) U4.4/Aag2	Relative *RLuc* expression (%) U4.4/Aag2
Negative control	Negative control siRNA (Ambion AM4635)	N/A	100
Positive control	*RLuc* siRNA (Ambion AM4630)	N/A	30.5/23.8
1016 (cold)	5’ –GAGGGAUUCCUAGUGUGCAAG -3’ 3’ –GCCUCCCUAAGGAUCACACGU -3’	0/0	21.7/31.2
1268 (hot)	5’ –UGGGCGAGGGAAUACAAGGCA -3’ 3’ –UCACCCGCUCCCUUAUGUUCC -5’	393/253	91.6/103.6
2257 (hot)	5’ –UCCGGGAUCAGGCAAGUCUGC -3’ 3’ –CAAGGCCCUAGACCGUUCAGA -5’	341/79	60.5/92.7
2460 (cold)	5’ –UCGCUUGCCAUUCCGGUACUC -3’ 3’ -AAAGCGAACGGUAAGGCCATG -5’	0/0	51.8/36.6
3456 (cold)	5’ –UCGCAGAAAGAAAAAUCCAAC -3’ 3’ –ATAGCGUCUUUCUUUUUAGGU -5’	0/0	20.6/39
3549 (hot)	5’ –CGGUUAAAGGCAGUAGGGUUG -3’ 3’ –GAGCCAAUUUCCGUCAUCCCA -5’	300/261	21.4/42.2
5129 (cold)	5’ –GACTCGTCTTCCACTGCCAGC -3’ 3’ –GGCUGAGCAGAAGGUGACGGU -5’	0/0	39/38.1
6547 (cold)	5’ –GUUUAUUAACACUGUUUUGAA -3’ 3’ –AACAAAUAAUUGUGACAAAAC -5’	0/0	24.7/41.2
7305 (hot)	5’ –UGGCGAGGGACAUUAAGGCGU -3’ 3’ –GAACCGCUCCCUGUAAUUCCG -5’	397/245	94.1/106.1
8340 (hot)	5’ –CGAGGAUAACGUGGAUAGGCC -3’ 3’ –GAGCUCCUAUUGCACCUAUCC -3’	324/753	97.5/81.4
9887 (cold)	5’ -UGCCGAACGUGGUGGGGUUCC -3’ 3’ –TTACGGCUUGCACCACCCCAA -5’	0/1	43.7/90.2
10181 (hot)	5’ –AGGCGUACGUCGAUCGAUCGG -3’ 3’ –GCUCCGCAUGCAGCUAGCUAG -5’	177/316	62.2/70.3
10499 (hot)	5’ –ACGACCUGUACGCGAACACGG -3’ 3’ –AUUGCUGGACAUGCGCUUGUG -5’	252/1,116	89.7/97.7

10645 (cold)	5’ –CAAAUCAAAACGAACCCUGUC -3’ 3’ –CGGUUUAGUUUUGCUUGGGAC -5’	0/1	81.7/102.4

Table 5.3 List of siRNA mimics.

Summary of siRNA mimics location, sequence and ability to inhibit viral marker gene expression.

The optimum concentration of viRNA mimic for silencing SFV4(3H)-*RLuc* was determined. 1.25 x 10^5 U4.4 cells per well were cultured in 24-well plates overnight before transfection with hot- and cold-spot viRNA mimics (4 each of hot or cold spots). The cultures were then infected with SFV4(3H)-RLuc (MOI=1) 24 hours post-transfection. Luciferase activities were measured at 12 hours post-infection. The experiment was carried out at 6 different final concentrations of viRNA: 3, 6, 12, 25, 50, and 100 nM. Every concentration tested was carried out in triplicate (figure 5.10).

The results showed a general silencing efficiency pattern where positive control siRNA against *RLuc* silenced *RLuc* expression most efficiently at all concentrations. Cold-spot viRNA mimics (blue lines) were the next most efficient, then hot-spot mimics and then the negative control.

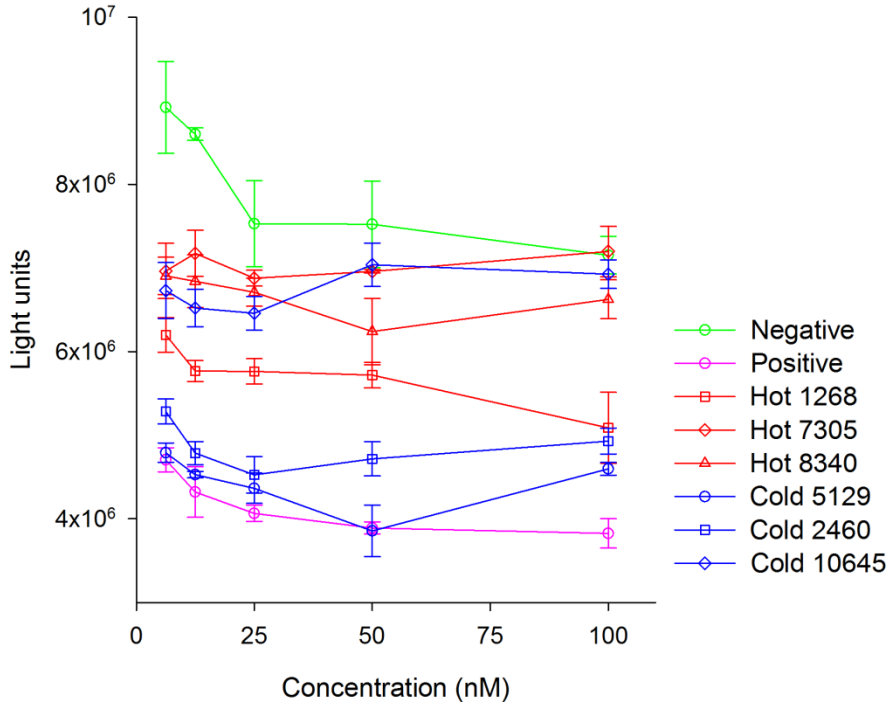

Figure 5.10: The ability to silence *RLuc* expression of viRNA mimics and controls siRNAs in different concentrations.

U4.4 cultures were transfected with siRNA duplexes including: a positive control siRNA targeting *RLuc*, a negative control scrambled siRNA and 4 cold- and 4 hot- viRNA mimics for 24 h at final concentrations of 3, 6, 12, 25, 50 or 100 nM (X-axis), then infected with SFV4(3H)-*RLuc* (MOI=1). *RLuc* activities (Y axis) were determined at 12 hours post-infection. The experiment was carried out in triplicate and error bars represent standard error.

There was no clear dose response and a second experiment was therefore carried out using lower concentrations of siRNAs. This dose response showed cold spot-derived viRNAs have a similar silencing ability to that of the positive control siRNA. In contrast, hot spot-derived viRNA mimics resembled the negative siRNA. As the concentration of siRNAs used rose, the luciferase activity decreased (figure 5.11). 10 nM was chosen as the standard concentration for testing different viRNA mimics.

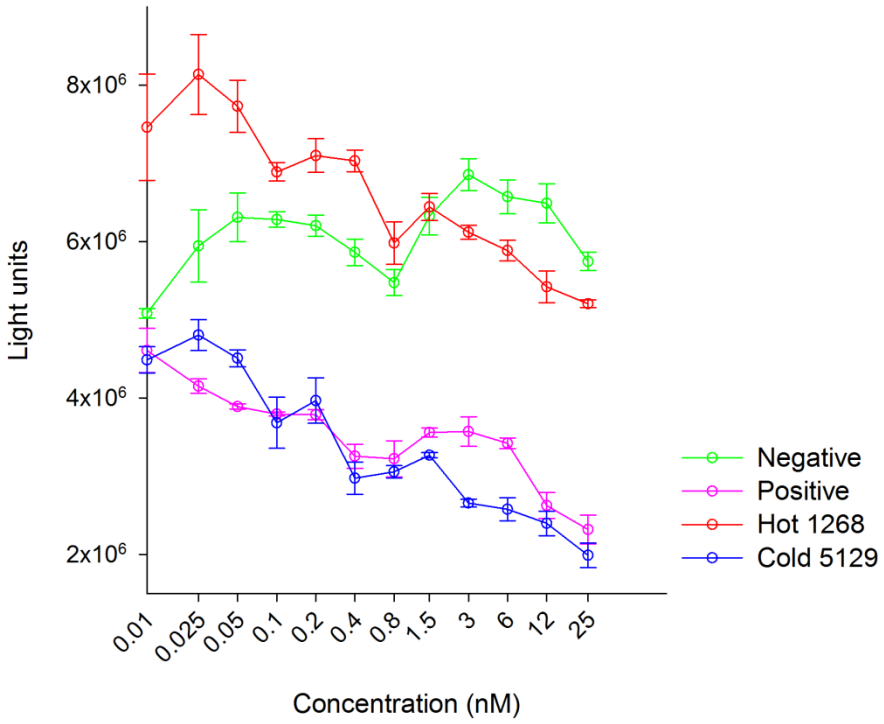

Figure 5.11: Investigation of siNRA dosage and ability to silence *RLuc* expression.

U4.4 cultures were transfected with siRNA duplexes including: a positive control siRNA targeting *RLuc*, a negative control scrambled siRNA, 1 cold-spot and 1 hot-spot viRNA mimics for 24 h at final concentrations ranging from 0.01 to 25 nM (X-axis), then infected with SFV4(3H)-*RLuc* (MOI=1). *RLuc* activities were determined at 12 hours post-infection (Y axis). The experiment was carried out in triplicate and error bars represent standard error.

Once the optimum concentration was determined, all 7 hot- and 7 cold-spot viRNA mimics (Table 5.3) were compared. As described above, cultures were tranfected with siRNA in 24-well plates for 24 hours followed by infection with SFV4(3H)-*RLuc* (MOI=1). Luciferase activities were measured at 12 hours post-infection. The experiment was carried out in triplicate (figure 5.12). All luciferase measurements were normalised to the negative control (100%). The results indicated that the overall

ability of cold-spot viRNA mimics to target SFV4 viral RNA is significantly higher than hot-spot viRNA mimics (P = 0.0379 by a statistical comparison of hot and cold groups with a Mann-Whitney U test). The findings support the earlier results shown in figure 5.10 and 5.11.

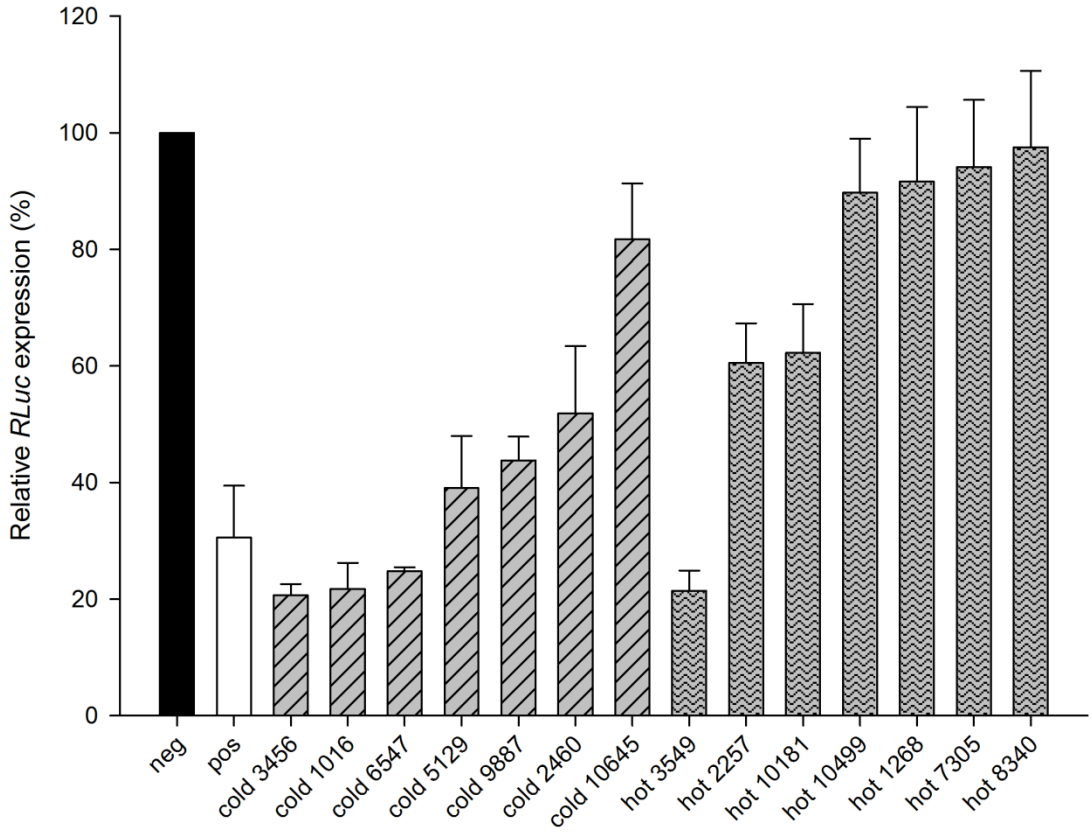

Figure 5.12: Synthetic siRNA mimics of SFV genome hot and cold spot viRNAs and their effect on virus replication in U4.4 cells.

Ae. albopictus-derived U4.4 cells were transfected with viRNA mimics (10 nM, Table 5.3) for 24 h, followed by reporter SFV4(3H)-*RLuc* infection (MOI=1). *RLuc* activities (read-out for SFV replication) were determined at 12 hours post-infection and normalised to negative-control scrambled siRNA (100% relative *RLuc* expression). Statistical analysis was performed by comparing the activities of hot and cold spot mimic siRNA groups (Mann-Whitney Test, P = 0.0379). This experiment was performed in triplicate for each siRNA and repeated three times; bars show the average relative *RLuc* activities for each siRNA from all three experiments, and error bars represent standard errors.

This experiment was repeated with *Ae. aegypti*-derived Aag2 cells as described above, with the same selection of viRNAs mimics (Table 5.3, column 3). The same silencing effects were observed, with cold-spot viRNAs mimics being significantly

more efficient than hot-spot mimics (P = 0.0379 by Mann-Whitney U test) at inhibiting SFV replication (Figure 5.13). This result suggests cold spot viRNAs are more efficient at mediating RNAi silencing than hot spot viRNAs in mosquito cells of different species.

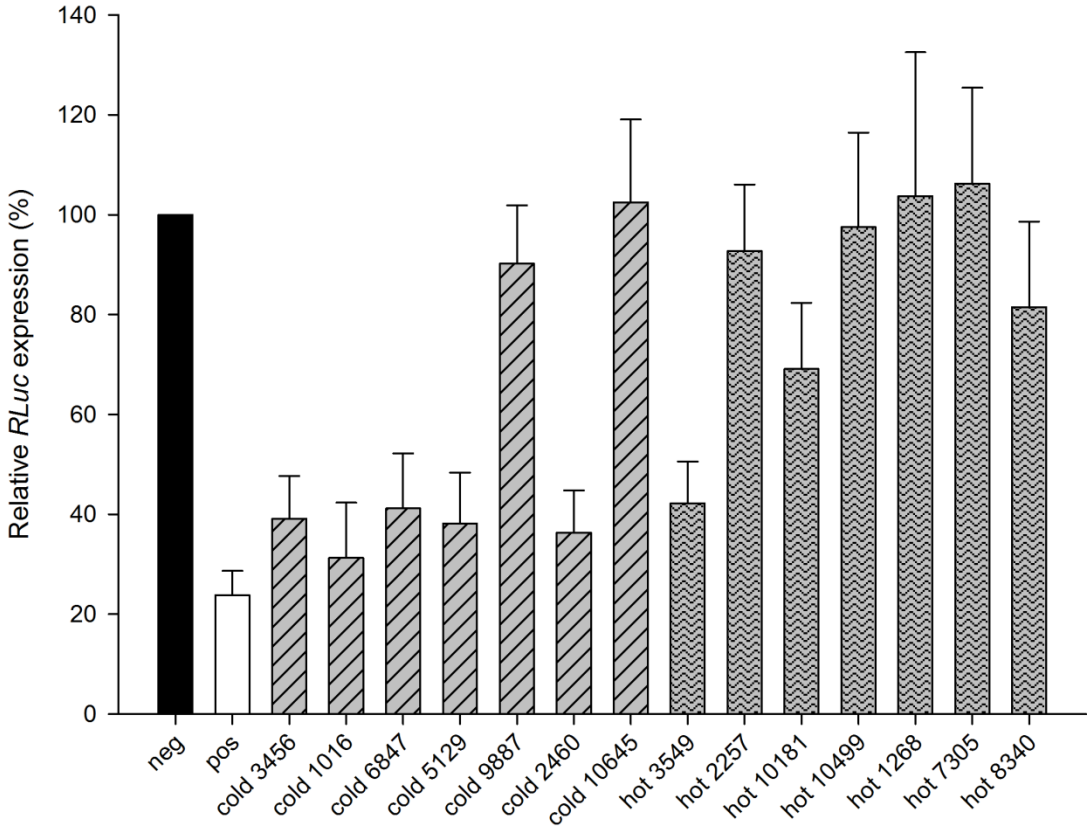

Figure 5.13: Synthetic siRNA mimics of SFV genome hot and cold spot viRNAs and their effect on virus replication in Aag2 cells.

Ae. aegypti-derived Aag2 cells were transfected with viRNA mimics (10 nM, Table 5.3) for 24 h, followed by reporter SFV4(3H)-*RLuc* infection (MOI=1). *RLuc* activities (read-out for SFV replication) were determined at 12 hours post-infection and normalised to negative-control scrambled siRNA (100% relative *RLuc* expression). Statistical analysis was performed by comparing the activities of hot and cold spot mimic siRNAs groups (Mann-Whitney Test, P = 0.0379). This experiment was performed in triplicate for each siRNA and repeated three times; bars show the average relative *RLuc* activities for each siRNA from all three experiments, and error bars represent standard errors.

Summary of Findings

SFV4-derived viRNAs in Aedes albopictus-derived U4.4 cells

- viRNAs derived from SFV4 infected U4.4 cells were sequenced by Solexa Illumina deep sequencing technology. A total of 3.2 x 10^6 small RNA were sequenced. 7.5 x 10^4 reads were derived from viral nucleic acid. This represents 2.1% of all small RNA isolated from U4.4 cells.
- viRNA were 20-26 nt in length. 21 nt long viRNAs were found to be the predominant species and accounted for 91.1% of all 20-26 nt sequences.
- The biogenesis of viRNAs from genome and genome complementary RNA was asymmetric. 60% of all the 21 nt viRNAs mapped to the genome and 40% to the complementary genome.
- There was no obvious skewing towards a particular base at the first position. There was no bias in GC-content and no obvious common sequence motifs.
- 21 nt viRNAs were generated over the entire SFV genome and genome complement in a non-random manner. Some areas generated high frequencies of viRNAs and other areas no or very few viRNAs; these are referred to ‘hot spots’ and ‘cold spots’ respectively. The hot and cold spots were spread throughout the length of the whole genome.
- Replicate experiments showed similar patterns of viRNA frequency with some identical hot and cold spots but also some variation.

SFV-derived viRNAs in Aedes aegypti-derived Aag2 cells

- viRNA identified were 20-25 nt in length. 21 nt long viRNAs were found to be the predominant species and accounted for 97.6% of these sequences.
- 59.6% of all 21 nt viRNA mapped to the SFV genome and 40.4% mapped to the genome complement.
- The biogenesis of viRNAs from genome and genome complementary RNAs was asymmetric. 59.6% of all the 21 nt viRNAs mapped to the genome and 40.4% to the complementary genome.

- There was no obvious skewing towards a particular base at the first position. There was no bias in GC-content and no obvious common sequence motifs.
- 21 nt viRNAs were also generated over the entire SFV genome and genome complement in a non-random manner. However, many hot spots mapped to the structural region of the genome.
- Comparison of the viRNA frequencies between U4.4 and Aag2 cells showed that there were identical hot and cold spots but also some differences.

viRNA origins in mosquito U4.4 cells

- Infection with SFV1(3F)-IRES-ZsGreen VRPs resulted in 50% of the cells being green indicating that replicon replication had occurred and that the EMCV IRES did not produce a viable replicon. Unfortunately, therefore this did not provide a system to analyse viRNA production in the absence of virus/replicon replication.
- Non-green cells in the SFV1(3F)-IRES-ZsGreen infected culture were successfully sorted into a separate population by FACS. The viRNA population in these cells was compared to that in the SFV1(3F)- ZsGreen infected culture.
- There was an approximately 21-fold reduction in viRNAs in the (non-green) SFV1(3F)-IRES-ZsGreen infected cells compared to the SFV1(3F)-ZsGreen infected cells. However the absence of IRES derived viRNAs suggest SFV1(3F)-IRES-ZsGreen stock contained contaminating of SFV1(3F)-ZsGreen replicons.
- In both cultures approximately 70% of 21 nt RNA mapped to the genomic RNA.
- In comparison to biogenesis of viRNAs from SFV4 infected cells. There was a 10% bias towards viRNAs generated from the genomic RNA in the replicon infected cells.
- MFED values generated by secondary structure prediction were close to zero along the entire SFV genome, which indicated an absence of structured RNA, with the exception of the 5’ untranslated region.

- The frequency pattern of 21-nt genome-derived viRNAs was aligned and compared with the pairing and MFED values.
- viRNA frequencies were put into ordered catagories. There was no correlation with MFED values.
- The relationship between pairing values and viRNA frequency catagories was analysed, again there was no significant association.
- A long-distance pairing analysis of the genome identified 22 regions with complementary sequences which could allow folding back to form secondary structures. These regions produced no viRNAs or only a low frequency of viRNAs.

Ability of hot spot- and cold spot-derived viRNAs to inhibit SFV replication

- Transfection of U4.4 cells with hot- and cold-spot viRNA mimics for 24 hours followed by infection with SFV4(3H)-*RLuc* indicated that the overall ability of cold-spot viRNA mimics to target SFV4 viral RNA was significantly higher than of hot-spot viRNAs.
- The same viRNA mimics were studied in Aag2 cells. The same silencing effects were observed, with cold-spot viRNAs mimics being significantly more efficient than hot-spot mimics.

Discussion

RNAi is the most direct form of defence against arboviruses in mosquitoes. The mechanism of RNAi has been well studied. However, there is little insight on i) viral dsRNA substrate for Dicer ii) dicer's preference of viral dsRNA substrate and iii) whether dsRNA processing is identical in different host species of the same genus. This study has addressed some of these questions. To answer these questions, Illumina Solexa, a new powerful sequencing technology was used to characterise SFV-derived viRNAs produced during the acute phase of infection in SFV4 infected *Ae. albopictus* U4.4 cells. The technology sequenced 3 million (and later 12 M) pieces of small RNA. 2.1% of these small RNA sequences were derived from 21-26 nt viral RNA. The predominant viRNA species was 21 nt in length; they were

generated asymmetrically from the SFV genome (60%) and genome complement (40%); and distributed along the length of the SFV genome and complement in a non-random manner. The loci on the genome/genome complementary RNA generating high frequency of viRNAs were named "hot-spots", whilst "cold-spots" referred to areas that generated few or no detectable viRNAs. This finding is in perfect agreement with previous findings form *Ae. aegypti* infected with Sindbis virus (Myles *et al.*, 2008). These authors (Myles 2008, figure 1b and c) also showed that the predominating viRNA is 21 nt and that viRNA distribution across the genome and complementary genome is non-random with hot- and cold- spots. These findings indicated that key features of alphavirus-induced antiviral RNAi are conserved across aedine and anopheline mosquitoes (Myles *et al*., 2010). In the present study, the 21 nt viRNAs showed no obvious skewing towards a particular base at the first base position, no bias in GC-content and no obvious common sequence motifs. This indicated that Dicer in U4.4 cells does not have a preference of viral dsRNA substrate. This finding is very different from siRNA derived from *Brassica juncea* infected with plant virus turnip mosaic virus (TuMV) which shows a GC preference in siRNA hotspots (Ho, 2007). This suggests that differences in host species and Dicer affect the biogenesis of viRNA. The difference in viRNA generation was also apparent when a similar experiment was carried out on a mosquito of a different genus, *Culex pipiens quinquefasciatus* and a non-alphavirus (West Nile Virus) (Brackney *et al*., 2009). Their viRNA species were more evenly distributed (from 19-23 nt) instead of a single predominant species as observed in the present study. Nevertheless, the viRNA frequency pattern remains in agreement with non-random distribution of viRNAs (Brackney *et al*., 2009). Therefore, the biogenesis of viRNA in *Ae. aegypti*-derived Aag2 cells was investigated to determine whether dsRNA processing is identical in different species of the same mosquito genus. The predominant viRNA species in Aag2 was also 21 nt in length; generated asymmetrically from the SFV genome (60%) and genome complement (40%); and distributed along the length of the SFV genome and genome complement in a non-random manner with hot- and cold-spots. Comparison of the viRNA frequencies between U4.4 and Aag2 cells showed that they shared identity in hot and cold spots. However, the distribution made up an overall pattern with many hot spots mapped to

the structural region of the genome. This could suggest that replication of SFV had entered the late phase in Aag2 cells at 24 hours post-infection which would lead to a higher level of subgenomic RNA as substrate for Dicer.

The non-random distribution of U4.4 and Aag2 derived viRNAs along the SFV genome and genome complementary RNA had raised questions on i) what substrate/origin gave rise to robust generation of hot-spot viRNAs, and ii) how different viRNAs differ in their abilities in mediating RNAi. In virus infection, it is highly likely that viRNAs are derived from all three sources: i) double-stranded regions in single-stranded viral genome, ii) in genome complementary RNA molecules, and iii) replication intermediate duplex. In an attempt to gain insight into viRNA generation from replication intermediates, non-replicating VRP SFV1(3F)-IRES-ZsGreen was used. This was designed to locate viRNA peaks that would be eliminated when replication was eliminated. Unlike insect-only viruses, SFV does not possess RNAi inhibitor proteins and replication intermediates are not being protected, so it is believed that replication intermediates may be a major source of viRNA (Myles *et al*., 2010). Unfortunately, the EMCV IRES element did not provide a system to analyse viRNA production in the absence of virus/replicon replication. According to the Solexa sequencing data, IRES was absent in the isolated non-green cells (Table 5.1 & 5.2). The reason why these cells are non-green but not containing any detectable IRES sequence is unclear. However, the presence of ZsGreen viRNAs, similar viRNA distribution pattern between SFV1(3F)-IRES-ZsGreen and SFV1(3F)-ZsGreen (Figure 5.7A&B) and 21-fold less viRNAs in the non-green isolated cell infected SFV1(3F)-IRES-ZsGreen compared with SFV1(3F)-ZsGreen infected cells suggested that a low level of SFV1(3F)-ZsGreen replication was occurring in non-green cells. A simpler strategy such as introduction of a point mutation or a stop codon in the virus replicase sequence or use uncapped SFV genomic transcripts and transfection could be used. However these strategies do not provide a large amount of SFV genomic transcripts to produce a viRNA for analysis. Alternately, establishing a stable cell line constitutively expressing SFV genomic RNA which contains a mutation in the replicase sequence may provide a viable system to address this investigation. In both replicon (SFV1(3F)-IRES-ZsGreen & SFV1(3F)-ZsGreen) infected cultures, approximately 70% of 21 nt viRNAs were

mapped to the genome RNA which is 10% more than in virus infected cultures. However, the reason behind this observation is unclear.

The second approach to identify the substrate/origin of hot spot viRNAs was to estimate RNA secondary structures on the single-stranded viral genome and determine if those highly structured areas were correlated to viRNA hot-spots. SFV is not known to have any inverted repeats or functional RNA structures, unlike some plant viruses where genomic RNA is highly structure and perfectly paired, which could serve as substrates for Dicer (Ho *et al*., 2006). MFED and pairing analyses predicted possible secondary structures on SFV4 genomic RNA. Like other alphavirus, the most likely secondary structure is at the 5' end of the genome and the rest of the genome contains only a few areas with a high probability of secondary structures. These powerful secondary structure prediction methods allowed analyses to determine whether predicted secondary structure locations had any correlation with observed viRNA hot-spots. Unfortunately, no correlation was found between: i) means of MFED values and different categories of viRNA frequencies; ii) pairing values and different categories of viRNA frequencies; iii) specific distant-pairing regions of the genomic RNA and high viRNA frequency. These (i & ii) suggested within each category, locations with similar levels of viRNA generation did not have a similar probability of secondary structure formation and (iii) viRNA hot-spots were not generated from locations where long-distance pairing could take place on the SFV genome. The lack of any correlation indicated that the vast majority of viRNAs are not specifically generated from genomic secondary structures. Like the 5' region of the alphavirus, the 3' terminus of the flavivirus genome contains secondary structure, and these structures do not appear to be a target to generate excess viRNAs during mosquito infection by West Nile virus (Brackney *et al*., 2009). Therefore, the origin of alphavirus-induced dsRNA remains inconclusive.

Areas that generated high frequency of viRNA (hot-spots), and reappeared in different sequencing experiments must be in a conformation, position or replication state that increases the chance of access by Dcr-2. For example, the genomic RNA nucleotide position 10499 and genome complementary position 461 and 9769 nt consistently generated high viRNA frequency throughout all four U4.4 sequencing

experiments (figure 5.14). Those locations that consistently generate few or no viRNAs may not provide much access to Dcr-2, or alternatively they could be less available, either temporally or spatially during replication. For example, newly synthesized RNAs remain closely associated and protected by replication complexes (Frolova *et al*, 2010; Geiss *et al*., 2005).

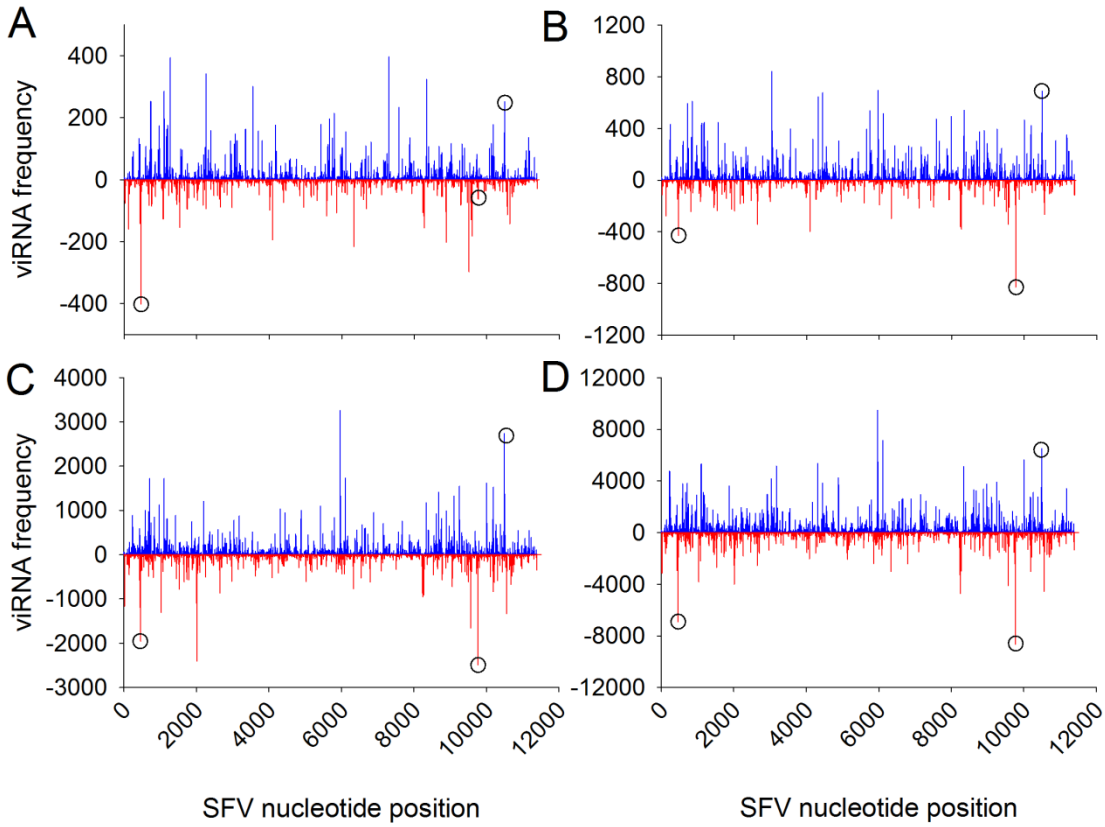

Figure 5.14: Comparison of 21 nt viRNA distributions from SFV4-infected U4.4 cells.

(A) Produced in late 2008 with maximum depth of 400 reads. (B) Produced in early 2009 with maximum depth of 400 reads. (C) Produced in early 2010 with maximum depth of 3000 reads. (D) Produced in 2010 following C with maximum depth of 10000 reads. Circles indicate exact locations where high amounts of viRNA were generated in the majority of the different sequencing experiments.

The robust generation of hot- or cold-spots at exactly the same location of the SFV genome raised the question of how different viRNAs differ in their ability to mediate RNAi. It is unclear whether this non-randomised generation serves any purpose. The results showed that the overall ability of cold-spot viRNA mimics to target SFV4 viral RNA was significantly higher than for hot-spot viRNAs in both U4.4 and Aag2

cells (P = 0.0379 and P = 0.0379, respectively by a statistical comparison of hot and cold groups with a Mann-Whitney U test). This suggests that Dicer and the RISC complex vary in their specificity or ability to bind and process RNA. Hot-spot viRNAs could be generated from areas which are structured (secondary + tertiary + quaternary) but remain accessible to the small ds-RNA binding protein Dicer. However, the larger RISC complex may not find the same site to be as accessible. Therefore hot-spot viRNAs may not be very effective for target degradation. The converse may be applied in that areas that are easy for RISC to access (big open area and single-stranded) may not be a good substrate for Dicer (non-structured single stranded area). A similar phenomenon was observed in *Potato spindle tuber viroid* (PSTVd) where secondary structures within the viroid generate most siRNA but at the same time these secondary structures are highly resistant to RISC-mediated cleavage (Itaya *et al.*, 2007). To date, evidence of viRNA-based RNAi diversion has been described in Cauliflower mosaic pararetrovirus (CaMV) in which the non-coding part of the virus genome spawns massive quantities of viRNAs to prevent less abundant viRNAs produced from other genome regions from being assembled into AGO-RISCs. The expression of this non-coding part of CaMV on an attenuated geminivirus rescued infectivity and accumulated higher DNA titres (Blevins *et al.*, 2011). Also, in human adenovirus, highly structured virus-associated RNAs appear to function as suppressors of RNAi by acting as competitive substrates and antagonists of Dicer (Andersson *et al.*, 2005; Lu & Cullen, 2004). The two results (precise hot-spot generation and difference in hot/cold spot silencing efficiency) and the fact that alphaviruses lack an RNAi inhibitor, suggested that alphaviruses have been under selective pressure by RNAi and their genomes have been selected to allow more viRNA generation at areas that may least compromise virus replication. We will not know if this is true until we have mutated the hot viRNA generation area and compared the attenuation effect with a mutation in the cold area, but natural selection definitely would not allow an RNAi susceptible strain to be the predominant genotype when the host cell of the virus has RNAi as a viral defence mechanism. Perhaps acquiring a viral suppressor of RNAi (VSR) may seem more sensible than sacrificing replication rate through evolution. However, alphaviruses require persistent infection in order to complete their life cycle, experiments have

demonstrated that the co-expression of RNAi-inhibitory protein B2 of Flock House virus (*Nodaviridae*, insect virus) in Sindbis virus during infection in *Ae. aegypti* dramatically increased the mortality rate of the mosquito (Cirimotich *et al.*, 2009; Myles *et al.*, 2008). Therefore, a viRNA-based diversion mechanism may lead to a better balance between virus and host survival and persistence.

Table of contents

Chapter 6: RNAi in *Aedes aegypti* mosquitoes

Introduction

The ability of alphaviruses to infect cells of the mosquito *Ae. albopictus* has previously been studied in three cell lines, C6/36, C7-10, and U4.4 derived from larvae (Singh, 1967). C6/36 is one of twenty clones (C6, clone 6) isolated from cultured *Ae. albopictus* cells, one characteristic of this clone is the ability to produce high virus yield up to 7 days after dengue and Chikungunya virus infections. Sub-clone 36, one of the 43 sub-clones of C6, showed mild to extensive cytopathic effects several days post-infection with Chikungunya or Dengue viruses (Igarashi, 1978). C7-10 cells are also a sub-cloned population originating from Singh's cells and display cytopathic effect upon Sindbis virus infection (Sarver & Stollar, 1977). In the previous chapters of this thesis I studied SFV in these three cell lines and then studied the detailed reponse of one cell line, U4.4, to SFV infection. Given the variability between cell lines and the observations with different constructs of SFV, I wanted to investigate events *in vivo* in mosquitoes. To do this, protocols had to be developed to keep, infect and study the course of infection in mosquitoes. This chapter describes the establishment of these systems and their use.

SFV1 VRP infection of *Aedes aegypti* mosquitoes

Due to lack of an insectary to allow infection of live mosquitoes with propagating virus, this experiment was designed to infect live mosquitoes with non-propagating SFV1-d1eGFP VRPs. The SFV1-d1eGFP construct is as described in Chapter 1 and in Figure 1.7B. The expression of eGFP is driven by subgenomic promoter to provide a high level of expression. The infection of mosquitoes with SFV was designed to be carried out with droplets of mouse blood mixed with SFV1-d1eGFP VRPs placed on the top of the nylon mesh of the feeding container (open air environment). SFV is relatively stable in aerosols of tissue homogenates (Benbough, 1969), however aerosols of purified virus are rapidly inactivated (de Jong *et al.*, 1976). Therefore, the stability of purified SFV in mouse blood was determined. To

determine the stability of the infectivity of SFV in this open air environment, a naturally occurring strain of SFV, A7(74), was mixed with fresh mouse blood (final conc. 1 x 10^5 PFU/ml) at 28^{o}C and allowed to rest in an opened eppendorf tube for up to 3 hours. Virus titres were determined at 0, 0.5, 1, 1.5, 2, and 3 hours by plaque assays. SFV A7(74) was mixed with 10% fructose PBSA as a control (final conc. 2.5 x 10^7 PFU/ml). The experiment was carried out in triplicate. The experiment showed that the SFV A7(74) titre did not decrease over the course of 3 hours (Figure 6.1A). This indicates mouse blood is suitable for maintaining SFV infectivity for up to 3 hours in open air. In the control suspension of virus without mouse blood the SFV titre steadily declined from 7 x 10^6 to 2.5 x 10^4 PFU/ml (Figure 6.1B).

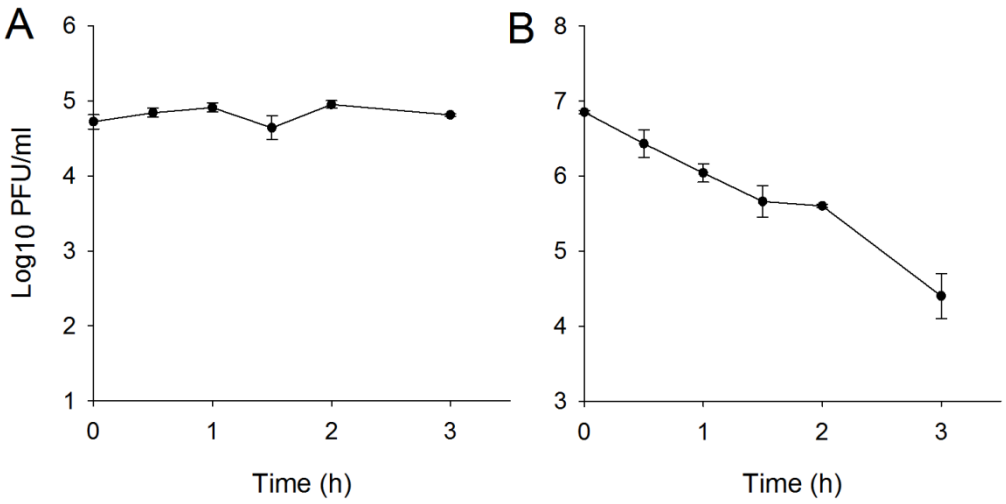

Figure 6.1: Infectivity of SFV A7(74) in open air in mouse blood.

The infectivity of SFV A7(74) determined in (A) fresh mouse blood and (B) 10% fructose PBSA. SFV A7(74) was added to three replicate tubes of fresh mouse blood (final conc. 1 x 10^5 PFU/ml) or 10% fructose PBSA (final conc. 2.5 x 10^7 PFU/ml). The tubes were left open for 3 hours and samples were taken for plaque assay at various times. Each point represents the mean titre from the three replicate tubes and the error bars show the standard error of the mean.

To infect and visualise SFV infection in the live mosquito, mosquitoes were fed with SFV VRP-spiked blood meals containing 10^5 infectious units (IU)/µl of SFV1-d1eGFP VRPs. Mosquitoes were kept alive for 5 days before they were dissected. To search for evidence of infection, midguts were observed under UV microscopy. Out of the 50 infected mosquitoes, none showed obvious expression of eGFP in the midgut. Figure 6.2A shows the midgut of a control mosquito which is highly

autofluorescent. Figure 6.2B shows the midgut of a SFV1-eGFP VRP-fed mosquito. There is a possible focus of fluorescence (location enlarged in Figure 6.2C). It is difficult to draw conclusions from this study, either infection was difficult to establish, or the time after infection that the midgets were examined was not appropriate, or the eGFP signal was too weak to observe given the high background autofluoresence.

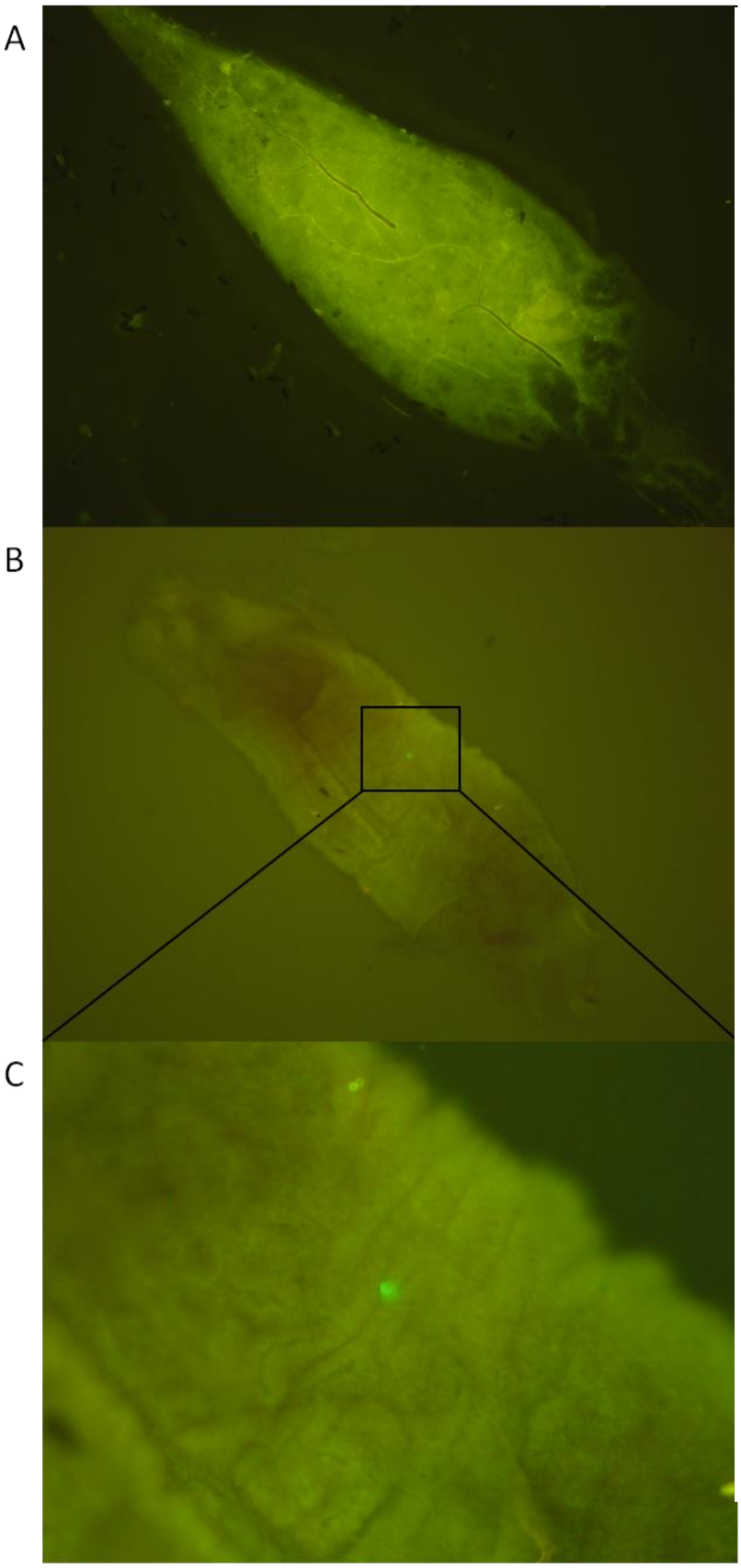

Figure 6.2 Midguts of SFV-eGFP infected *Aedes aegypti*

Photomicrographs of *Ae. aegypti* midgut dissected at day 5 post-infection, fixed with 4% paraformaldehyde under UV spectrum at 10X magnification. (A) A midgut from a healthy non-infected control female mosquito. (B) SFV1-eGFP infected midgut. (C) enlarged view of possible expression of eGFP.

Immunostaining of paraffin sections of mosquitoes

As an alternative to fluorescence microscopy and to avoid the problem with auto-fluorescence, immunostaining of paraffin processed sections was carried out. Mosquitoes fed with SFV1-d1eGFP VRP spiked blood meals ($1x10^5$ (IU)/μl) were kept alive for 5 days and then fixed in 4% paraformaldehyde. Fixed mosquitoes were processed and sectioned. Sections were then stained with an antibody against the viral protein nsP3. Both fluorochrome and diaminobenzidine (DAB) immunostaining were used (Figure 6.3A and B). The fixed paraffin section also showed a high degree of autofluorescence at 230-260 nm. There is a possibility that the autofluorescence would mask the fluorescence signal coming from the fluorochrome. DAB staining avoided autofluorescence and brown staining was located in the thorax of the sectioned mosquito (Figure 6.3B). However, blood contains peroxidise and that could also break down DAB to produce brown pigment.

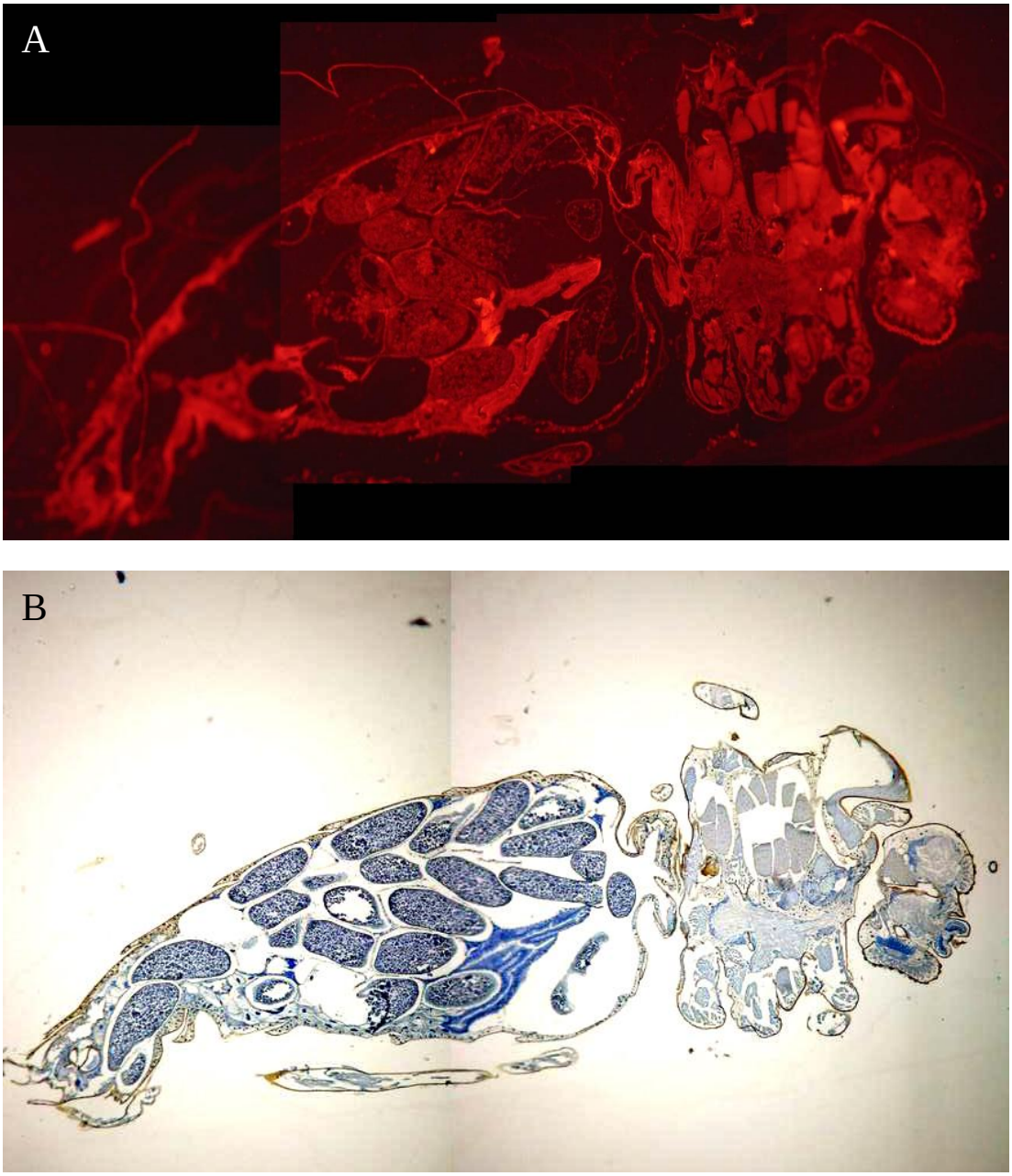

Figure 6.3: Immuno-staining of paraffin sectioned *Ae. aegypti* on day 5 post-infection with SFV1-d1eGFP.

A polyclonal rabbit antibody against SFV nsP3 was used on paraffin sectioned SFV1-d1eGFP infected *Ae. Aegypti* on day 5 post-infection (A) A photomicrograph of a paraffin sectioned mosquito under 230-260 nm. A secondary antibody bound to a fluorochrome was used. No specific fluorescence was observed within any cells. There was a high degree of autofluorescence. (B) A photomicrograph of a paraffin sectioned mosquito under visible light. A secondary antibody bound to a horseradish peroxidise was used.

Characterisation of a new virus, SFV4(3H)-*RLuc*-p19.

The next approach was not to optimise visualisation of virus in the midgut but to first seek evidence of virus infection and replication in this tissue using viruses containing *Renilla* luciferase. It was also planned to use a virus containing an RNAi inhibitor as well as luciferase to overcome the host RNAi response which could be restricting the infection. SFV4(3H)-*RLuc* and SFV4(3H)-*RLuc*-p19 which express *Renilla* luciferase and in the latter virus also expresses the RNAi inhibitor p19, were used to infect mosquitoes. The p19 protein was from *Cymbidium ringspot virus (CymRSV)* and is a well-characterised inhibitor of RNA silencing which sequesters small RNA duplex. To ensure a high level of P19 expression to accommodate amount of viRNA generated in virus infection, the gene was cloned at the 3'-end of a duplicated subgenomic promoter (Figure 6.4. However, this means P19 under the control of a subgenomic promoter would only provide the counter RNAi effect late in infection. This virus was generated in the laboratory of Professor Andres Merits (University of Tartu) but it had not been characterised. To characterise SFV4(3H)-*RLuc*-p19, a virus growth curve was produced. Aliquots of 5 x 10^5 U4.4 cells were infected synchronously at MOI of 10 and 100 µl of supernatant was collected at 12, 24, 48, 72, 96 and 120 h post-infection. The supernatant in the cultures was completely replaced with fresh media each time after the supernatant was collected. Supernatant samples were kept in eppendorf tubes at -80^{o}C and titrated by plaque assay. In figure 6.5, the results are compared to figure 3.4 (production of infectious SFV4 virus in U4.4 cells), showing that the pattern is very similar with high levels of virus production observed from 0 to 24 hours post-infection. Thereafter, virus production dropped to low levels as the culture entered the persistent phase of infection. This indicated that the recombinant SFV4(3H)-*RLuc*-p19 virus replicated well in U4.4 cells.

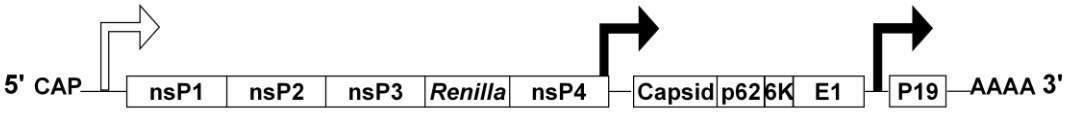

Figure 6.4: A Schematic representation of the SFV4(3H)-*RLuc*-P19.

SFV4(3H)-*RLuc*-p19 is based on SFV4 construct with *RLuc* protein gene inserted between nsP3 and nsP4 sequence. A subgenomic promoter is duplicated at the 3' end of the structural genes followed by an insertion of RNAi inhibitor P19.

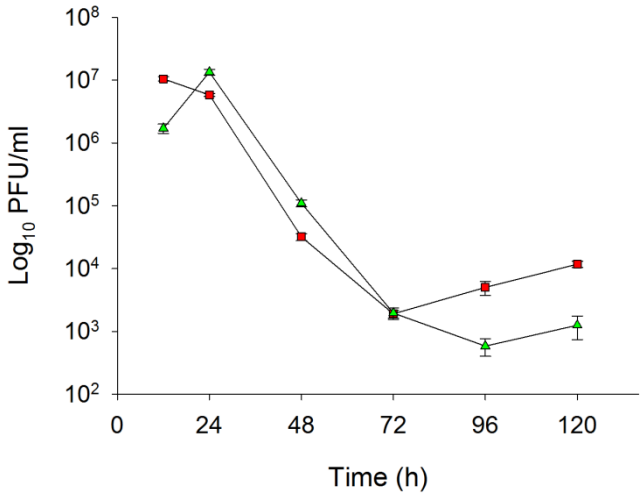

Figure 6.5: SFV4(3H)-*RLuc*-p19 production between time intervals up to 120 hours post-infection.

U4.4 cells were infected synchronously with SFV4(3H)-*RLuc*-p19 (▲)(MOI=10). Supernatants were collected for titration at 12, 24, 48, 72, 96 and 120 h post-infection. Virus titre (Y axis) is represented in Log_{10}(PFU). Each time point is the mean of triplicate samples. The error bars indicate the standard error of the mean. Data for SFV4 production in U4.4 cells (■) was taken from Figure 3.4 and used here for comparison.

The effect of the p19 RNAi inhibitor was first tested in vitro, U4.4 cultures were infected with SFV4(3H)-*RLuc*-p19 (MOI= 0.001 or 10) and virus titre determined at 24 and 48 hours post-infection. Parallel cultures were infected with SFV4(3H)-*RLuc* or SFV4 as controls. In the case of infection with MOI of 0.001, titres of all three viruses increased from 24-48 hours. SFV4 produced the higher titre out of the three viruses followed by SFV4(3H)-*RLuc*-p19 and SFV(3H)-*RLuc* (Figure 6.6). That

SFV4(3H)-*RLuc* produced the lowest titre, suggests that insertion of the foreign marker gene attenuates virus replication. Interestingly, SFV4(3H)-*RLuc*-p19 had a higher titre than SFV4(3H)-*RLuc* at both MOI 0.001 and 10, indicating that insertion of p19 partially rescues the phenotype. After the discussion during the PhD viva, a statistic analysis between the virus titres was decided to be determined, however this particular data file on the harddrive was corrupted beyond repair.

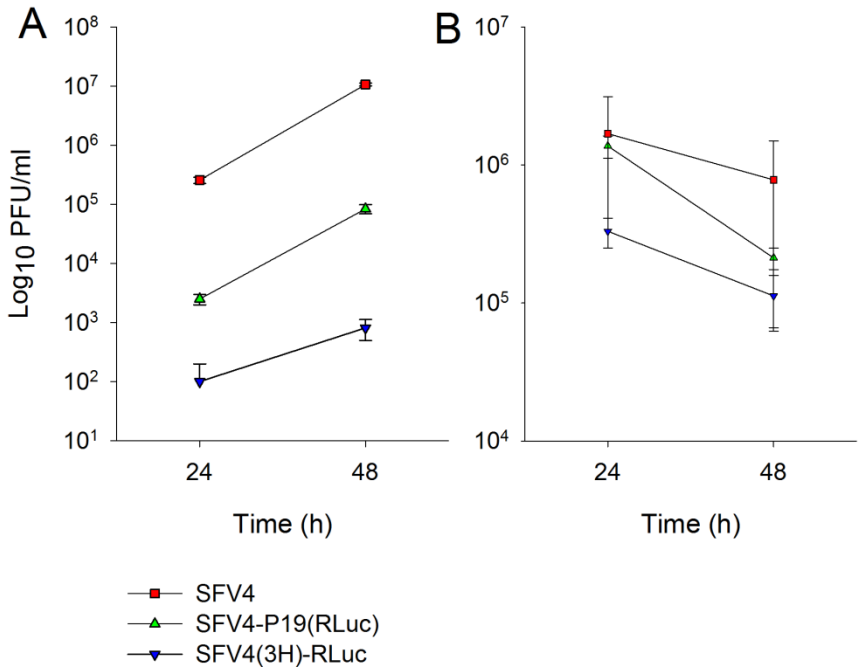

Figure 6.6: Virus titres of SFV4(3H)-*RLuc*-p19, SFV4(3H)-*RLuc* and SFV4 at 24 and 48 hours post-infection

U4.4 cultures were infected with the indicated viruses at (A) MOI 0.001 (B) MOI 10. Virus titres were determined at 24 and 48 hours by plaque assay. Each point is the mean of triplicate samples. The error bars indicate the standard error of the mean.

Infection of *Aedes aegypti* mosquitoes with SFV4(3H)-*RLuc*-p19 and SFV4(3H)-*RLuc*

To see the effect of p19 on SFV replication in whole mosquitoes, *Ae. aegypti* were orally infected with SFV4(3H)-*RLuc*-p19 or SFV4(3H)-*RLuc* as control. To prepare mosquitoes for oral infection, sugar and water sources were removed 24 hours prior to infection. Twenty female mosquitoes were transferred to infection containers. SFV4(3H)-*RLuc*-p19 was mixed with blood and ATP to a final concentration of 10^7 PFU/ml. Five drops (10 ul each) of blood mix were placed on top of the nylon mesh of the feeding container. Eighty female mosquitoes (divided between four containers) were given SFV4(3H)-*RLuc*-p19 blood mix. SFV4(3H)-*RLuc* blood mix was used to infect 80 female mosquitoes as a control. One hour was allowed for blood feeding at 28^{o}C. After feeding was finished, unfed mosquitoes were removed and discarded. To determine virus replication, whole mosquitoes were ground and lysed in an eppendorf tube with a disposable tissue homogeniser in passive lysis buffer on post-infection days (PID) 2, 3, 4, and 5, and viral marker gene expression was determined by luciferase assay. The results are showed in table 6.1. In the SFV4(3H)-*RLuc* group only one mosquito had detectable luciferase activity. This was detected on PID 5. In the SFV4(3H)-*RLuc*-p19 group, 2 mosquitoes were luciferase positive, one at day 2 and one at day 4. The luciferase activity was noticeably higher in SFV4(3H)-*RLuc*-p19 infected mosquitoes; the luciferease activity detected on PID 2 and 4 of SFV4(3H)-*RLuc*-p19 infected mosquitoes were 6.5 times and 43 times higher than the activity detected in the SFV4(3H)-*RLuc* infected mosquito on PID 5. However, numbers are too small to determine whether or not this was significant.

	SFV4(3H)-*RLuc*		SFV4(3H)-*RLuc*-p19	
PID	No. of *RLuc* +ve/-ve mosquitoes	Average *RLuc* activity (+ve/-ve)	No. of *RLuc* +ve/-ve mosquitoes	Average *RLuc* activity (+ve/-ve)
2	0/11	NA/252	1/10	9117/230
3	0/10	NA/198	0/8	NA/211
4	0/9	NA/148	1/14	60319/148
5	1/9	1395/232	0/11	NA/213

Table 6.1 Renilla luciferase detection in mosquitoes fed with SFV4(3H)-*RLuc* or SFV4(3H)-*RLuc*-p19 infected blood meals.

Luciferase expression in SFV4(3H)-*RLuc*-p19 and SFV4(3H)-*RLuc* blood fed mosquitoes was determined on PID 2, 3, 4 and 5. Average *RLuc* activity (+ve/ve): average of *Rluc* activity between *RLuc* positive mosquitoes and *RLuc* negative (background) mosquitoes, respectively.

Infection of *Aedes aegypti* mosquitoes with SFV4(3H)-*RLuc* and SFV4-st*RLuc* viruses

In an attempt to make the assay more sensitive a virus expressing higher levels of luciferase (SFV4-st*RLuc* in which the expression of luciferase is under the control of subgenomic promoter) was used. *Ae. aegypti* were given SFV4(3H)-*RLuc* and SFV4-st*RLuc* blood meals as described above. Twenty mosquitoes were fed and unfed mosquitoes were removed. Fed mosquitoes were ground and lysed in an eppendorf tube with disposable tissue homogenisers in passive lysis buffer on post-infection day (PID) 7 and viral marker gene expression was determined by luciferase assay (Table 6.2). In the SFV4(3H)-*RLuc* group only 2 out of 9 mosquitoes had detectable luciferase activity. None was detected from mosquitoes fed with SFV4-st*RLuc* virus. The use of SFV4-st*RLuc* virus did not infect mosquitoes more successfully than SFV4(3H)-*RLuc* virus, therefore it is inconclusive that whether luciferase unders the control of the subgenomic promoter (SFV4-st*RLuc*) is more readily detectable than that luciferase in the replicase genes in live mosquitoes.

	SFV4(3H)-*RLuc*		SFV4-st*RLuc*	
PID	No. of *RLuc* +ve/-ve mosquitoes	Average *RLuc* activity (+ve/-ve)	No. of *RLuc* +ve/-ve mosquitoes	Average *RLuc* activity (+ve/-ve)
7	2/9	63874/310	0/14	NA/292

Table 6.2 Renilla luciferase detection in mosquitoes fed with SFV4(3H)-*RLuc* or SFV4-st*RLuc* infected blood meals.

SFV4(3H)-*RLuc* and SFV4-st*RLuc* blood fed mosquitoes were kept alive and luciferase expression was determined on PID 7. Average *RLuc* activity (+ve/ve): average of *Rluc* activity between *RLuc* positive mosquitoes and *RLuc* negative (background) mosquitoes, respectively.

Summary of Findings

Infection of mosquitoes with SFV

- SFV was found to be stable in blood on exposure to open air environment for at least 3 hours.
- The midgut of a mosquito is highly auto-fluorescent.
- Fluorescence microscopy found no obvious expression of eGFP in the midguts of 50 mosquitoes fed with SFV1-d1eGFP VRP blood meal.
- Immunostaining of paraffin-processed sections of mosquitoes fed with SFV1-d1eGFP VRP blood meals did not identify any infection in the midgut of mosquitoes.

Characterisation of SFV4(3H)-RLuc-p19 virus

- Virus production of SFV4(3H)-*RLuc*-p19 in U4.4 cells was very similar to SFV4.
- Addition of p19 to SFV4(3H)-*RLuc* significantly increased virus production.

Infection of Aedes aegypti with SFV4(3H)-RLuc-p19 and SFV4(3H)-RLuc

- Infection was difficult to establish.

- Only 2/80 mosquitoes had detectable luciferase activity after being fed with SFV4(3H)-*RLuc*-p19 and 1/80 mosquitoes had detectable luciferase activity after being fed with SFV4(3H)-*RLuc*.
- The luciferease activities detected on PIDs 2 and 4 from SFV4(3H)-*RLuc*-p19 infected mosquitoes were higher than that detected in the SFV4(3H)-*RLuc* infected mosquito on PID 5.

Infection of Aedes aegypti with SFV4(3H)-RLuc and SFV4-stRLuc viruses

- Two out of nine mosquitoes fed with SFV4(3H)-*RLuc* had detectable luciferase activity at PID 7.
- No mosquito fed with SFV4-st*RLuc* virus had detectable luciferase activity at PID 7.
- SFV4-st*RLuc* virus did not infect mosquitoes more successfully than SFV4(3H)-*RLuc* virus.

Discussion

The goal of this series of experiment was to use SFV1-d1eGFP to establish and visualise SFV infection in the midgut of *Ae. aegypti*, and then to assess the effect on SFV infection of the p19 protein of CymRSV, a protein that inhibits RNAi, with SFV4(3H)-*RLuc*, SFV4(3H)-*RLuc*-p19 and SFV4-st*RLuc* viruses. Fifty female mosquitoes were fed with SFV1-d1eGFP VRP but none produced any obvious expression of eGFP in the midgets (PID 5). The absence of observable eGFP signal could be explained by non-propagating VRP not producing a strong signal or by infection itself being difficult to establish by non-propagating VRPs. Therefore, paraffin sections of SFV1-d1eGFP VRP infected mosquitoes were produced. Unfortunately, immunostaining of paraffin-processed sections of mosquitoes also did not identify any infection in the midguts. Although infection of *Ae. aegypti* with SFV VRPs was unsuccessful, successful infection (by intrathoracic injection) and immunostaining of Sindbis virus infected *Ae. albopictus* has been demonstrated by Myles and co-worker. Immunofluorescence assay showed that anterior and posterior

midguts of Sindbis infected mosquitoes were intensively stained on day 2 post-infection (Myles *et al*., 2004).

The characterisation of SFV4(3H)-*RLuc*-P19 showed a very similar level of virus production to SFV4 with a high amount of virus being produced up to 24 hours post-infection, followed by low virus production from 72 hours onwards. This indicated that the p19 RNAi inhibitor did not have an obvious effect on the time of transition from acute to persistent phase of infection (Figure 6.5). The effect of the p19 RNAi inhibitor was then tested in U4.4 cultures at low and high MOI (MOI= 0.001 or 10) at 24 and 48 hours post-infection (Figure 6.6). The results showed SFV4 had the highest titre and SFV4(3H)-*RLuc*-p19 had a higher titre than SFV4(3H)-*RLuc* at MOI 0.001. This appeared to be the same at MOI =10 however statistical analysis could not be carried out deal to data corruption. This indicated that SFV4(3H)-*RLuc*-p19 had a less compromised replication rate than SFV4(3H)-*RLuc*, suggesting p19 partially rescued the SFV4(3H)-*RLuc* phenotype by reducing the RNAi pressure on virus replication. Interestingly, in the case of infection with MOI of 0.001, titres of all three viruses increased from 24-48 hours, whereas the titre appeared to decrease from 24 to 48 hours in infection with MOI of 10. Once again, this decrease at MOI=10 could not be confirmed by statistical analysis because the data file is corrupted beyond repair. It is unlikely that virus particles disappeared or eliminated from 24 to 48 hours post-infection.

Infection of *Ae. aegypti* with SFV4(3H)-*RLuc*, SFV4(3H)-*RLuc*-p19 and SFV4-st*RLuc* was established. However, the number of mosquitoes which became infected and expressed viral marker genes was too little to carry out statistical analysis to show whether replication of SFV4(3H)-*RLuc*-p19 is different from SFV4(3H)-*RLuc*. This study was recently continued by another student (Julio Rodriguez) in our laboratory with a Hemotek feeding apparatus (Discovery Workshops, UK). The new feeding apparatus greatly increased the proportion of mosquitoes which fed on the blood meal and 50-60% of the fed mosquitoes were infected. This suggested that feeding mosquitoes with an infected blood meal at 28^{o}C is inefficient. It is essential to have equipment to keep the blood meal warm for future experiments.

Infection of mosquitoes with SFV4(3H)-*RLuc*-p19 and SFV4(3H)-*RLuc* only produced three mosquitoes that expressed luciferase. Two became infected with SFV4(3H)-*RLuc*-p19 and luciferase expression was detected one each on PID 2 and 4. The luciferase activity of these two SFV4(3H)-*RLuc*-p19 infected mosquitoes were 6.5 and 43 times (PID 2 & 4, respectively) higher than the one infected with SFV4(3H)-*RLuc* detected on PID 5. Although the number of infected mosquitoes was too few to make a significant comparison, the increase of luciferase activity in SFV4(3H)-*RLuc*-p19 infected mosquitoes indicated an increase in infection level which has been previously reported by Cirimotich and co-workers. They described the use of a recombinant SINV that expresses a *Flock house virus* (FHV) B2 protein to study the effects of RNAi on mosquito infection. The report showed the level of infection and dissemination rate were increased when mosquitoes were infected with SINV-B2, and that inhibition of RNAi during infection was highly pathogenic and significantly shortened the mosquitoes' lifespan (Cirimotich *et al*., 2009). P19 and B2 are of different origins and act differently; P19 is from *Tombusviruses* of the *Tombusviridae* (plant virus) and binds and sequesters only 21 nt double stranded small RNAs, whereas B2 is from FHV of the *Nodaviridae* (insect virus) and binds to siRNAs and longer dsRNAs (Lingel et al., 2005; Mérai et al., 2006); however they both function to prevent small RNAs from being incorporated into the RISC.

By understanding the effect of the RNAi inhibitor in SINV-P19 infection in *Ae. aegypti* (Cirimotich *et al*., 2009), and the enhanced spread of SFV expressing P19 in U4.4 mosquito cell culture (Attarzadeh-Yazdi *et al*., 2009), it is intriguing to speculate that the outcome of a more successful SFV4(3H)-*RLuc*-p19 infection in *Ae. aegypti* mosquitoes might also show an enhanced rate of replication and mortality.

References

Abu-Elyazeed, R., el-Sharkawy, S., Olson, J., Botros, B., Soliman, a, Salib, a, Cummings, C. & Arthur, R. (1996). Prevalence of anti-Rift-Valley-fever IgM antibody in abattoir workers in the Nile delta during the 1993 outbreak in Egypt. *Bulletin of the World Health Organization* **74**, 155-8.

Adelman, Z. N., Sanchez-vargas, I., Travanty, E. A., Carlson, J. O., Beaty, B. J., Blair, C. D. & Olson, K. E. (2002). RNA Silencing of Dengue Virus Type 2 Replication in Transformed C6 / 36 Mosquito Cells Transcribing an Inverted-Repeat RNA Derived from the Virus Genome. *Journal of virology* **76**, 12925-12933.

Agaisse, H. & Perrimon, N. (2004). The roles of JAK/STAT signaling in Drosophila immune responses. *Immunological reviews* **198**, 72-82.

Aguilar, P. V., Weaver, S. C. & Basler, C. F. (2007). Capsid protein of eastern equine encephalitis virus inhibits host cell gene expression. *Journal of virology* **81**, 3866-76.

Ahmad, K. (2000). More deaths from Rift Valley fever in Saudi Arabia and Yemen. *Lancet* **356**, 1422.

Aitken, T. H. G., Tesh, R. B., Beaty, B. J. & Rosen, L. (1979). Transovarial transmission of yellow fever virus by mosquitoes (Aedes aegypti). *The American journal of tropical medicine and hygiene* **28**, 119. ASTMH.

Al-Hazmi, M., Ayoola, E. A., Abdurahman, M., Banzal, S., Ashraf, J., El-Bushra, A., Hazmi, A., Abdullah, M., Abbo, H., & other authors. **(2003).** Epidemic Rift Valley fever in Saudi Arabia: a clinical study of severe illness in humans. *Clinical infectious diseases : an official publication of the Infectious Diseases Society of America* **36**, 245-52.

Alexopoulou, L., Holt, A. C., Medzhitov, R. & Flavell, R. A. (2001). Recognition of double-stranded RNA and activation of NF-kB by Toll-like receptor 3. *Nature* **413**, 732–738. [London: Macmillan Journals], 1869-.

Amor, S., Scallan, M. F., Morris, M. M., Dyson, H. & Fazakerley, J. K. (1996). Role of immune responses in protection and pathogenesis during Semliki Forest virus encephalitis. *The Journal of general virology* **77 (Pt 2** , 281-91.

Andersson, M. G., Haasnoot, P. C. J., Xu, N., Berenjian, S. & Berkhout, B. (2005). Suppression of RNA Interference by Adenovirus Virus-Associated RNA †. *Journal of virology* **79**, 9556-9565.

Anishchenko, M., Bowen, R. a, Paessler, S., Austgen, L., Greene, I. P. & Weaver, S. C. (2006). Venezuelan encephalitis emergence mediated by a phylogenetically predicted viral mutation. *Proceedings of the National Academy of Sciences of the United States of America* **103**, 4994-9.

Arbouzova, N. I. & Zeidler, M. P. (2006). JAK/STAT signalling in Drosophila: insights into conserved regulatory and cellular functions. *Development (Cambridge, England)* **133**, 2605-16.

Armstrong, P. M. & Andreadis, T. G. (2010). Eastern Equine Encephalitis Virus in Mosquitoes and Their Role as Bridge Vectors. *Emerging Infectious Diseases* **16**, 1869-1874.

Atasheva, S., Gorchakov, R., English, R., Frolov, I. & Frolova, E. (2007). Development of Sindbis viruses encoding nsP2/GFP chimeric proteins and their application for studying nsP2 functioning. *Journal of virology* **81**, 5046-57.

Atkins, G. J., Carter, J. & Sheahan, B. J. (1982). Effect of alphavirus infection on mouse embryos. *Infection and immunity* **38**, 1285-90.

Attardo, G. M., Higgs, S., Klingler, K. a, Vanlandingham, D. L. & Raikhel, A. S. (2003). RNA interference-mediated knockdown of a GATA factor reveals a link to anautogeny in the mosquito Aedes aegypti. *Proceedings of the National Academy of Sciences of the United States of America* **100**, 13374-9.

Attarzadeh-Yazdi, G., Fragkoudis, R., Chi, Y., Siu, R. W. C., Ulper, L., Barry, G., Rodriguez-Andres, J., Nash, A. a, Bouloy, M., & other authors. **(2009).** Cell-to-cell spread of the RNA interference response suppresses Semliki Forest virus (SFV) infection of mosquito cell cultures and cannot be antagonized by SFV. *Journal of virology* **83**, 5735-48.

Avadhanula, V., Weasner, B. P., Hardy, G. G., Kumar, J. P. & Hardy, R. W. (2009). A novel system for the launch of alphavirus RNA synthesis reveals a role for the Imd pathway in arthropod antiviral response. *PLoS pathogens* **5**, e1000582.

BLACKWELL, J. L. & BRINTON, M. A. (1997). Translation elongation factor-1 alpha interacts with the 3 ’ stem-loop region of West Nile virus Translation Elongation Factor-1 Alpha Interacts with the 3J Stem-Loop Region of West Nile Virus Genomic RNA. *Journal of virology* **71**, 6433.

Bagny, L., Delatte, H., Elissa, N., Quilici, S. & Fontenille, D. (2009). Aedes (Diptera: Culicidae) vectors of arboviruses in Mayotte (Indian Ocean): distribution area and larval habitats. *Journal of medical entomology* **46**, 198-207.

Balachandran, S., Roberts, P. C., Brown, L. E., Truong, H., Pattnaik, a K., Archer, D. R. & Barber, G. N. (2000). Essential role for the dsRNA-

dependent protein kinase PKR in innate immunity to viral infection. *Immunity* **13**, 129-41.

Barillas-Mury, C., Han, Y. S., Seeley, D. & Kafatos, F. C. (1999). Anopheles gambiae Ag-STAT, a new insect member of the STAT family, is activated in response to bacterial infection. *The EMBO journal* **18**, 959-67.

Barry, G., Breakwell, L., Fragkoudis, R., Attarzadeh-Yazdi, G., Rodriguez-Andres, J., Kohl, A. & Fazakerley, J. K. (2009). PKR acts early in infection to suppress Semliki Forest virus production and strongly enhances the type I interferon response. *The Journal of general virology* **90**, 1382-91.

Barry, G., Fragkoudis, R., Ferguson, M. C., Lulla, A., Merits, A., Kohl, A. & Fazakerley, J. K. (2010). Semliki forest virus-induced endoplasmic reticulum stress accelerates apoptotic death of mammalian cells. *Journal of virology* **84**, 7369-77.

Bauer, S., Kirschning, C. J., Häcker, H., Redecke, V., Hausmann, S., Akira, S., Wagner, H. & Lipford, G. B. (2001). Human TLR9 confers responsiveness to bacterial DNA via species-specific CpG motif recognition. *Proceedings of the National Academy of Sciences of the United States of America* **98**, 9237-42.

Baulcombe, D. (2004). RNA silencing in plants. *Nature* **431**, 356-63.

Benbough, J. E. (1969). The effect of relative humidity on the survival of airborne Semliki forest virus. *The Journal of general virology* **4**, 473-7.

Berglund, P., Garoff, H. & Atkins, G. (1993). Semliki Forest virus expression system: production of conditionally infectious recombinant particles. *Nature Biotechnology* **11**, 916-920.

Berglund, P., Smerdou, C., Fleeton, M. N. & others. **(1998).** Enhancing immune responses using suicidal DNA vaccines. *Nature biotechnology* **16**, 562–565. Nature Publishing Group.

Bernstein, E., Denli, A. M., Hannon, G. J. & Gene, H.-dependent. **(2001).** The rest is silence. *RNA Society* **7**, 1509-1521.

Bessaud, M., Peyrefitte, C. N., Pastorino, B. a M., Gravier, P., Tock, F., Boete, F., Tolou, H. J. & Grandadam, M. (2006). O'nyong-nyong Virus, Chad. *Emerging infectious diseases* **12**, 1248-50.

Black, W. C., Bennett, K. E., Gorrochótegui-Escalante, N., Barillas-Mury, C. V., Fernández-Salas, I., de Lourdes Muñoz, M., Farfán-Alé, J. a, Olson, K. E. & Beaty, B. J. (2002). Flavivirus susceptibility in Aedes aegypti. *Archives of medical research* **33**, 379-88.

Blandin, S., Moita, L. F., Köcher, T., Wilm, M., Kafatos, F. C. & Levashina, E. a. (2002). Reverse genetics in the mosquito Anopheles gambiae: targeted disruption of the Defensin gene. *EMBO reports* **3**, 852-6.

Blevins, T., Rajeswaran, R., Aregger, M., Borah, B. K., Schepetilnikov, M., Baerlocher, L., Farinelli, L., Meins, F., Hohn, T. & Pooggin, M. M. (2011). Massive production of small RNAs from a non-coding region of Cauliflower mosaic virus in plant defense and viral counter-defense. *Nucleic acids research* **39**, 5003-14.

Bonn, D. (2006). How did chikungunya reach the Indian Ocean? *The Lancet infectious diseases* **6**, 543.

Bosio, C., Fulton, R., Salasek, M., Beaty, B. & Black IV, W. (2000). Quantitative trait loci that control vector competence for dengue-2 virus in the mosquito Aedes aegypti. *Genetics* **156**, 687-698.

Boutros, M., Agaisse, H. & Perrimon, N. (2002). Sequential activation of signaling pathways during innate immune responses in Drosophila. *Developmental cell* **3**, 711-22.

Brackney, D. E., Beane, J. E. & Ebel, G. D. (2009). RNAi targeting of West Nile virus in mosquito midguts promotes virus diversification. *PLoS pathogens* **5**, e1000502.

Brackney, D. E., Scott, J. C., Sagawa, F., Woodward, J. E., Miller, N. a, Schilkey, F. D., Mudge, J., Wilusz, J., Olson, K. E., & other authors. (2010). C6/36 Aedes albopictus Cells Have a Dysfunctional Antiviral RNA Interference Response. *PLoS neglected tropical diseases* **4**, e856.

Bradish, C. J., Allner, K. & Maber, H. B. (1971). The virulence of original and derived strains of Semliki forest virus for mice, guinea-pigs and rabbits. *The Journal of general virology* **12**, 141-60.

Braks, M., Honório, N., Lourençqo-De-Oliveira, R., Juliano, S. & Lounibos, L. (2003). Convergent habitat segregation of Aedes aegypti and Aedes albopictus (Diptera: Culicidae) in southeastern Brazil and Florida. *Journal of medical entomology* **40**, 785-94.

Breakwell, L., Dosenovic, P., Karlsson Hedestam, G. B., D'Amato, M., Liljeström, P., Fazakerley, J. & McInerney, G. M. (2007). Semliki Forest virus nonstructural protein 2 is involved in suppression of the type I interferon response. *Journal of virology* **81**, 8677-84.

Brown, S., Hu, N. & Hombría, J. C. (2001). Identification of the first invertebrate interleukin JAK/STAT receptor, the Drosophila gene domeless. *Current biology* **11**, 1700-5.

Caley, I. J., Betts, M. R., Davis, N. L., Swanstrom, R., Frelinger, A. J. & Johnston, R. E. (1999). Venezuelan equine encephalitis virus vectors expressing HIV-1 proteins: vector design strategies for improved vaccine efficacy. *Vaccine* **17**, 3124-3135.

Campbell, C. L., Keene, K. M., Brackney, D. E., Olson, K. E., Blair, C. D., Wilusz, J. & Foy, B. D. (2008). Aedes aegypti uses RNA interference in defense against Sindbis virus infection. *BMC microbiology* **8**, 47.

Caplen, N., Zheng, Z., Falgout, B. & Morgan, R. (2002). Inhibition of Viral Gene Expression and Replication in Mosquito Cells by dsRNA-Triggered RNA Interference. *Molecular Therapy* **6**, 243-251.

Chan, K. L., Ho, B. C. & Chan, Y. C. (1971). Aedes aegypti (L.) and Aedes albopictus (Skuse) in Singapore City. 2. Larval habitats. *Bulletin of the World Health Organization* **44**, 629-33.

Chang, T. L., Jr, J. V., Delportillo, A. & Klotman, M. E. (2005). Dual role of α-defensin-1 in anti – HIV-1 innate immunity. *Journal of Clinical Investigation* **115**, 765-773.

Chebath, J., Benech, P., Revel, M. & Vigneron, M. (1987). Constitutive expression of (2'-5') oligo A synthease confers resistance to picornavirus infection. *Nature* **330**, 587-8.

Chen, J., Miller, D. & Katow, S. (1995). Expression of the rubella virus structural proteins by an infectious Sindbis virus vector. *Archives of virology* 2075-2084.

Chen, Z. J. (2005). Ubiquitin signalling in the NF-κB pathway. *Nature cell biology* **7**, 758-765.

Choe, K.-M., Werner, T., Stöven, S., Hultmark, D. & Anderson, K. V. (2002). Requirement for a peptidoglycan recognition protein (PGRP) in Relish activation and antibacterial immune responses in Drosophila. *Science (New York, NY)* **296**, 359-62.

Christophides, G. K., Zdobnov, E., Barillas-Mury, C., Birney, E., Blandin, S., Blass, C., Brey, P. T., Collins, F. H., Danielli, A., & other authors. (2002). Immunity-related genes and gene families in Anopheles gambiae. *Science (New York, NY)* **298**, 159-65.

Cirimotich, C. M., Scott, J. C., Phillips, A. T., Geiss, B. J. & Olson, K. E. (2009). Suppression of RNA interference increases alphavirus replication and virus-associated mortality in Aedes aegypti mosquitoes. *BMC microbiology* **9**, 49.

Cogoni, C. & Macino, G. (1997). Isolation of quelling-defective (qde) mutants impaired in posttranscriptional transgene-induced gene silencing in Neurospora

crassa. *Proceedings of the National Academy of Sciences of the United States of America* **94**, 10233-8.

Condreay, L. D. & Brown, D. T. (1986). Exclusion of superinfecting homologous virus by Sindbis virus-infected Aedes albopictus (mosquito) cells. *J Virol* **58**, 81-86.

Cox, J., Grillet, M. E., Ramos, O. M., Amador, M. & Barrera, R. (2007). Habitat segregation of dengue vectors along an urban environmental gradient. *The American journal of tropical medicine and hygiene* **76**, 820-6.

Daher, K. a, Selsted, M. E. & Lehrer, R. I. (1986). Direct inactivation of viruses by human granulocyte defensins. *Journal of virology* **60**, 1068-74.

Darnell Jr., J. E. (1997). STATs and Gene Regulation. *Science* **277**, 1630-1635.

Davey, M. W. & Dalgarno, L. (1974). Semliki Forest virus replication in cultured Aedes albopictus cells: studies on the establishment of persistence. *The Journal of general virology* **24**, 453-63.

Davies, F. G. (1975). Observations on the epidemiology of Rift Valley fever in Kenya. *The Journal of hygiene* **75**, 219-30.

Davis, M., Sagan, S. M., Pezacki, J. P., Evans, D. J. & Simmonds, P. (2008). Bioinformatic and physical characterizations of genome-scale ordered RNA structure in mammalian RNA viruses. *Journal of virology* **82**, 11824-36.

Davis, N. L., Willis, L. V., Smith, J. F. & Johnston, R. E. (1989). In vitro synthesis of infectious venezuelan equine encephalitis virus RNA from a cDNA clone: analysis of a viable deletion mutant. *Virology* **171**, 189-204.

Delatte, H., Dehecq, J., Thiria, J., Domerg, C., Paupy, C. & Fontenille, D. (2008). Geographic distribution and developmental sites of Aedes albopictus (Diptera: Culicidae) during a Chikungunya epidemic event. *Vector borne and zoonotic diseases* **8**, 25-34.

Delaunay, P., Jeannin, C., Schaffner, F. & Marty, P. (2009). [News on the presence of the tiger mosquito Aedes albopictus in metropolitan France]. *Archives de pédiatrie : organe officiel de la Sociéte française de pédiatrie* **16 Suppl 2**, S66-71. Elsevier.

Deonarain, R., Alcami, a., Alexiou, M., Dallman, M. J., Gewert, D. R. & Porter, a. C. G. (2000). Impaired Antiviral Response and Alpha/Beta Interferon Induction in Mice Lacking Beta Interferon. *Journal of Virology* **74**, 3404-3409.

Diebold, S. S., Kaisho, T., Hemmi, H., Akira, S. & Reis e Sousa, C. (2004). Innate antiviral responses by means of TLR7-mediated recognition of single-stranded RNA. *Science* **303**, 1529-31.

Donnelly, M. L., Hughes, L. E., Luke, G., Mendoza, H., ten Dam, E., Gani, D. & Ryan, M. D. (2001). The "cleavage" activities of foot-and-mouth disease virus 2A site-directed mutants and naturally occurring "2A-like" sequences. *The Journal of general virology* **82**, 1027-41.

Dostert, C., Jouanguy, E., Irving, P., Troxler, L., Galiana-Arnoux, D., Hetru, C., Hoffmann, J. a & Imler, J.-L. (2005). The Jak-STAT signaling pathway is required but not sufficient for the antiviral response of drosophila. *Nature immunology* **6**, 946-53.

Doyle, S., Vaidya, S., O'Connell, R., Dadgostar, H., Dempsey, P., Wu, T., Rao, G., Sun, R., Haberland, M., & other authors. **(2002).** IRF3 mediates a TLR3/TLR4-specific antiviral gene program. *Immunity* **17**, 251-63.

Dubensky Jr, T. W., Driver, D. A., Polo, J. M., Belli, B. A., Latham, E. M., Ibanez, C. E., Chada, S., Brumm, D., Banks, T. A., & other authors. **(1996).** Sindbis virus DNA-based expression vectors: utility for in vitro and in vivo gene transfer. *Journal of virology* **70**, 508. Am Soc Microbiol.

Eritja, R., Escosa, R., Lucientes, J., Marquès, E., Roiz, D. & Ruiz, S. (2005). Worldwide invasion of vector mosquitoes: present European distribution and challenges for Spain. *Biological Invasions* **7**, 87-97.

Ertürk-Hasdemir, D., Broemer, M., Leulier, F., Lane, W. S., Paquette, N., Hwang, D., Kim, C.-H., Stöven, S., Meier, P. & Silverman, N. (2009). Two roles for the Drosophila IKK complex in the activation of Relish and the induction of antimicrobial peptide genes. *Proceedings of the National Academy of Sciences of the United States of America* **106**, 9779-84.

Fayzulin, R., Gorchakov, R., Petrakova, O., Volkova, E. & Frolov, I. (2005). Sindbis virus with a tricomponent genome. *Journal of virology* **79**, 637–643. Am Soc Microbiol.

Fazakerley, J. K., Pathak, S., Scallan, M., Amor, S. & Dyson, H. (1993, August). Replication of the A7(74) strain of Semliki Forest virus is restricted in neurons. *Virology*.

Fazakerley, J. K., Boyd, A., Mikkola, M. L. & Kaariainen, L. (2002). A single amino acid change in the nuclear localization sequence of the nsP2 protein affects the neurovirulence of Semliki Forest virus. *Journal of virology* **76**, 392. Am Soc Microbiol.

Fazakerley, J. K. (2002). Pathogenesis of Semliki Forest virus encephalitis. *Journal of neurovirology* **8 Suppl 2**, 66-74.

Ferrandon, D., Imler, J.-L. & Hoffmann, J. A. (2004). Sensing infection in Drosophila: Toll and beyond. *Seminars in Immunology* **16**, 43-53.

Ferrandon, D., Imler, J.-L., Hetru, C. & Hoffmann, J. a. **(2007).** The Drosophila systemic immune response: sensing and signalling during bacterial and fungal infections. *Nature reviews Immunology* **7**, 862-74.

Finkelstein, Y., Faktor, O., Elroy-Stein, O. & Levi, B. Z. (1999). The use of bi-cistronic transfer vectors for the baculovirus expression system. *Journal of biotechnology* **75**, 33-44.

Fire, A., Albertson, D., Harrison, S. W. & Moerman, D. G. (1991). Production of antisense RNA leads to effective and specific inhibition of gene expression in C. elegans muscle. *Development (Cambridge, England)* **113**, 503-14.

Fire, A., Xu, S., Montgomery, M., Kostas, S., Driver, S. & CC, M. (1998). Potent and specific genetic interference by double-stranded RNA in Caenorhabditis elegans. *Nature* **391**, 806-811.

Fitzgerald, K. a, Rowe, D. C., Barnes, B. J., Caffrey, D. R., Visintin, A., Latz, E., Monks, B., Pitha, P. M. & Golenbock, D. T. (2003). LPS-TLR4 signaling to IRF-3/7 and NF-kappaB involves the toll adapters TRAM and TRIF. *The Journal of experimental medicine* **198**, 1043-55.

Flynt, A., Liu, N., Martin, R. & Lai, E. C. (2009). Dicing of viral replication intermediates during silencing of latent Drosophila viruses. *Proceedings of the National Academy of Sciences of the United States of America* **106**, 5270-5.

Fragkoudis, R., Chi, Y., Siu, R. W. C., Barry, G., Attarzadeh-Yazdi, G., Merits, a, Nash, a a, Fazakerley, J. K. & Kohl, a. **(2008).** Semliki Forest virus strongly reduces mosquito host defence signaling. *Insect molecular biology* **17**, 647-56.

Fragkoudis, R., Tamberg, N., Siu, R., Kiiver, K., Kohl, A., Merits, A. & Fazakerley, J. K. (2009). Neurons and oligodendrocytes in the mouse brain differ in their ability to replicate Semliki Forest virus. *Journal of neurovirology* **15**, 57-70.

Frolova, E., Frolov, I. & Schlesinger, S. (1997). Packaging signals in alphaviruses. *Journal of virology* **71**, 248-58.

Frolova, E. I., Fayzulin, R. Z., Cook, S. H., Griffin, D. E., Rice, C. M. & Frolov, I. (2002). Roles of nonstructural protein nsP2 and alpha/beta interferons in determining the outcome of Sindbis virus infection. *Journal of virology* **76**, 11254. Am Soc Microbiol.

Frolova, E., Gorchakov, R. & Garmashova, N. (2006). Formation of nsP3-specific protein complexes during Sindbis virus replication. *Journal of virology* **80**, 4122.

Frolova, E. I., Gorchakov, R., Pereboeva, L., Atasheva, S. & Frolov, I. (2010). Functional Sindbis virus replicative complexes are formed at the plasma membrane. *Journal of virology* **84**, 11679-95.

Fros, J. J., Liu, W. J., Prow, N. a, Geertsema, C., Ligtenberg, M., Vanlandingham, D. L., Schnettler, E., Vlak, J. M., Suhrbier, A., & other authors. **(2010).** Chikungunya virus nonstructural protein 2 inhibits type I/II interferon-stimulated JAK-STAT signaling. *Journal of virology* **84**, 10877-87.

Garmashova, N., Gorchakov, R., Volkova, E., Paessler, S., Frolova, E. & Frolov, I. (2007). The Old World and New World alphaviruses use different virus-specific proteins for induction of transcriptional shutoff. *Journal of virology* **81**, 2472-84.

Garoff, H., Frischauf, A., Simons, K. & Lehrach, H. (1980). Nucleotide sequence of cdna coding for Semliki Forest virus membrane glycoproteins. *Nature* **288**, 236-241.

Geiss, B. J., Pierson, T. C. & Diamond, M. S. (2005). Actively replicating West Nile virus is resistant to cytoplasmic delivery of siRNA. *Virology journal* **2**, 53.

Georgel, P., Naitza, S., Kappler, C., Ferrandon, D., Zachary, D., Swimmer, C., Kopczynski, C., Duyk, G., Reichhart, J. M. & Hoffmann, J. a. **(2001).** Drosophila immune deficiency (IMD) is a death domain protein that activates antibacterial defense and can promote apoptosis. *Developmental cell* **1**, 503-14.

Geuking, P., Narasimamurthy, R. & Basler, K. (2005). A genetic screen targeting the tumor necrosis factor/Eiger signaling pathway: identification of Drosophila TAB2 as a functionally conserved component. *Genetics* **171**, 1683-94.

Ghosh, A., Sarkar, S. N. & Sen, G. C. (2000). Cell growth regulatory and antiviral effects of the P69 isozyme of 2-5 (A) synthetase. *Virology* **266**, 319-28.

Glasgow, G. M., Sheahan, B. J., Atkins, G. J., Wahlberg, J. M., Salminen, a & Liljeström, P. (1991). Two mutations in the envelope glycoprotein E2 of Semliki Forest virus affecting the maturation and entry patterns of the virus alter pathogenicity for mice. *Virology* **185**, 741-8.

Glasgow, G. M., Killen, H. M., Liljeström, P., Sheahan, B. J. & Atkins, G. J. (1994). A single amino acid change in the E2 spike protein of a virulent strain of Semliki Forest virus attenuates pathogenicity. *The Journal of general virology* **75 (Pt 3)**, 663-8.

Glasgow, L. A. (1966). Leukocytes and interferon in the host response to viral infections II. Enhanced interferon response of leukocytes from immune animals. *Journal of Bacteriology* **91**, 2185–2191. Am Soc Microbiol.

Gorchakov, R. & Frolova, E. (2005). Inhibition of transcription and translation in Sindbis virus-infected cells. *Journal of virology* **79**, 9397.

Gottar, M., Gobert, V., Michel, T., Belvin, M., Duyk, G., Hoffmann, J. a, Ferrandon, D. & Royet, J. (2002). The Drosophila immune response against Gram-negative bacteria is mediated by a peptidoglycan recognition protein. *Nature* **416**, 640-4.

Gould, E. a & Higgs, S. (2009). Impact of climate change and other factors on emerging arbovirus diseases. *Transactions of the Royal Society of Tropical Medicine and Hygiene* **103**, 109-21.

Gubler, D. J. (1998). Dengue and dengue hemorrhagic fever. *Clinical microbiology reviews* **11**, 480-96.

Guzmán, M. G., Kouri, G. P., Bravo, J., Soler, M., Vazquez, S. & Morier, L. (1990). Dengue hemorrhagic fever in Cuba, 1981: a retrospective seroepidemiologic study. *The American journal of tropical medicine and hygiene* **42**, 179-84.

Gérardin, P., Barau, G., Michault, A., Bintner, M., Randrianaivo, H., Choker, G., Lenglet, Y., Touret, Y., Bouveret, A., & other authors. (2008). Multidisciplinary prospective study of mother-to-child chikungunya virus infections on the island of La Réunion. *PLoS medicine* **5**, e60.

HOVANESSIAN, A. G. & KERR, I. M. (1979). The (2 -5) Oligoadenylate (pppA2 -5 A2 -5 A) Synthetase and Protein Kinase (s) from Interferon-Treated Cells. *European Journal of Biochemistry* **93**, 515–526. Wiley Online Library.

Hahn, C. S., Hahn, Y. S., Braciale, T. J. & Rice, C. M. (1992). Infectious Sindbis virus transient expression vectors for studying antigen processing and presentation. *Proceedings of the National Academy of Sciences of the United States of America* **89**, 2679-83.

Hahon, N. & Zimmerman, W. D. (1970). Chikungunya virus infection of cell monolayers by cell-to-cell and extracellular transmission. *Applied and Environmental Microbiology* **19**, 389. Am Soc Microbiol.

Hall, A. H. S. & Alexander, K. A. (2003). RNA Interference of Human Papillomavirus Type 18 E6 and E7 Induces Senescence in HeLa Cells †. *Journal of virology* **77**, 6066-6069.

Halstead, S., Udomsakdi, S., Singharaj, P. & Nisalak, A. (1969). Dengue and chikungunya virus infection in man in Thailand, 1962-1964. *The American Journal of Tropical Medicine and Hygiene* **18**, 984-996.

Hamilton, A. & Baulcombe, D. (1999). A Species of Small Antisense RNA in Posttranscriptional Gene Silencing in Plants. *Science* **286**, 950-952.

Hammond, S. M., Bernstein, E., Beach, D. & Hannon, G. J. (2000). An RNA-directed nuclease mediates post-transcriptional gene silencing in Drosophila cells. *Nature* **404**, 293-6.

Harbach, R. E. (2011). Mosquito Taxonomic Inventory, 16 February 2011. *http://mosquito-taxonomic-inventoryinfo/*.

Harley, D., Sleigh, A. & Ritchie, S. (2001). Ross River Virus Transmission , Infection , and Disease : a Cross-Disciplinary Review. *Clinical Microbiology Reviews* **14**, 909-932.

Hashimoto, C., Hudson, K. L. & Anderson, K. V. (1988). The Toll gene of Drosophila, required for dorsal-ventral embryonic polarity, appears to encode a transmembrane protein. *Cell* **52**, 269-79.

Hayes, C. G. (2001). West Nile virus: Uganda, 1937, to New York City, 1999. *Annals of the New York Academy of Sciences* **951**, 25-37.

Hedengren, M., Asling, B., Dushay, M. S., Ando, I., Ekengren, S., Wihlborg, M. & Hultmark, D. (1999). Relish, a central factor in the control of humoral but not cellular immunity in Drosophila. *Molecular cell* **4**, 827-37.

Helenius, a, Morein, B., Fries, E., Simons, K., Robinson, P., Schirrmacher, V., Terhorst, C. & Strominger, J. L. (1978). Human (HLA-A and HLA-B) and murine (H-2K and H-2D) histocompatibility antigens are cell surface receptors for Semliki Forest virus. *Proceedings of the National Academy of Sciences of the United States of America* **75**, 3846-50.

Helenius, a, Kartenbeck, J., Simons, K. & Fries, E. (1980). On the entry of Semliki forest virus into BHK-21 cells. *The Journal of cell biology* **84**, 404-20.

Higa, Y., Yen, T. N., Kawada, H., Son, H. T., Hoa, N. T. & Takagi, M. (2010). Geographic Distribution of Aedes aegypti and Aedes albopictus Collected from Used Tires in Vietnam. *Journal of the American Mosquito Control Association* **26**, 1-9.

Ho, D. D. & Hirsch, M. S. (1985). Acute viral encephalitis. *Medical Clinics of North America* **69**, 415-29.

Ho, T. (2007). Evidence for targeting common siRNA hotspots and GC preference by plant Dicer-like proteins. *FEBS Lett* **581**, 3267-3272.

Ho, T., Pallett, D., Rusholme, R., Dalmay, T. & Wang, H. (2006). A simplified method for cloning of short interfering RNAs from Brassica juncea infected with Turnip mosaic potyvirus and Turnip crinkle carmovirus. *Journal of virological methods* **136**, 217-23.

Hoffmann, J. & Reichhart, J.-M. (2002). Drosophila innate immunity: an evolutionary perspective. *Nature immunology* **3**, 121-6.

Hoffmann, J. a. **(2003).** The immune response of Drosophila. *Nature* **426**, 33-8.

Hornung, V., Ellegast, J., Kim, S., Brzózka, K., Jung, A., Kato, H., Poeck, H., Akira, S., Conzelmann, K.-K., & other authors. **(2006).** 5'-Triphosphate RNA is the ligand for RIG-I. *Science* **314**, 994-7.

Igarashi, a. (1978). Isolation of a Singh's Aedes albopictus Cell Clone Sensitive to Dengue and Chikungunya Viruses. *Journal of General Virology* **40**, 531-544.

Isaacs, a. & Lindenmann, J. (1957). Virus Interference: I. The Interferon. *CA: A Cancer Journal for Clinicians* **38**, 280-290.

Ishak, H., Miyagi, I., Toma, T. & Kamimura, K. (1997). Breeding habitats of Aedes aegypti (L) and Aedes. albopictus (Skuse) in villages of Barru, South Sulawesi, Indonesia. *The Southeast Asian journal of tropical medicine and public health* **28**, 844-50.

Itaya, A., Zhong, X., Bundschuh, R., Qi, Y., Wang, Y., Takeda, R., Harris, A. R., Molina, C., Nelson, R. S. & Ding, B. (2007). A structured viroid RNA serves as a substrate for dicer-like cleavage to produce biologically active small RNAs but is resistant to RNA-induced silencing complex-mediated degradation. *J Virol* **81**, 2980-2994.

Izant, J. G. & Weintraub, H. (1984). Inhibition of thymidine kinase gene expression by anti-sense RNA: a molecular approach to genetic analysis. *Cell* **36**, 1007-15.

Jing-Hsiung, O., Straussa, E. G., Straussa, J. H. & Simons, K. (1983). The 5'-terminal sequences of the genomic RNAs of several alphaviruses. *Journal of Molecular Biology* **168**, 1-15.

Johnsen, I. B., Nguyen, T. T., Ringdal, M., Tryggestad, A. M., Bakke, O., Lien, E., Espevik, T. & Anthonsen, M. W. (2006). Toll-like receptor 3 associates with c-Src tyrosine kinase on endosomes to initiate antiviral signaling. *The EMBO journal* **25**, 3335-46.

Johnson, B. W., Olson, K. E., Allen-Miura, T., Rayms-Keller, a, Carlson, J. O., Coates, C. J., Jasinskiene, N., James, a a, Beaty, B. J. & Higgs, S. (1999). Inhibition of luciferase expression in transgenic Aedes aegypti mosquitoes by Sindbis virus expression of antisense luciferase RNA. *Proceedings of the National Academy of Sciences of the United States of America* **96**, 13399-403.

de Jong, J. C., Harmsen, M., Plantinga, a D. & Trouwbrost, T. (1976). Inactivation of Semliki Forest Virus in aerosols. *Applied and environmental microbiology* **32**, 315-9.

Jorgensen, R. A., Atkinson, R. G., Forster, R. L. S. & Lucas, W. J. (1998). An RNA-based information superhighway in plants. *Science* **279**, 1486-1487.

Joshi, R. L., Ravel, J. M., Haenni, A.-lise, Monod, I. J., Vii, U. P. & Jussieu, P. (1986). Interaction of turnip yellow mosaic virus Val-RNA with eukaryotic elongation factor EF-1 [alpha]. Search for a function. *The EMBO journal* **5**, 1143-1148.

Jupp, P., McIntosh, B. & Blackburn, N. (1986). Experimental assessment of the vector competence of Culex (Culex) neavei Theobald with West Nile and Sindbis viruses in South Africa. *Transactions of the Royal Society of Tropical Medicine and Hygiene* **80**, 226–230. Elsevier.

Kaneko, T., Yano, T., Aggarwal, K., Lim, J.-H., Ueda, K., Oshima, Y., Peach, C., Erturk-Hasdemir, D., Goldman, W. E., & other authors. **(2006).** PGRP-LC and PGRP-LE have essential yet distinct functions in the drosophila immune response to monomeric DAP-type peptidoglycan. *Nature immunology* **7**, 715-23.

Karlsson, G. & Liljeström, P. (2003). Live viral vectors: Semliki Forest virus. *Methods in Molecular Medincine* **87**, 69-82.

Kato, H., Takeuchi, O., Sato, S., Yoneyama, M., Yamamoto, M., Matsui, K., Uematsu, S., Jung, A., Kawai, T., & other authors. **(2006).** Differential roles of MDA5 and RIG-I helicases in the recognition of RNA viruses. *Nature* **441**, 101-5.

Kawai, T., Takeuchi, O., Fujita, T., Inoue, J., Mühlradt, P. F., Sato, S., Hoshino, K. & Akira, S. (2001). Lipopolysaccharide stimulates the MyD88-independent pathway and results in activation of IFN-regulatory factor 3 and the expression of a subset of lipopolysaccharide-inducible genes. *Journal of immunology* **167**, 5887-94.

Keene, K. M., Foy, B. D., Sanchez-Vargas, I., Beaty, B. J., Blair, C. D. & Olson, K. E. (2004). RNA interference acts as a natural antiviral response to O'nyong-nyong virus (Alphavirus; Togaviridae) infection of Anopheles gambiae. *Proceedings of the National Academy of Sciences of the United States of America* **101**, 17240-5.

Kemp, C. & Imler, J.-L. (2009). Antiviral immunity in drosophila. *Current opinion in immunology* **21**, 3-9.

Kenney, J. L., Adams, a P. & Weaver, S. C. (2010). Transmission potential of two chimeric western equine encephalitis vaccine candidates in Culex tarsalis. *The American journal of tropical medicine and hygiene* **82**, 354-9.

Ketting, R. F., Haverkamp, T. H., van Luenen, H. G. & Plasterk, R. H. (1999). Mut-7 of C. elegans, required for transposon silencing and RNA interference, is a homolog of Werner syndrome helicase and RNaseD. *Cell* **99**, 133-41.

Khoo, C. C. H., Piper, J., Sanchez-Vargas, I., Olson, K. E. & Franz, A. W. E. (2010). The RNA interference pathway affects midgut infection- and escape barriers for Sindbis virus in Aedes aegypti. *BMC microbiology* **10**, 130.

Khush, R. S., Cornwell, W. D., Uram, J. N. & Lemaitre, B. (2002). A ubiquitin-proteasome pathway represses the Drosophila immune deficiency signaling cascade. *Current biology : CB* **12**, 1728-37.

Kielian, M. (1995). Membrane fusion and the alphavirus life cycle. *Advances in virus research* **45**, 113-51.

Kim, V. N. (2008). Sorting out small RNAs. *Cell* **133**, 25-6.

Kiwanuka, N., Sanders, E. J., Rwaguma, E. B., Kawamata, J., Ssengooba, F. P., Najjemba, R., Were, W. a, Lamunu, M., Bagambisa, G., & other authors. (1999). O'nyong-nyong fever in south-central Uganda, 1996-1997: clinical features and validation of a clinical case definition for surveillance purposes. *Clinical infectious diseases* **29**, 1243-50.

Klimstra, W. B., Ryman, K. D. & Johnston, R. E. (1998). Adaptation of Sindbis virus to BHK cells selects for use of heparan sulfate as an attachment receptor. *Journal of virology* **72**, 7357-66.

Klotman, M. E. & Chang, T. L. (2006). Defensins in innate antiviral immunity. *Nature reviews Immunology* **6**, 447-56.

Knipe, D. (1996). *Fields Virology*. Lippincott Williams & Wilkins.

Kouri, G. P., Guzmán, M. G., Bravo, J. R. & Triana, C. (1989). Dengue haemorrhagic fever/dengue shock syndrome: lessons from the Cuban epidemic, 1981. *Bulletin of the World Health Organization* **67**, 375-80.

van der Krol, A., Lenting, P. E., Veenstra, J., van der Meer, I. M., Gerats, A. G. M., MOI, J. N. M. & Stuitje, A. R. (1988). An antisense chalcone synthase gene in transgenic plants inhibits flower pigmentation. *Nature* **333**, 866-869.

Kulasegaran-Shylini, R., Atasheva, S., Gorenstein, D. G. & Frolov, I. (2009). Structural and functional elements of the promoter encoded by the 5' untranslated region of the Venezuelan equine encephalitis virus genome. *Journal of virology* **83**, 8327-39.

Kumar, A., Haque, J., Lacoste, J., Hiscott, J. & Williams, B. (1994). Double-Stranded RNA-Dependent Protein Kinase Activates Transcription Factor NF- B by Phosphorylating I B. *Proceedings of the National Academy of Sciences* **91**, 6288-6292.

Kurkela, S., Manni, T., Myllynen, J., Vaheri, A. & Vapalahti, O. (2005). Clinical and laboratory manifestations of Sindbis virus infection: prospective study, Finland, 2002-2003. *The Journal of infectious diseases* **191**, 1820-9.

Kurt-Jones, E. a, Popova, L., Kwinn, L., Haynes, L. M., Jones, L. P., Tripp, R. a, Walsh, E. E., Freeman, M. W., Golenbock, D. T., & other authors. (2000). Pattern recognition receptors TLR4 and CD14 mediate response to respiratory syncytial virus. *Nature immunology* **1**, 398-401.

Lacomme, C. (2005). Plant Virus-Derived Small Interfering RNAs Originate Predominantly from Highly Structured Single-Stranded Viral RNAs †. *Journal of virology* **79**, 7812-7818.

de Lamballerie, X., Leroy, E., Charrel, R. N., Ttsetsarkin, K., Higgs, S. & Gould, E. a. (2008). Chikungunya virus adapts to tiger mosquito via evolutionary convergence: a sign of things to come? *Virology journal* **5**, 33.

Lanciotti, R. S. (1999). Origin of the West Nile Virus Responsible for an Outbreak of Encephalitis in the Northeastern United States. *Science* **286**, 2333-2337.

Lecellier, C.-henri & Voinnet, O. (2004). RNA silencing : no mercy for viruses ? *Immunological Reviews* **198**, 285-303.

Lemaitre, B., Kromer-Metzger, E., Michaut, L., Nicolas, E., Meister, M., Georgel, P., Reichhart, J. M. & Hoffmann, J. a. (1995). A recessive mutation, immune deficiency (imd), defines two distinct control pathways in the Drosophila host defense. *Proceedings of the National Academy of Sciences of the United States of America* **92**, 9465-9.

Lemaitre, B., Nicolas, E., Michaut, L., Reichhart, J. M. & Hoffmann, J. a. (1996). The dorsoventral regulatory gene cassette spätzle/Toll/cactus controls the potent antifungal response in Drosophila adults. *Cell* **86**, 973-83.

Leulier, F., Rodriguez, a, Khush, R. S., Abrams, J. M. & Lemaitre, B. (2000). The Drosophila caspase Dredd is required to resist gram-negative bacterial infection. *EMBO reports* **1**, 353-8.

Leulier, F., Vidal, S., Saigo, K., Ueda, R. & Lemaitre, B. (2002). Inducible Expression of Double-Stranded RNA Reveals a Role for dFADD in the Regulation of the Antibacterial Response in Drosophila Adults. *Current Biology* **12**, 996-1000.

Levine, B. (1996). Bcl-2 protects mice against fatal alphavirus encephalitis. *Proceedings of the National Academy of Sciences* **93**, 4810-4815.

Li, R., Li, Y., Kristiansen, K. & Wang, J. (2008). SOAP: short oligonucleotide alignment program. *Bioinformatics (Oxford, England)* **24**, 713-4.

Li, S., Peters, G. a, Ding, K., Zhang, X., Qin, J. & Sen, G. C. (2006). Molecular basis for PKR activation by PACT or dsRNA. *Proceedings of the National Academy of Sciences of the United States of America* **103**, 10005-10.

Lidbury, B. a, Simeonovic, C., Maxwell, G. E., Marshall, I. D. & Hapel, a J. (2000). Macrophage-induced muscle pathology results in morbidity and mortality for Ross River virus-infected mice. *The Journal of infectious diseases* **181**, 27-34.

Liljeström, P. & Garoff, H. (1991). A new generation of animal cell expression vectors based on the Semliki Forest virus replicon. *Nature Biotechnology* **9**, 1356–1361. Nature Publishing Group.

Lin, C.-C., Chou, C.-M., Hsu, Y.-L., Lien, J.-C., Wang, Y.-M., Chen, S.-T., Tsai, S.-C., Hsiao, P.-W. & Huang, C.-J. (2004). Characterization of two mosquito STATs, AaSTAT and CtSTAT. Differential regulation of tyrosine phosphorylation and DNA binding activity by lipopolysaccharide treatment and by Japanese encephalitis virus infection. *The Journal of biological chemistry* **279**, 3308-17.

Lin, R.-J., Chang, B.-L., Yu, H.-P., Liao, C.-L. & Lin, Y.-L. (2006). Blocking of interferon-induced Jak-Stat signaling by Japanese encephalitis virus NS5 through a protein tyrosine phosphatase-mediated mechanism. *Journal of virology* **80**, 5908-18.

Lingel, A., Simon, B., Izaurralde, E. & Sattler, M. (2005). The structure of the flock house virus B2 protein, a viral suppressor of RNA interference, shows a novel mode of double-stranded RNA recognition. *EMBO reports* **6**, 1149-55.

Liu, Y. & Zhang, X. (2007). Murine coronavirus-induced oligodendrocyte apoptosis is mediated through the activation of the Fas signaling pathway. *Virology* **360**, 364-75.

Loewy, a, Smyth, J., von Bonsdorff, C. H., Liljeström, P. & Schlesinger, M. J. (1995). The 6-kilodalton membrane protein of Semliki Forest virus is involved in the budding process. *Journal of virology* **69**, 469-75.

Logue, C. H., Sheahan, B. J. & Atkins, G. J. (2008). The 5’ untranslated region as a pathogenicity determinant of Semliki Forest virus in mice. *Virus genes* **36**, 313-21.

Lu, S. & Cullen, B. R. (2004). Adenovirus VA1 Noncoding RNA Can Inhibit Small Interfering RNA and MicroRNA Biogenesis. *Journal of virology* **78**, 12868-12876.

Lund, J. M., Alexopoulou, L., Sato, A., Karow, M., Adams, N. C., Gale, N. W., Iwasaki, A. & Flavell, R. a. (2004). Recognition of single-stranded RNA

viruses by Toll-like receptor 7. *Proceedings of the National Academy of Sciences of the United States of America* **101**, 5598-603.

Lvov, D. K., Butenko, a M., Gromashevsky, V. L., Larichev, V. P., Gaidamovich, S. Y., Vyshemirsky, O. I., Zhukov, a N., Lazorenko, V. V., Salko, V. N., & other authors. **(2000).** Isolation of two strains of West Nile virus during an outbreak in southern Russia, 1999. *Emerging infectious diseases* **6**, 373-6.

MacRae, I. J., Zhou, K. & Doudna, J. a. **(2007).** Structural determinants of RNA recognition and cleavage by Dicer. *Nature structural & molecular biology* **14**, 934-40.

Macrae, I. J., Li, F., Zhou, K., Cande, W. Z. & Doudna, J. a. **(2006).** Structure of Dicer and mechanistic implications for RNAi. *Cold Spring Harbor symposia on quantitative biology* **71**, 73-80.

Madani, T. a, Al-Mazrou, Y. Y., Al-Jeffri, M. H., Mishkhas, A. a, Al-Rabeah, A. M., Turkistani, A. M., Al-Sayed, M. O., Abodahish, A. a, Khan, A. S., & other authors. **(2003).** Rift Valley fever epidemic in Saudi Arabia: epidemiological, clinical, and laboratory characteristics. *Clinical infectious diseases : an official publication of the Infectious Diseases Society of America* **37**, 1084-92.

Malathi, K., Dong, B., Gale, M. & Silverman, R. H. (2007). Small self-RNA generated by RNase L amplifies antiviral innate immunity. *Nature* **448**, 816-9.

Marié, I., Durbin, J. E. & Levy, D. E. (1998). Differential viral induction of distinct interferon-alpha genes by positive feedback through interferon regulatory factor-7. *The EMBO journal* **17**, 6660-9.

Mathews, D. H., Sabina, J., Zuker, M. & Turner, D. H. (1999). Expanded sequence dependence of thermodynamic parameters improves prediction of RNA secondary structure. *Journal of molecular biology* **288**, 911-40.

Mathey-Prevot, B. & Perrimon, N. (1998). Mammalian and Drosophila blood: JAK of all trades? *Cell* **92**, 697-700.

Mathiot, C. C., Grimaud, G., Garry, P., Bouquety, J. C., Mada, a, Daguisy, a M. & Georges, a J. (1990). An outbreak of human Semliki Forest virus infections in Central African Republic. *The American journal of tropical medicine and hygiene* **42**, 386-93.

Matsumoto, M., Kikkawa, S., Kohase, M., Miyake, K. & Seya, T. (2002). Establishment of a monoclonal antibody against human Toll-like receptor 3 that blocks double-stranded RNA-mediated signaling. *Biochemical and biophysical research communications* **293**, 1364-9.

McInerney, G. M., Kedersha, N. L., Kaufman, R. J., Anderson, P. & Liljestrom, P. (2005). Importance of eIF2alpha phosphorylation and stress granule assembly in alphavirus translation regulation. *Molecular Biology of the Cell* **16**, 3753-3763.

Medeiros, R. B., Resende, R. D. O. & A, A. C. D. (2004). The Plant Virus Tomato Spotted Wilt Tospovirus Activates the Immune System of Its Main Insect Vector , Frankliniella occidentalis. *Journal of virology* **78**, 4976-4982.

Meegan, J. M. (1979). The Rift Valley fever epizootic in Egypt 1977–1978 1. Description of the epizootic and virological studies. *Transactions of the Royal Society of Tropical Medicine and Hygiene* **73**, 618-623.

Meister, M. & Lagueux, M. (2003). Drosophila blood cells. *Cellular Microbiology* **5**, 573-580.

Melancon, P. & Garoff, H. (1987). Processing of the Semliki Forest virus structural polyprotein: role of the capsid protease. *Journal of virology* **61**, 1301-9.

Mi, S., Cai, T., Hu, Y., Chen, Y., Hodges, E., Ni, F., Wu, L., Li, S., Zhou, H., & other authors. **(2008).** Sorting of small RNAs into Arabidopsis argonaute complexes is directed by the 5' terminal nucleotide. *Cell* **133**, 116-27.

Michel, T., Reichhart, J. M., Hoffmann, J. a & Royet, J. (2001). Drosophila Toll is activated by Gram-positive bacteria through a circulating peptidoglycan recognition protein. *Nature* **414**, 756-9.

Misra, U. K. & Kalita, J. (2010). Overview: Japanese encephalitis. *Progress in neurobiology* **91**, 108-20. Elsevier Ltd.

Monath, T. P. (2001). Yellow fever: an update. *The Lancet Infectious Diseases* **1**, 11–20. Elsevier.

Morris-Downes, M. M., Phenix, K. V., Smyth, J., Sheahan, B. J., Lileqvist, S., Mooney, D. a, Liljeström, P., Todd, D. & Atkins, G. J. (2001). Semliki Forest virus-based vaccines: persistence, distribution and pathological analysis in two animal systems. *Vaccine* **19**, 1978-88.

Morrison, T., Whitmore, A., Shabman, R., Lidbury, B., Mahalingam, S. & Heise, M. T. (2006). Characterization of Ross River virus tropism and virus-induced inflammation in a mouse model of viral arthritis and myositis. *Journal of virology* **80**, 737.

Mudiganti, U., Hernandez, R., Ferreira, D. & Brown, D. T. (2006). Sindbis virus infection of two model insect cell systems--a comparative study. *Virus research* **122**, 28-34.

Mudiganti, U., Hernandez, R. & Brown, D. T. (2010). Insect response to alphavirus infection--establishment of alphavirus persistence in insect cells involves inhibition of viral polyprotein cleavage. *Virus research* **150**, 73-84. Elsevier B.V.

Muñnoz, J., Eritja, R., Alcaide, M., Montalvo, T., Soriguer, R. & Figuerola, J. (2011). Host-feeding patterns of native Culex pipiens and invasive Aedes albopictus mosquitoes (Diptera: Culicidae) in urban zones from Barcelona, Spain. *Journal of medical entomology* **48**, 956-60.

Myles, K. M., Pierro, D. J. & Olson, K. E. (2004). Comparison of the transmission potential of two genetically distinct Sindbis viruses after oral infection of Aedes aegypti (Diptera: Culicidae). *Journal of medical entomology* **41**, 95-106.

Myles, K. M., Wiley, M. R., Morazzani, E. M. & Adelman, Z. N. (2008). Alphavirus-derived small RNAs modulate pathogenesis in disease vector mosquitoes. *Proceedings of the National Academy of Sciences of the United States of America* **105**, 19938-43.

Myles, K. M., Morazzani, E. M. & Adelman, Z. N. (2010). Origins of alphavirus-derived small RNAs in mosquitoes. *Biotechnology* **6**, 387-391.

Mérai, Z., Kerényi, Z., Kertész, S., Magna, M., Lakatos, L. & Silhavy, D. (2006). Double-stranded RNA binding may be a general plant RNA viral strategy to suppress RNA silencing. *Journal of virology* **80**, 5747-56.

Naitza, S., Rosse, C., Kappler, C., Georgel, P., Belvin, M., Gubb, D., Camonis, J., Hoffmann, J. A., Reichhart, J.-marc, & other authors. (2002). against Gram-Negative Infection Requires the Death Protein dFADD. *Immunity* **17**, 575-581.

Napoli, C., Lemieux, C. & Jorgensen, R. (1990). Introduction of a Chimeric Chalcone Synthase Gene into Petunia Results in Reversible Co-Suppression of Homologous Genes in trans. *The Plant cell* **2**, 279-289.

Nasidi, A., Monath, T., DeCock, K., Tomori, O., Cordellier, R., Olaleye, O., Harry, T., Adeniyi, J., Sorungbe, A., & other authors. (1989). Urban yellow fever epidemic in western Nigeria, 1987. *Transactions of the Royal Society of Tropical Medicine and Hygiene* **83**, 401–406. Elsevier.

Nickens, D. G. & Hardy, R. W. (2008). Structural and functional analyses of stem-loop 1 of the Sindbis virus genome. *Virology* **370**, 158-72.

Niklasson, B., Espmark, Ä. & Lundström, J. (1988). Occurrence of arthralgia and specific IgM antibodies three to four years after Ockelbo disease. *The Journal of infectious diseases* **157**, 832–835. JSTOR.

Nishiya, T., Kajita, E., Miwa, S. & Defranco, A. L. (2005). TLR3 and TLR7 are targeted to the same intracellular compartments by distinct regulatory elements. *The Journal of biological chemistry* **280**, 37107-17.

Norder, H., Lundström, J. O., Kozuch, O. & Magnius, L. O. (1996). Genetic relatedness of Sindbis virus strains from Europe, Middle East, and Africa. *Virology* **222**, 440–445. Elsevier.

Nowotny, M. & Yang, W. (2009). Structural and functional modules in RNA interference. *Current opinion in structural biology* **19**, 286-93.

Oberste, M. S., Fraire, M., Navarro, R., Zepeda, C., Zarate, M. L., Ludwig, G. V., Kondig, J. F., Weaver, S. C., Smith, J. F. & Rico-Hesse, R. (1998). Association of Venezuelan equine encephalitis virus subtype IE with two equine epizootics in Mexico. *The American journal of tropical medicine and hygiene* **59**, 100-7.

Oliver, K. R. & Fazakerley, J. K. (1998). Transneuronal spread of Semliki Forest virus in the developing mouse olfactory system is determined by neuronal maturity. *Neuroscience* **82**, 867-77.

Oliver, K. R., Scallan, M. F., Dyson, H. & Fazakerley, J. K. (1997). Susceptibility to a neurotropic virus and its changing distribution in the developing brain is a function of CNS maturity. *Journal of Neurovirology* **3**, 38-48.

Patterson, K. D. (1992, April). Yellow fever epidemics and mortality in the United States, 1693-1905. *Social science & medicine (1982).*

Peleg, J. (1968). Growth of arboviruses in monolayers from subcultured mosquito embryo cells. *Virology* **35**, 617-619.

Petrakova, O., Volkova, E., Gorchakov, R., Paessler, S., Kinney, R. M. & Frolov, I. (2005). Noncytopathic replication of Venezuelan equine encephalitis virus and eastern equine encephalitis virus replicons in mammalian cells. *Journal of virology* **79**, 7597. Am Soc Microbiol.

Pichlmair, A., Schulz, O., Tan, C. P., Näslund, T. I., Liljeström, P., Weber, F. & Reis e Sousa, C. (2006). RIG-I-mediated antiviral responses to single-stranded RNA bearing 5'-phosphates. *Science (New York, NY)* **314**, 997-1001.

Pichlmair, A., Schulz, O., Tan, C.-P., Rehwinkel, J., Kato, H., Takeuchi, O., Akira, S., Way, M., Schiavo, G. & Reis e Sousa, C. (2009). Activation of MDA5 requires higher-order RNA structures generated during virus infection. *Journal of virology* **83**, 10761-9.

Pierro, D. J., Myles, K. M., Foy, B. D., Beaty, B. J. & Olson, K. E. (2003). Development of an orally infectious Sindbis virus transducing system that

efficiently disseminates and expresses green fluorescent protein in Aedes aegypti. *Insect molecular biology* **12**, 107-16.

Plumet, S., Herschke, F., Bourhis, J.-M., Valentin, H., Longhi, S. & Gerlier, D. (2007). Cytosolic 5'-triphosphate ended viral leader transcript of measles virus as activator of the RIG I-mediated interferon response. *PloS one* **2**, e279.

Pluskota, B., Storch, V., Braunbeck, T., Beck, M. & Becker, N. (2008). First record of Stegomyia albopicta (Skuse) (Diptera : Culicidae) in Germany. *European Mosquito Bulletin* **26**, 1-5.

Polo, J. M., Belli, B. a, Driver, D. a, Frolov, I., Sherrill, S., Hariharan, M. J., Townsend, K., Perri, S., Mento, S. J., & other authors. **(1999).** Stable alphavirus packaging cell lines for Sindbis virus and Semliki Forest virus-derived vectors. *Proceedings of the National Academy of Sciences of the United States of America* **96**, 4598-603.

Powers, A. N. N. M., Brault, A. C., Shirako, Y., Strauss, E. G., Kang, W., Strauss, J. H. & Weaver, S. C. (2001). Evolutionary Relationships and Systematics of the Alphaviruses. *Journal of virology* **75**, 10118-10131.

Powers, a M., Brault, a C., Tesh, R. B. & Weaver, S. C. (2000). Re-emergence of Chikungunya and O'nyong-nyong viruses: evidence for distinct geographical lineages and distant evolutionary relationships. *The Journal of general virology* **81**, 471-9.

Prikhod'ko, E. a & Miller, L. K. (1996). Induction of apoptosis by baculovirus transactivator IE1. *Journal of virology* **70**, 7116-24.

Pugachev, K. V., Mason, P. W., Shope, R. E. & Frey, T. K. (1995). Double-subgenomic Sindbis virus recombinants expressing immunogenic proteins of Japanese encephalitis virus induce significant protection in mice against lethal JEV infection. *Virology* **212**, 587-94.

Quiroz, E., Aguilar, P. V., Cisneros, J., Tesh, R. B. & Weaver, S. C. (2009). Venezuelan equine encephalitis in Panama: fatal endemic disease and genetic diversity of etiologic viral strains. *PLoS neglected tropical diseases* **3**, e472.

Ranki, M. & Ulmanen, I. (1979). Semliki Forest virus-specific nonstructural protein is associated with ribosomes. *FEBS letters* **108**, 299-302.

Reinert, J. F., Harbach, R. E., Anice, M. & Sallum, M. (2005). Checklist of aedine mosquito species (Diptera , Culicidae , Aedini) occurring 249 in Middle and South America (south of the United States) reflecting current generic and subgeneric status. *Revista Brasileira de Entomologia* **49**, 249-252.

Renault, P., Solet, J.-L., Sissoko, D., Balleydier, E., Larrieu, S., Filleul, L., Lassalle, C., Thiria, J., Rachou, E., & other authors. **(2007).** A Major

Epidemic of Chikungunya Virus Infection on Réunion Island, France, 2005–2006. *Am J Trop Med Hyg* **77**, 727-731.

Rice, C. M., Levis, R., Strauss, J. H. & Huang, H. V. (1987). Production of infectious RNA transcripts from Sindbis virus cDNA clones: mapping of lethal mutations, rescue of a temperature-sensitive marker, and in vitro mutagenesis to generate defined mutants. *Journal of virology* **61**, 3809. Am Soc Microbiol.

Rinaldo Jr, C. R., Overall Jr, J. C. & Glasgow, L. A. (1975). Viral replication and interferon production in fetal and adult ovine leukocytes and spleen cells. *Infection and immunity* **12**, 1070. Am Soc Microbiol.

Rincón, M., Flavell, R. a & Davis, R. J. (2001). Signal transduction by MAP kinases in T lymphocytes. *Oncogene* **20**, 2490-7.

Robertson, S., Hull, B., Tomori, O., Bele, O., LeDuc, J. & Esteves, K. (1996). Yellow fever: a decade of reemergence. *The journal of the American Medical Association* **276**, 1157-62.

Robin, S., Ramful, D., Zettor, J., Benhamou, L., Jaffar-Bandjee, M.-C., Rivière, J.-P., Marichy, J., Ezzedine, K. & Alessandri, J.-L. (2010). Severe bullous skin lesions associated with Chikungunya virus infection in small infants. *European journal of pediatrics* **169**, 67-72.

Robin, Y., Bourdin, P., Le Gonidec, G. & Heme, G. (1974). Virus de la foret de Semliki et encephalomyelites equines au Senegal. *Ann Microbiol (Inst Pasteur)* **125**, 235-241.

Robinson, M. (1955). An epidemic of virus disease in Southern Province, Tanganyika Territory, in 1952–53. I. Clinical features. *Transactions of the Royal Society of Tropical Medicine* **49**, 28-32.

Rock, F. L., Hardiman, G., Timans, J. C., Kastelein, R. a & Bazan, J. F. (1998). A family of human receptors structurally related to Drosophila Toll. *Proceedings of the National Academy of Sciences of the United States of America* **95**, 588-93.

Roiz, D., Eritja, R., Molina, R., Melero-Alcibar, R. & Lucientes, J. (2008). Initial distribution assessment of Aedes albopictus (Diptera: Culicidae) in the Barcelona, Spain, area. *Journal of medical entomology* **45**, 347-52.

Romi, R., Di Luca, M. & Majori, G. (1999). Current status of Aedes albopictus and Aedes atropalpus in Italy. *Journal of the American Mosquito Control Association* **15**, 425-427.

Romi, R. (2001). Aedes albopictus in Italy: an underestimated health problem. *Ann Ist Super Sanita* **37**, 241-7.

Royet, J. (2004). Infectious non-self recognition in invertebrates: lessons from Drosophila and other insect models. *Molecular immunology* **41**, 1063-75.

Rämet, M., Manfruelli, P., Pearson, A., Mathey-Prevot, B. & Ezekowitz, R. A. B. (2002). Functional genomic analysis of phagocytosis and identification of a Drosophila receptor for E. coli. *Nature* **416**, 644-8.

Samanidou-Voyadjoglou, A., Patsoula, E., Spanakos, G. & Vakalis, N. C. (2005). Cofirmation of Aedes Albopictus (SKuse) (Diptera: Culicidae) in Greece. *Journal of the European Mosquito Control Association* **19**, 10-11.

Samanta, M., Iwakiri, D., Kanda, T., Imaizumi, T. & Takada, K. (2006). EB virus-encoded RNAs are recognized by RIG-I and activate signaling to induce type I IFN. *The EMBO journal* **25**, 4207-14.

Samuel, C. E. (2001). Antiviral Actions of Interferons. *Clinical Microbiology Reviews* **14**, 778-809.

Samuel, M. A., Whitby, K., Keller, B. C., Marri, A., Barchet, W., Williams, B. R. G., Silverman, R. H., Gale, M. & Diamond, M. S. (2006). PKR and RNase L contribute to protection against lethal West Nile Virus infection by controlling early viral spread in the periphery and replication in neurons. *Journal of virology* **80**, 7009-19.

Sanchez-vargas, I., Travanty, E. A., Keene, K. M., Franz, A. W., Beaty, B. J., Blair, C. D. & Olson, K. E. (2004). RNA interference, arthropod-borne viruses, and mosquitoes. *Virus research* **102**, 65-74.

Sanders, H. R., Foy, B. D., Evans, A. M., Ross, L. S., Beaty, B. J., Olson, K. E. & Gill, S. S. (2005). Sindbis virus induces transport processes and alters expression of innate immunity pathway genes in the midgut of the disease vector, Aedes aegypti. *Insect biochemistry and molecular biology* **35**, 1293-307.

Santagati, M. G., Määttä, J. a, Itäranta, P. V., Salmi, a a & Hinkkanen, a E. (1995). The Semliki Forest virus E2 gene as a virulence determinant. *The Journal of general virology* **76 (Pt 1)**, 47-52.

Santagati, M. G., Määttä, J. a, Röyttä, M., Salmi, a a & Hinkkanen, a E. (1998). The significance of the 3'-nontranslated region and E2 amino acid mutations in the virulence of Semliki Forest virus in mice. *Virology* **243**, 66-77.

Sarver, N. & Stollar, V. (1977). Sindbis virus-induced cytopathic effect in clones of Aedes albopictus (Singh) cells. *Virology* **80**, 390-400.

Scallan, M. F., Allsopp, T. E. & Fazakerley, J. K. (1997). bcl-2 acts early to restrict Semliki Forest virus replication and delays virus-induced programmed cell death. *Journal of virology* **71**, 1583-90.

Schaffner, F. (2000, April). Première observation d'Aedes albopictus (Skuse, 1894) en France métropolitaineFirst record of Aedes albopictus (Skuse, 1894) in metropolitan France. *Comptes Rendus de l'Académie des Sciences - Series III - Sciences de la Vie*.

Scherbik, S. V., Paranjape, J. M., Stockman, B. M., Silverman, R. H. & Brinton, M. A. (2006). RNase L Plays a Role in the Antiviral Response to West Nile Virus. *Journal of virology* **80**, 2987-2999.

Schwartz, O. & Albert, M. L. (2010). Biology and pathogenesis of chikungunya virus. *Nature reviews Microbiology* **8**, 491-500.

Scott, J. C., Brackney, D. E., Campbell, C. L., Bondu-Hawkins, V., Hjelle, B., Ebel, G. D., Olson, K. E. & Blair, C. D. (2010). Comparison of dengue virus type 2-specific small RNAs from RNA interference-competent and -incompetent mosquito cells. *PLoS neglected tropical diseases* **4**, e848.

Silva, M. L. C. R., Galiza, G. J. N., Dantas, A. F. M., Oliveira, R. N., Iamamoto, K., Achkar, S. M. & Riet-Correa, F. (2011). Outbreaks of Eastern equine encephalitis in northeastern Brazil. *Journal of veterinary diagnostic investigation : official publication of the American Association of Veterinary Laboratory Diagnosticians, Inc* **23**, 570-5.

Silverman, N. & Maniatis, T. (2001). NF-kappaB signaling pathways in mammalian and insect innate immunity. *Genes & development* **15**, 2321-42.

Sim, S. & Dimopoulos, G. (2010). Dengue virus inhibits immune responses in Aedes aegypti cells. *PloS one* **5**, e10678.

Simizu, B., Yamamoto, K., Hashimoto, K. & Ogata, T. (1984). Structural proteins of Chikungunya virus. *Journal of virology* **51**, 254-8.

Simmonds, P., Tuplin, A. & Evans, D. J. (2004). Detection of genome-scale ordered RNA structure (GORS) in genomes of positive-stranded RNA viruses: Implications for virus evolution and host persistence. *RNA* **10**, 1337-51.

Simmonds, P., Karakasiliotis, I., Bailey, D., Chaudhry, Y., Evans, D. J. & Goodfellow, I. G. (2008). Bioinformatic and functional analysis of RNA secondary structure elements among different genera of human and animal caliciviruses. *Nucleic acids research* **36**, 2530-46.

Singh, I. & Helenius, a. **(1992).** Role of ribosomes in Semliki Forest virus nucleocapsid uncoating. *Journal of virology* **66**, 7049-58.

Singh, K. R. P. (1967). Cell cultures derived from larvae of Aedes albopictus (Skuse) and Aedes aegypti (L.). *Curr Sci* **36**, 506-508.

Smerdou, C. & Liljeström, P. (1999). Two-helper RNA system for production of recombinant Semliki forest virus particles. *Journal of virology* **73**, 1092-8.

Smithburn, K. C. & Haddow, A. J. (1944). Semliki Forest virus. I. Isolation and pathogenic properties. *Journal of immunology* **49**, 141-157.

Smithburn, K., Hughes, T., Burke, A. & Paul, J. (1940). A neurotropic virus isolated from the blood of a native of Uganda. *The American Journal of Tropical Medicine and Hygiene* **1**, 471–492. ASTMH.

Sourisseau, M., Schilte, C., Casartelli, N., Trouillet, C., Guivel-Benhassine, F., Rudnicka, D., Sol-Foulon, N., Le Roux, K., Prevost, M.-C., & other authors. (2007). Characterization of reemerging chikungunya virus. *PLoS pathogens* **3**, e89.

Souza-Neto, J. a, Sim, S. & Dimopoulos, G. (2009). An evolutionary conserved function of the JAK-STAT pathway in anti-dengue defense. *Proceedings of the National Academy of Sciences of the United States of America* **106**, 17841-6.

Spencer, E., Jiang, J. & Chen, Z. J. (1999). Signal-induced ubiquitination of I B ␣ by the F-box protein Slimb / ␤ -TrCP. *Genes & Development* 284-294.

Stokes, A., Bauer, J. H. & Hudson, N. P. (1928). Experimental transmission of yellow fever to laboratory animals. *The American Journal of Tropical Medicine and Hygiene* **1**, 103. ASTMH.

Strauss, J. H. & Strauss, E. G. (1994). The alphaviruses: gene expression, replication, and evolution. *Microbiological reviews* **58**, 491-562.

Stöven, S., Ando, I., Kadalayil, L., Engström, Y. & Hultmark, D. (2000). Activation of the Drosophila NF-kappaB factor Relish by rapid endoproteolytic cleavage. *EMBO reports* **1**, 347-52.

Szittya, G., Moxon, S., Pantaleo, V., Toth, G., Rusholme Pilcher, R. L., Moulton, V., Burgyan, J. & Dalmay, T. (2010). Structural and functional analysis of viral siRNAs. *PLoS pathogens* **6**, e1000838.

Sánchez-Vargas, I., Scott, J. C., Poole-Smith, B. K., Franz, A. W. E., Barbosa-Solomieu, V., Wilusz, J., Olson, K. E. & Blair, C. D. (2009). Dengue virus type 2 infections of Aedes aegypti are modulated by the mosquito's RNA interference pathway. *PLoS pathogens* **5**, e1000299.

Söderhäll, K. & Cerenius, L. (1998). Role of the prophenoloxidase-activating system in invertebrate immunity Kenneth S6derh ill and Lage Cerenius. *Current Opinion in Immunology* **10**, 23-28.

Taddeo, B., Luo, T. R., Zhang, W. & Roizman, B. (2003). Activation of NF-kappaB in cells productively infected with HSV-1 depends on activated protein kinase R and plays no apparent role in blocking apoptosis. *Proceedings of the National Academy of Sciences of the United States of America* **100**, 12408-13.

Takeuchi, O. & Akira, S. (2007). Recognition of viruses by innate immunity. *Immunological reviews* **220**, 214-24.

Takkinen, K. (1986). Complete nucleotide sequence of the nonstructural protein genes of Semliki Forest virus. *Nucleic Acids Research* **14**, 5667.

Tamberg, N., Lulla, V., Fragkoudis, R., Lulla, A., Fazakerley, J. K. & Merits, A. (2007). Insertion of EGFP into the replicase gene of Semliki Forest virus results in a novel, genetically stable marker virus. *The Journal of general virology* **88**, 1225-30.

Tan, L. V., Ha, D. Q., Hien, V. M., van der Hoek, L., Farrar, J. & de Jong, M. D. (2008). Me Tri virus: a Semliki Forest virus strain from Vietnam? *The Journal of general virology* **89**, 2132-5.

Tarbatt, C. J., Glasgow, G. M., Mooney, D. a, Sheahan, B. J. & Atkins, G. J. (1997). Sequence analysis of the avirulent, demyelinating A7 strain of Semliki Forest virus. *The Journal of general virology* **78 (Pt 7)**, 1551-7.

Tauszig, S., Jouanguy, E., Hoffmann, J. a & Imler, J. L. (2000). Toll-related receptors and the control of antimicrobial peptide expression in Drosophila. *Proceedings of the National Academy of Sciences of the United States of America* **97**, 10520-5.

Taylor, R., Hurlbut, H., Work, T., Kingston, J. & Frothingham, T. (1955). Sindbis virus: a newly recognized arthropodtransmitted virus. *The American journal of tropical medicine and hygiene* **4**, 844-62.

TenBroeck, C. & Merrill, M. H. (1933). A serological difference between eastern and western equine encephalomyelitis virus. *Proc Sot Exp Biol Med* **31**, 217-220.

Tesh, R. (1982). Arthritides caused by mosquito-borne viruses. *Annual review of medicine* **33**, 31–40. Annual Reviews 4139 El Camino Way, PO Box 10139, Palo Alto, CA 94303-0139, USA.

Thomas, J. M., Klimstra, W. B., Ryman, K. D. & Heidner, H. W. (2003). Sindbis virus vectors designed to express a foreign protein as a cleavable component of the viral structural polyprotein. *Journal of virology* **77**, 5598. Am Soc Microbiol.

Thompson, W. H., Kalfayan, B. & Anslow, R. O. (1965). Isolation of California Encephalitis Group Virus From a Fatal Human Illness. *American journal of epidemiology* **81**, 245-53.

Travanty, E. a, Adelman, Z. N., Franz, A. W. E., Keene, K. M., Beaty, B. J., Blair, C. D., James, A. a & Olson, K. E. (2004). Using RNA interference to develop dengue virus resistance in genetically modified Aedes aegypti. *Insect biochemistry and molecular biology* **34**, 607-13.

Trock, S. C., Meade, B. J., Glaser, a L., Ostlund, E. N., Lanciotti, R. S., Cropp, B. C., Kulasekera, V., Kramer, L. D. & Komar, N. (2000). West Nile virus outbreak among horses in New York State, 1999 and 2000. *Emerging infectious diseases* **7**, 745-7.

Tsai, T. F. (1991). Arboviral infections in the United States. *Infectious Disease Clinics of North America* **5**, 73-102.

Tsetsarkin, K. a, Vanlandingham, D. L., McGee, C. E. & Higgs, S. (2007). A single mutation in chikungunya virus affects vector specificity and epidemic potential. *PLoS pathogens* **3**, e201.

Tuplin, A., Evans, D. J. & Simmonds, P. (2004). Detailed mapping of RNA secondary structures in core and NS5B-encoding region sequences of hepatitis C virus by RNase cleavage and novel bioinformatic prediction methods. *The Journal of general virology* **85**, 3037-47.

Vaidyanathan, R. & Scott, T. W. (2006). Apoptosis in mosquito midgut epithelia associated with West Nile virus infection. *Apoptosis* **11**, 1643-51.

Vanlandingham, Dana L Tsetsarkin, K., Hong, C., Klingler, K., McElroy, K. L., Lehane, M. J. & Higgs, S. (2005). Development and characterization of a double subgenomic chikungunya virus infectious clone to express heterologous genes in Aedes aegypti mosqutioes. *Insect Biochemistry and Molecular Biology* **35**, 1162-1170.

Vasiljeva, L., Valmu, L., Kääriäinen, L. & Merits, a. (2001). Site-specific protease activity of the carboxyl-terminal domain of Semliki Forest virus replicase protein nsP2. *The Journal of biological chemistry* **276**, 30786-93.

Vasiljeva, L., Merits, A., Golubtsov, A., Sizemskaja, V., Kääriäinen, L. & Ahola, T. (2003). Regulation of the sequential processing of Semliki Forest virus replicase polyprotein. *The Journal of biological chemistry* **278**, 41636-45.

Vazeille, M., Moutailler, S., Coudrier, D., Rousseaux, C., Khun, H., Huerre, M., Thiria, J., Dehecq, J.-S., Fontenille, D., & other authors. (2007). Two Chikungunya isolates from the outbreak of La Reunion (Indian Ocean) exhibit different patterns of infection in the mosquito, Aedes albopictus. *PloS one* **2**, e1168.

Vazeille, M., Jeannin, C., Martin, E., Schaffner, F. & Failloux, A.-B. (2008). Chikungunya: a risk for Mediterranean countries? *Acta tropica* **105**, 200-2.

Ventoso, I., Sanz, M. A., Molina, S., Berlanga, J. J., Carrasco, L. & Esteban, M. (2006). Translational resistance of late alphavirus mRNA to eIF2alpha phosphorylation: a strategy to overcome the antiviral effect of protein kinase PKR. *Genes & development* **20**, 87-100.

Volkova, E., Frolova, E., Darwin, J. R., Forrester, N. L., Weaver, S. C. & Frolov, I. (2008). IRES-dependent replication of Venezuelan equine encephalitis virus makes it highly attenuated and incapable of replicating in mosquito cells. *Virology* **377**, 160-9.

Vähä-Koskela, M. J. V., Tuittila, M. T., Nygårdas, P. T., Nyman, J. K.-E., Ehrengruber, M. U., Renggli, M. & Hinkkanen, A. E. (2003). A novel neurotropic expression vector based on the avirulent A7(74) strain of Semliki Forest virus. *Journal of neurovirology* **9**, 1-15.

Wang, K. S., Kuhn, R. J., Strauss, E. G., Ou, S. & Strauss, J. H. (1992). High-affinity laminin receptor is a receptor for Sindbis virus in mammalian cells. *Journal of virology* **66**, 4992-5001.

Wang, W., Owen, S. M., Rudolph, D. L., Cole, M., Hong, T., Waring, A. J., Lal, R. B., Lehrer, R. I. & Cole, A. M. (2004). Activity of α- and θ-Defensins against Primary Isolates of HIV-1. *The Journal of Immunology* **173**, 515-520.

Watling, D., Serafinowska, H. T., Reese, C. B. & Kerr, I. M. (1985). Analogue inhibitor of 2-5A action: effect on the interferon-mediated inhibition of encephalomyocarditis virus replication. *The EMBO journal* **4**, 431-6.

Watts, D. M., Pantuwatana, S., Yuill, T. M., DeFoliart, G. R., Thompson, W. H. & Hanson, R. P. (1975). Transovarial transmission of LaCrosse virus in Aedes triseriatus. *Annals of the New York Academy of Sciences* **266**, 135-43.

Weaver, S. C. & Reisen, W. K. (2010). Present and future arboviral threats. *Antiviral research* **85**, 328-45.

Weaver, S. C., Ferro, C., Barrera, R., Boshell, J. & Navarro, J.-C. (2004). Venezuelan equine encephalitis. *Annual review of entomology* **49**, 141-74.

Weber, A. N. R., Tauszig-Delamasure, S., Hoffmann, J. a, Lelièvre, E., Gascan, H., Ray, K. P., Morse, M. a, Imler, J.-L. & Gay, N. J. (2003). Binding of the Drosophila cytokine Spätzle to Toll is direct and establishes signaling. *Nature immunology* **4**, 794-800.

Wek, R. C., Jiang, H.-Y. & Anthony, T. G. (2006). Coping with stress: eIF2 kinases and translational control. *Biochemical Society transactions* **34**, 7-11.

Wengler, G. (1984). Identification of a transfer of viral core protein to cellular ribosomes during the early stages of alphavirus infection. *Virology* **134**, 435-42.

Wengler, G. (1987). The mode of assembly of alphavirus cores implies a mechanism for the disassembly of the cores in the early stages of infection. *Archives of Virology* **94**, 1-14.

Wiley, M. R., Roberts, L. O., Adelman, Z. N. & Myles, K. M. (2010). Double subgenomic alphaviruses expressing multiple fluorescent proteins using a Rhopalosiphum padi virus internal ribosome entry site element. *PloS one* **5**, e13924.

Willems, W. R., Kaluza, G., Boschek, C. B., Bauer, H., Hager, H., Schütz, H. J. & Feistner, H. (1979). Semliki forest virus: cause of a fatal case of human encephalitis. *Science (New York, NY)* **203**, 1127-9.

Williams, M., Woodall, J. & Gillett, J. (1965). O'Nyong-Nyong fever: An epidemic virus disease in East Africa: VII. Virus isolations from man and serological studies up to July 1961. *Transactions of the Royal Society of Tropical Medicine and Hygiene* **59**, 186-97.

Woolaway, K. E., Lazaridis, K., Belsham, G. J., Carter, M. J. & Roberts, L. O. (2001). The 5' Untranslated Region of Rhopalosiphum padi Virus Contains an Internal Ribosome Entry Site Which Functions Efficiently in Mammalian , Plant , and Insect Translation Systems. *Journal of virology* **75**, 10244-10249.

Wyers, F., Petitjean, a M., Dru, P., Gay, P. & Contamine, D. (1995). Localization of domains within the Drosophila Ref(2)P protein involved in the intracellular control of sigma rhabdovirus multiplication. *Journal of virology* **69**, 4463-70.

Xi, Z., Ramirez, J. L. & Dimopoulos, G. (2008). The Aedes aegypti toll pathway controls dengue virus infection. *PLoS pathogens* **4**, e1000098.

Yazdani, R. & Kaushik, V. V. (2007). Chikungunya Fever. *Rheumatology (Oxford, England)* **46**, 1214-5; author reply 1215.

Yoneyama, M. & Fujita, T. (2009). RNA recognition and signal transduction by RIG-I-like receptors. *Immunological reviews* **227**, 54-65.

Zambon, R. a, Nandakumar, M., Vakharia, V. N. & Wu, L. P. (2005). The Toll pathway is important for an antiviral response in Drosophila. *Proceedings of the National Academy of Sciences of the United States of America* **102**, 7257-62.

Zambon, R. a, Vakharia, V. N. & Wu, L. P. (2006). RNAi is an antiviral immune response against a dsRNA virus in Drosophila melanogaster. *Cellular microbiology* **8**, 880-9.

Zamore, P. D., Tuschl, T., Sharp, P. a & Bartel, D. P. (2000). RNAi: double-stranded RNA directs the ATP-dependent cleavage of mRNA at 21 to 23 nucleotide intervals. *Cell* **101**, 25-33.

Zdobnov, E. M., von Mering, C., Letunic, I., Torrents, D., Suyama, M., Copley, R. R., Christophides, G. K., Thomasova, D., Holt, R. a, & other authors. **(2002).** Comparative genome and proteome analysis of Anopheles gambiae and Drosophila melanogaster. *Science* **298**, 149-59.

Zheng, X., Silverman, R. H., Zhou, a, Goto, T., Kwon, B. S., Kaufman, H. E. & Hill, J. M. (2001). Increased severity of HSV-1 keratitis and mortality in mice lacking the 2-5A-dependent RNase L gene. *Investigative ophthalmology & visual science* **42**, 120-6.

Zhou, R., Silverman, N., Hong, M., Liao, D. S., Chung, Y., Chen, Z. J. & Maniatis, T. (2005). The role of ubiquitination in Drosophila innate immunity. *The Journal of biological chemistry* **280**, 34048-55.

Zhou, a, Paranjape, J., Brown, T. L., Nie, H., Naik, S., Dong, B., Chang, a, Trapp, B., Fairchild, R., & other authors. **(1997).** Interferon action and apoptosis are defective in mice devoid of 2',5'-oligoadenylate-dependent RNase L. *The EMBO journal* **16**, 6355-63.

Zuker, M. (2000). Calculating nucleic acid secondary structure. *Current opinion in structural biology* **10**, 303-10.

Zuker, M. (2003). Mfold web server for nucleic acid folding and hybridization prediction. *Nucleic Acids Res* **31**, 3406-3415.

Zuker, M. & Stiegler, P. (1980). information This paper presents a new computer method for folding an RNA molecule Nucleic Acids Research. *Nucleic Acids Research* **9**, 133-148.

Appendix I: Common Solutions and Reagents

Common solutions and reagents used in this thesis are appended here:

TNE buffer

To make 10X TNE buffer for long-term storage of viruses and virus-like particles the following recipe was followed:

In 800 ml of dH_2O 12.1 g of Trizma Base (Sigma, UK), 3.7 g of disodium EDTA (Sigma, UK) and 116.8 g NaCl (Sigma, UK) were added. The pH was adjusted to 7.4 and the solution was made up to a final volume of 1 L. Following autoclaving 10X TNE buffer was diluted with nuclease-free water (Sigma, UK) to give 1X TNE and used.

In vitro transcription

Reagents used in the *in vitro* transcription reaction were

10X SP6 buffer. This was custom made and it contained the following:

400 mM HEPES potassium salt (Sigma, UK) pH adjusted to 7.4.

60 mM magnesium acetate tetrahydrate (Sigma, UK).

20 mM Spermidine trihydrochoride (Sigma, UK).

The buffer was filter sterilised using a 0.22 µm filter (Sartorius, bought through SLS, UK).

M^7GpppG (cap analog) was purchased from Amersham Biosciences, UK.

DTT was purchased from Sigma, UK.

rNTPs used were purchased from Amersham Biosciences, UK in the form of stock solutions (40 mM) ATP, CTP, UTP and GTP.

H_2O (DNase, RNase-free water) was purchased from Sigma, UK.

RNAsin inhibitor was purchased from Promega, UK.

SP6 RNA polymerase was purchased from Amersham Biosciences, UK.

Immunostaining

Triton X-100 was purchased from BDH, UK.

Proteinase K was purchased from Sigma, UK.

To-Pro nuclear marker was a Molecular Probes product (Invitrogen, UK).

Propidium iodide containing mounting medium was purchased from VectorLabs, USA.

PBS was purchased in the form of tablets from VWR international (UK branch).

CAS block is a Zymed, US product. The company is now part of Invitrogen, UK.

Cell Lines

All media used in this thesis were purchased from Gibco, UK. The company is now part of Invitrogen, UK.

Reverse transcription and Polymerase Chain Reaction (PCR)

For RT-PCR the SuperScript II RNase H^+ reverse transcriptase enzyme kit (Invitrogen, UK) was used. OligodT primer, dNTPs and RNasin inhibitor were purchased from Promega, UK. Nuclease-free water was purchased from Sigma, UK. For PCR, *Pfx* DNA polymerase was purchased from Invitrogen, UK. *Taq* polymerase was purchased from Promega.

Agarose Gel Electrophoresis

Agarose gels were made using 0.5M TBE buffer and agarose powder purchased from Promega, UK. The synthesis of the TBE buffer was:

<u>1 litre 5X TBE buffer stock</u>

54 g Tris Base

27.5 g boric acid

20 ml 0.5M EDTA (pH 8)

All reagents were from Sigma, UK.

DNA ladders used for size comparisons were purchased from New England Biolabs, UK.

Bacterial Techniques

Two different strains of recombinant *E. coli* bacteria were used during this project. DH5α (Invitrogen, UK) and XL-10 gold (Stratagene, UK). To grow liquid cultures LB (Luria-Bertani) medium was used. The composition of LB medium was 10 grams tryptone, 5 grams of yeast extract, 10 grams of NaCl. This was purchased as premixed powder from Fischer, UK and 15 grams of the powder mix were added to 500 ml of dH_2O. The medium was then autoclaved and used.

Following transformation a rich medium was used to help recovery of bacteria. The medium of choice was SOC (Invitrogen, UK). The composition of SOC medium is as that of LB with the addition of KCl, $MgCl_2$, $MgSO_4$ and glucose

Appendix II: Supplemental material

pSFV1 with IRES in EcoRV and with duplication of the N-terminus of nsP1

GATGGCGGATGTGTGACATACACGACGCCAAAAGATTTTGTTCCAGCTCCTGCCACCTCCGCTAC
GCGAGAGATTAACCACCCACGATGGCCGCCAAAGTGCATGTTGATATTGAGGCTGACAGCCCATT
CATCAAGTCTTTGCAGAAGGCATTTCCGTCGTTCGAGGTGGAGTCATTGCAGGTCACACCAAATG
ACCATGCAAATGCCAGAGCATTTTCGCACCTGGCTACCAAATTGATCGAGCAGGAGACTGACAAA
GACACACTCATCTTGGATGGGTAATAACCCCCCCCCCCCTAACGTTACTGGCCGAAGCCGCTTGG
AATAAGGCCGGTGTGCGTTTGTCTATATGTTATTTTCCACCATATTGCCGTCTTTTGGCAATGTG
AGGGCCCGGAAACCTGGCCCTGTCTTCTTGACGAGCATTCCTAGGGGTCTTTCCCCTCTCGCCAA
AGGAATGCAAGGTCTGTTGAATGTCGTGAAGGAAGCAGTTCCTCTGGAAGCTTCTTGAAGACAAA
CAACGTCTGTAGCGACCCTTTGCAGGCAGCGGAACCCCCCACCTGGCGACAGGTGCCTCTGCGGC
CAAAAGCCACGTGTATAAGATACACCTGCAAAGGCGGCACAACCCCAGTGCCACGTTGTGAGTTG
GATAGTTGTGGAAAGAGTCAAATGGCTCTCCTCAAGCGTATTCAACAAGGGGCTGAAGGATGCCC
AGAAGGTACCCCATTGTATGGGATCTGATCTGGGGCCTCGGTGCACATGCTTTACATGTGTTTAG
TCGAGGTTAAAAAAACGTCTAGGCCCCCCGAACCACGGGGACGTGGTTTTCCTTTGAAAAACACG
ATGATAATATGGCCGCCAAAGTGCATGTTGATATTGAGGCTGACAGCCCATTCATCAAGTCTTTG
CAGAAGGCATTTCCGTCGTTCGAGGTGGAGTCATTGCAGGTCACACCAAATGACCATGCAAATGC
CAGAGCATTTTCGCACCTGGCTACCAAATTGATCGAGCAGGAGACTGACAAAGACACACTCATCT
TGGATATCGGCAGTGCGCCTTCCAGGAGAATGATGTCTACGCACAAATACCACTGCGTATGCCCT
ATGCGCAGCGCAGAAGACCCCGAAAGGCTCGTATGCTACGCAAAGAAACTGGCAGCGGCCTCCGG
GAAGGTGCTGGATAGAGAGATCGCAGGAAAAATCACCGACCTGCAGACCGTCATGGCTACGCCAG
ACGCTGAATCTCCTACCTTTTGCCTGCATACAGACGTCACGTGTCGTACGGCAGCCGAAGTGGCC
GTATACCAGGACGTGTATGCTGTACATGCACCAACATCGCTGTACCATCAGGCGATGAAAGGTGT
CAGAACGGCGTATTGGATTGGGTTTGACACCACCCCGTTTATGTTTGACGCGCTAGCAGGCGCGT
ATCCAACCTACGCCACAAACTGGGCCGACGAGCAGGTGTTACAGGCCAGGAACATAGGACTGTGT
GCAGCATCCTTGACTGAGGGAAGACTCGGCAAACTGTCCATTCTCCGCAAGAAGCAATTGAAACC
TTGCGACACAGTCATGTTCTCGGTAGGATCTACATTGTACACTGAGAGCAGAAAGCTACTGAGGA
GCTGGCACTTACCCTCCGTATTCCACCTGAAAGGTAAACAATCCTTTACCTGTAGGTGCGATACC

Supplemental data 1: The genomeic sequence of the SFV1(3F)-IRES-ZsGreen from 1 - 1690 nt.

SFV1(3F)-IRES-ZsGreen contains duplicated N-terminus of nsP1 (highlighted in blue). IRES element is located at 276 – 853 nt, between the EcoRV site between the duplicated N-terminus of nsP1 (highlighted in green).